UNIVERSITY OF HULL

"THE SEDIMENTOLOGY AND PETROLOGY OF THE NEW RED SANDSTONE OF THE ELGIN BASIN, NORTH EAST SCOTLAND"

being a Thesis submitted for the Degree of

Doctor of Philosophy

in the University of Hull

by

David Williams, B.Sc.

AUGUST, 1973

LIST OF CONTENTS

		Page Number
ACKNOWLEDGEMENTS		
SUMMARY		
CHAPTER 1	INTRODUCTION	1
CHAPTER 2	HISTORY OF PREVIOUS RESEARCH	3
CHAPTER 3	STRATIGRAPHY OF THE ELGIN BASIN	9
CHAPTER 4	HOPEMAN SANDSTONE : WATERLAIN FACIES	18
	Sheetflood deposits	19
	Playa deposits	24
CHAPTER 5	HOPEMAN SANDSTONE : AEOLIAN FACIES	30
	Seif dunes	30
	Barchan dunes	34
	Contorted dunes	41
CHAPTER 6	PETROGRAPHY OF THE HOPEMAN SANDSTONE	49
	Classification of sandstones	49
	Classification of the Hopeman Sandstone	52
	Detrital components of the Hopeman Sandstone	60
	Roundness and sphericity	67
	Grain size analysis	69
CHAPTER 7	BURGHEAD BEDS : POINT BAR DEPOSITS	84
	Comparison of the Burghead Beds with modern day point bars	85
	The ideal cycle	86
	Locality descriptions	92
	Palaeocurrent analysis and provenance	98
	Grain size analysis	100
	Petrological classification of the point bar deposits	108
	Detrital components of the point bar deposits	111

LIST OF CONTENTS

		Page Number
CHAPTER 15	MORAY FIRTH BOREHOLE DATA	204
	Ideal cycle	206
CHAPTER 16	PALAEOGEOGRAPHY, FRAMEWORK AND HISTORY OF THE NEW RED SANDSTONE ELGIN BASIN	208
	Pediment Zone	210
	Sand Sea Zone	210
	Intertidal Zone	211
	Evaporite Zone	212
REFERENCES		

ACKNOWLEDGEMENTS

This research was undertaken during the tenure of a Natural Environment Research Council research studentship; receipt of this assistance is gratefully acknowledged.

Acknowledgements are also extended to all members of the department staff for their invaluable help and advice throughout the three years of my research. I should also like to thank Dr. J. S. Peacock (I.G.S.), David Fish (Hamilton Brothers Oil Company), Malcolm Rider (Total Oil Marine) and Dr. A. A. Walker (University of Newcastle) for their co-operation and discussions regarding many aspects of the Elgin Basin.

Particular thanks are due to Professor M. R. House and my supervisor, Dr. Brian Waugh. Professor House has always been a source of both encouragement and knowledge, and has extended the use of facilities at the department in the most beneficial way. My supervisor, Dr. Brian Waugh, has been a source of inspiration at many times during my research and has always encouraged me, both in my especialised field, and also in the broader aspects of geology. His help has been invaluable in many respects and my appreciation cannot be expressed too deeply.

Finally I should like to thank Mrs. Anne King for typing my thesis and for making such a first class presentation. Miss Nancy Tan has kindly corrected a few minor errors.

Summary of Thesis submitted for the Doctor of Philosophy degree

by DAVID WILLIAMS

on

"THE SEDIMENTOLOGY and PETROLOGY of the NEW RED SANDSTONE of the ELGIN BASIN, NORTH EAST SCOTLAND"

The New Red Sandstone Elgin Basin occupied the approximate position of the present day Moray Firth. The basin was dominantly continental in character although periodic marine incursions occurred from the main Norwegian Basin to the east.

To the south of the basin at Elgin, deposition began during the Upper Permian with a series of sheetflood deposits which graded laterally into seif dunes to the north. Deposition during the Triassic is dominated by aeolian barchan dunes although minor point bar, playa and floodplain deposits were present. A caliche horizon terminates deposition during the late Triassic. The sediments were derived from the south and south west from an Old Red Sandstone, Moinian and Dalradian source. Fluorite and barytes cementing the dune sandstones were probably introduced prior to the Upper Triassic although remobilisation occurred in association with the galena-haematite-silica-calcite mineralisation during the Middle or Upper Jurassic. The mineralising fluids were introduced along contemporaneous faults.

In the west of the Elgin basin, a series of distal alluvial fan deposits were laid down during the late Triassic in the Golspie area. They were derived from the Old Red Sandstone and Moinian to the west. As at Elgin, faulting and accompanying mineralisation occurred during the Middle or Upper Jurassic.

Boreholes in the Moray Firth indicate that evaporites and intertidal deposits were laid down in the centre of the basin from the early Permian to the end of the Triassic. The four major environmental zones recognisable in the Permo-Triassic Elgin Basin are (a) Pediment Zone, (b) Sand Sea Zone, (c) Intertidal Zone, and (d) Evaporite Zone.

Palaeowind analyses indicate that the basin was influenced by the north easterly Trade Winds throughout the Permian and Lower Triassic although the presence of south westerly winds during the Upper Triassic may indicate a change in climatic conditions.

CHAPTER 1

INTRODUCTION

The New Red Sandstone Elgin Basin is situated in the north east of Scotland and occupies the approximate position of the present day Moray Firth (Fig. 1.1). The basin was dominantly continental in character although periodic marine incursions occurred from the main Norwegian Basin to the east. The basin is bounded to the west by the Northern Highlands and to the south by the Grampian Highlands. Geophysical investigations suggest that the eastern boundary was marked by the Banff-Shetland Islands Arc (Collette, 1968) and the northern boundary by a series of high density metamorphic rocks (McQuillin, 1968).

The Elgin district is situated along the southern shore of the Moray Firth (Fig. 1.2) and occupies a broad coastal plain between the River Findhorn to the west and the River Spey to the east. The general structure of the Elgin district is represented by a series of gently northward dipping strata which are repeated by a series of east west post-Liassic faults, downthrowing to the south (Fig. 1.3). The main exposures are seen along the coastal tract between Burghead and Lossiemouth in a series of post glacial cliffs, present day cliffs and overgrown quarries. A few minor quarries also occur inland along the Carden Hill-Spynie ridge (145622 - 222655) and the Duffus-Clarkly Hill ridge (128683 - 170686).

To the west of the Moray Firth, a north east to south west trending fault with datable Kimmeridgian activity (Gallagher, 1971; Hallam, 1970), separates a narrow coastal tract of Mesozoic strata from the pre-Carboniferous rocks of the Northern Highlands (Fig. 1.2). The Mesozoic sediments are mainly Jurassic in age but, to the south, in the Golspie area, marls and clastic sediments underlie fossiliferous Liassic sediments. These underlying sediments are unfossiliferous, but their similarity to deposits in the Elgin district, and their stratigraphic position suggests they are Triassic in age (Read, 1925).

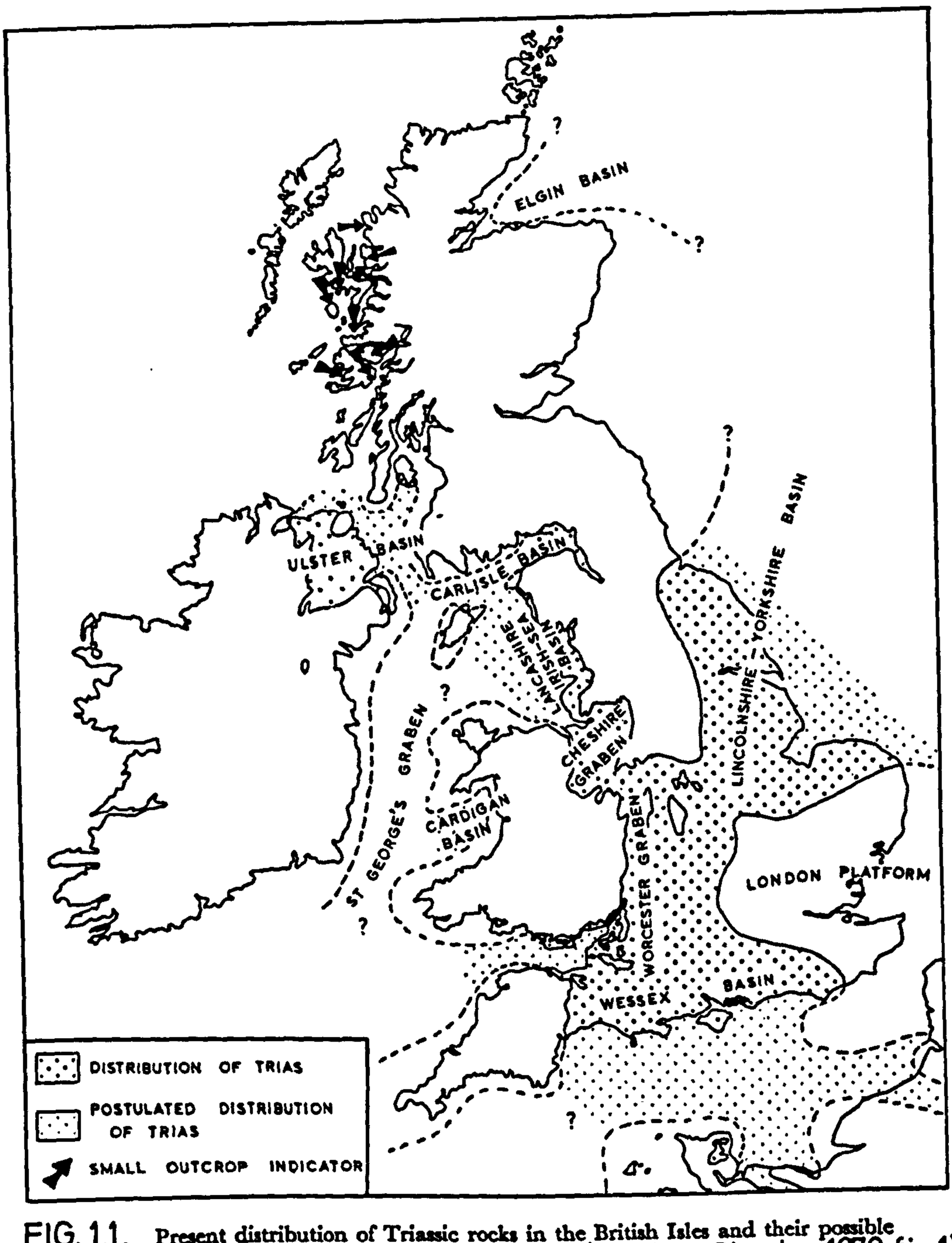

FIG. 1.1. **Present distribution of Triassic rocks in the British Isles and their possible distribution off-shore** (Audley-Charles, 1970, fig. 1).

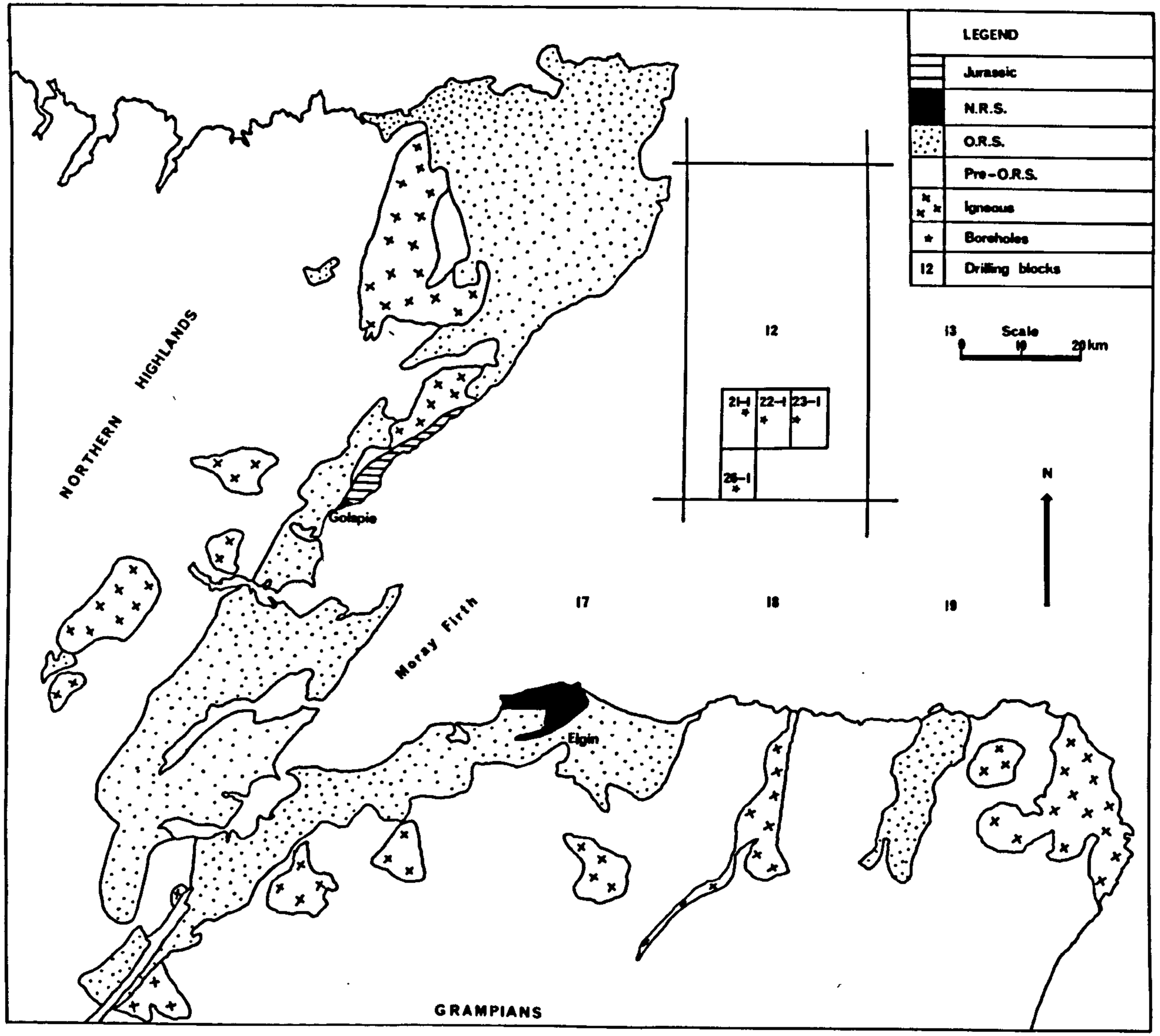

Fig. 1.2. Geology of the Moray Firth area.

Fig. 1.2 shows the position of the four major boreholes which had been drilled in the Moray Firth up to and including October, 1971. The author is indebted to Hamilton Brothers Oil Company for access to the drilling log of borehole 12/26-1 and to Total Oil Marine for a synopsis of the important results from boreholes 12/21-1, 12/22-1 and 12/23-1. The results indicate dominantly marine to near shore sedimentation compared to the continental sedimentation seen at Golspie and Elgin.

Comparison of the sediments with those seen in modern day environments has enabled the author to establish the depositional framework of the Elgin Basin during New Red Sandstone times. These results have been supplemented by petrological studies in an attempt to locate the source of the sediments and to study the diagenetic history of the Elgin Basin. Foreset analyses of both aeolian and waterlain deposits were also used to establish the dominant directions of sediment transport.

The thesis has collated evidence from both onshore and offshore localities in an attempt to define the depositional framework, environmental significance and diagenetic history of the Elgin Baisn during New Red Sandstone times.

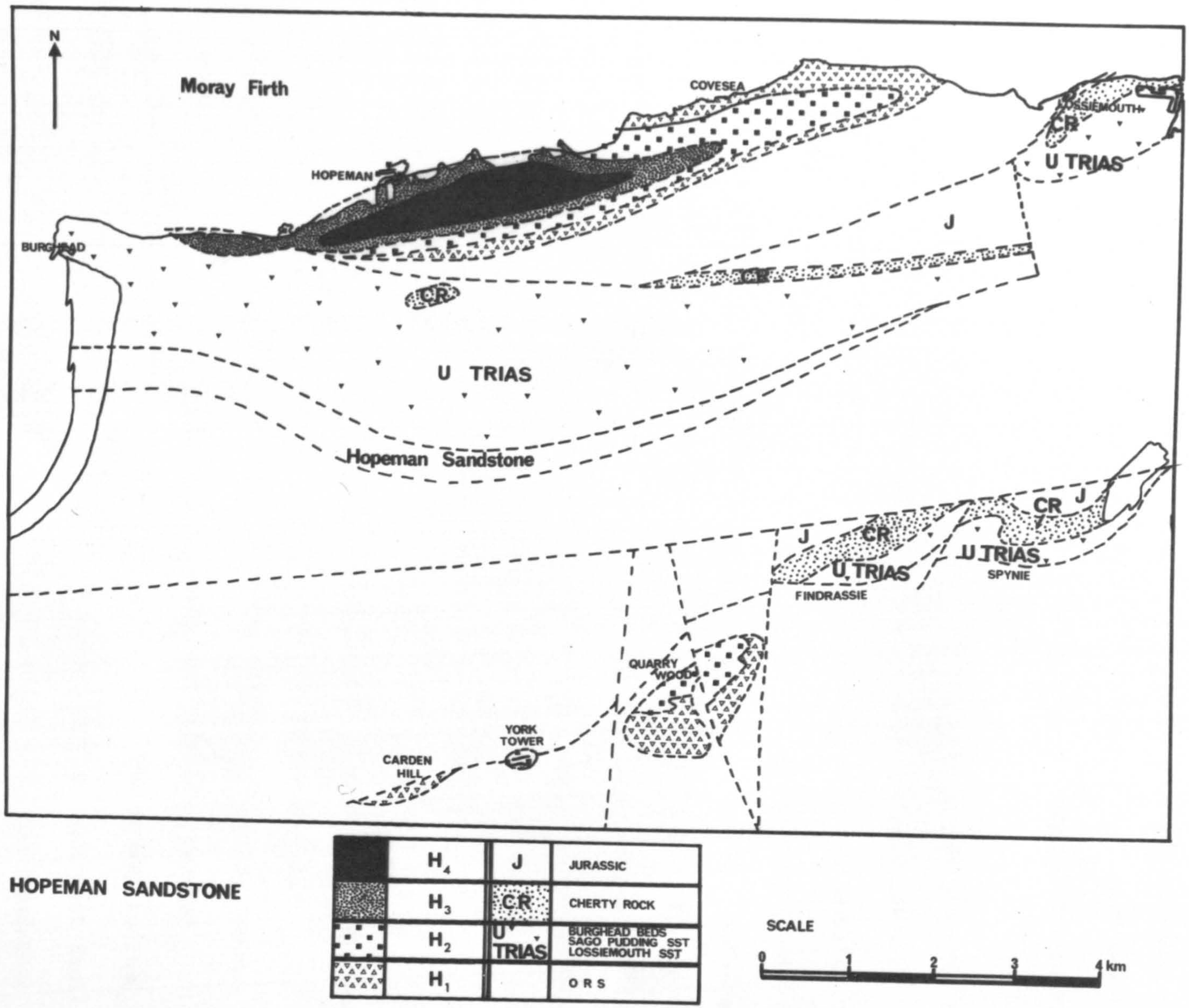

Figure 1.3. Geology of the Elgin district

CHAPTER 2

HISTORY OF PREVIOUS RESEARCH

Previous research on the New Red Sandstone of the Elgin Basin is almost entirely confined to the Elgin district where the discovery of reptilian remains in the mid nineteenth century has been a subject of considerable discussion and controversy even up to the present day. During the early part of the twentieth century, clarification of their stratigraphic significance enabled such workers as Watson and Hickling (1914), Mackie (1897, 1901 and 1925) and later Westoll (1951) to differentiate the various sedimentary environments with reference to their stratigraphic position.

Owing to the close structural and environmental characteristics of the New Red Sandstone and the Old Red Sandstone, during the early part of the nineteenth century, the Permo-Triassic of the Elgin district was thought to be Devonian in age. Quarries to the south of Elgin had yielded both reptilian remains and Holyptychius nobillissimus suggesting to early workers that the reptiles were also Devonian in age. However, in Murchison (1859), prominent geologists were divided into two different parties, one supporting a Devonian age for the reptilian bearing sandstones and the other a New Red Sandstone age. Feelings ran high and one palaeontologist was heard to say that he would not believe that they were Devonian in age unless he saw a reptile with Holyptychius in its mouth!

In 1896, Huxley's conviction (in Judd, 1873) that the reptiles were Permo-Triassic in age was further strengthened by his knowledge that Hyperodapedon also occurred in the Triassic beds from Warwickshire, Devon and India. However, the problem of Holyptychius and reptilian remains occurring in the same quarry still had to be explained. The answer to the problem was finally solved by Judd (1873). He noted that an east west fault system had brought together the New Red Sandstone and the Old Red Sandstone so that both were seen in the same quarry. His theory was confirmed by the Royal Society excavation in the Old Millstone Quarry (184637) during 1885 which yielded the following section:

Coarse sandstone, white to pale yellow, often felspathic and gritty, becoming pebbly downwards. Five reptiles recovered from one horizon and one from the course of stone below 20 feet (6.5 metres)

grades into

Conglomerate. Pebbles of white and purple quartz up to fist size, about 4 feet (1.3 metres),

sharp contact

Finely laminated pink and red sandstone with much false bedding. Yielded at base Holoptychius nobillissimus.

The section showed that the New Red Sandstone and the Old Red Sandstone were separated by a conglomerate and, apart from Phillips (1886), the New Red Sandstone unconformity was accepted by all workers from the date of the excavation.

During the following decade, reptilian remains continued to be discovered, not only at Quarry Wood but also at Spynie, Findrassie and Lossiemouth (Fig. 1.2). Newton (1893) not only confirmed the New Red Sandstone age but was able to differentiate two distinct reptilian faunas. He noted that the reptilian remains found at Quarry Wood were entirely different from the other Elgin localities. He distinguished an Upper Triassic (Lossiemouth Sandstone) from a Lower Triassic/? Upper Permian fauna (Hopeman Sandstone) and listed the following genera from each locality:

Upper Triassic

Lossiemouth: Stagonolepsis, Hyperodapedon, Telerpton.

Spynie: Hyperodapedon, Telerpton and a Ceratodus tooth.

Findrassie: Stagonolepsis, Dasygnathus.

? Upper Permian/Lower Triassic.

Quarry Wood: Two forms of Dicynodont, Gordonia and Geikia accompanied by Elginia allied to Pareiasaurus.

Watson (1909) distinguished three distinct reptile localities in the Elgin district and was also able to confirm the conclusions of Newton (1893). He noted that at Quarry Wood, a pebbly sandstone separated the New Red Sandstone and the Old Red Sandstone and that this was in turn overlain by

a false bedded horizon. He also confirmed Newton's interpretation that the Spynie, Findrassie and Lossiemouth areas were characterized by a distinctive group of sandstones. The third area he regarded as the coastal section between Covesea and Burghead where only reptilian footprints had been found.

He concluded therefore that there were three types of Reptilian Sandstone in the neighbourhood of Elgin;

(a) Lossiemouth Beds

(b) Cutties Hillock Beds

(c) Cummingstone Beds

Whilst Watson regarded the Lossiemouth Beds as undeniably Triassic in age, he concluded that the Cutties Hillock Beds contained a completely different assemblage, more akin to the Permian fauna of Texas and Russia. The footprints of the Cummingstone Beds he correlated with similar footprints in the Permian of Mansfield and Thuringia. The similarities in the petrology and cross bedding of the Cutties Hillock Beds and the Cummingstone Beds led Watson to suggest that they were of the same age. These beds are now known as the Hopeman Sandstone.

As knowledge of other Permo-Triassic reptilian localities increased, Watson and Hickling (1914) were able to define the ages even more precisely. The reptiles Gordonia, Geikia and Elginia from the Cutties Hillock Beds were shown to be slightly later than those of the Upper Permian Pareiasaurus Beds of Russia, or equivalent to the Cisticephalus zone of South Africa, the extreme top of the Permian. The Lossiemouth Beds were compared in age to the Middle Trias Lettenkohle of Germany. They also suggested that the reptiles were all terrestrial except for Hyperodapedon and Stenometopon from the Lossiemouth Beds which may have been river forms.

No significant reference to the stratigraphy of the Elgin district was made again until the year of the 1948 International Geological Congress in London. A paper by Watson et al., (1948) and the guide to "The Vertebrate-bearing strata of Scotland" (Westoll, 1951) were the first to document the existence of the Burghead Beds. These authors were able to differentiate

the fluviatile nature of the Burghead Beds from the aeolian Lossiemouth Sandstone and Hopeman-Cummingstone Beds. The following succession is taken from Watson et al. (1948, p. 6.):

Sandstone of Lossiemouth, Spynie and Findrassie	c. 200 ft.
(A Middle or Lower Upper Triassic age is indicated)	
Burghead Beds (New name)	c. 250 ft.
Sandstone of Cutties Hillock and Hopeman-Cummingstone	c. 200 ft.

Further work on the reptilian remains by Walker (1961) enabled the position of the Lossiemouth Sandstone to be placed near to the Carnian-Norian boundary which was younger than had previously been thought. He also noted the diversity of the forms and the remarkable degree of articulation of the remains. Walker suggested that this indicated little or no transportation of the specimens had occurred.

Although much detailed research on the reptilian remains has been undertaken from the mid nineteenth century to the present day, little work has been carried out on the petrological and sedimentological characteristics of the sandstones. However, between 1897 and 1901, three papers by Mackie (1897, 1901a and 1901b) brought about a substantial step forward in the understanding of the Elgin sandstones.

His first paper on the "Sands and Sandstones of Eastern Moray" compared the recent aeolian Culbin Sands to some of the large scale cross-bedded sandstones of Hopeman. He therefore interpreted the Hopeman Sandstone as being aeolian in character. The second paper dealt with the pebbly sandstone at the base of the New Red Sandstone at Quarry Wood. He noticed its consistent nature at five separate localities and the discordant character of the contact with the Old Red Sandstone. Most important of all, he interpreted the three sided nature of the pebbles as being due to sand blast action in an arid environment. The rounded edges were due to later re-deposition by water, a hypothesis far ahead of its time. His final paper dealt with the barytes and fluorite cements of the Hopeman Sandstone and suggested that they were derived from saline lakes.

Various workers made passing references to the lithology of the reptilian bearing sandstone but it was left once again to Mackie to further petrological studies of the sandstones. In 1925, Mackie's heavy mineral analyses confirmed the threefold stratigraphic division established by Watson and Hickling (1914). He also noticed the deficiency of heavy minerals in the aeolian sandstones compared to the fluviatile sandstones.

Shotton (1956) not only confirmed the aeolian nature of the Hopeman and Lossiemouth Sandstones but was also able to suggest that the Hopeman Sandstone was formed by a north easterly wind. He thought that the easterly wind together with the arid climate of the New Red Sandstone indicated that the British Isles occupied a position in the Trade Wind Belt at this time.

However, the most important step forward in more recent times has been the publication of the Elgin Memoir (Peacock et al., 1968). The memoir summarized all previous research and represented the first detailed account on all aspects of the Elgin New Red Sandstone.

In comparison with Elgin, research on the Golspie New Red Sandstone is limited to work by Judd (1873) and Read (1925). Judd (1873) was the first to recognise the Triassic age of the marls and sandstones at Golspie; he demonstrated that the rocks were overlain conformably by sediments with a Lower Lias fauna. He also recognised a cherty limestone which he found to be similar in character to the Cherty Rock at Elgin.

The most recent account of geology of the Golspie area is that of Read (1925). He was able to recognise three main units in the Triassic. The uppermost pebbly sandstone he suggested was Rhaetic in age and the underlying cherty limestones and calcareous sandstones as Upper Triassic in age. (The Rhaetic was included in the Jurassic at this time.)

The decade between 1960 and 1970 marked the advent of exploration for oil and gas in the North Sea. The first geophysical results published in this connection by Collette (1960) showed a large negative anomaly occupying the Moray Firth. He interpreted the anomaly as being due to a granite. More recent surveys have now however shown that the anomaly is more probably due

to the presence of a large sedimentary basin. Recent Geophysical data obtained by Collette (1968), McQuillin (1968) and Eden et al., (1970) have enabled the limits of the basin to be more accurately defined.

CHAPTER 3

STRATIGRAPHY OF THE ELGIN BASIN

Understanding of the stratigraphy of the New Red Sandstone is complicated by the limited number and isolation of the onshore exposures and the marked lateral variation in the facies. Detailed correlation over a wide area is therefore extremely difficult. It is therefore intended to deal first with local stratigraphy and then consider its relevance to the Elgin Basin as a whole.

The main onshore locality of the New Red Sandstone is seen to the south of the Elgin Basin at Elgin. The most recent stratigraphical classification is taken from the Elgin Memoir (Peacock, 1968, p. 54.) and is based on the work of Watson and Hickling (1914), Mackie (1925), Westoll (1951) and Walker (1961).

Cherty Rock	Upper Triassic
Sandstones of Lossiemouth, Spynie and Findrassie	Upper Triassic
Burghead Beds	Triassic
Sandstones of Cutties Hillock and Hopeman	Upper Permian and Triassic

The Cutties Hillock Sandstones have yielded reptilian remains identified by Walker (1961) as Upper Permian in age. The Hopeman Sandstone has not yielded any identifiable fossil material but their petrological similarities have been compared by Watson and Hickling (1914) and Mackie (1925) to those of the Cutties Hillock Sandstones. This view is taken here, and it is suggested that the term Cutties Hillock Sandstone be omitted from future publications. They are hereafter referred to as the inland exposures of the Hopeman Sandstone.

The inland exposures of the Hopeman Sandstone consists of two main phases. The lowest phase is represented by a series of pebbly sandstones lying discordantly on the Old Red Sandstone and are interpreted by the author as sheetflood deposits (see Chapter 4). They reach a maximum of 4 metres in

thickness but this is extremely variable. The presence of dreikanter pebbles with rounded edges suggests that they were exposed to the wind prior to their incorporation into the sheetflood deposits.

Reptilian remains have been recovered from just above this horizon at the base of the overlying second phase. They have been identified by Watson and Hickling(1914) as being equivalent in age to the Cisticephalus zone of the Karroo Basin. They were thought to be Permian in age but extremely close to the Triassic boundary. Recent opinion is however divided as to whether the Cisticephalus zone is equivalent to the Upper Permian or very Early Triassic in age (Walker, personal communication, 1971).

The second phase at Quarry Wood consists of approximately 30 metres of large scale cross bedded sandstones. The well rounded quartz grains and the unidirectional foresets are indicative of fossil barchan dunes. The sheetflood phase is therefore denoted the H1 phase and the barchan dune phase as H2 (Fig. 3.1).

On the coastal exposures between Covesea and Cummingstone, the basal contact between the Hopeman Sandstone and the Old Red Sandstone is not seen. However, at Covesea Skerries Lighthouse, the Old Red Sandstone and the Hopeman Sandstone are only separated by 250 metres; the contact between the two groups is thought to be an unconformity (Peacock, 1968, p.58).

Regional mapping of the coastal exposures of the Hopeman Sandstone indicate that four distinct phases of aeolian deposition are present. The phases are separated by periods of flooding which may be preserved as playa deposits. The lowest phase is represented by seif dunes and the succeeding ones by barchan dunes.

The main problem of correlating the inland and the coastal exposures of the Hopeman Sandstone is dependent upon the relative ages of the seif dunes and the H1 sheetflood deposits of Quarry Wood. Evidence suggests that the source area lay to the south. In modern day deposits, seif dunes are normally found closer to the source than barchan dunes. The presence of barchan dunes as the H2 phase at Quarry Wood therefore indicates that the seif

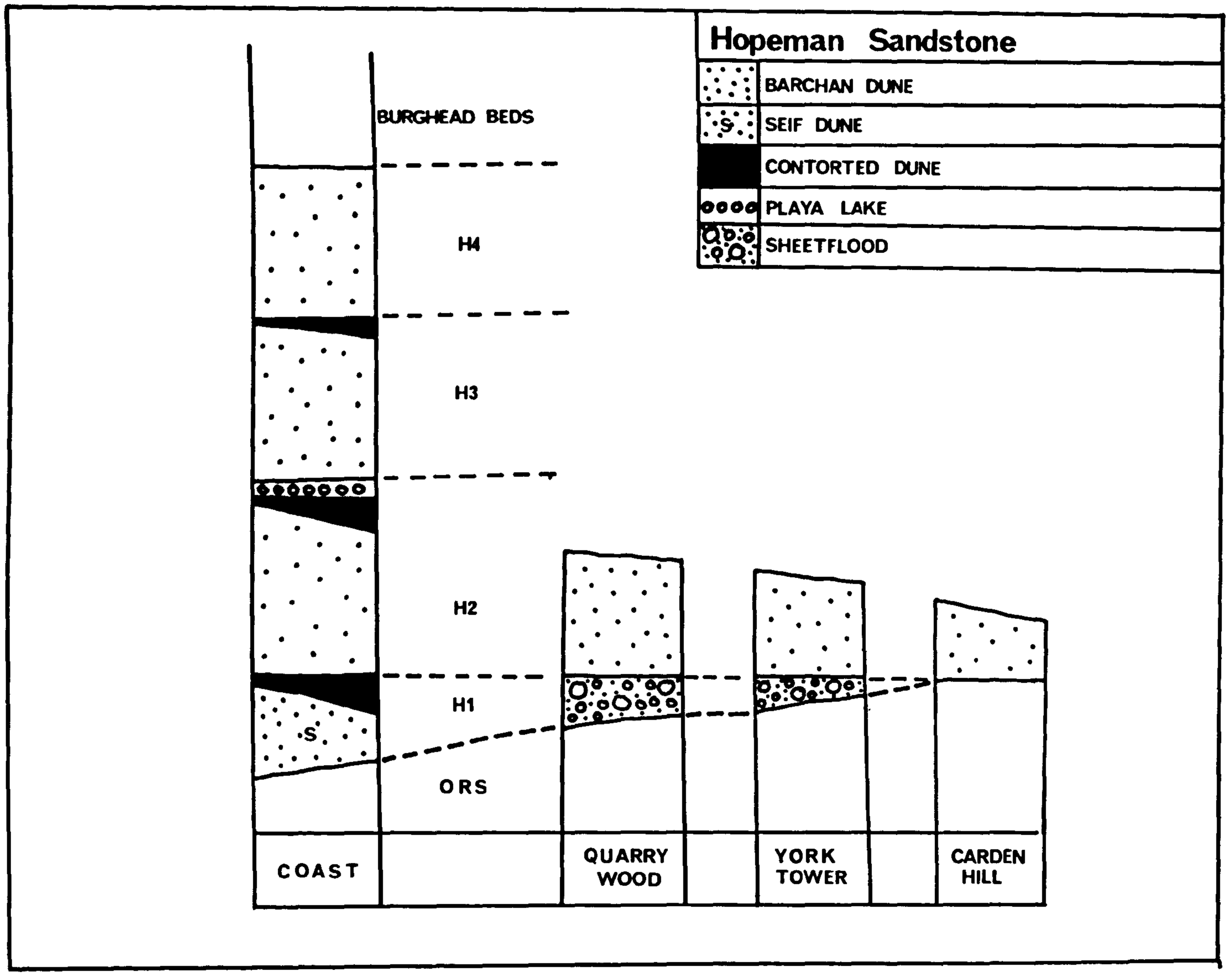

Fig. 3.1. Correlation of the inland and coastal exposures of the Hopeman Sandstone.

dunes of Covesea are probably H1 or earlier. Modern day desert regions in Libya show that sheetflood deposits merge into seif dune deposits within a distance of 2 miles from the source (McKee and Tibbitts, 1962). It seems probable that a similar transition occurs in the Hopeman Sandstone where the sheetflood deposits of Quarry Wood are contemporaneous with the seif dunes at Covesea. Thus, the seif dunes are also denoted H1, the succeeding barchan dunes being denoted H2, H3 and H4 phases respectively.

Thus the H1 phase is possibly of Upper Permian age, with the succeeding phases being Triassic in age. The Hopeman Sandstone, which is 200 feet thick in the Clarkly Hill borehole (Peacock, 1968) thins rapidly to the east until at Lossiemouth and Spynie it is completely absent (Table 3.2). The Clarkly Hill borehole also shows that the Hopeman Sandstone is overlain by the Burghead Beds which are fluviatile in origin. The junction between the two horizons appears to be conformable. Evidence discussed in later chapters suggests that the fluvial system migrated over the aeolian dunes from the west.

No reptilian remains have been recovered from the Burghead Beds but evidence suggests that they were in part contemporaneous with the fossiliferous Lossiemouth Sandstones to the east. The Lossiemouth Sandstone is underlain by a maximum of 4 metres of fluviatile sandstones. They are interpreted as the flood plain facies of the Burghead Beds (see Fig. 3.2).

In the Clarkly Hill borehole (Table 3.1) the Burghead Beds are represented in the upper part by coarse grained point bar deposits and in the lower part by floodplain deposits. The main problem is, with which horizon in the Burghead Beds are the floodplain deposits of Lossiemouth contemporaneous.

There are three main possibilities:

1. It is equivalent to the first period of flooding at the base of the Burghead Beds (72·5 metres in the Clarkly Hill borehole, see Table 3.1).

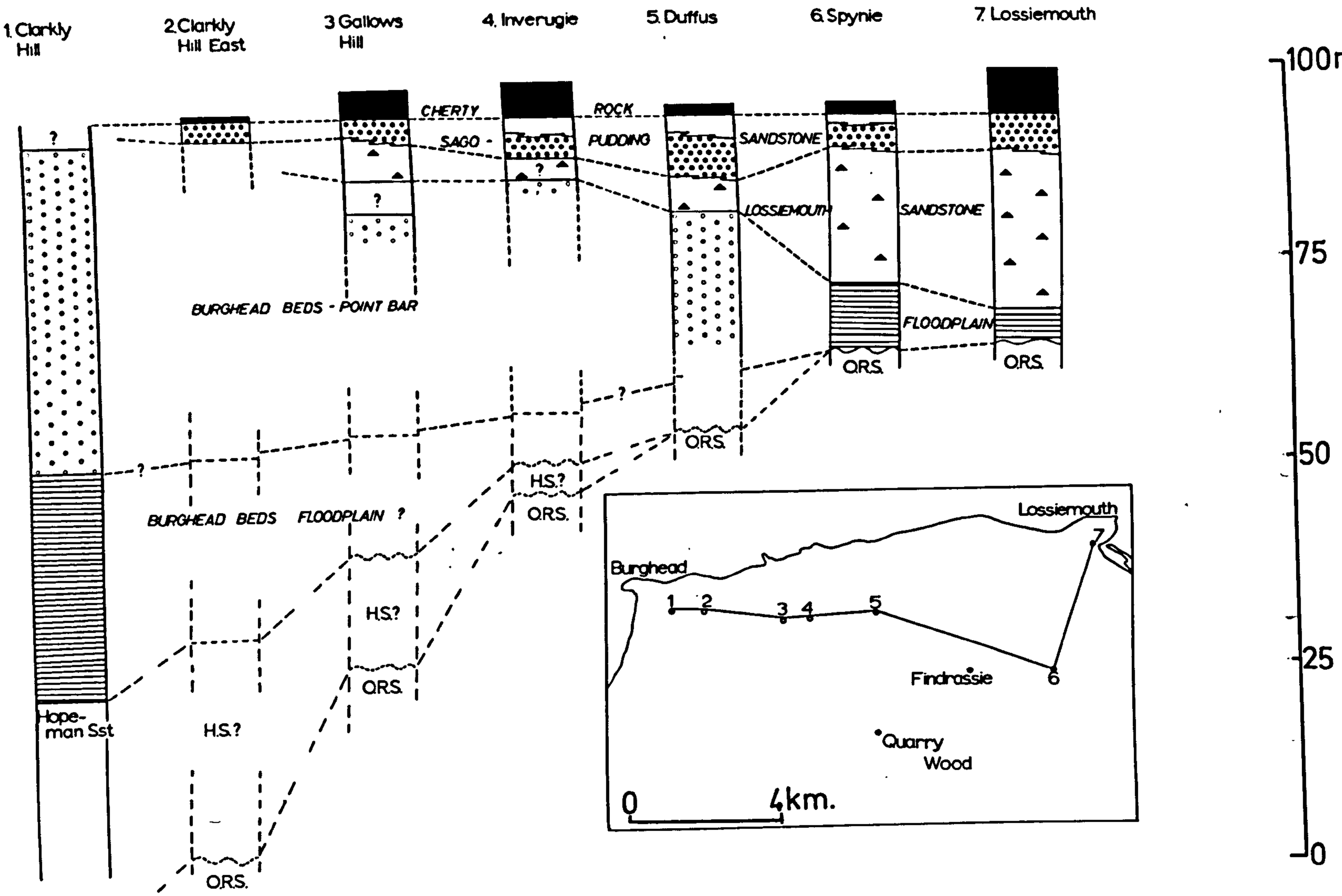

Fig. 3.2. Correlation of the New Red Sandstone of the Elgin district.

TABLE 3.1

CLARKLY HILL BOREHOLE (12706833, 59·5 metres O.D.) (taken from Peacock, 1968)

Permian and Triassic

	Thickness (in metres)	Depth
Burghead Beds		
Sandstone, friable, cross-bedded, yellow brown to greyish brown, fine to coarse grained, with bands of pebbles, poorly cemented. Thin beds of silt and clay, horizons of silt pellets. Dip 5 degrees.	41·5	41·5
Sandstone, friable, greyish-orange to pale grey, fine to medium grained. Pyritic cement below 60 metres depth.	31·0	72·5
Hopeman Sandstone		
Sandstone, medium to coarse grained, friable, dune bedded.	32·5	105·0
Sandstone, friable, medium to coarse grained, gritty. Quartz pebbles frequent towards the base. Sets of cross bedding up to 5 metres.	27·0	132·0
Interbedded sandstone and siltstone. Many pebbles.	0·5	132·5
presumed unconformity		
Old Red Sandstone	11·0	143·5

TABLE 3.2

SPYNIE QUARRY BOREHOLE (22286559, 25·5 metres O.D.) (taken from Peacock, 1968)

	Thickness (in metres)	Depth
Triassic		
Sandstone, pinkish grey (5YR 7/1), siliceous at top, calcareous below.	9·5	9·5
Siltstone and fine grained sandstone, grey, pinkish and pale orange (10YR 7/2-8/2), calcareous. Dip 5-7 degrees.	6·5	16·0
Sandstone, brownish yellow, fine and coarse grained, interbedded with siltstone; calcareous. Grey, brown and violet at the base.	1·5	17·5
No evidence of angular discordance		
Old Red Sandstone	54·0	71·5

2. It represents the period of maximum flooding towards the east at the base of the coarse grained point bar deposits (41·5 metres in the Clarkly Hill borehole).
3. The maximum period of flooding occurred at an intermediate position (between 0 and 72·5 metres in the Clarkly Hill borehole).

Towards the top of the Burghead Beds, there is evidence that aeolian deposition was encroaching towards the west and replacing the fluvial deposits. It is therefore probable that the maximum extension of the Burghead Beds "fluvial system" to the east occurred near to the base of the coarse grained point bar deposits. The floodplain deposits at Lossiemouth are therefore thought to be contemporaneous with the base of the point bar deposits (Fig. 3·2).

BURGHEAD	LOSSIEMOUTH
Cherty Rock	Cherty Rock
Sago Pudding Sandstone	SagoPudding Sandstone
Burghead Beds (Point Bar)	Lossiemouth Sandstone Burghead Beds (Floodplain)
Burghead Beds (Floodplain)	Non deposition

Walker (1961) suggested that Stagonolepsis, Dasygnathus and its allies, collected from near the base of the Lossiemouth Sandstone, indicated an age close to the Carnian-Norian boundary. The Lossiemouth Sandstone is therefore Norian and possibly Rhaetian in age.

The Lossiemouth Sandstone is overlain by the Sago Pudding Sandstone and the Cherty Rock (see Fig. 3.2). The Sago Pudding Sandstone represents a waterlain sandstone which was subsequently reworked by the wind to produce a bimodal "Sago Pudding" effect. The Cherty Rock is interpreted as an altered

caliche horizon and is overlain by a series of marls with a Lower Lias fauna. The Cherty Rock, Sago Pudding Sandstone, Lossiemouth Sandstone and the upper part of the Burghead Beds at Burghead (Point bar deposits) therefore represent deposition during the Norian and the Rhaetian. The lower part of the Burghead Beds at Burghead (Clarkly Hill) and phases H2-4 of the Hopeman Sandstone can therefore be equated with the Middle and Lower Triassic and possibly part of the Upper Triassic (Carnian). The H1 phase of the Hopeman Sandstone is probably Upper Permian in age (Fig. 3.4).

New Red Sandstone strata also outcrop to the south west of the Moray Firth and Golspie in Sutherland. A narrow faulted coastal tract between Golspie and Helmsdale has brought up a series of Mesozoic strata ranging from Triassic to Kimmeridgian in age. Although no fauna or flora have been recovered from the Triassic strata they are conformably overlain by Lower Liassic marls. Judd (1873) first recognised the similarity between the cherty limestone of Golspie and the Cherty Rock of Lossiemouth. Even in thin section he found them absolutely indistinguishable.

The Triassic strata are exposed along the foreshore between Dunrobin Castle (852007) and Golspie Burn (840000). The following classification is taken from Read (1925):

Lower Lias	
Pebbly grits	300 feet
Cherty limestone	?50 feet
Calcareous sandstone	?20 feet

The pebbly grits are only seen near to their base but their coarse nature would suggest that they were deposited in a similar position in the basin to the Burghead Beds ..... that is, near to the source. The sandstones are extremely poorly exposed but appear to represent a series of distal alluvial fan deposits.

The cherty limestone represents a caliche horizon which grades down into the underlying calcareous sandstone. It is extremely similar to

the Cherty Rock of Lossiemouth and was thought to be contemporaneous with it by all previous authors. (Read, 1925; Judd, 1873). Modern day caliche horizons are extremely variable in nature and grade laterally into playas, dunes and many other desert facies. Thus, although the caliche at Golspie and Elgin reflect increasingly favourable climatic conditions for the formation of caliche horizons, there is no factual reason to believe they were formed contemporaneously.

In fact, two factors show that it is indeed unlikely that they are contemporaneous. Firstly, the Cherty Rock of Elgin is an extremely old caliche whereas the caliche which was formed at Golspie represents only the initial stages of caliche formation. Secondly, 300 feet of sediments overlie the caliche at Golspie, whilst at Elgin there is a complete absence of any overlying sediments. Conditions necessary for the formation of caliche already existed before the Rhaetic (Craig, 1965) and it is thought that the cherty limestone of Golspie is probably Keuper in age. The pebbly sandstones are therefore Rhaetic and possibly partly Keuper in age.

Recent geophysical surveys have suggested that the Moray Firth represents a large sedimentary basin and has probably been so since Permian times (Craig, 1965). Borehole data obtained from Hamilton Brothers Oil Company and Total Oil Marine have yielded the following results:-

1. The Elgin Basin was open to the east, probably from the very beginning of the Permian.
2. An important marine incursion occurred during some part of the Zechstein but terrigenous sedimentation persisted.
3. After the marine incursion a thick series of siltstones accumulated.
4. In their lower part these bear some evidence of marine influence but appear to have been continental for the most part. Evidence is not conclusive.
5. A marine incursion (after a period of erosion) closed the Permo Triassic.

HAMILTON BROS OIL CO WELL 12 / 26 - 1

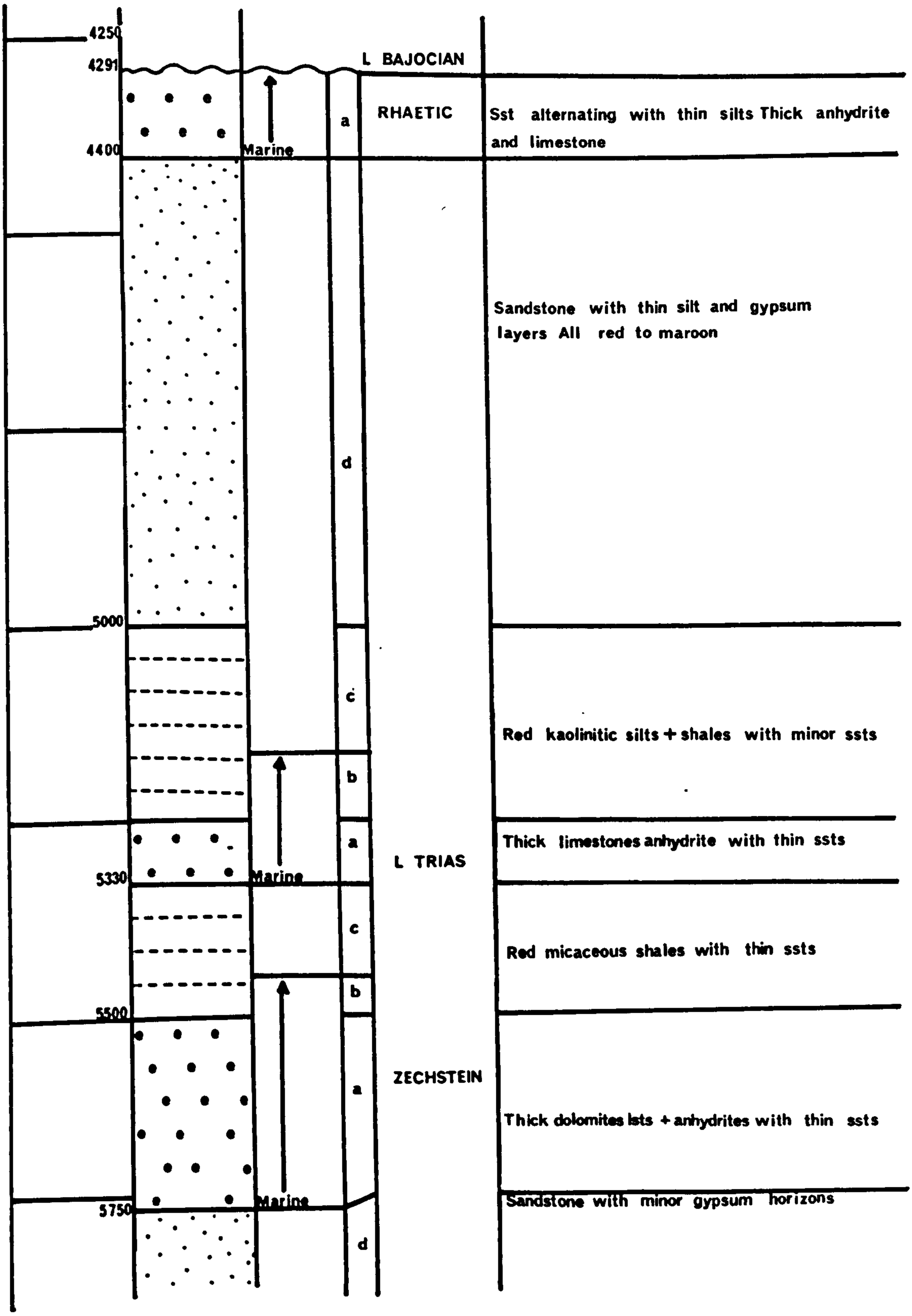

Fig. 3.3. Hamilton Brothers Oil Company borehole 12/26-1.

Figure 3.3 shows the generalised sequence of sediments from Hamilton Brothers Oil Company borehole 12/26-1. Comparison of the results with those from Total Oil Marine have yielded the following conclusions. Marine sedimentation only occurred in the centre of the basin and then only for short periods. Sedimentation in the centre of the basin began in early Permian times whilst in the Elgin and Golspie areas, it did not begin until the late Permian and the Triassic (see Fig. 3.4).

As there is no evidence of Carboniferous sedimentation in the area, it is suggested that deposition in the Elgin basin began during the Lower Permian. Progressive recession of the source resulted in deposition in the late Permian at Elgin and probably late Trias at Golspie. This is evidenced by sheetfloods and alluvial fan deposits at the base of the succession which are generally acknowledged to represent deposition near to the source area.

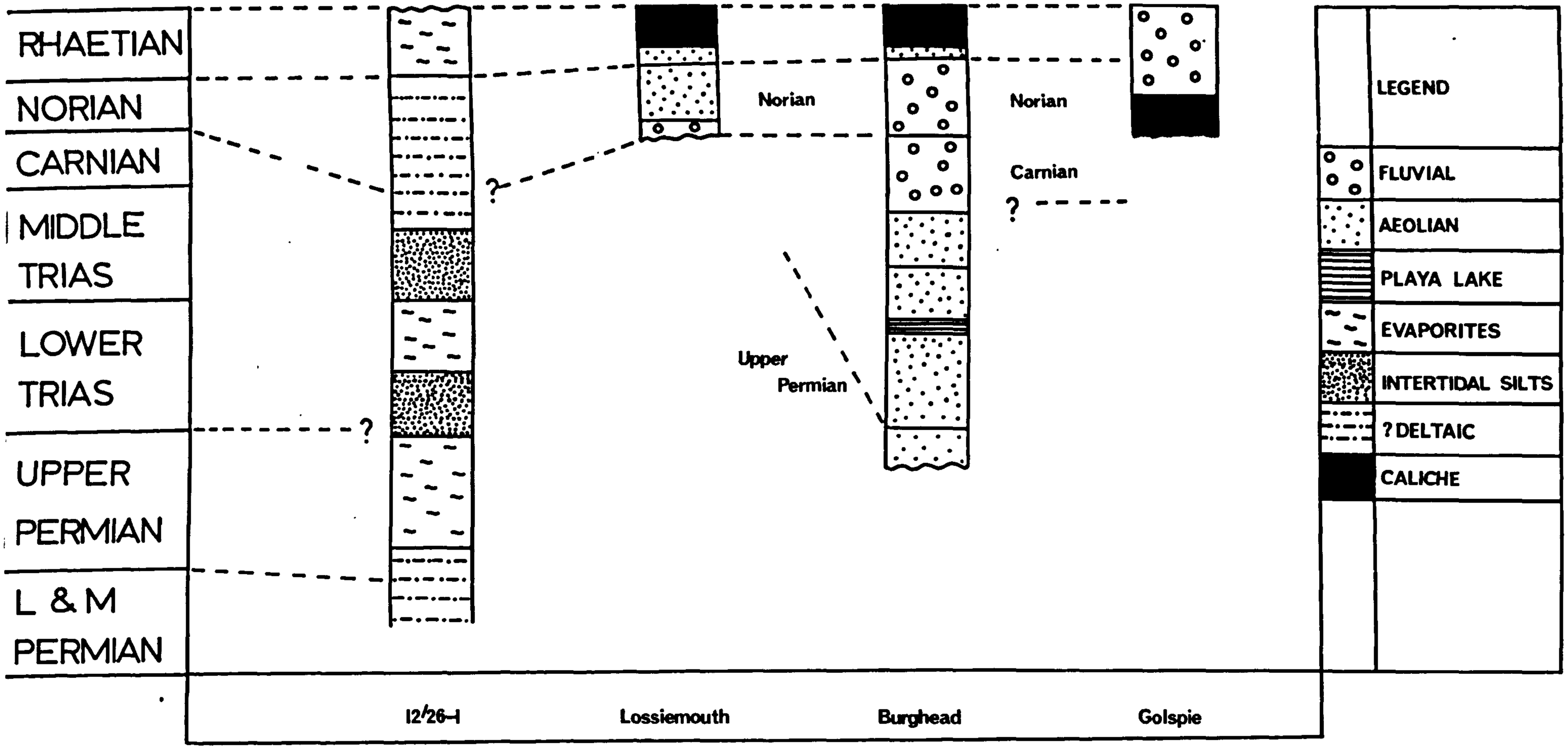

Fig. 3.4. Stratigraphy of the New Red Sandstone Elgin Basin.

CHAPTER 4

HOPEMAN SANDSTONE; WATERLAIN FACIES

The most widespread horizon in the Elgin district is the Hopeman Sandstone which is exposed along the coast between Masonshaugh Quarry (121692) and Covesea (204704) and in a few minor inland quarries along the Quarry Wood ridge. The sandstones were deposited in an arid to semi-arid environment and are dominantly aeolian in character. They are mainly characterised by large scale dune cross bedded sandstones but some minor horizontally bedded and structureless sandstones indicate deposition by water. The waterlain horizons represent flash flood sediments deposited during periods of high rainfall. Although the deposits have a limited occurrence at the present day, they are thought to have been more extensive at the time of deposition and have since been reworked and redeposited by aeolian agencies.

Evidence for their former presence is often seen in studies of the many contorted horizons in the dunes of the Hopeman Sandstone. Where waterlain horizons are still preserved, there is sufficient evidence to suggest that they were the singular cause of the contortions in the underlying dunes. Injection structures also suggest the presence of water. However, at many localities there is no evidence of waterlain deposits overlying the contorted dunes, suggesting that they may have been removed by the wind.

In modern day deserts waterlain horizons are represented by three main facies:

1. Alluvial fan and sheetflood deposits represent deposition near to the source area. They are poorly sorted sediments, the coefficient of sorting increasing and the grain size decreasing away from the source area. Sheetflood deposits are laterally extensive and represent "en masse" deposition of the talus material and are not channelled as in the case of the alluvial fan deposits.
2. Playa deposits are often the end product of the sheetflood deposition where the gradient is sufficiently reduced to allow the settling out of

the finer material in a tranquil environment. They are deposited in the centre of desert basins and are often ephemeral in character.

3. Desert fluvial deposits are formed in wadis, braided rivers or as extremely wide meandering streams. The type of fluvial system is clearly related to the gradient and discharge of the area in which they were deposited (Allen, 1970).

Sheetflood and playa deposits can be recognised in the Hopeman Sandstone.

SHEETFLOOD DEPOSITS

The poor sorting, structureless nature, coarse mode and basal position of the sheetflood deposits distinguish them from the well sorted foreset bedding of the aeolian sandstones. These distinguishing parameters all suggest a supersaturated flow of sediment which is in character with sediments deposited close to a mountain source following torrential rainfall in an arid to semi arid environment.

The clearest evidence of sheetflood deposits is seen inland at Quarry Wood in the H1 phase of the Hopeman Sandstone. They lie discordantly on the Old Red Sandstone and reach a maximum thickness of 3 metres. The unconformity is clearly lower to the west, as at York Tower, they rest on the Alves Beds (lowest Upper Old Red Sandstone) whilst at Quarry Wood, they rest on the Rosebrae Beds (highest Upper Old Red Sandstone). Their presence as the basal member of the Hopeman Sandstone lends support to the theory that they were deposited close to the mountain source, as the deposits become more basinal in character as they get younger. The absence of the sheetflood deposits at Carden Hill and Covesea indicates that the deposits did not extend far to the south or west (Fig. 4.1.).

The sheetflood deposits are yellow brown in colour and vary from soft friable to hard siliceous pebbly sandstones. The upper contact of the sheet flood with the aeolian sandstones is gradational so that the dune sandstones

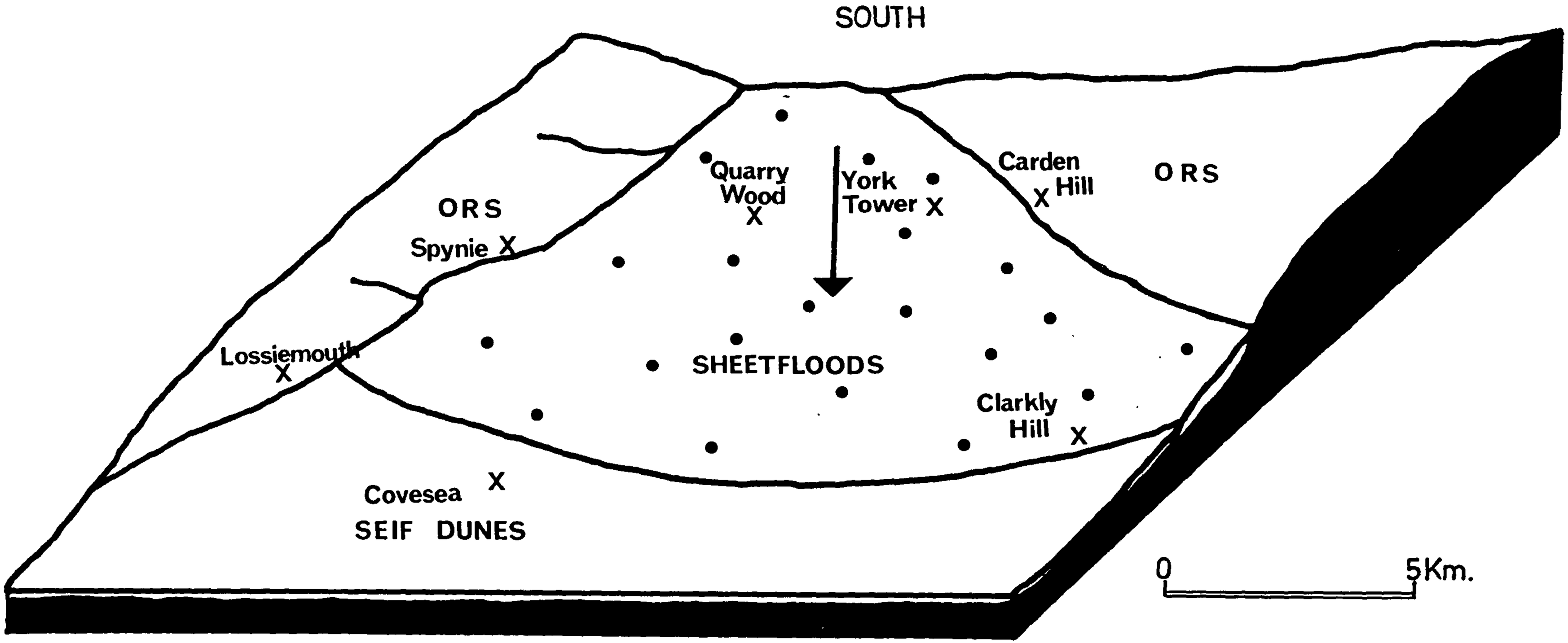

Fig. 4.1. Distribution of the H1 sheetflood deposits.

have retained a similar lithology; they can however be differentiated by their bedding characteristics. This is clearly due to later reworking of the sheet-flood deposits by the wind.

The most easterly exposure is seen at the old quarry 400 metres north west of Laverockloch Farm (193637) (Fig. 4.2.). The pebbly sandstones at this locality occupy the base of the quarry floor although minor exposures are seen in the easterly face of the quarry. Plate 4.1A illustrates the sheetflood deposits resting on the Old Red Sandstone at this locality. The thickness of the sheetflood deposits is approximately 2 metres although the upper contact is gradational and therefore difficult to measure accurately.

Sheetflood deposits are again seen at the Old Millstone Quarry at Quarry Wood (Fig. 4.2.). At the present day, the junction with the Old Red Sandstone is not seen but the section was described in the Royal Society excavation of 1885 (see Chapter 2).

At Rosebrae Quarry (173633), 3 metres of sheetflood deposits are seen lying discordantly on the Rosebrae Beds of the Upper Old Red Sandstone. South of the Old Millstone Quarry, a number of glaciated exposures are seen extending southwards towards the Danish Camp (Fig. 4.2.). These exposures are documented in the primary survey of the Geological Survey but are now obscured by the Forestry Commission plantations.

West of Quarry Wood, the sheetflood deposits are present at York Tower Quarry. The north face of the quarry is occupied by 15 metres of Rosebrae Beds overlain by the sheetflood deposits towards the top; unfortunately, the contact is inaccessible. The downfaulted southern face is occupied by the aeolian sandstones of the H2 phase, the junction with the sheetflood deposits being at the base of the quarry where the pebbly sandstones are exposed on the quarry floor.

No evidence of sheetflood deposition is seen at Carden Hill where dune sandstones of the H2 phase rest directly on the Old Red Sandstone.

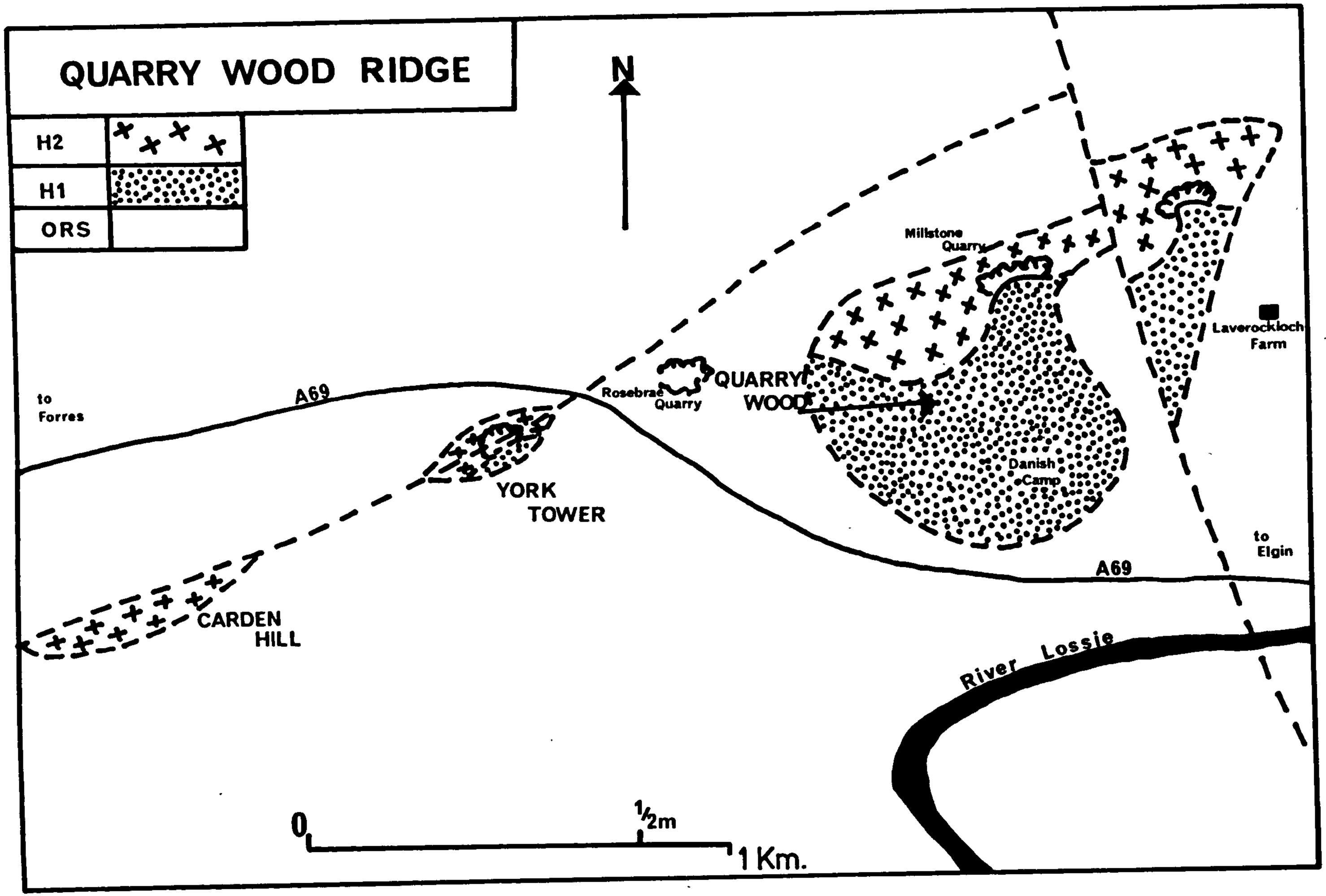

Fig. 4.2. Inland exposures of the Hopeman Sandstone.

In the Clarkly Hill borehole, the base of the Hopeman Sandstone is represented by one metre of interbedded silts and pebbly sandstones; pebbles reach 30 mm in diameter. The interbedded nature of the sediments suggest several periods of sheetflood deposition, the silts representing the final settling out phase of the sheetfloods and indicating that Clarkly Hill was towards the distal end of sheetflood deposition.

This interpretation is substantiated by the presence of seif dunes at the equivalent horizon at Covesea. The absence of sheetflood deposits at Covesea, Spynie, Findrassie, Lossiemouth and Carden Hill is interpreted as non deposition rather than subsequent erosion (Fig. 4.1.).

Sedimentary structures in the sheetflood horizon are almost non existent although rare traces of horizontal lamination are seen. Pebble horizons show no distinct alignment and are randomly distributed throughout the sandstone. The high degree of weathering and silicification may have obliterated all traces of the original bedding but this is thought to be unlikely as sheet-flood deposits from the New Red Sandstone of Devon described by Laming (1966) show a similar lack of structure near to the source area. Their mode of deposition can be compared to that of mudflows where the highly saturated sediment does not promote good sorting. Thus, the high sediment:water ratio results in a lack of grading, random distribution of pebbles throughout the sandstone and lack of bedding structures.

Pebbles reach a maximum diameter of 90 mm in diameter and are set in a matrix varying from coarse sand to silt. The pebbles are frequently wind faceted but the edges show later rounding due to transportation by water. This dreikanter-like appearance suggests that the pebbles were originally products of sandblast action near to the mountain source and were subsequently incorporated into the sheetfloods (Mackie, 1901).

The distribution of the maximum pebble sizes from each locality shows a rapid decrease in size towards the north, indicating a southerly source. Measurement of pebble orientations at Quarry Wood gives a mean direction of N3°E.

The presence of seif dunes at the equivalent horizon at Covesea and a thinner sequence of pebbly sandstones at Clarkly Hill indicate that the sheetflood deposits died out rapidly to the north (Fig. 4.1.).

The composition of the pebbles in the sheetflood deposits is basically of quartzites with minor granulites and chert. Present day deposits to the south of Quarry Wood consist of Old Red Sandstone, Moinian and Dalradian strata. The following succession of the pre-Permian strata of the Elgin district is taken from the Elgin memoir (p. 4):

OLD RED SANDSTONE	
Upper	Rosebrae Beds (sandstones)
	Cornstone Beds (calcareous sandstones and limestones)
	Scaat Craig Beds (mainly pebbly sandstones)
	Alves Beds (mainly pebbly sandstones)
Middle	Sandstones, conglomerates and nodule beds
Middle or Lower	Buckie Beds (breccias, limestones and sandstones)
DAIRADIAN	
	Carnfield Actinolite Flags
	Findlater Flags
	West Sands Mica Schist
	Cullen Quartzite
MOINIAN	
	Psammitic granulite, quartzites, pelitic schists

Analysis of 200 pebbles from the sheetflood deposits give the following results:

Vein Quartz	24 per cent
Metaquartzite	44 per cent
Psammitic Granulite	8 per cent
Feldspathic Psammitic Granulite	12 per cent
Chert	2 per cent

TABLE 4.1.

A PERCENTAGE COMPOSITION OF MIDDLE OLD RED SANDSTONE CONGLOMERATE PEBBLES (ELGIN MEMOIR, Page 33)

	a	b	c	d	e	f	g	h	i
Quartzite	87	65	68	82	76	78	62	70	77
Feldspathic flags/psammitic granulite	7	32	24	13	18	16	32	20	14
Micaceous flags and mica schist	-	-	6	1	-	1	5	-	4
Vein quartz	1	2	2	3	2	1	1	2	2
Granite	1	1	-	1	2	1	-	4	-
Microgranite	-	-	-	-	-	1	-	2	3
Feldspar porphyry	-	-	-	-	-	1	-	-	-
Andesite	-	-	-	-	-	1	-	1	-
Quartz porphyry	1	-	-	-	-	-	-	1	-
Limestone	-	-	-	-	2	-	-	-	-
Sandstone	3	-	-	-	-	-	-	-	-

B AVERAGE PERCENTAGE OF PEBBLE TYPES IN THE MIDDLE OLD RED SANDSTONE AND THE HOPEMAN SANDSTONE SHEETFLOOD DEPOSITS

	Middle Old Red Sandstone	Sheetfloods
Quartzites	74%	78%
Granulites	20%	20%
Others	6%	2%

From a preliminary study, it would appear that 98 per cent of the pebbles were derived from a metamorphic source area of Dalradian and Moinian. However, the chert can be equated with locally derived cornstones from just south of Elgin indicating that the Old Red Sandstones were more important than the pebble analyses suggest.

Table 4.1 illustrates that the composition of pebbles in the Middle Old Red Sandstone sandstones and conglomerates show a similar ratio of rock types to those of the sheetflood deposits of the Hopeman Sandstone. If the pebbles were derived directly from the Moinian and Dalradian strata, one would expect to find more evidence of such easily recognisable horizons as the Carnfield Actinolite Flags and the West Sands Mica Schists. However, if the pebbles were polycyclic in origin, only the harder quartzites and granulites would be preserved upon retransportation. It is the author's contention that the source area of the sheetflood deposits was dominantly Old Red Sandstone, the pebbles of Moinian and Dalradian being polycyclic in origin from the Old Red Sandstone sandstones and conglomerates. (Table 4.1.). The sandstones and silts probably disaggregate to form the constituent matrix of the sheetfloods. The source area is thought to have been within a few miles of Quarry Wood in a southerly direction.

PLAYA DEPOSITS

Playa lake deposits are exposed in the upper horizons of the H2 phase, 100 metres north of the site of the old Inverugie Castle (15507035, Fig. 4.3.). They overlie contorted beds of the H2 phase and are themselves overlain by barchan dune sandstones of the H3 phase. From their relationship to the underlying and overlying dune sandstones, it can be deduced that the playas of the Hopeman Sandstone were formed in the "sand sea". Although their outcrop is relatively small at the present day, evidence for their former presence over a wider area will be discussed in the following chapter under the section dealing with contorted beds. The contorted horizons are thought to be formed by the

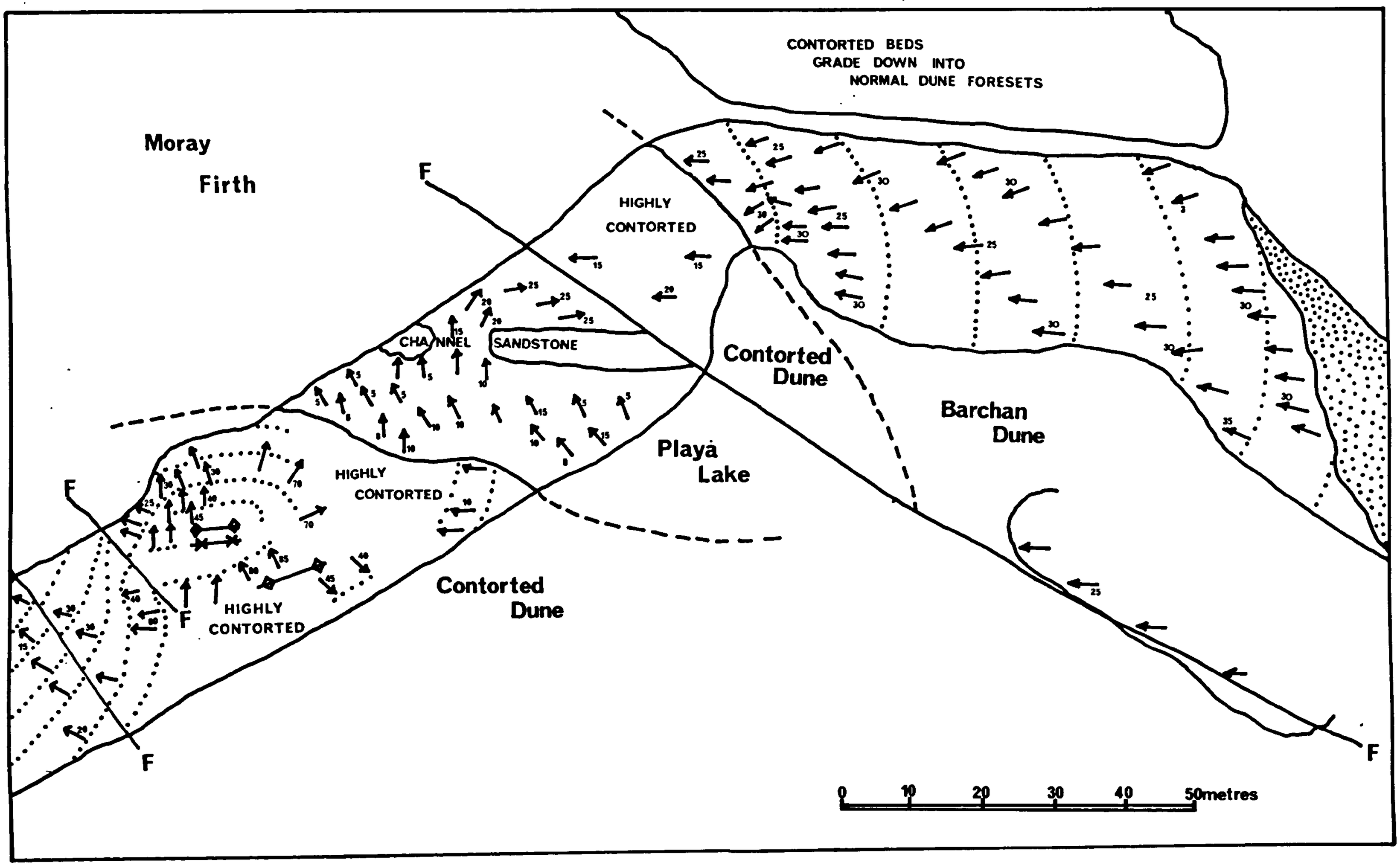

Fig. 4.3. H2 playa deposits at the site of the old Inverugie Castle(15507035).

saturation of dune sandstone by floodwater; thus, although there may be no waterlain deposits present now, contorted horizons signify their former presence.

Glennie (1970) recognises two main divisions of playa lake deposits:

(a) Inland playas - formed by floodwaters from the mountain source.

(b) Coastal playas - formed by marine flooding.

The playas of the Hopeman Sandstone are inland playas and appear to represent the end product of sheetflood deposition when the floodwaters reached the centre of the basin. Their formation appears to have been similar to those of the Djofra Graben, Libya (Glennie, 1970) where floodwaters are trapped by sand dune barriers and a playa lake is formed.

Although details of the sedimentary structures have not been described, knowledge of the environment of deposition has enabled a theoretical sequence of events to be postulated (Fig. 4.4.);

1. At the entrance to the playa, the sheetfloods are channelled between the dunes and scour down into the underlying dune sands. Where the waters are trapped in inter dune areas, the effective velocity of the floods is reduced to zero and plane laminated graded units are laid down.
2. As the floods are ephemeral in character, the playa gradually dries out forming ripple marked sandstones and silts. Renewed flooding will form another fining upward cycle from plane laminated beds to ripple marked sediments.

Table 4.2. shows 7·6 metres of H2 playa lake deposits which are exposed at the site of the old Inverugie Castle. Fig. 4.4. shows an idealised sequence of events which has been postulated to explain these deposits.

1. <u>Channel sandstones</u>

It is suggested that floodwaters were channelled between the dunes on the edges of the playa, until finally, the waters were dammed up in the inter dune areas. As the playa is formed in a sand sea, the centre of the playa migrates with the dunes and therefore channel deposits may overlie characteristic graded units formed in the centre of the playa.

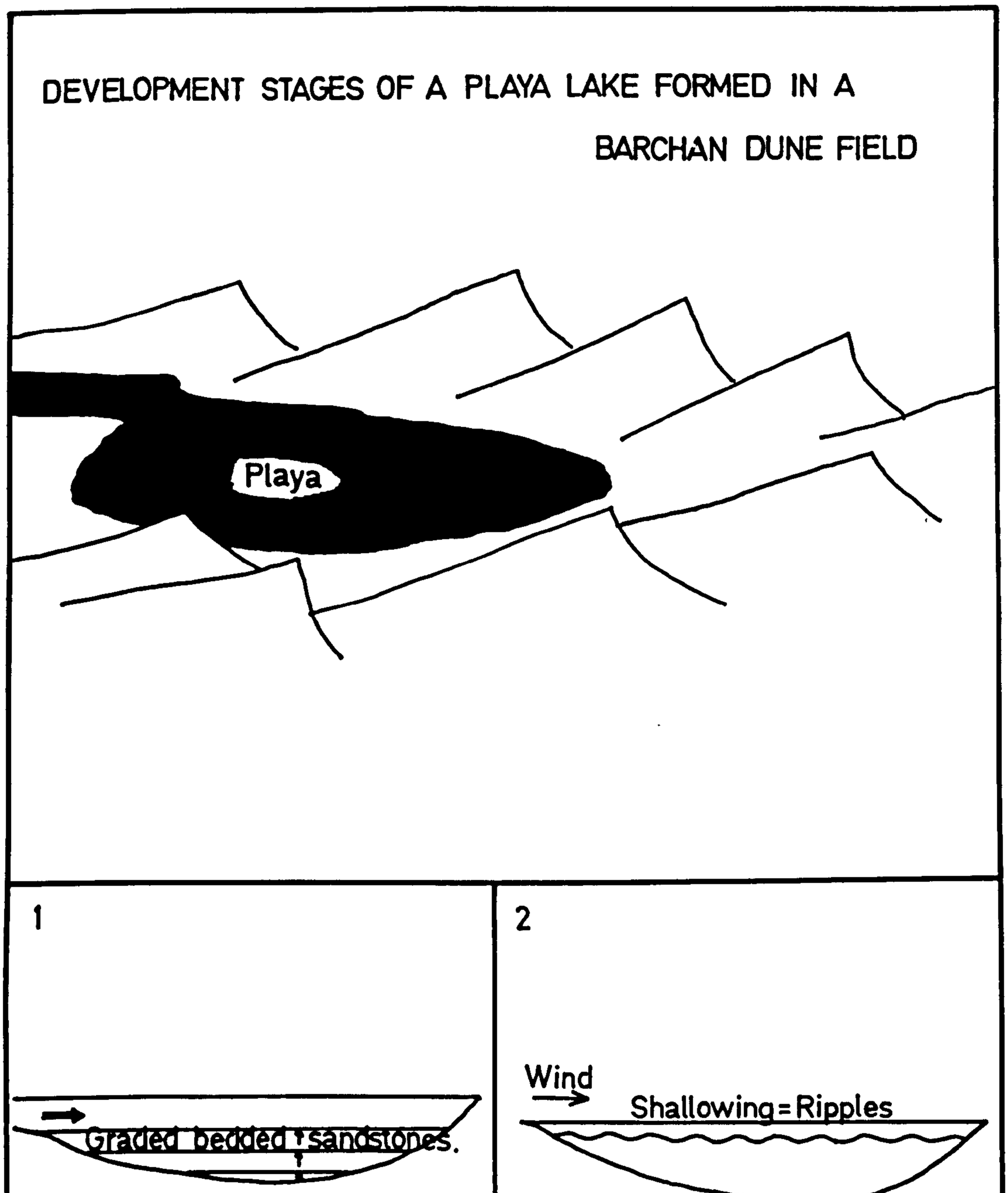

Fig. 4.4. Ideal sequence of the Hopeman Sandstone playa deposits.

University Library

TABLE 4.2.

PLAYA LAKE DEPOSITS AT THE SITE OF THE OLD INVERUGIE CASTLE (15507035)

Faulted contact with contorted beds of the H2 phase

2 metres	Channel sandstones cut down into finely laminated, fine to medium grained sandstone up to a maximum depth of 2 metres. Laminated sandstones are often graded bedded and may be ripple marked in the finer part of the graded bedded unit.
3 metres	Finely laminated bedded units varying from fine to medium grained sandstones. Evidence of ripple marks and halite pseudomorphs at the top of the graded units.
0·6 metres	Finely laminated graded units varying from grits to silty sandstones.
2 metres	Graded bedded units from pebbly sandstones to silty sandstones. Ripple marks and eroded ripple marks are present in the upper parts of the units.

Disconformity at the base at the contact with the underlying H2 contorted dune unit.

EXPLANATION OF PLATE 4.1.

HOPEMAN SANDSTONE WATERLAIN

A. Sheetflood deposits of the H1 phase unconformably overlying the Rosebrae Beds (Upper Old Red Sandstone) in an old quarry 400 metres north west of Laverockloch Farm(19$637).

B. Channel sandstone cutting down into plane laminated playa deposits at the site of the old Inverugie Castle (15507035). The channel is massively bedded although silt galls do appear at the base.

C. Ripple marked medium grained sandstones in the H2 playa deposits (15507035).



a



b

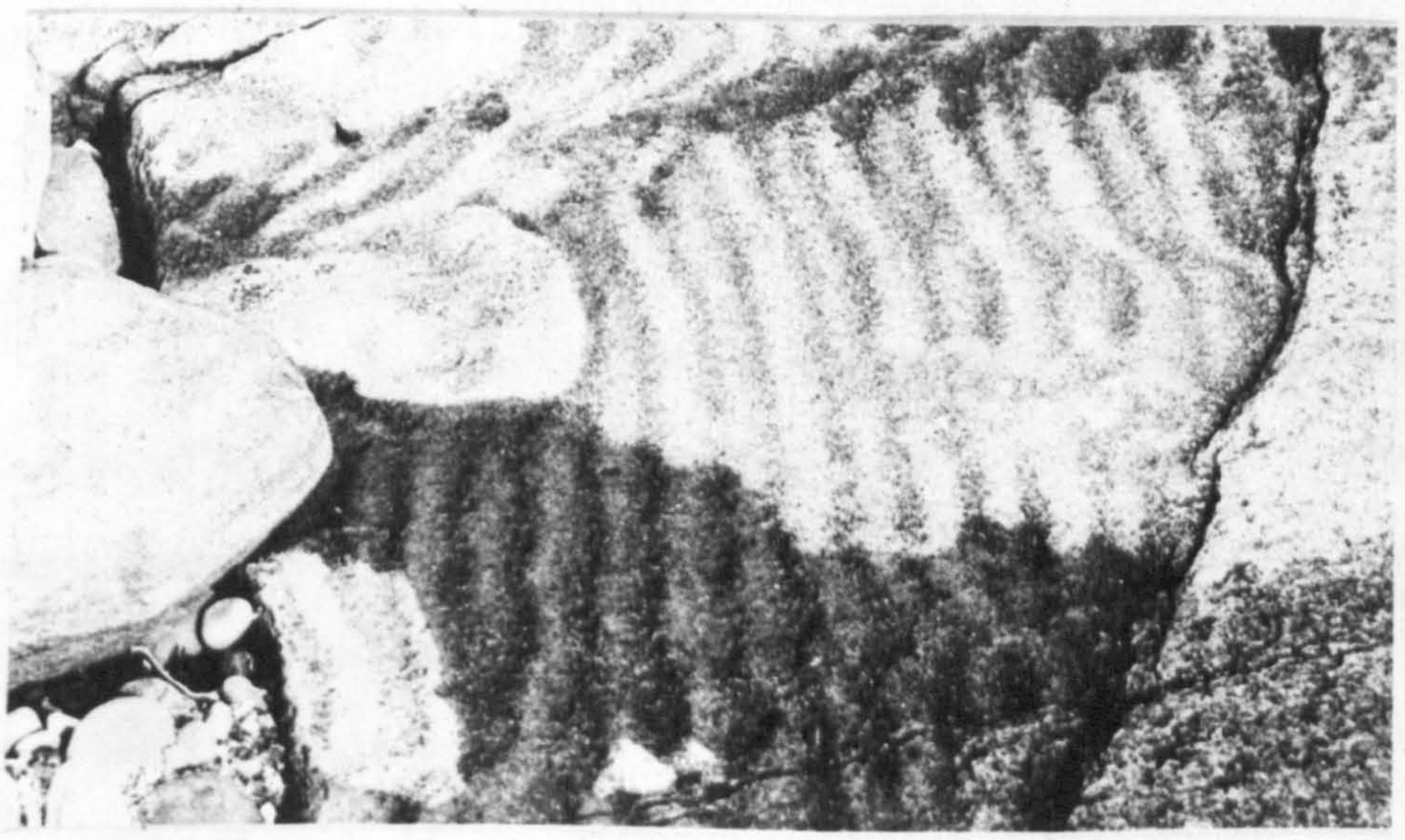

c

PLATE 4.1.

The channel is 3-4 metres in width, 2-3 metres in depth and can be traced laterally for 30 metres at the present day. The lithology of the sediments is similar to that found in the graded bedded units but grain size indicates that they are more poorly sorted. Plate 4.1B shows the channel cutting down into the plane laminated horizons. At the base of the channel, silt galls are common and may reach up to 100 mm in length and 10-20 mm in thickness. The channel appears to have eroded silts from the top most unit of the preceding dessication cycle. The channel shows an east to west current direction.

2. Graded bedded units

Graded bedded units represent the lowest unit of the cycle and are formed where the passage of floodwaters is barred by the dunes and a lake is formed. As the effective velocity of the water is zero, the coarsest material is deposited first producing graded bedding. The units are generally between 10-40 mm in thickness, each phase representing renewed flooding. Several graded units may be present without any evidence of ripple marked sandstones but this is probably due to their removal by deflation rather than non deposition. In some cases, the graded units can only be recognised in thin section. Comparison of the grain size of the playa deposits with those of the dune sandstones (see Chapter 6) suggests that the playa deposits were derived mainly from the dune sands. Thus, although the floodwaters probably brought in minor amounts of silt, sandstones and pebbles, the major proportion of the sediment appears be aeolian in origin explaining the absence of thick silts.

3. Ripple marked sandstones/silts

The graded bedded units are thought to have been deposited when the playa was relatively deep. As evaporation and groundwater drainage occurred, shallow water sedimentation became established as evidenced by the presence of ripple marks. The ripples are thought to have been formed by the wind acting on the surface of the shallow playa, the ripples being a reflection of the prevailing north east wind of the Hopeman Sandstone. This is substantiated by south east to north west orientation of the crests of the ripples and their assymetry towards the south west. Interference ripples are seen in some cases

but are not common. The wavelength of the ripples is generally between 40-60 mm. Plate 4.2C illustrates the ripples.

4. Complete dessication

Evidence of complete dessication is rarely seen, but when it occurs, it is characterised by fine grained sandstone and silts, sometimes with evidence of halite pseudomorphs. No evidence of mud cracks is seen but their former presence is postulated. It is clear that this horizon is rarely preserved owing to the removal of the fine sediment by deflation upon complete dessication.

CHAPTER 5

HOPEMAN SANDSTONE - AEOLIAN FACIES

Aeolian sandstones predominate in the Hopeman Sandstone, the waterlain horizons representing less than 5 per cent of the sandstones. Both seif dunes and barchan dunes have been recognised. The seif dunes are present in the H1 phase and are laterally equivalent to the sheetfloods deposits seen inland at Quarry Wood. It is thought that the seif dunes were formed on the edges of the sand sea nearest to the mountain source (Fig. 5.1.). Barchan dunes are the dominant type of dunes present in the Hopeman Sandstone; they occur in the H2-4 phases on the coast and the H2 phase inland. Contorted horizons occur both in the barchan dunes and the seif dune phases.

Differentiation of the seif dunes and barchan dunes was based on work on modern dunes published by McKee and Tibbitts (1964) and McKee (1966). McKee (1966), following initial work by Bagnold (1954), was able to show that different types of dunes could be recognised purely by studying their internal structure. Thus, by detailed study of the foresets, various dune types found in fossil aeolian deposits could be recognised. McKee and Tibbits (1964) showed that seif dunes were characterised by bidirectional foresets which were at right angles to the axis of the dune, which in turn, runs parallel to the mean wind direction. The foresets are therefore at right angles to the mean wind direction. McKee (1966) showed that the large scale foresets found in barchan dunes were the result of migration of the slipface of the dune in a lee-ward direction. Foresets in fossil dunes of the barchan type should therefore show unidirectional foresets reflecting the characteristic leeward dipping curved slipface of the barchan dune. Fig. 5.7. shows the foreset analyses of the Hopeman Sandstone and the characteristic foreset patterns of both seif and barchan dunes.

SEIF DUNES

A seif dune of the H1 phase is exposed along the foreshore between Covesea Skerries Lighthouse (204704) and the Gordonstoun Lookout Post (175707).

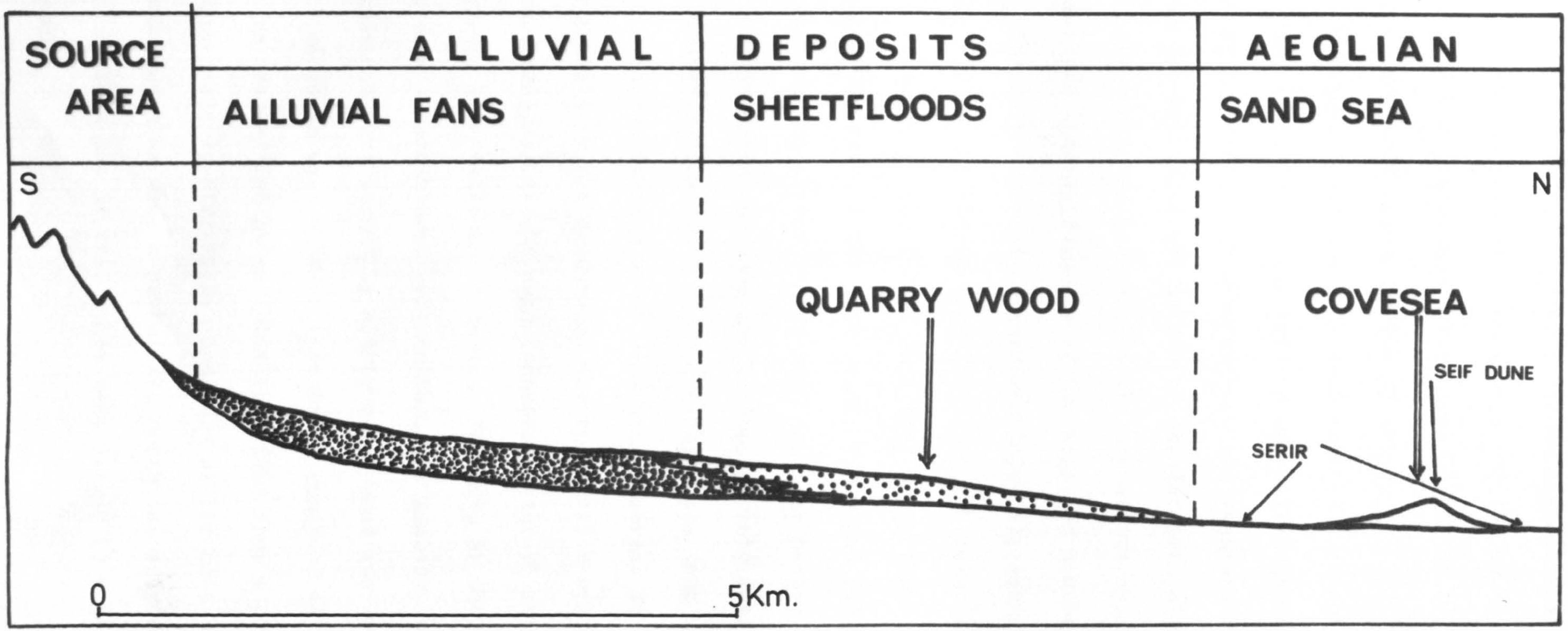

Fig. 5.1. Reconstruction of the Elgin district during the H1 phase.

At Covesea Skerries Lighthouse, the foresets of the seif dune are extremely contorted but the northerly dipping foresets suggest that they represent the northerly limb of the seif dune seen further to the west. The absence of the characteristic south westerly dipping foresets of the H2 barchan dunes in the area preclude that they belong to the H2 phase.

However, between Gordonstoun Lookout Post and the bay east of Covesea village (Fig. 5.3.), the axis of the seif dune runs almost parallel to the coast. At low tide, both the northern and southern limbs of the dune are seen showing the bidirectional nature of the foresets at right angles to the dune axis. The contorted horizons at the top of the seif dune are overlain by the planar and tabular foresets of the basal H2 barchan dune.

The seif dunes at Covesea are laterally equivalent to the sheetflood deposits seen inland at Quarry Wood (Fig. 5.1.). This relationship appears to be a fossil analogue of the Zallaf Sand Sea, Libya (McKee and Tibbitts, 1964). Discussing the position of the seif dunes, McKee and Tibbits note that bordering the south east margin of the Zallaf Sand Sea near Sebhah, is an extensive serir or gravel covered plain which merges southwards into fans of the rocky plateau area. The gravel surface then changes within less than a mile to one of pure sand.

At Sebhah, strong south east winds prevail in the morning while north east winds prevail in the afternoon; the result is a seif dune with an east-west orientation. Analysis of the dune foresets of the H1 seif dunes yields a rose diagram showing bidirectional foresets. The axis of the seif dune has an east-north-east to west-south-west orientation. By analogy, the seif dunes of the Hopeman Sandstone were formed by either north east and south east winds, or north west and south west winds. Palaeowind analyses of other Permo-Triassic localities in the British Isles (Shotton, 1956) show a prevailing wind from an east to north easterly direction. Analysis of the H2-4 barchan phases of the Hopeman Sandstone also show a prevailing north easterly direction. It is therefore concluded that the H1 seif dunes were formed by north east and south easterly winds.

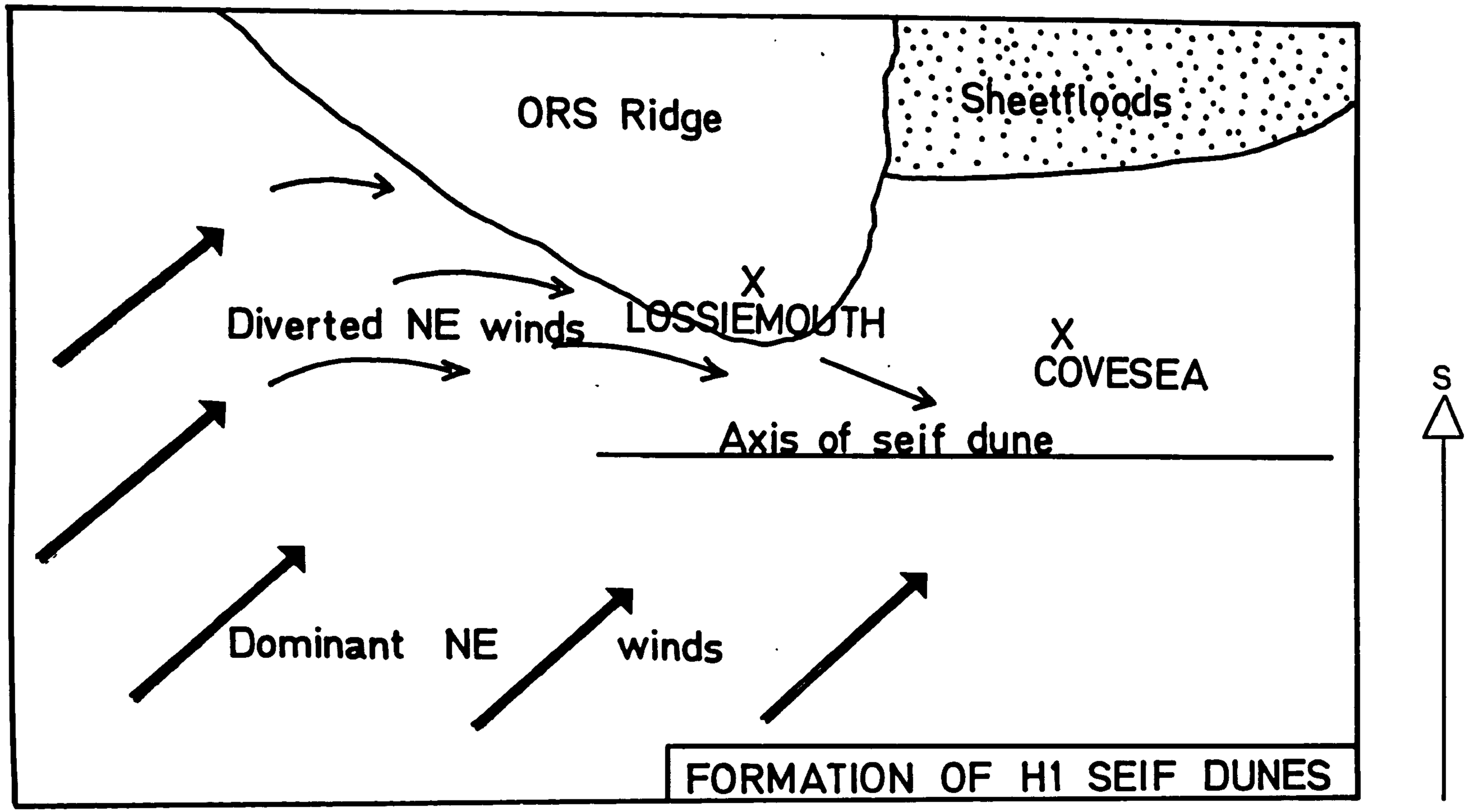

Fig. 5.2. Formation of the H1 phase seif dune

The north east wind is present as the dominant wind throughout Hopeman Sandstone times. The problem is then, to account for the presence of the south east wind in the H1 phase and its subsequent absence in the succeeding phases of dune formation. The proximity of the mountain source during H1 times and its subsequent recession in later formations provides the most logical reason for the presence of the south east wind. It may be interpreted as a local valley wind, but an alternative explanation is the diversion of the dominant north east wind by a ridge in the Lossiemouth area. (Fig. 5.2,).

Evidence for a ridge in the Lossiemouth area is seen both in Hopeman Sandstone times and also during the deposition of the Sago Pudding Sandstone. To the west, at Clarkly Hill, the total thickness of the Hopeman Sandstone is over 60 metres; this thins rapidly to the east until at Lossiemouth, the Hopeman Sandstone is completely absent. It is therefore suggested that this ridge diverted the main north east winds producing an eddying effect and a resultant subsiduary east to south east wind. (Fig. 5.2.). Erosion of the ridge during succeeding phases explains the later absence of the south east winds.

Glennie (1970) suggest that seif dunes are formed by unidirectional winds of high velocity and barchan dunes by winds of lower velocity. This may be the case in the large seif sand seas of Arabia and Australia but, in many cases, seif dunes are confined to narrow areas close to the mountain source in a dominantly barchan dune field. As in the case of the Hopeman Sandstone, these seif dunes appear to be linked to their proximity to the mountain source rather than the wind velocity.

Folk (1970) also suggests that seif dunes do not form by the "two wind" mechanism but, instead, form through the activity of paired helical vortices with horizontal axes (Bagnold, 1953) which trend parallel with the great geostrophic wind systems, specifically the trade winds. This theory adequately explains the large areas of seif dunes in the Australian and Arabian deserts but not the isolated seif dunes in dominantly barchan dune fields e.g. Libya (Glennie, 1970). It is suggested that a two wind interference system can produce the paired helical

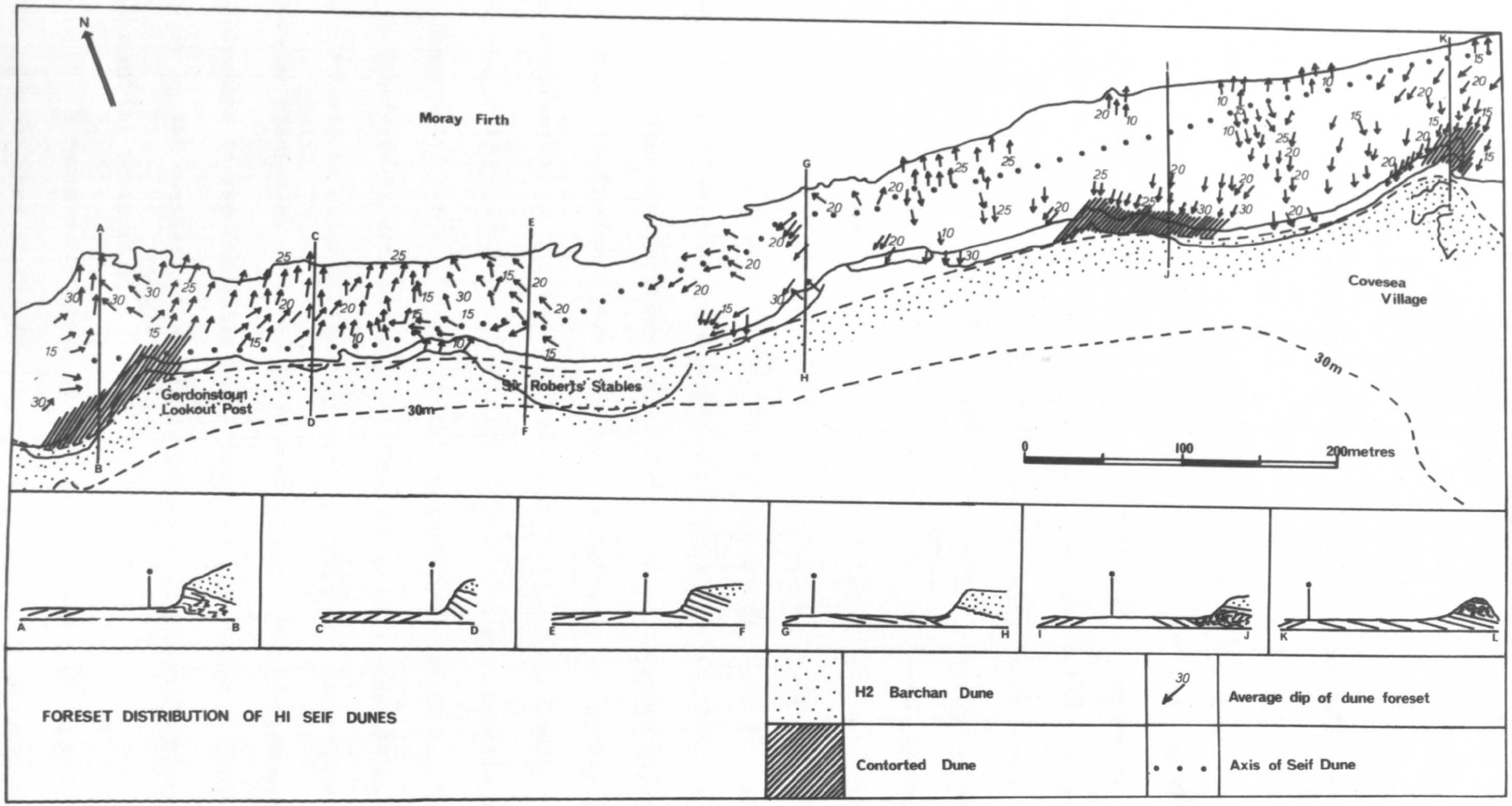

Fig. 5.3. Distribution of the foresets in the H1 seif dune.

vortices with horizontal axes, thus explaining the frequent occurrence of seif dunes near to mountain sources.

Foreset analysis of the seif dune of the H1 phase results in a bidirectional rose diagram trending at right angles to the axis of the dune. The east west orientation of the foreshore between Gordonstoun Lookout Post and the bay east of Covesea village exposes the axis of the seif dune almost parallel to the coastline. The crest and the base of the dune are not exposed but the axial parts of the dune can readily be differentiated from the peripheral zones.

The axis of the seif dune (Fig. 5.3) runs east-north-east to west-south-west. In parts there is an arcuate form to the axis, this being interpreted as seif dunes with barchanoid slipfaces as illustrated by Glennie (1970, p. 94). This interpretation is supported by the presence of complimentary arcuate foresets in the southern limb of the dune. There is evidence for termination of the seif dune at Gordonstoun Lookout Post where the normal north-south dipping foresets are replaced by east-west dipping foresets. Near to the axis of the dune, foresets dip both north and south at high angles. The dip of the foresets is generally greater than 20 degrees and is often 30 degrees. Bounding surfaces also dip at high angles, generally between 15-20 degrees (Fig. 5.4).

Near the periphery of the dune, low angle cross-strata dipping at between 5 and 10 degrees are more common. Some foresets may dip gently in the opposite direction to the main direction; their dip is generally less than 5 degrees. Asymmetrical scours are also present. Some foresets may reach 25-30 degrees but these are rare on the periphery of the dune. Bounding surfaces between the foresets are also gentler than those seen near the axis of the dune. Contorted horizons occur on the edges of the dunes and are probably due to the flood-water channelled into the inter dune areas. Their relevance is discussed with reference to the contorted dunes later in the chapter. Contorted dunes are only seen on the southerly limb of the dune but this may be due to the limited exposure of the northern limb.

A maximum thickness of 15 metres of the seif dunes is exposed at the present day; the base of the dune is not seen but it is thought to rest

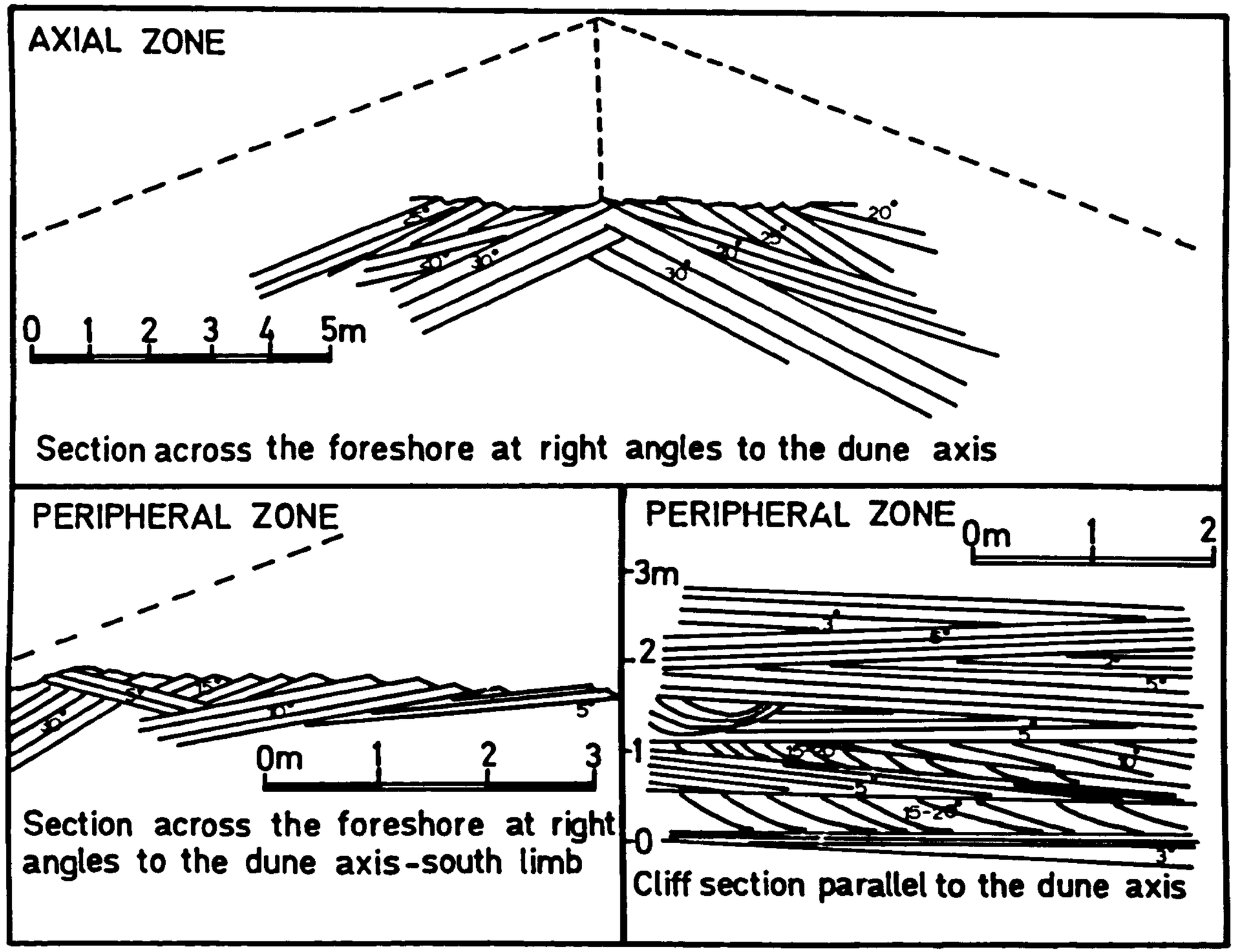

Fig. 5.4. Internal structures of the H1 seif dune at Covesea.

unconformably on the Old Red Sandstone a few metres below the foreshore. It is suggested that the original seif dunes were probably between 25-30 metres in height. No evidence for inter dune areas is seen at the present day owing to the limited outcrop of the H1 phase.

BARCHAN DUNES

Barchan dunes occur in the inland exposures of the H2 phase and the H2-4 phases on the coast. Inland they rest directly on the sheetflood deposits of the H1 phase whilst on the coast they rest on the seif dunes of the H1 phase.

The easternmost exposure of the H2 phase at Quarry Wood is seen at the old quarry, 400 metres north west of Laverockloch Farm (193637). A thickness of 10 metres of barchan sandstones overlie the sheetfloods of the H1 phase. The westerly face of the quarry shows a vertical section of gently dipping to almost horizontal dune foresets. In the northerly face, the foresets dip towards the west at 15-20 degrees.

Individual laminae of the foresets are well sorted although the laminae possess a variation in grain size from fine to coarse sandstones. Pebbles up to 10 mm in diameter are seen in some of the coarser laminae and tend to be more common towards the junction with the sheetflood deposits. The mean grain size of the barchan dunes at this locality is much coarser than those seen on the coast suggesting they they have been derived directly from the underlying sheetflood deposits. The fine material would have been removed in suspension.

Although most of the foresets are dipping to the west, some dip gently in an easterly direction. This denotes the relative instability at the base of the dune rather than a change in wind direction.

Dunes of the H2 phase are again seen at the Old Millstone Quarry where they again overlie sheetflood deposits. There is no clear contact with the sheetflood deposits but a gradation up into the large scale dune foresets. This reflects the reworking of the sheetfloods by the wind. Pebbles are again common at the base of the dunes but die out within a few metres of the sheetflood

deposits. Although most of the Old Millstone Quarry is now overgrown, the contact with the H1 phase is well seen in the northern face of the quarry, Exposures of the basal parts of the dunes are also seen in the eastern and southern faces of the quarry.

Analysis of the foreset directions also reflects the basal nature of the barchan dunes at Quarry Wood. Fig. 5.5. shows that there is no preferred orientation of the foresets although minor nodes occur at 270, 230 and 150 degrees. This represents preservation of the windward foresets as well as the leeward foresets, a feature characteristic of the basal dune. This interpretation is substantiated by the coarse nature and the relatively poor sorting coefficient of this horizon.

Dune sandstones are again exposed on the summit of Quarry Wood Hill where they show large scale cross bedded units, the foresets dipping towards the south west. An old quarry (18326355), 100 metres south west of the summit of Quarry Wood Hill shows a maximum of 10 metres of dune bedded sandstones. This quarry shows dune foresets of the middle horizons of the barchan dune, Fig. 5.5. illustrates the foresets dipping uniformly in a south westerly direction compared to the poorly orientated basal parts of the dune.
The laminae are still relatively coarse but only isolated pebbles are present compared to the basal parts of the dune exposed at the Old Millstone Quarry.

Dune sandstones of the H2 phase are also exposed in the southern face of York Tower Quarry. Although the contact with the underlying H1 phase is seen, the basal parts of the dune are not present; the foresets dip uniformly in a west south westerly direction representing the middle unit of the barchan dune. The area therefore is a surface on to which the barchan dunes migrated as there is no evidence of the basal parts of the dunes ever being present.

On the coast, barchan dunes outcrop in the cliffs and along the foreshore between Gordonstoun Lookout Post (176708) and Masonshaugh Quarries (126692). Several quarries also expose the barchan dunes along the coast (Fig. 5.6.).

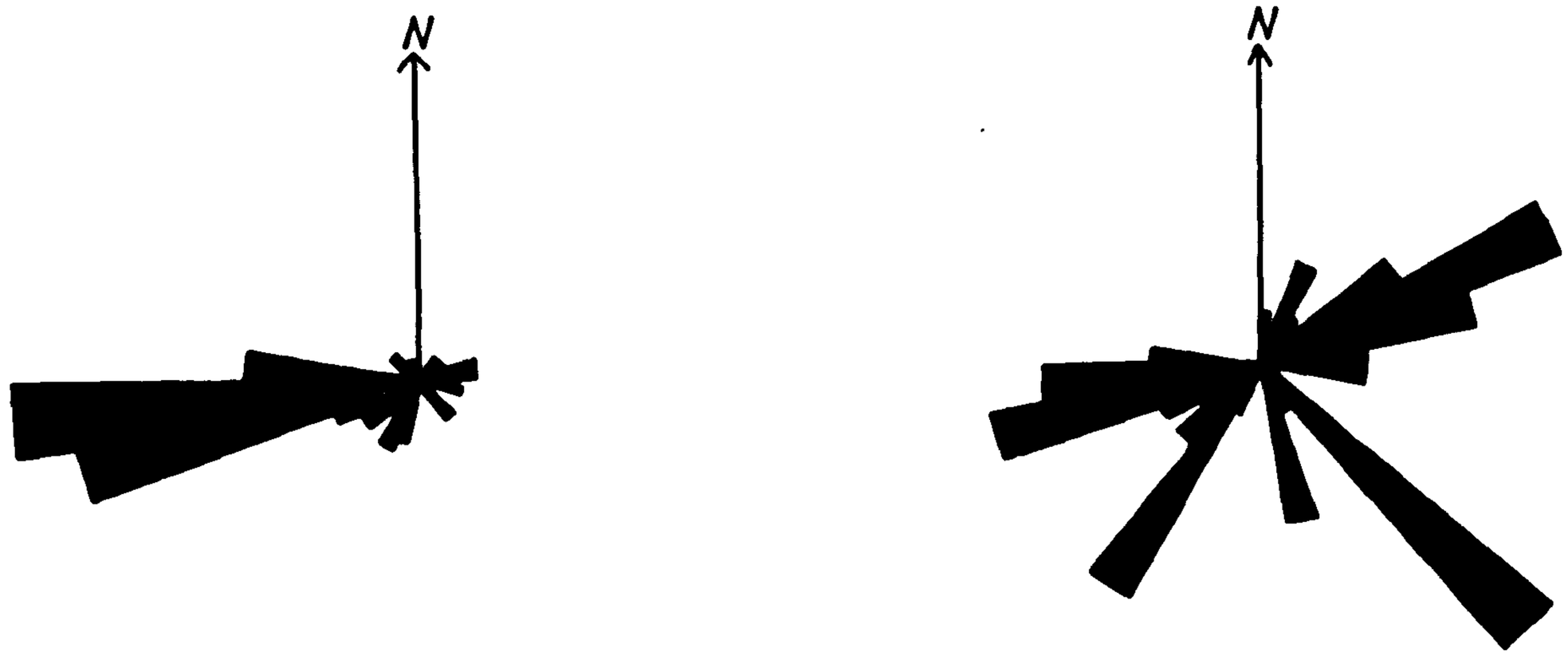

Middle and upper dune *Lower dune*

Foreset analysis Quarry Wood

Fig. 5.5. Differentiation of the lower and middle H2 barchan dune phase at Quarry Wood.

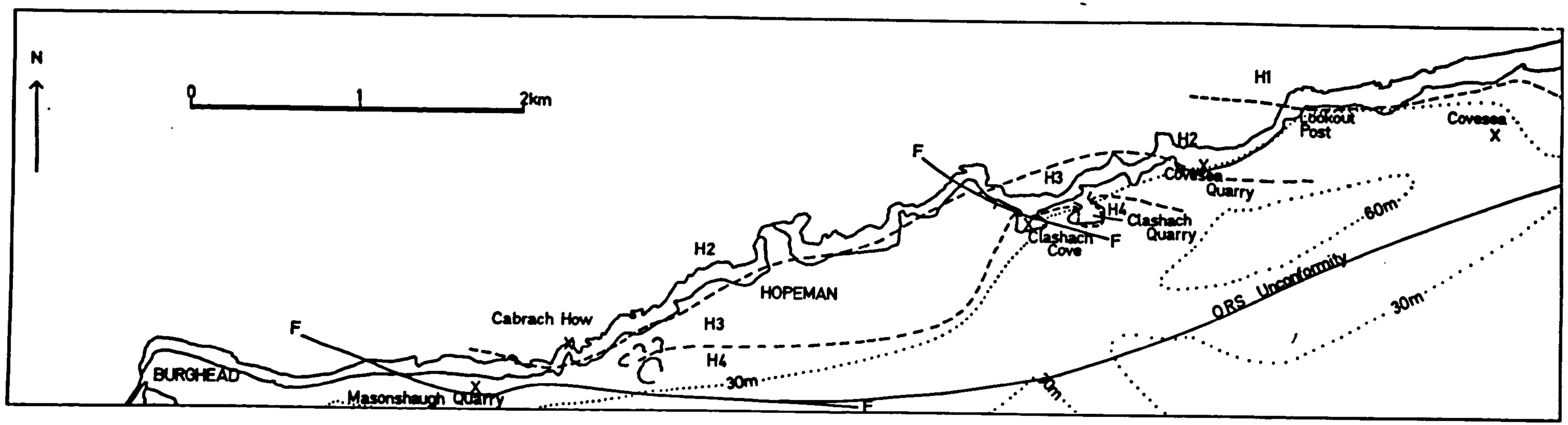

Fig. 5.6. Distribution of the four phases of the Hopeman Sandstone.

In the cliffs below Gordonstoun Lookout Post, low angle tabular planar and planar foresets, representing the basal horizon of the H2 phase, overlie the contorted horizons at the top of the H1 phase. The basal horizon of the H2 phase is undisturbed showing the intra-formational character of the contorted horizons below.

Westwards along the cliff section, up to 30 metres of large scale cross bedded sandstones are exposed in the cliffs and along the foreshore 800 metres to the west, the cliffs north of Covesea Quarry show the H2/3 contact. The cross bedded units vary in thickness between 20-30 metres and clearly depict the middle portions of the H2 barchan dune. The angle of foreset dip varies between 10-30 degrees, the value being highest at the top of the cliffs and steadily decreasing towards the base. The foresets are cut by high angled bounding surfaces varying from 30 degrees at the top to 15 degrees at the base. Four major bounding surfaces are present along the 800 metres of coastline; these are thought to represent the erosional surfaces between separate dunes. Minor bounding surfaces are also present but these are only a few metres in length and illustrate erosional surfaces within dunes.

The cliffs north of Covesea Quarry (16907035) expose large scale foresets grading up into contorted beds. A continuation of the lower horizons in the foreshore shows the characteristic curved slipface of the barchan dune (Plate 5.2B.). The barchan dune sandstones grade up into 15 metres of contorted beds representing disturbed barchan dune foresets. The bay to the west of this locality shows the equivalent horizon to the contorted beds to be undisturbed. A bounding surface just above this horizon represents the boundary between the H2 and H3 phases at this point. The basal unit of the H3 phase is not seen at this locality indicating that the slipface of the barchan dune migrated on to this horizon.

Along the foreshore between the H2/H3 contact (16707049) west of Covesea Quarry and Clashach Cove (16007014), large scale cross bedding of the middle dune unit of the H3 phase is present. In the cliff section (16327027) to the north east of Clashach Quarry, high angle tabular planar and planar foresets of the upper unit of H3 are seen. At 16387024, this horizon is overlain by coarse grained low angle planar foresets of the basal unit of the H4 phase. A similar contact is again seen from Clashach Cove (16007014) to north west of Clashach Quarry. (16187014).

In Clashach Quarry, the main face of the quarry shows the development of 20 metres of large scale cross bedding of the H3 phase. Reptilian footprints seen on the leeward dipping foresets in the eastern part of the quarry are of H3 age. At the top of the quarry 5 metres of large scale cross bedded

sandstones of the middle unit of the H4 phase rest on the H3 phase. An erosion surface separates the two phases; H3 cross bedding generally dips to the south west whilst those of the H4 dip to the north west and probably represent the "wings" of the succeeding barchan dune phase.

Dune sandstones of the H3 phase outcrop along the cliffs and the foreshore from Clashach Cove to a point just north of the site of Inverugie Castle. (15707027). Here the beds of the H3 phase are underlain by the contorted beds at the top of the H2 phase.

At Clashach Cove (159701), a fault displaces the beds to the south by 3-4 metres. The easterly face of the cove exposes dune sandstones of the H4 phase and the westerly beach exposes sandstones of the H3 phase. The fault is continued to the north west where it can be seen on the foreshore at 155703. It is also seen in a small disused quarry 20 metres to the south of this point. At 155703, the playa lake deposits of the H2 phase are faulted against the contorted beds of the H2 phase.

Dune sandstones of the H2 phase outcrop along the foreshore between the playa deposits at (155703) and Cabrach Well (133692). Only the upper horizons are seen, these being represented by contorted bedding and basin and dome structures. Some undisturbed bedding is present at Hopeman Harbour.

Sandstones of the basal H4 unit and part of the H3 dune sandstones outcrop in the post glacial cliffs to the east of Hopeman. At Roddoch Wells, the contorted beds mark the upper limit of the H2 sandstones; they are overlain by planar and tabular basal sandstone foresets of the H3 phase. West of the H2-H3 contact at Roddoch Wells (131692) to the foreshore north of Masonshaugh Quarry, large scale foreset cross bedding represents the dunes of the H3 phase. At this point (121693), the Hopeman Sandstones are faulted against the Burghead Beds to the west.

At Greenbrae Quarry, the main working face consists of well defined dune bedding of the H4 phase; reptilian footprints are again seen at this locality. A small disused part of the quarry (13836934) marks the boundary between the H3 and H4 phases where massive contorted beds are overlain by low angle planar beds of the basal H4 unit.

The Hopeman Sandstone is also exposed in a few old quarries on Covesea Hill (182705). These resemble the dune sandstones at Greenbrae Quarry but their exact position cannot be defined accurately. An infilled quarry 350 metres north east of Burnside (169697) was noted in the Elgin Memoir (p.61) but has since become overgrown. The presence of thinly bedded sandstones and weathered out clay galls may represent the playa lake deposits of the H2 phase.

In the Clarkly Hill Borehole up to 60-70 metres of Hopeman Sandstone are present. The H1 phase of sheet-flood deposits occupies the lowest metre of the New Red Sandstone. Horizons of slumped bedding at 132.0 metres and 105 metres are thought to represent the equivalent contorted horizons of H1 and H2 seen on the coast. Thus the H3 and H4 phases would be represented by 32·5 metres and the H2 phase by 26·5 metres of dune bedded sandstones.

The thickness of each phase is clearly highly variable as the H2 phase reaches up to 30-35 metres in thickness on the coast. The following values are thought to represent the approximate thickness of each phase.

H4 25 metres

H3 30 metres

H2 35 metres

H1 4 metres (sheetfloods) and 25 metres (seif dunes)

Thus the maximum thickness of the Hopeman sandstone is probably about 120 metres but at any one point it is probably nearer to 60-70 metres and may be completely absent, as at Lossiemouth.

Foreset analysis

Comparison of dune foresets with those of modern barchan dunes is based on the work of McKee (1966). However it must be remembered when comparing fossil dune forests with those of recent dunes that the windward foresets are seldom preserved in fossil dunes. The leeward foresets are invariably preserved and measurement of these foresets show the characteristic curved slipfaces of the barchan dunes in an arc of 60-90 degrees. Although the slipfaces of modern barchan dunes often show an arc of the slipface of as much as 120 degrees, in fossil dunes the "wings" of the dunes are normally eroded and thus not preserved. Measurements of the direction of the foresets substantiates the view that the dunes were formed by unidirectional winds to form barchan dunes; these winds vary between east-north easterly and north easterly.

Studies of the types of the foresets enable three main units to be differentiated: i.e. upper, middle and lower.

(a) Lower

The lower parts of the dune may be recognised by their unconformable relationship to the underlying horizons; however, they may also be recognised by their sedimentary structures and their grain size characteristics (Chapter 6). The early stages of dune formation are here defined as the lower dune unit. In some areas where the early stages are not present, the middle dune unit may rest directly on the underlying horizon.

Plate 5·1A shows the characteristic foreset bedding of the lower dune unit. As can be seen in Fig. 5.5 the lower dune unit does not reflect the unidirectional foresets seen higher up in the dune. They reflect the relative instability of the foresets at the beginning of dune formation.

Windward dipping foresets may occasionally comprise up to 50 per cent of the foresets present but are generally between 10 to 20 per cent. They usually dip at angles of less than 5 degrees but may reach up to 10 degrees. Tabular planar sets are dominant, with rare wedge planar (as defined by McKee, 1966, p. 56). The lower dune unit seldom attains a thickness of more than 5 metres.

Leeward dipping foresets are more common and begin to show the formation of the characteristic avalanche slip faces; these are represented by foresets dipping at angles between 25-30 degrees.

In sections parallel to the dominant wind direction, the foresets dip at 25-30 degrees but thinner sets of cross strata may dip at 5-15 degrees. Wedge planar foresets are commonly up to 2-3 metres in thickness but tabular planar foresets seldom exceed 2 metres. Asymmetrical scours are present, but not common.

In sections at right angles to the dominant wind direction, the foresets are more tabular planar in nature. The dips are gentler and bounding surfaces are generally less than 10 degrees and often horizontal. Small scour structures are more common in this section.

Individual laminae are well sorted but in general the lower dune unit reflects a coarser grain size than the overlying units. Standard deviation is also high. Evidence in the succeeding section on the contorted dunes suggests that these grain size characteristics are sometimes due to reworking of playa lake deposits.

(b) Middle

The middle dune units reflect the unidirectional nature of the dominant wind and are in essence the preserved leeward slipfaces of the barchan dunes. The slipfaces of the dunes are often seen in plan view on the foreshore. Directional analysis of the foresets show a spread through an arc of up to 90 degrees, symmetrical about the mean and representing the preserved slipfaces of the dunes.

Fig. 5·7 shows the foreset readings measured from the middle dune unit. Measurements from the lower dune unit are not included in the results as their analyses do not reflect the true dominant wind direction. Numerous readings of foreset directions were measured at several localities from each phase, rendering the results statistically valid.

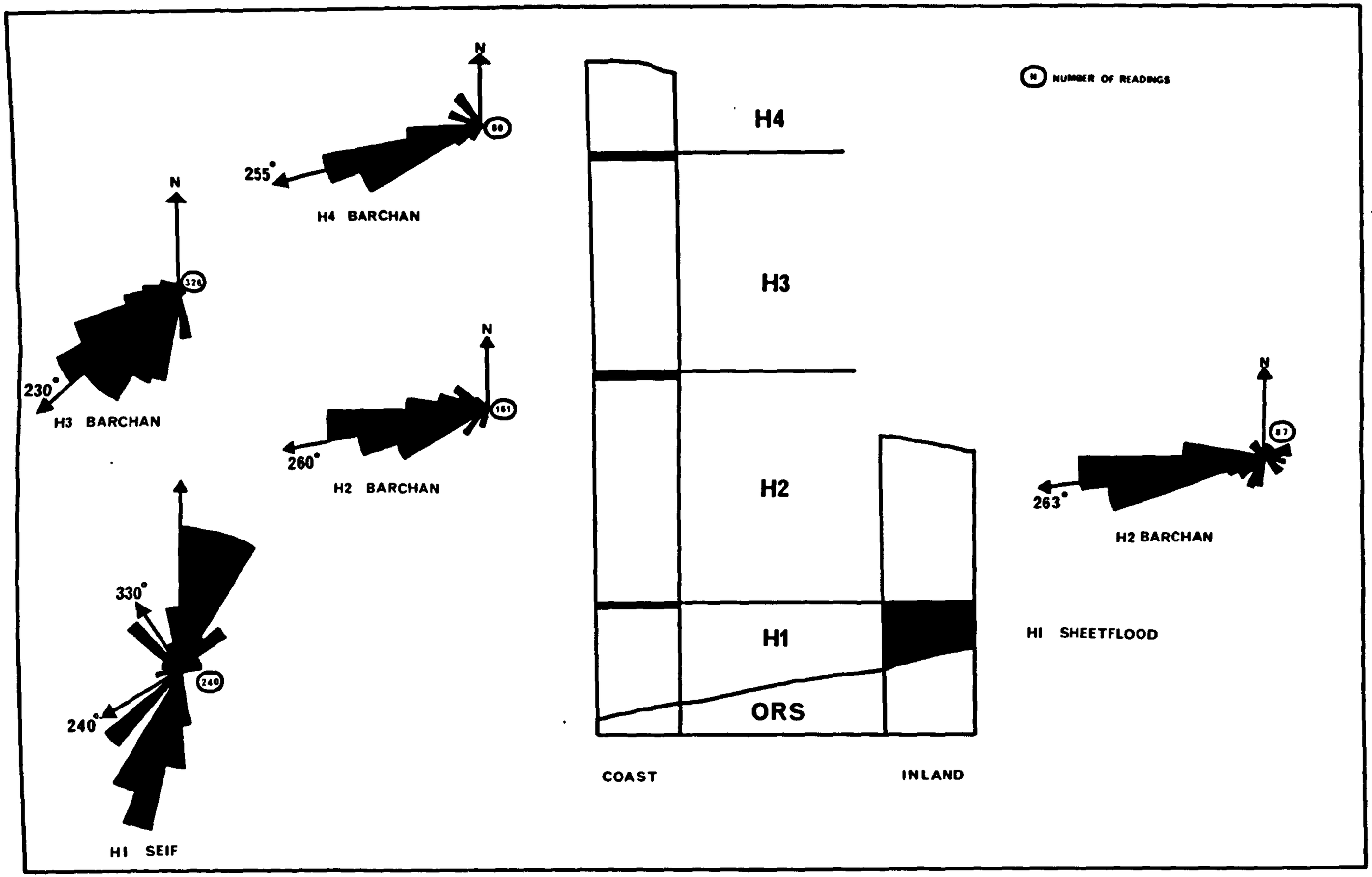

Fig. 5.7. Foreset analysis of the Hopeman Sandstone.

Measurements from the H2 phase on the coast give a mean wind direction from the east north east; similar measurements from the H2 barchan dunes inland give a remarkably similar reading and again suggest that the dominant wind was from the east north east. Figs. 5·5, 5·7, 5·8.

Measurements from the H3 phase (Fig. 5·9) show a mean direction from a north easterly direction. Although only 30 degrees difference exists between the mean of the H2 and H3 phases, this difference is remarkably uniform at all localities. The H4 phase is again more easterly in direction but a minor direction from the south east is present at many localities (Fig. 5·10).

Thus, throughout Hopeman Sandstone times, the dominant wind direction was from a north east to east north easterly direction. It may be argued that the results are statistically invalid as the expected 100-120 degrees arc of the slipface is here only represented by one of 70-80 degrees. However, the extra 40 degrees is represented by the wings of the barchan which are seldom preserved. The direction of dip of the foresets at the wings show greatest deviation from the mean dominant wind.

As the middle dune units are the preserved slipfaces of the dune, they should therefore indicate the maximum angles of the slipfaces. Large scale sets of foresets up to 30 metres in thickness have a maximum dip of approximately 30-35 degrees but this angle decreases to the base of the foreset to 20 degrees or less. They are cut by bounding surfaces which flatten towards the base. At the top they dip at 25-30 degrees decreasing towards the base to 15-20 degrees. The major bounding surfaces are thought to represent the contact between two dunes where a later dune has migrated over a previously formed dune. Minor asymmetrical scours and bounding surfaces occur within these larger units. The bounding surfaces are generally within 5 degrees of the foreset dip.

Grain size is uniform in individual laminae and sorting is good relative to that of the lower dune unit.

(c) <u>Upper</u>

The upper dune unit is seldom present owing to the erosion or the contorting of the unit prior to the deposition of the succeeding phase. The middle unit of the dune is often the highest unit of the barchan which is present.

In general, the foresets are similar to those of the lower dune but they can be clearly differentiated from them by their grain size. The upper unit is well sorted and has a grain size akin to that of the middle dune.

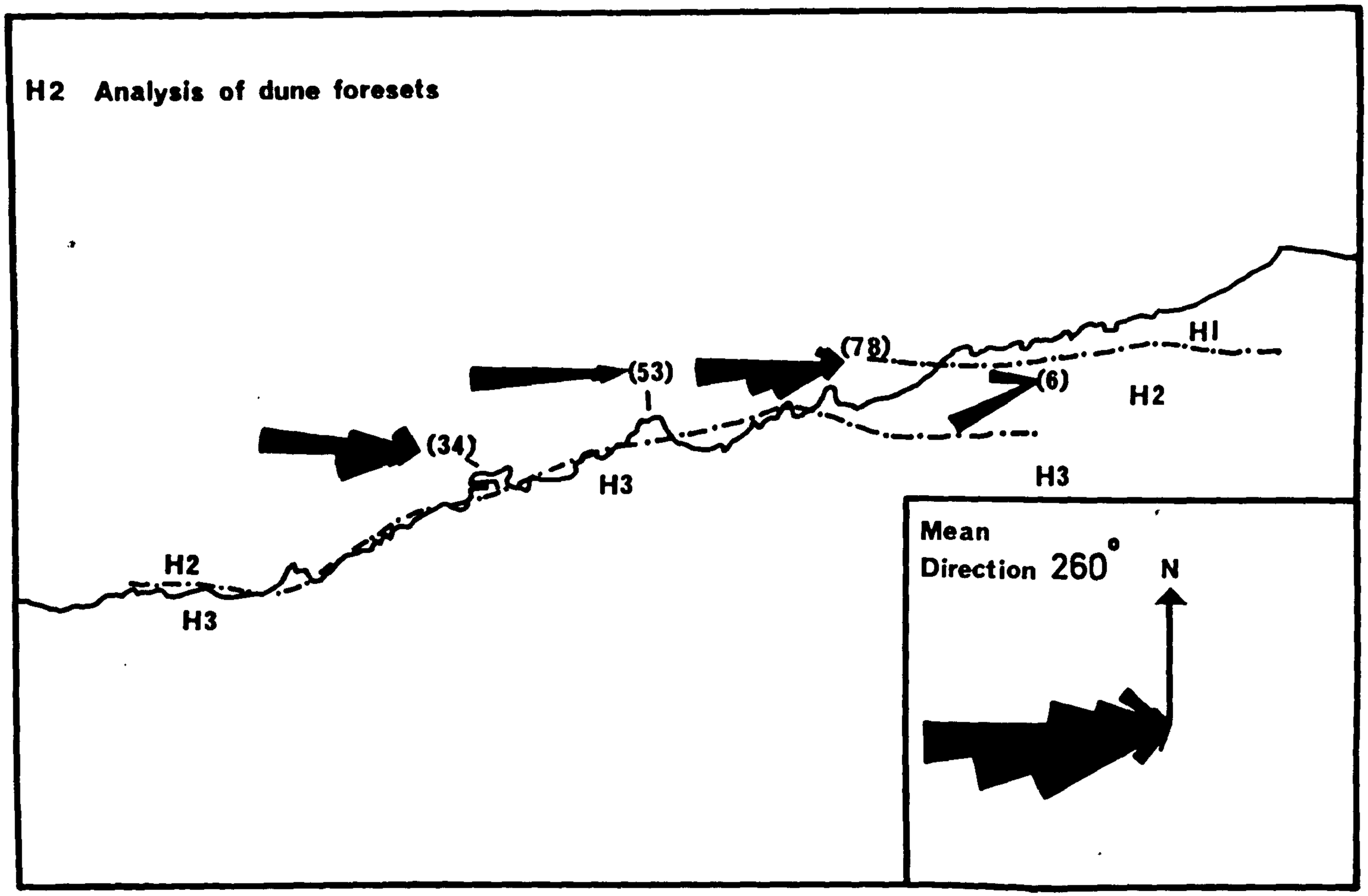

Fig. 5.8. Foreset analysis of the H2 phase.

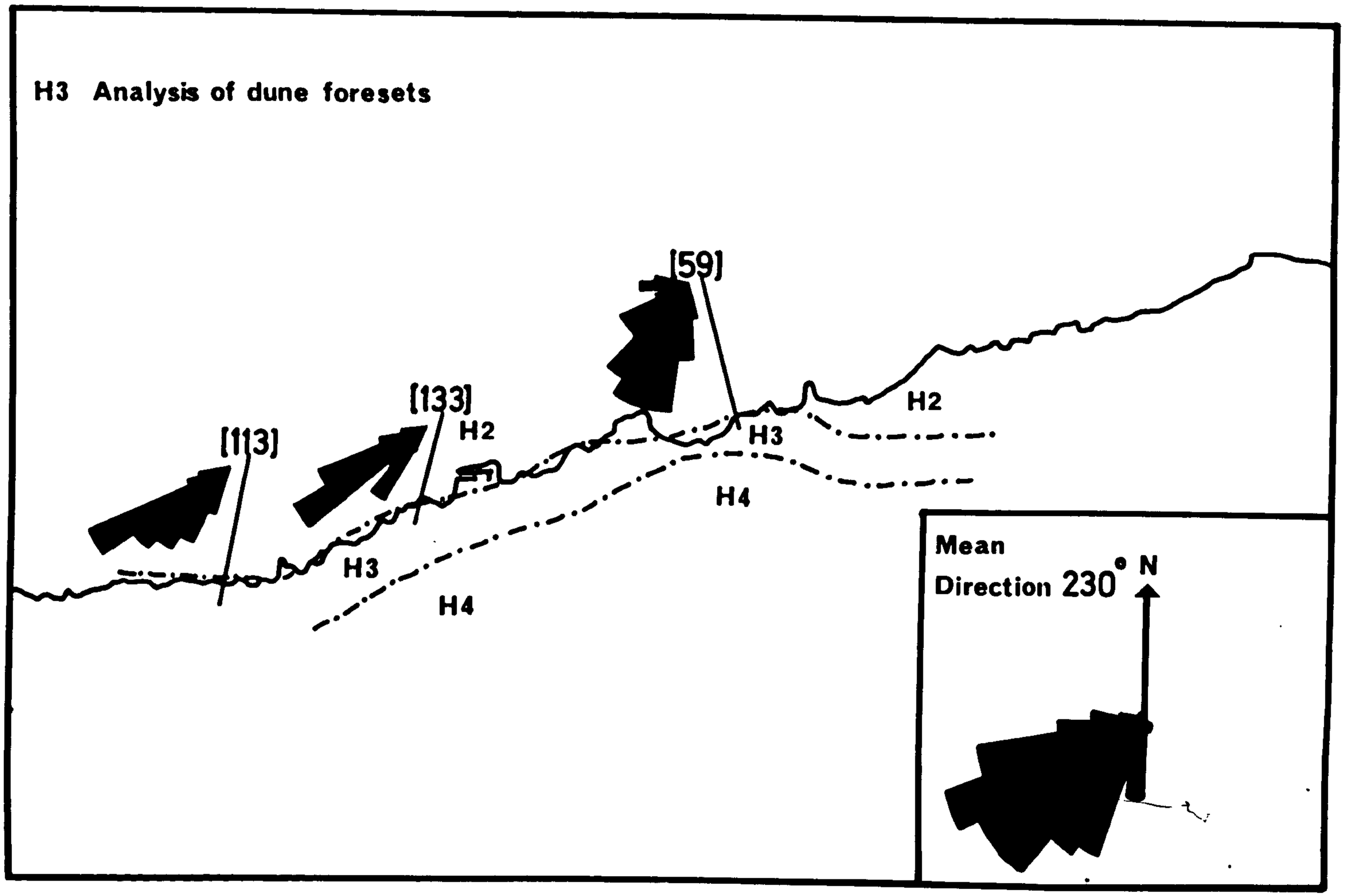

Fig. 5.9. Foreset analysis of the H3 phase.

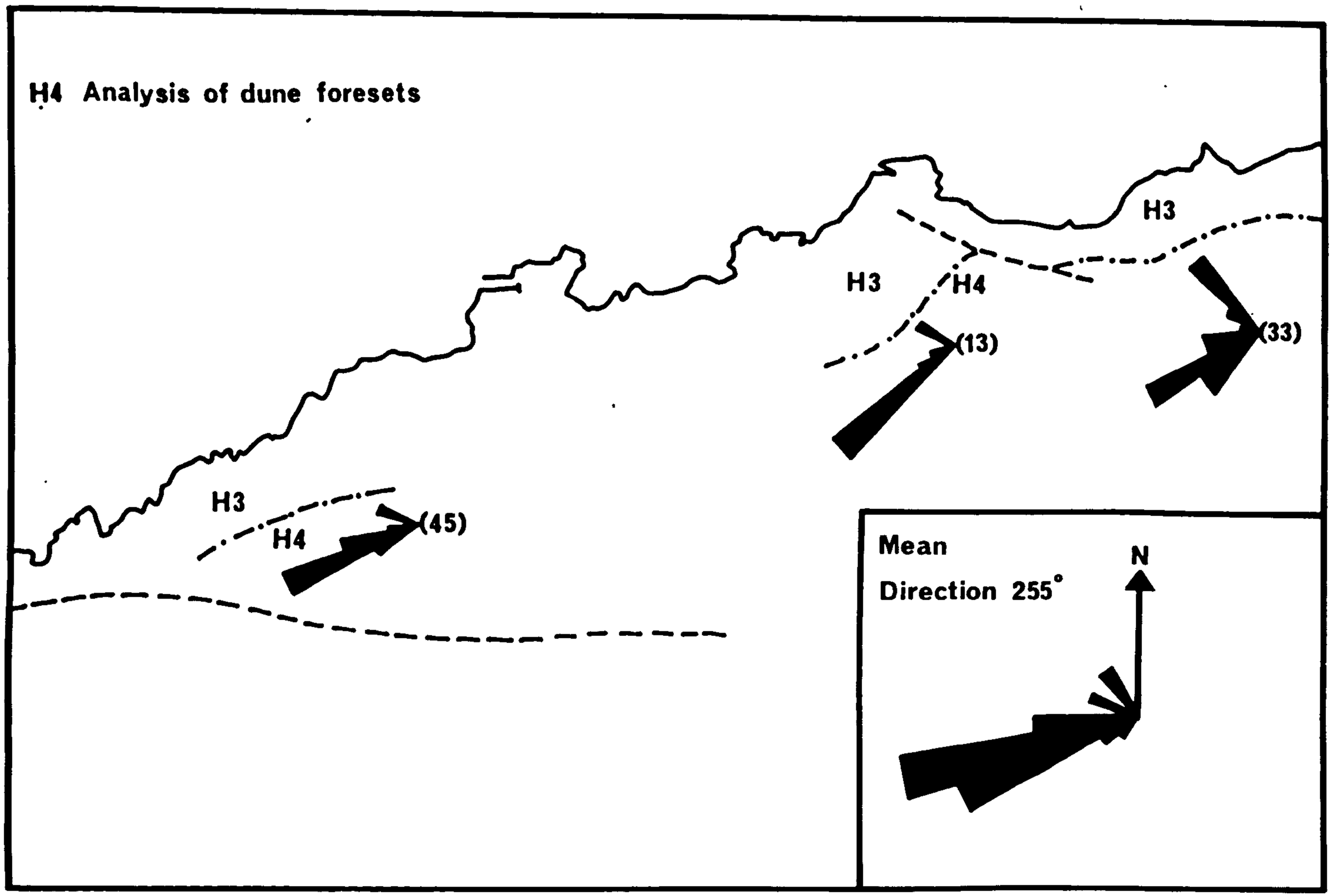

Fig. 5.10. Foreset analysis of the H4 phase.

Foresets show remarkable variation in dip in a short distance compared to the large foresets in the middle dune unit. Windward dipping foresets are present and may dip up to 15 degrees but are generally less than 10 degrees. Leeward dipping foresets are invariably steeper with a maximum of 30 degrees.

Wedge planar bedding is more common than tabular planar bedding, thus distinguishing them from the lower dune unit. Assymetrical scours are also present but rare, and slumping and contortions often occur. Sections at right angles to the dominant wind show similar wedge and tabular planar bedding but generally at a lower angle to those parallel to the dominant wind.

Upper dune foreset bedding is seen north of Clashach Quarry where lower dune foresets of the H4 phase overlie the upper dune foresets of the H3 phase. There is no evidence that upper dune units of the H2 phase are present but large scale contortions in this phase may have obscured them. It is clear that the dune crest is liable to erosion by the succeeding dunes; this is the reason put forward for the limited exposure of the upper units at the present day.

CONTORTED DUNES

The contorted bedding of the Hopeman Sandstone has been described by Peacock (1966). Although the localities of the contortions have been recorded in detail by this author, the sedimentological studies embodied in this thesis have shed light on the probable cause of the contortions. Contorted dunes occur in the upper unit or the top of the middle unit of the dunes and are overlain by playa lake deposits or the basal unit of the succeeding dune phase.

Contorted beds occur at the top of the H1 phase seif dunes from Covesea Skerries Lighthouse to Gordonstoun Lookout Post. Structures in the cliffs north east of Covesea Skerries Lighthouse show fragments of laminated sandstones in a groundmass of structureless sandstones. All stages of folding can be seen from open to tight folds, the cores of the tight folds being replaced by broken laminae or structureless sandstones. Peacock (1966, Fig. 2, p. 159) shows the general form of the structures at this locality. Fragments of laminated sandstones (the original foreset bedding) range from 0·02 to 1.5 metres in length but are generally only 10-20 mm in thickness. They show little or no orientation and probably represent the more consolidated horizons of the dune sandstones. The structureless sandstones represent the unconsolidated horizons of the dune sandstone. On the foreshore, a series of basin and dome structures lie just above normal dune bedded sandstones; the outlines of these structures is exaggerated by the barytes cement in the sandstones which makes them more resistant to weathering. The beds beneath and above the contorted horizon are undisturbed showing the intraformational character of the disturbance.

The bay north of Covesea Village shows the normal dune foresets grading up into 3 metres of contorted beds (Plate 5.2C). The foresets dip at much steeper angles than is normally seen in dune sandstones (i.e. greater than 33 degrees) and, where this angle is especially steep, the dune foresets are replaced by structureless sandstones with fragments of laminated sandstones in their groundmass. The contact of the contorted and the normal dune sandstones is fairly sharp, the contortions clearly being due to oversteepening of the dune foresets. The contorted beds are overlain by the undisturbed basal dune unit of the H2 barchan phase.

The bay north of Covesea Village and west to Gordonstoun Lookout Post shows a series of contorted horizons at the top of the H1 phase. The contortions are seen as isolated exposures along the section but the equivalent horizon to the contorted dune may be represented by normal dune bedded sandstones of the upper dune unit. Further to the west, at the Natural Arch (18537098), the contorted beds once again grade up from normal dune foresets; the foresets remain intact but the angles are far steeper than in normal dune sandstones, the angles varying greatly over a short distance.

Between Sculptors Cave and the cliffs north of the Lookout Post (17507081), the foresets may be vertical or even recumbent in form. However, they still retain the original traces of dune bedding except in the cores of the tight folds where they become structureless. They grade upwards from normal dune foresetsand are overlain by basal dune sandstones of the H2 phase.

Similar exposures also occur at the top of the H2 phase. In the cliffs north of Covesea Quarry, 15 metres of contorted beds overlie normal dune bedding (Plate 5.2A, 5.2B). Fragments of laminated sandstones up to 5 metres in length are randomly distributed in a groundmass of structureless sandstones. Overfolding of the laminae has taken place in many cases. The contact between the normal dune foresets and the contorted beds is fairly sharp although the contact cuts down less to the north than to the south. Thirty metres to the west of the cliff face, a gully exposes the equivalent

EXPLANATION OF PLATE 5.1.

AEOLIAN DUNE BEDDING

A. Alternating coarse and fine laminae in the basal barchan dune deposits of the H2 phase (182709). Tabular planar foresets dip at angles between 0 and 30 degrees.

B. Microfaulting in the H2 contorted dune horizon at Roddoch Wells (134693).

C. Small scale slumping in the contorted beds of the H2 phase at the site of the old Inverugie Castle (15507035). The slumped beds grade up into structureless sandstones.

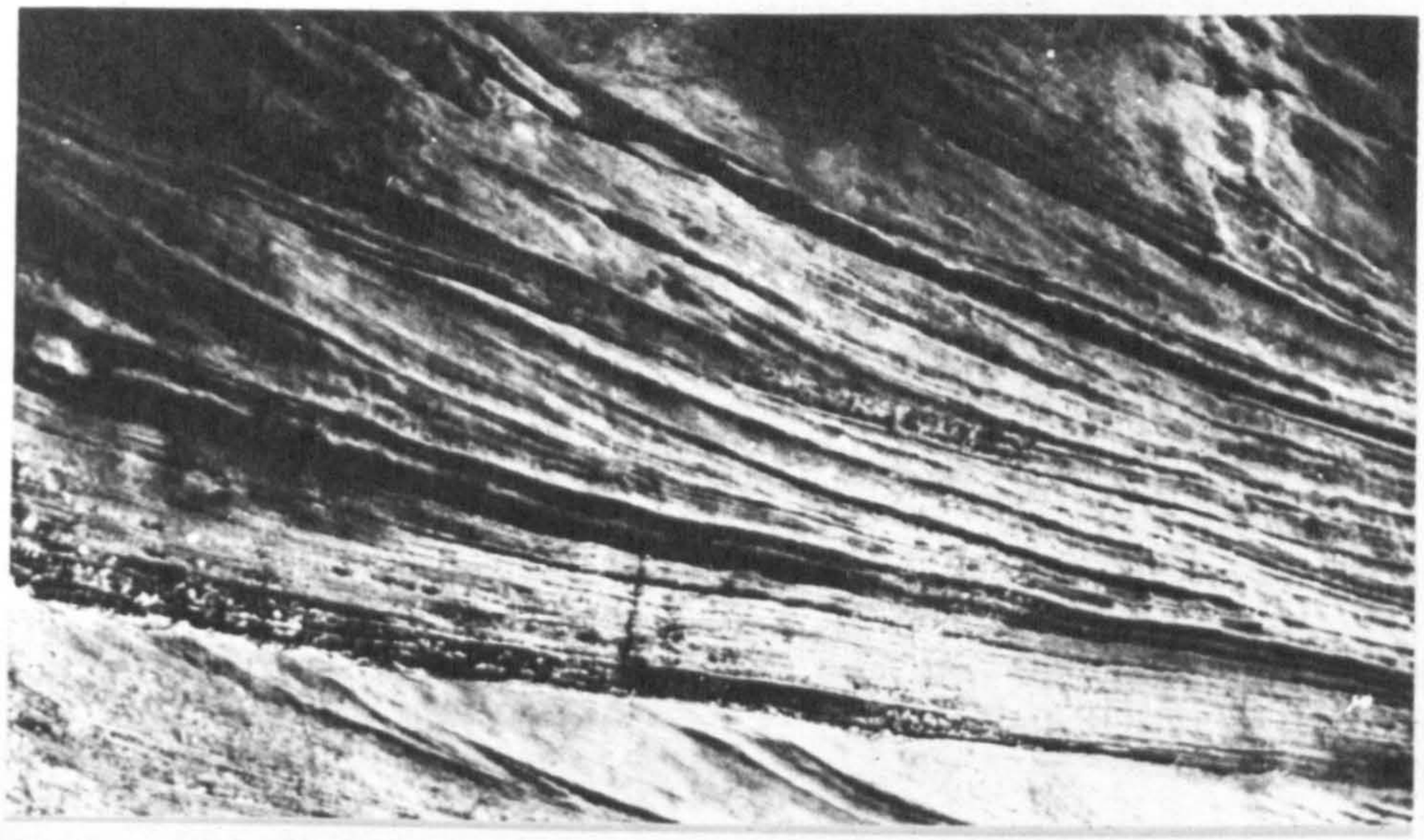

a



b

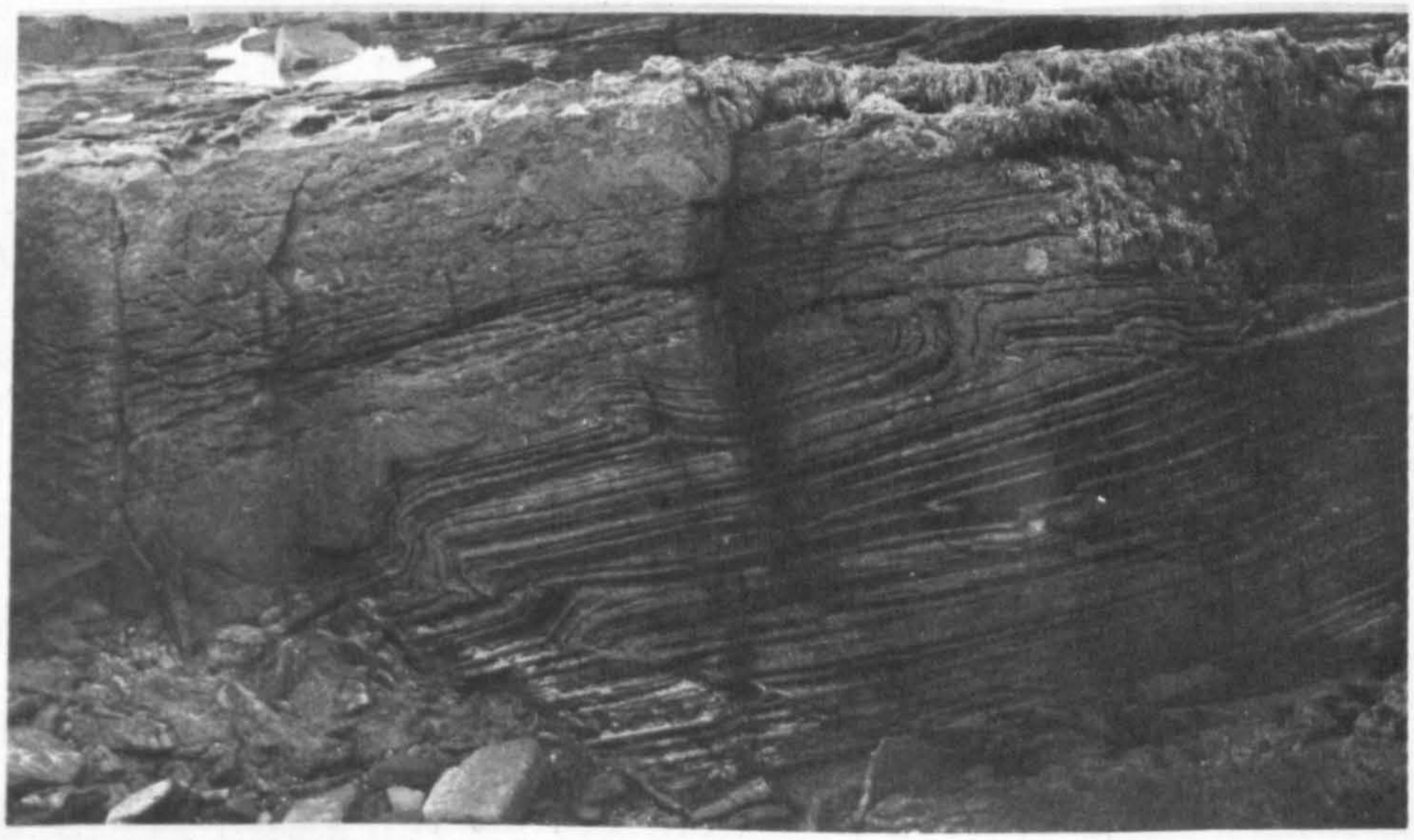

c

PLATE 5.1.

horizon but this is completely undisturbed and represented by normal dune foresets. In thin section, thesecan be divided into two main types. The thicker horizons illustrate all the characteristics of normal dune bedded sandstones. The second type however, are poorly cemented and only reach up to 1.5 metres in thickness. Sieve analyses indicate that they are relatively poorly sorted and have a coarser mean grain size than normal dune bedded sandstones. They also have a clay content of up to 15 per cent, a characteristic of playa deposits. These horizons are thought to represent redeposited playa sediments which formed prior to the main phase of flooding at the top of the H2 phase. The following is taken from this section:

3.0m	Dune sandstone	
0.3m	Reworked playa sediments	
2.0m	Dune sandstone	Contorted horizon
1.5m	Reworked playa sediments	
6.0m	Dune sandstone	
0.3m	Reworked playa sediments	
15.0m	Dune sandstone	

Contorted dune sandstones again outcrop at the top of the H2 phase, 100 metres north of the site of Inverpgie Castle (15607034). They are underlain by normal dune foresets and are overlain by playa deposits. Plate 5.1C illustrates small scale slump structures seen at this locality. To the west of the playa deposits (Fig. 4.3), the contortions show all stages of folding and accompanying faulting. Little or no orientation can be seen in the folding which has axes trending in many different directions.

To the west along the foreshore to Roddoch Bow, a series of basin and dome structures are seen at the top of the H2 phase. It is possible that they were formed by later tectonics but their uniformity in structure and their persistent occurrence at the top of the H2 phase would also suggest that they are due to the same cause as the contorted bedding. They may represent readjustment owing to the saturation of the overlying sandstones.

EXPLANATION OF PLATE 5.2.

CONTORTED DUNE BEDDING

A. Contorted dune bedding overlies normal barchan dune bedding at Covesea Quarry (16907035). The normal dune bedding dips away from the reader at 30 degrees. The contorted dunes are general structureless but occasional fragments of laminated sandstones are present in the groundmass.

B. Contorted dune bedding near to Covesea Quarry (16907035). The characteristic curved slipface of the barchan dunes underlying the contorted beds can be seen on the foreshore.

C. Normal seif dune foresets of the H1 phase grading up into structureless contorted bedding (188711).

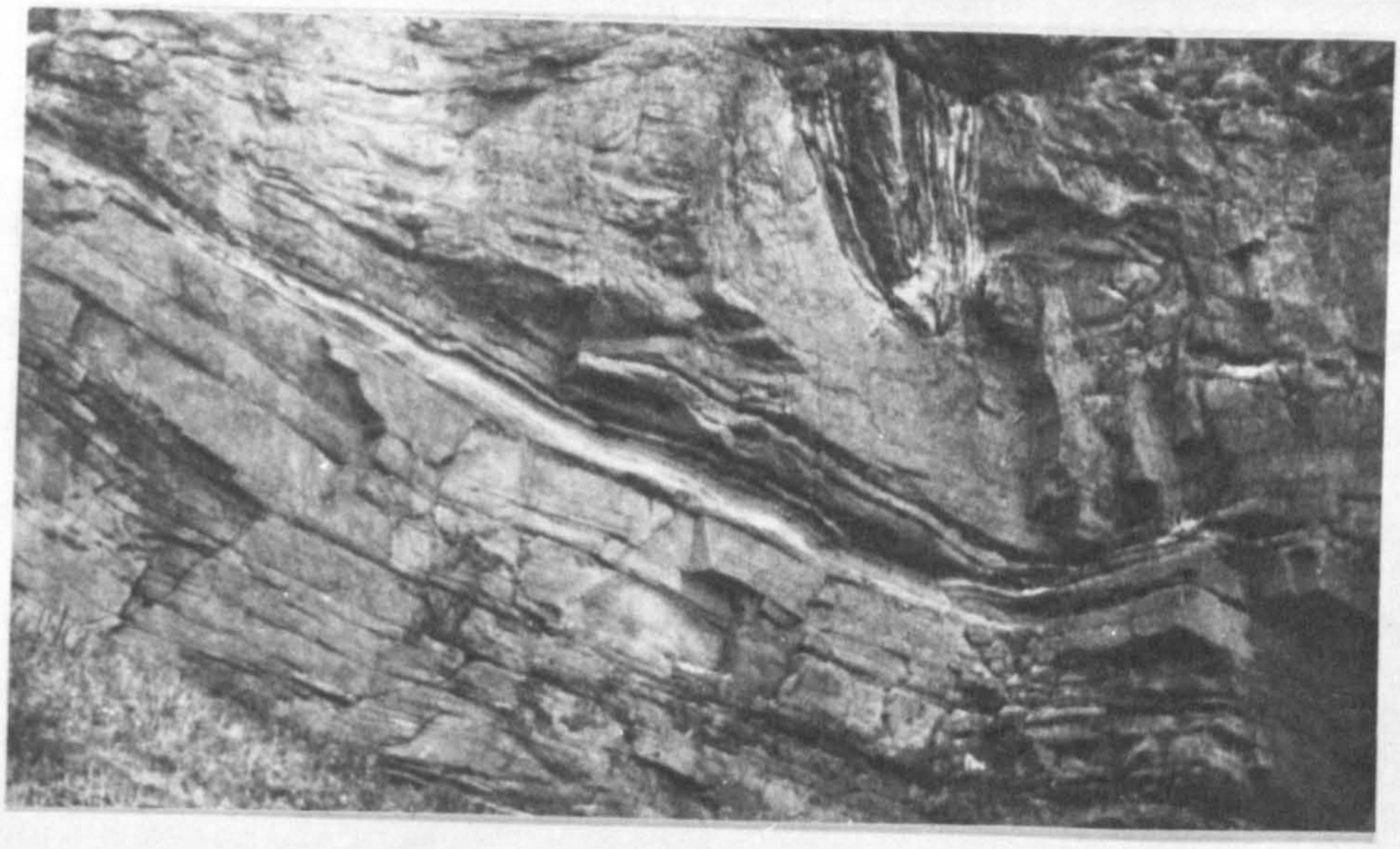

a



b

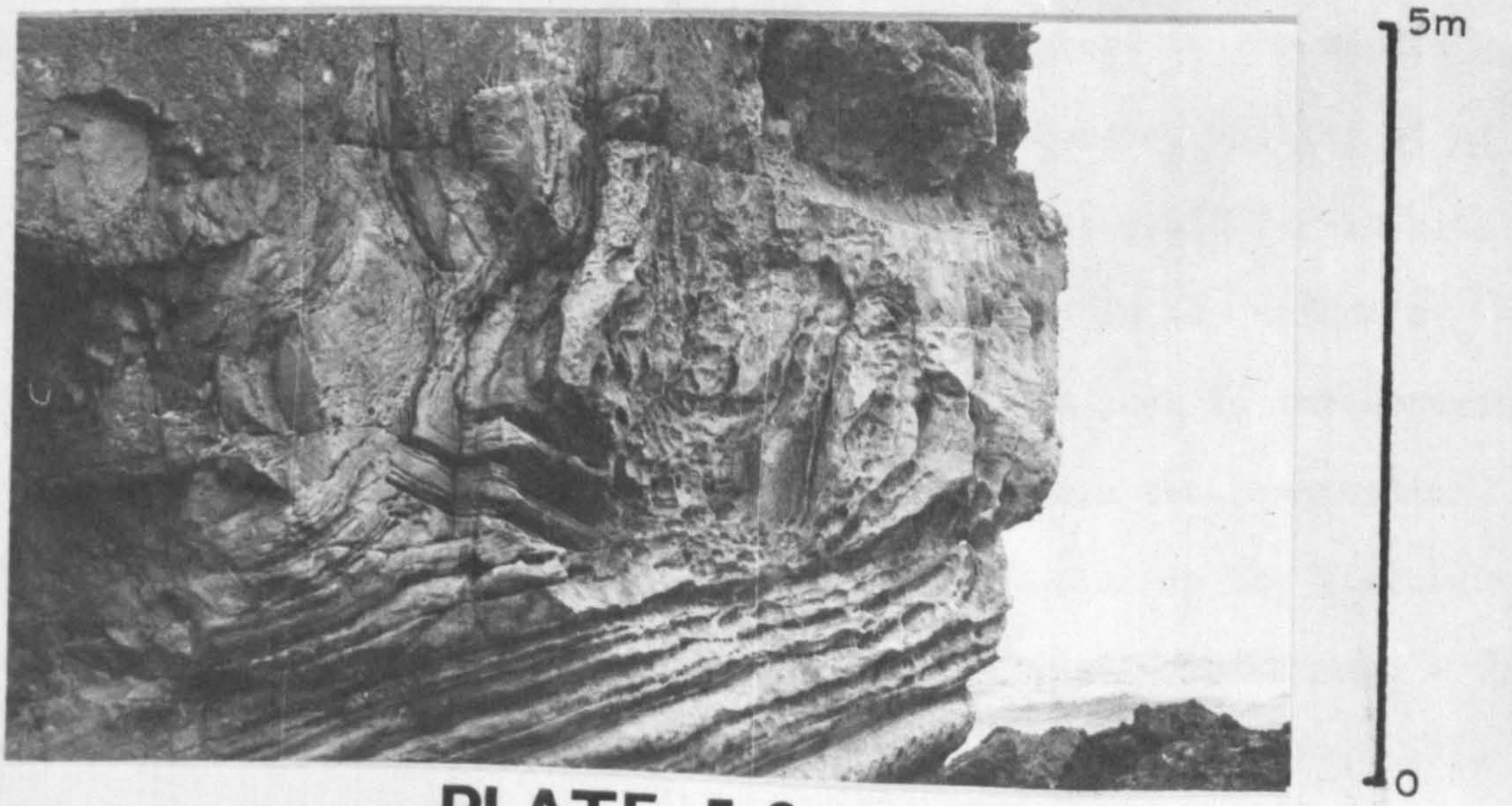

c

PLATE 5.2.

At Roddoch Bow (13206921), normal foreset bedding is folded and oversteepened but no structureless sandstones or fragments of laminated sandstones are seen at this locality. However, north east of Cabrach Well (13356928), at the same horizon, the effect of the contorting is more marked. Basin and dome structures are overlain by sandstones showing injection structures, microfaults (Plate5.2B) and structureless sandstones with small laminated fragments of dune foresets. The sandstones are overlain by basal dune deposits of the H3 phase.

In the disused quarry, north of the main working quarry of Greenbrae Quarry, structureless sandstones of the upper unit of the H3 phase are overlain by the basal unit of the H4 phase. It is thought that the position of the structureless sandstones and their structureless nature indicate that they are contorted dunes.

Causes of the contorted dunes

Contortions have been described by many authors (Cooper, 1943; Fairbridge, 1947; Kuenen, 1949; Rigby, 1958; Slater, 1927; Stewart, 1956; McKee and Weir, 1953; Jones, 1962; Selley et al, 1963) but in most cases, these have been in waterlain sediments and none of those so far documented have been on such a large scale as those present in the Hopeman Sandstone.

Jones (1962) documents the occurrence of contorted dunes due to earthquakes but evidence of associated movement is also seen in the underlying horizons which is not the case in the Hopeman Sandstone. Selley et al (1963) have suggested that contorted structures in the waterlain Torridonian sandstones originated during the movement of quicksands. In the author's experience, the structures are extremely similar to those seen in the Hopeman Sandstone although on a much smaller scale. Thus, although the Torridonian contortions are waterlain in origin, the lack of orientation in the structures of the Hopeman Sandstone would suggest that they had a similar quicksand origin.

Peacock (1966) also noted their similarity to the contortions in the Torridonian but found it difficult to envisage quicksands on such a large

scale in a desert environment: Bagnold (1941) did however note that sand is closely packed on the windward faces and loosely packed on the slipfaces, which led Peacock (1966) to suggest that the slipfaces could have acted as quicksands. He also suggested that the alternate wetting and drying of the sand would promote contortions when movement finally occurred. Peacock did not make any firm conclusions regarding the mechanism of the movement but he did consider the following possibilities; (a) gravity slumping due to over-loading on steep slipfaces by animals or rainfall; (b) undercutting of the dune slipfaces by floodwaters.

The formation of intra-formational recumbent folds has been studied experimentally by McKee, Reynolds and Baker (1962). They concluded (p.D159), "that either a rigid mass moving like ice or sudden movement of a body of sediment as by floodwater is capable of developing these structures in sediment that is saturated." Norris (1969) shows that dune sands tend to retain much of the available moisture in the nucleus of the dune. Recent excavations in the Persian Gulf (Fellowes, personal communication, 1971) have shown that this leads to relatively consolidated sands in the centre of the dune whereas on the periphery, the sands are completely unconsolidated.

The recent sedimentological study of the Hopeman Sandstone by the author has shown that at one locality there is evidence of playa deposits overlying the contortions and other evidence to suggest that, playa deposits at other contorted horizons were once present but have since been reworked by the wind. Identification of injection structures in the contorted horizons and the fact that some of the foresets retained their lamination during folding all tend to favour the theory that the dunes were partially or completely saturated when the contortions occurred.

It is suggested that the playa deposits are the mechanism which triggered off the movement while the dunes were saturated; this saturation may have been produced by the floodwaters themselves, by the accompanying rainfall and/or the natural moisture retained in the nucleus of the dune. Undercutting

of the slipfaces by the floodwaters, led to the collapse of the front of the dune with the consequent avalanching of some of the foresets. The periphery of the dune (both windward and leeward) which was made up of relatively unconsolidated sands produced the characteristic structureless sandstones as the laminae did not retain sufficient cohesion to be folded or faulted. However, the internal parts of the dune retained their lamination due to their greater consolidation and are now represented by the minor laminated fragments in the structureless sandstones. Although some of the folding is clearly due to slumping down the slipface by undercutting, quicksands also appear to have played a prominent role in the contortions. However, this is still in keeping with saturation by the floodwaters. In some cases, the normal dune foresets grade up into oversteepened foresets which show no signs of slumping or structureless sandstones. This appears to be due to the loose packing on the slipface of the dune producing a volume reduction (Sorby, 1908) when movement occurs and when the grains form a denser unit. Thus, the subsequent subsidence produces steep foresets in some cases and almost horizontal foresets in other cases. However, if the subsidence is too great, the foresets break up into structureless sandstones. This is seen in many cases where the normal dune foresets grade up into over-steepened foresets and finally into structureless sandstones (Plate 5.2).

In some cases the overloading was released by injection in the poorly consolidated sands, while in the well consolidate sands the pressure was released by brittle fracture in the form of microfaults. These two features are always closely related and appear to represent minor features of the contortions, possibly formed in the inter-dune areas where the relatively flat lying nature of the sediments would only allow relatively minor features to develop. Basin and dome structures in the H2 sandstones of the Hopeman district also appear to be mainly interdunal in character; repacking of the quartz grains upon saturation produces a volume reduction with the subsequent formation of basins of subsidence.

CHAPTER 6

PETROGRAPHY OF THE HOPEMAN SANDSTONE

The Hopeman Sandstone displays a characteristic orange to yellow orange colour in the field and this, together with the aeolian cross bedding, friable nature and excellent sorting clearly differentiates it from other horizons in the Elgin district. However, in boreholes, the Hopeman Sandstone exhibits the same grey colour seen in other horizons but they may still be identified by sedimentary structures and grain size characteristics.

The sandstones are normally exceedingly friable except at certain localities where they are cemented by calcite, fluorite and barytes. These cements are diagenetic in origin and are discussed together with the other diagenetic features of the Hopeman Sandstone in Chapter 13.

CLASSIFICATION OF SANDSTONES

There are various classifications which have been published in post war years, the most important of which are discussed below with reference to the most suitable classification for the Hopeman Sandstone.

McBride (1963), discussing various recent classifications, notes the tendency to subdivide sandstones on the basis of their mineral content, mineral and textural attributes or mineral, textural and structural attributes. Each classification has its own advantages and disadvantages and no one scheme is generally accepted for the universal classification of sandstones. However, if each case is taken on its own merit and the most suitable classification used, then the classification has achieved its purpose.

Folk's classification (1954) is an excellent example of a classification based solely on mineral attributes (Fig. 6.1B). Folk uses three end members, feldspar and igneous rock fragments, mica and metamorphic rock fragments and quartz and chert. However, practically, it is often difficult to recognize igneous and metamorphic rock fragments in thin section; there is also the question

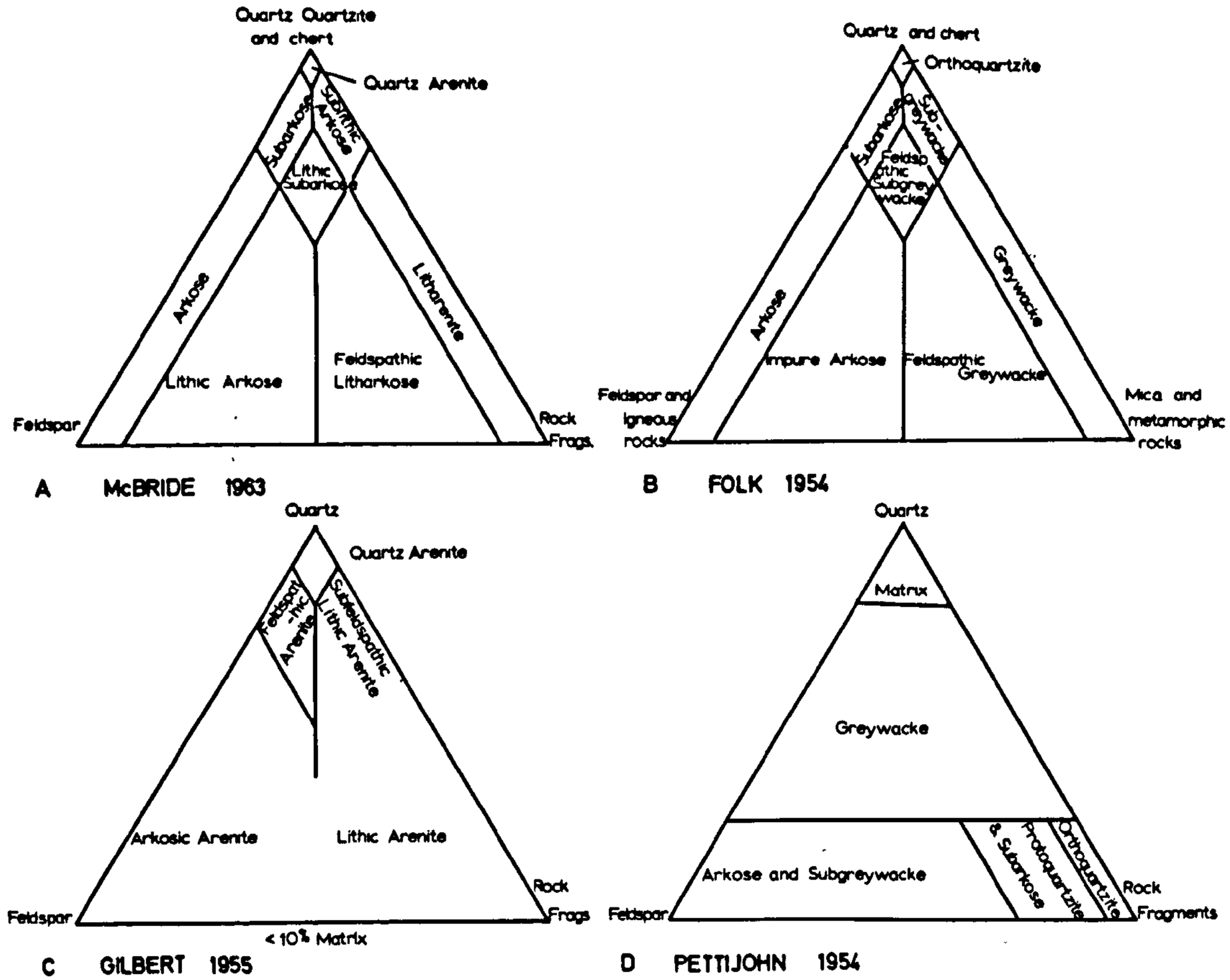

Fig. 6.1. Classification of sandstones.

as to whether metaquartzites are included in the same parameter as quartz or the metamorphic series, if indeed they can be differentiated. In the case of the Hopeman Sandstone, which appears to have been derived mainly from the Old Red Sandstone, many metamorphic rock fragments are present but these are dicyclic and thus show the original source rather than the actual source area. Furthermore, there is an objection to the grouping of all igneous rock fragments into one parameter as there is a marked mineralogical difference between volcanic and plutonic rocks.

Gilbert (1955) considered that quartz, rock fragments and feldspar were the most important parameters in sandstone classification (Fig. 6.1C). He proposed two classifications, one conforming to the greywacke clan with greater than 10 per cent clay, and one conforming to the arenite clan with less than 10 per cent clay. The parameters chosen by Gilbert (1955) are thought to be the most relevant in the classification of sandstones but the rather arbitrary figure of 10 per cent to differentiate the arenite and greywacke clan renders the scheme unsatisfactory. The sheetflood deposits of the Hopeman Sandstone have a clay content between 5-15 per cent but do not display any mineralogical or textural features of greywackes. McBride (1963) uses the same parameters as Gilbert (1955) but does not consider the clay content (Fig. 6.1A). However, in the classification of the Hopeman Sandstones, the clay content is necessary to differentiate the aeolian and waterlain sandstones so this classification was not considered.

Pettijohn (1954) considered that sand size particles were the result of the disintegration of plutonic igneous and supracrustal rocks. These two classes yield quartz and feldspar grains, and quartz and rock fragments, the ratio of the feldspar:rock fragments indicating the relative importance of the two sources. He also showed that the mineralogical and textural composition of the sandstones was a reflection of maturity. As quartz is undoubtedly the most stable and feldspar the most unstable common mineral present in arenaceous rocks, he proposed that the ratio of quartz:feldspar represented

a satisfactory maturity index. The fluidity of the depositing medium could also be related to the effective sorting coefficient of the sandstones, i.e. a low fluidity depositing medium would give rise to a poorly sorted sandstone and vice versa. He suggested that the ratio of the clay matrix to sand detritus therefore demonstrated the fluidity of the depositing medium. Pettijohn therefore proposed three parameters: (a) matrix, (b) feldspar and rock fragments, and (c) quartz and chert (Fig. 6.1D).

The classification of Pettijohn (1954) is favoured here as it makes the optimum utilisation of the true rock genesis by considering provenance, maturity and the fluidity of the depositing medium. However, when considering sandstones in the Elgin district, it has been found that sandstones of different mineralogical and textural attributes may fall into the same class, i.e. sandstones with a different type of rock fragment but the same percentage would be classified in the same clan. It is clear that the classification of Pettijohn (1954), although it shows an optimisation of the given parameters, is not solely sufficient to classify the Hopeman Sandstone. It is suggested that the parameters are numerically insufficient and that the following parameters are necessary to adequately define the sandstones of the type described here:

1. Rock Fragments

The importance of this parameter was first realised by Pettijohn (1954) and then by subsequent authors as a characteristic of supracrustal sources and thus an indicator of provenance.

2. Polycrystalline Quartz

The percentage of polycrystalline quartz is a measure of the relative distance of transport from the source area. Although it is to a certain extent governed by the grain size of the sediments its value is clearly demomonstrated in Fig. 6.5. Theoretically, the source area consists of 100 per cent polycrystalline grains, so a series through scree, alluvial fan, sheetflood and playa deposits should show a progressive decrease in the percentage of polycrystalline quartz grains. If also polycrystalline quartz grains are coupled

with rock fragments in the same parameter, this also discounts the question as to whether some grains are rock fragments of polycrystalline quartz grains.

3. Unimodal Quartz (strained and unstrained)

This is clearly the most common mineral in the arenites and therefore the basis for all classifications. Unimodal quartz is used here to differentiate it from polycrystalline quartz.

4, Feldspar

Pettijohn again recognised the importance of feldspars as an indicator of provenance from plutonic igneous rocks.

5. Clays

The clay to sand ratio provides an excellent measure of the fluidity of the depositing medium. The ratio is therefore important in the desert sandstones as a method of differentiating the aeolian and waterlain sandstones.

6. Mica

The presence of mica acts in a similar manner to that of clay and is therefore a function of fluidity, and another method of differentiating aeolian and waterlain sandstones.

It is the author's intention to propose a dual classification system for the classification of the Hopeman Sandstone. The first is the classification of Pettijohn (1954) and serves as a method of recognition of the sandstones in the arenite group. The second classification is shown in Fig. 6.2B and is a method whereby the various desert sandstone facies of the Hopeman Sandstone can be distinguished. The six parameters discussed above are grouped as follows:

1. Unimodal Quartz
2. Clay matrix and mica
3. Feldspar, chert, rock fragments and polycrystalline quartz

CLASSIFICATION OF THE HOPEMAN SANDSTONE

Modal analyses of thin sections of the Hopeman Sandstone were carried out using the standard point counting technique. Experiments were

A

Matrix or cement		detrital matrix >15% <75%	detrital matrix <15%		
sand fraction	feldspar > rocks	GREYWACKES (>5% feldspar, >10% rocks) feldspathic greywacke	ARKOSIC arkose	SANDSTONES subarkose or feldspathic quartzite	ORTHOQUARTZITES chert <5%
	rocks > feldspar	lithic greywacke	LITHIC subgreywacke	SANDSTONES protoquartzite	detrital >5%
	quartz+chert content	<75%	<75%	>75% <95%	>95%

(After Pettijohn + McBride)

B

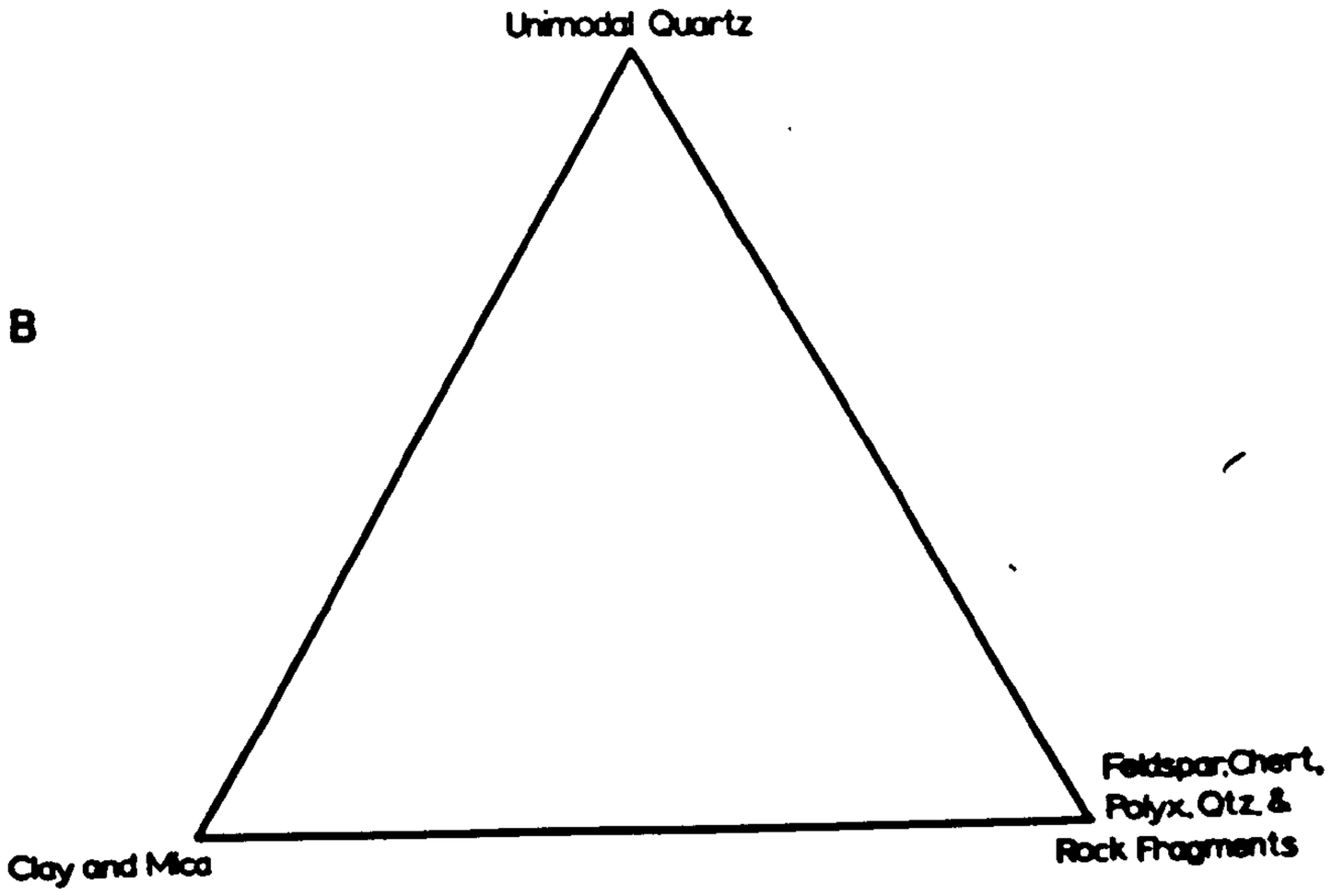

Fig. 6.2. Dual classification.

NUMBER	Unimodal Quartz	Clay and Mica	Rock Fragments, Chert, Feldspar and Polycrystalline Quartz
AEOLIAN SANDSTONES			
H1F28	57.9	0	42.1
H1F26	77.0	0	23.0
H1C18	63.7	0	36.3
H1C16	56.5	0	43.5
H1C6	70.1	0	29.9
H1C7	70.4	0	29.6
H1C8	72.0	0	28.0
H1C9	71.5	0	28.5
H1C10	71.1	0	28.9
H1C11	74.0	0	26.0
H1P40	74.8	0	25.3
H1P41	75.3	0	24.7
H1P36	69.6	0	30.4
H1P37	66.8	0	33.2
H1P38	68.8	0	31.2
H1P39	74.6	0	25.4
H4-9	71.6	0	28.4
H2C26	57.6	0	33.8
H2C27	55.8	9.6	28.2
H2C28	62.6	16.0	31.5
H2B29	60.0	6.0	28.75
H2B33	52.0	11.25	45.0
H3B37	65.0	3.25	35.0
H3B38	69.8	0	30.2
H3B39	75.6	0	24.4
H3B40	72.4	0	27.6
H3B41	75.5	0	24.5
H3B43	70.0	0	30.0
H4-8	79.4	0	20.6

TABLE 6.1. Relative percentage of unimodal quartz, clay and mica and other detrital components in the Hopeman Sandstone

NUMBER	Unimodal Quartz	Clay and Mica	Rock Fragments, Chert, Feldspar and Polycrystalline Quartz
PLAYA SANDSTONES			
H2F36A	71.6	0.6	27.8
H2F37A	48.0	7.4	44.6
H2F36B	60.3	9.3	30.5
H2F36C	60.4	14.4	25.2
H2F36D	66.0	0.6	23.4
H2F37B	45.0	1.8	53.2
H2F37C	60.0	5.0	35.0
H2F37D	63.0	6.5	30.5
H2F37E	56.0	12.0	32.0
H2F37F	52.0	1.0	47.0
SHEETFLOOD DEPOSITS			
QW-S1	9.0	15.0	76.0
QW-S2	66.0	10.5	23.5
QW-S3	45.0	13.5	41.5
QW-S4	47.0	16.5	36.5

TABLE 6.1 (continued)

NUMBER	Quartz	Feldspar	Rock Fragments
AEOLIAN			
H1F28	95.4	3.8	0.8
H1F25	95.8	3.8	0.4
H1C18	94.25	4.25	1.5
H1C16	98.0	2.0	0
H1C6	92.7	7.0	0.3
H1C7	95.1	3.6	1.3
H1C8	94.8	4.2	1.0
H1C9	95.0	5.0	0
H1C10	88.7	10.3	1.0
H1C11	91.7	8.3	0
H1P40	89.0	10.0	1.0
H1P41	93.7	6.3	0
H1P36	91.7	8.3	0
H1P37	93.1	6.6	0.3
H1P38	92.0	8.0	0
H1P40	96.7	3.3	0
H1P35	92.4	7.0	0.6
H4-9	94.0	4.0	2.0
H2C26	95.0	5.0	0
H2C27	93.4	6.2	0.4
H2C28	95.0	3.5	1.5
H2B29	94.75	4.25	1.0
H2B33	93.75	5.0	1.25
H3B37	96.0	2.0	2.0
H3B38	94.8	4.6	0.6
H3B39	89.4	10.3	0.3
H3B40	93.7	6.4	0
H3B41	93.2	5.4	1.4
H3B43	96.0	3.2	0.8
H4-8	95.1	4.3	0.6

TABLE 6.2. Relative percentage of quartz, feldspar and rock fragments in the Hopeman Sandstone

NUMBER	Quartz	Feldspar	Rock Fragments
PLAYA			
H2F36A	93.4	4.2	2.4
H2F37A	95.2	4.2	0.6
H2F36B	94.1	4.3	1.6
H2F36C	93.6	3.2	3.2
H2F36D	94.3	4.7	1.0
H2F37B	96.9	2.3	0.8
H2F37C	93.0	6.0	1.0
H2F37D	91.5	5.0	3.5
H2F36E	91.5	4.0	4.5
H2F36F	88.0	8.0	4.0
SHEETFLOOD			
QW-S1	66.5	5.0	21.5
QW-S2	77.0	8.0	4.0
QW-S3	47.6	3.5	35.0
QW-S4	70.5	8.0	7.5

TABLE 6.2 (continued)

carried out to find the most suitable number of counts per slide necessary to produce an accuracy of 1-3 per cent. It was found that 400 counts per slide was the minimum number of counts necessary to reproduce an experimental error of less than 3 per cent.

Results of the modal analyses are tabulated in Tables 6.1-2 and they are shown graphically on triangular diagrams in Fig. 6.3. The classification of McBride (1963) is also included.

The aeolian sandstones plot in the orthoquartzite and subarkose clan of Pettijohn's classification whereas in McBride's scheme they occur in the quartz arenite and subarkose clan. It can be seen from Fig. 6.3 that the terms orthoquartzite and quartz arenite are broadly synonomous. The playa deposits can be classified similarly and only vary from the aeolian sandstones in the percentage of clay which is present. This is a reflection of the basic derivation of the playa deposits from the aeolian sandstones.

The sheetflood deposits, as would be expected from their different source and mode of deposition, plot in a different clan from the aeolian and playa deposits. In Pettijohn's scheme they belong to the lithic sandstones whilst in that of McBride, they belong to the sublitharenites, litharenites and subarkose clans. Thus it can be seen that the variation in classification systems is not great but the advantages of the Pettijohn classification is in the ratios of the end members which classify maturity, fluidity and provenance, i.e. it is a truly genetic classification.

Applying the second method proposed by the author, aeolian deposits, which are completely devoid of mica and clays, plot on the line between unimodal quartz and detrital fragments (Fig. 6.3D). The playa deposits illustrate the same ratio of quartz:detrital fragments but can be differentiated from the aeolian sandstones by the presence of 1-12 per cent clay and mica. The contorted beds plot in the same field as the playa deposits suggesting that the dunes were contaminated by the floodwaters. It is also suggested that the medium to coarse material is all aeolian in character whereas the clays and mica were

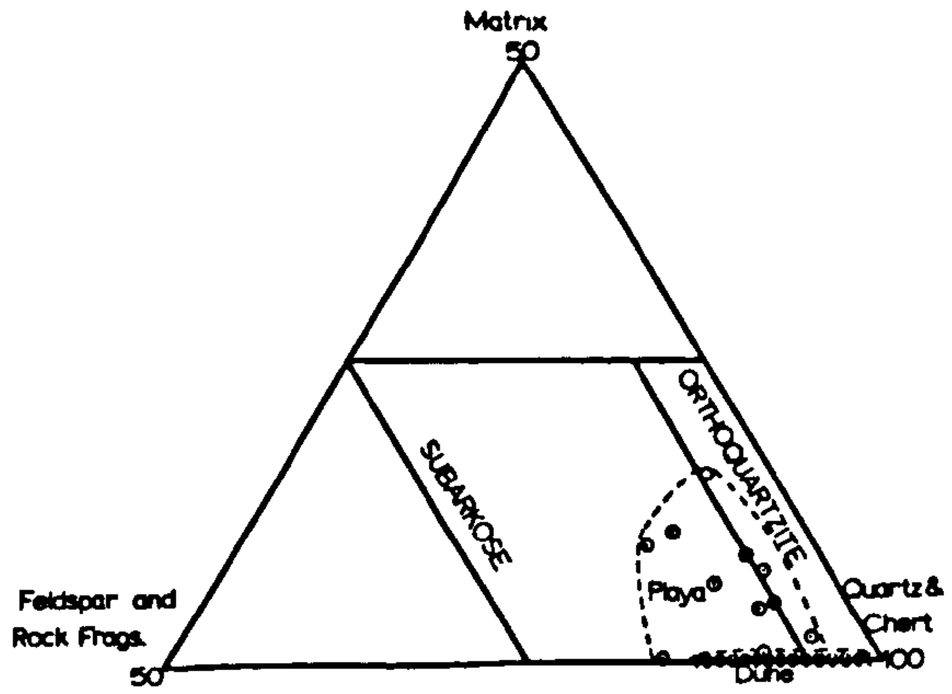

A Pettijohn 1954 (Feldspar>Rock Frags)

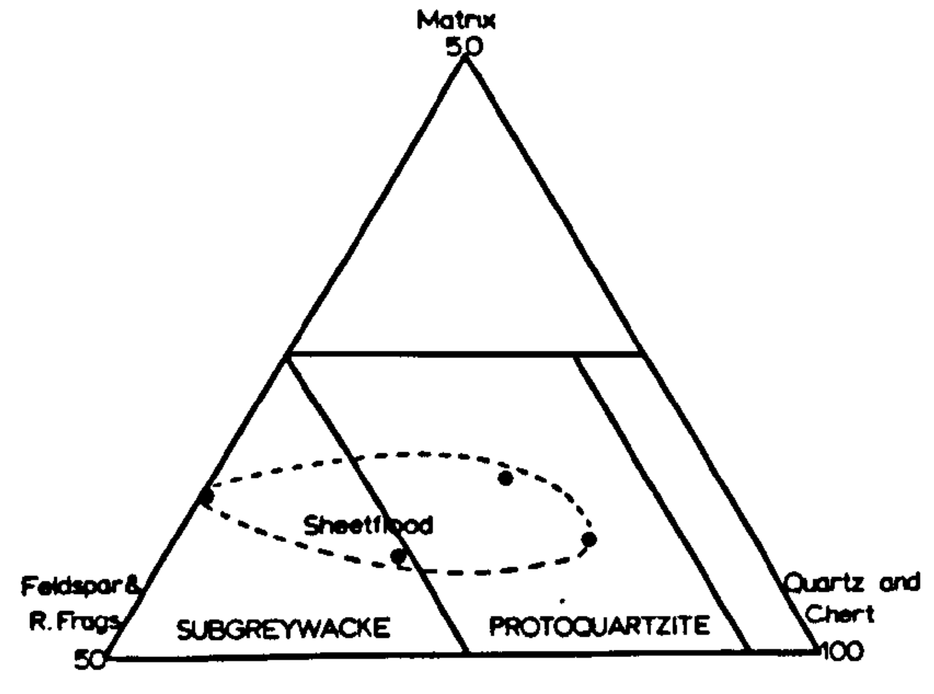

B Pettijohn 1954 (Rock Frags>Feldspar)

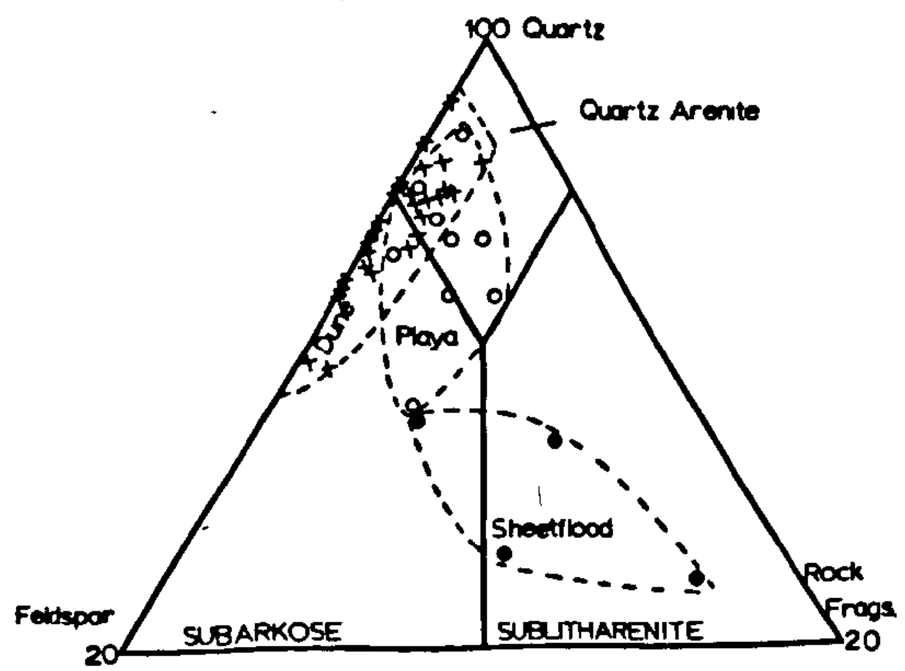

C McBride 1963

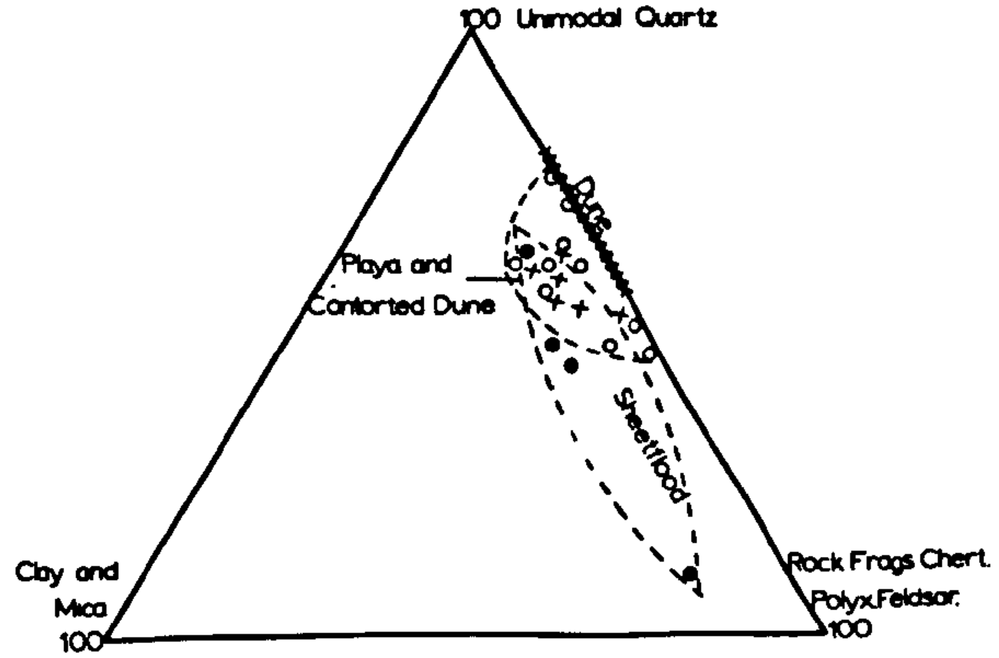

D Williams 1972

Fig. 6.3. Classification of the Hopeman Sandstone.

brought in by floodwaters; thus the difference between the playa, contorted and aeolian deposits is readily discernible.

The sheetflood deposits show a higher clay content and rock detritus component than the other deposits. This is a reflection of the proximity of the source, poor sorting and coarser grain size of the deposits.

These classifications can be supplemented by the descriptive and genetic parameters suggested by Pettijohn (1954).

Maturity index

Although Pettijohn demonstrated that the ratio of quartz:feldspar was a measure of the relative maturity, he did however recognise that sandstones derived from a supracrustal source would have a deceptively high maturity index. He therefore proposed an alternative index of the ratio quartz and chert:feldspar and rock fragments.

For the aeolian Hopeman Sandstone, the former index is 17:1 and the latter 15:1 indicating a relatively high degree of maturity. The playa deposits have indices of 20:1 and 19:1 respectively indicating a similar maturity as would be expected from rocks derived from the same source.

The sheetflood deposits reflect their differing origin and have ratios of 10:1 and 7:2. The difference in sheetflood ratios can be explained by their derivation from supracrustal rocks. Although they were derived mainly from the Old Red Sandstone, they are in fact dicyclic in origin as the original source was from the metamorphic Dalradian and Moinian rocks. The anomaly is therefore a higher percentage of feldspar than in the aeolian deposits. This may be due to the more local source and distance of transport of the sheetflood deposits, together with greater degree of attrition in aeolian transportation.

These values also reflect the corresponding textural maturity of the sandstones. The aeolian sandstones are well sorted and well rounded whereas the sheetfloods deposits are poorly sorted and angular in nature.

Provenance

The ratios of feldspar:rock fragments for the aeolian and playa deposits of the Hopeman Sandstone is 10:1 and 2:1 respectively suggesting that

the source was dominantly plutonic in nature. However, analyses of the detrital components of these sediments indicates a high percentage of quartzite and granulite fragments. In Pettijohn's classification, these components would be included in the quartz rather than the rock fragment parameter thus giving a relative deficiency in rock fragments. It is also thought that aeolian disaggregation of the rock fragments would lead to a deceptively low percentage of these grains. In conclusion, it is felt that supracrustal rocks played a more important role in the source area for the aeolian and playa deposits of the Hopeman Sandstone than is suggested by the above ratios.

The sheetflood deposits have a ratio of 1:3 indicating that supracrustal rocks were the most important source rocks. This is substantiated by pebble analyses which were discussed in Chapter 4. Thus, although the sheetflood deposits are dicyclic in origin, the ratio is clearly an indication of the original metamorphic Dalradian and Moinian source.

Fluidity

Fluidity of the depositing medium can be illustrated by the ratio of sand:clay (Pettijohn, 1954).

The aeolian sandstones of the Hopeman Sandstone indicate that the depositing medium had a high fluidity as no clay is present, i.e. the ratio is infinity. This is due to the retention of the fine material in suspension so only the sand and silt fractions are deposited. Mica is similarly absent so the relevance of the sand and clay as end members in the classification of desert sandstones can be clearly seen.

The playa deposits indicate a decrease in fluidity of the depositing medium compared to the aeolian sandstones, the ratio being 16:1. A further decrease is seen in the sheetflood deposits (6:1), this ratio clearly being a reflection of the high sediment:water ratio during their deposition and the resulting lack of sorting.

DETRITAL COMPONENTS OF THE HOPEMAN SANDSTONE

Theoretical considerations

It has already been shown in previous chapters that the sheetflood deposits were derived from south of Elgin whereas the aeolian sediments were deposited by north easterly winds. Quartz represents between 80-90 per cent of the total detrital components in these sandstones so if the two different source areas are to be differentiated by their detrital grains, different quartz types need to be distinguished.

There are three main types of quartz, strained, unstrained and polycrystalline. Blatt and Christie (1963) and Greensmith (1963) have shown that the relative percentage of each type of quartz enables variation in the provenance with time to be recognised. For a sandstone with little standard deviation in the mean grain size, as shown by Waugh (1967), this technique appears to be highly successful. However, where the mean grain size is highly variable, as in the Hopeman Sandstone, the variation of the percentage of polycrystalline quartz with grain size, conceals any other variation.

However, another technique can be applied to differentiate source areas. Fig. 6.5 illustrates that theoretically, a unit block of the source area is made up of 100 per cent polycrystalline quartz and an infinite mean grain size; increasing distance of derivation of sediments from the source area results in a decrease in grain size and a corresponding decrease in the percentage of polycrystalline quartz, until total disaggregation occurs. As different source areas have varying grain size characteristics, if mean grain size is plotted against the percentage of polycrystalline quartz, theoretically, samples from the same source with the same mean grain size will have the same percentage of polycrystalline quartz. Thus, two different source areas will have different arithmetic properties.

Fig. 6.5 illustrates mean grain size plotted against the percentage of polycrystalline quartz for the various environments of the Hopeman Sandstone, clearly differentiating the sheetflood from the aeolian and playa deposits.

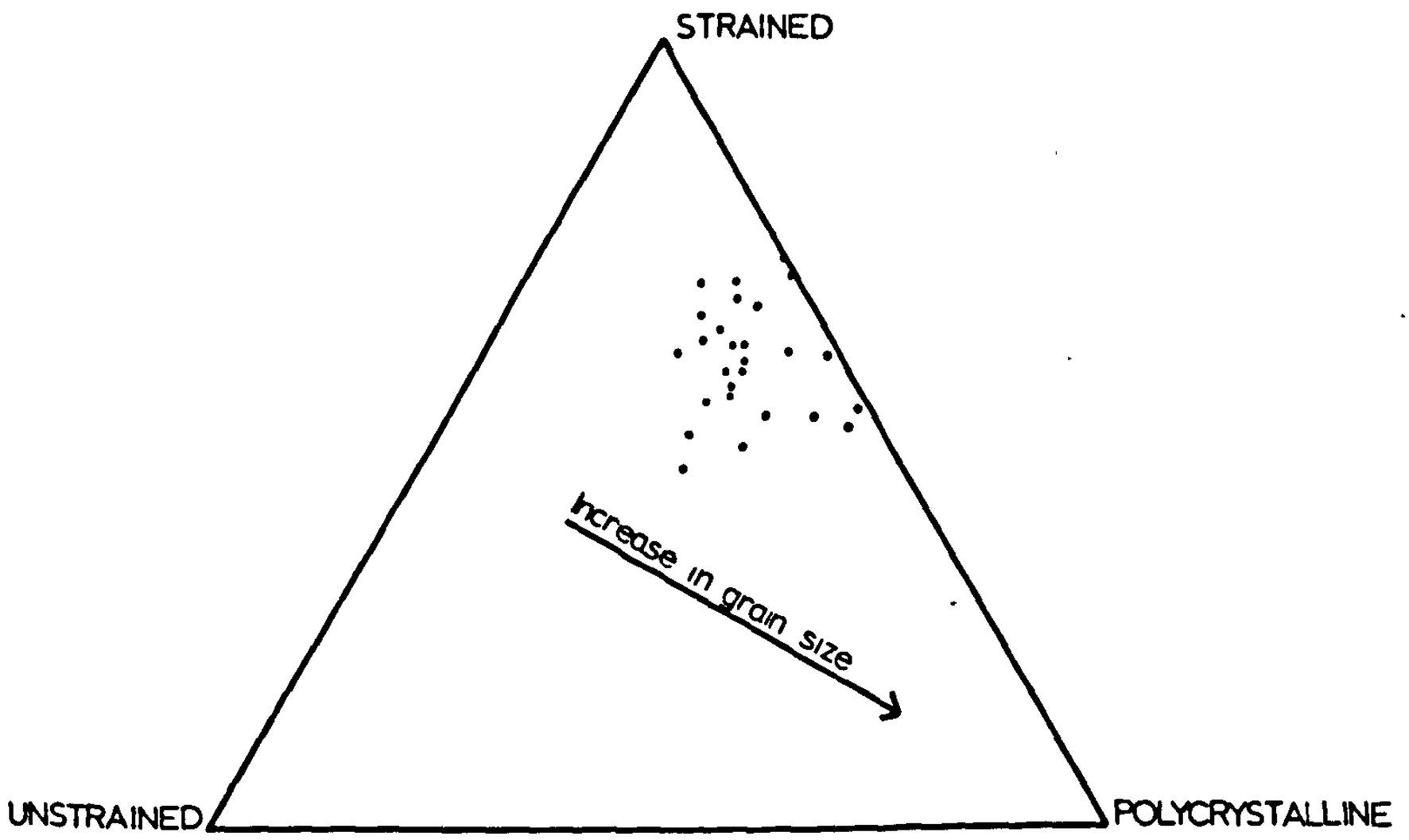

Fig. 6.4. Ratio of quartz types in the Hopeman Sandstone.

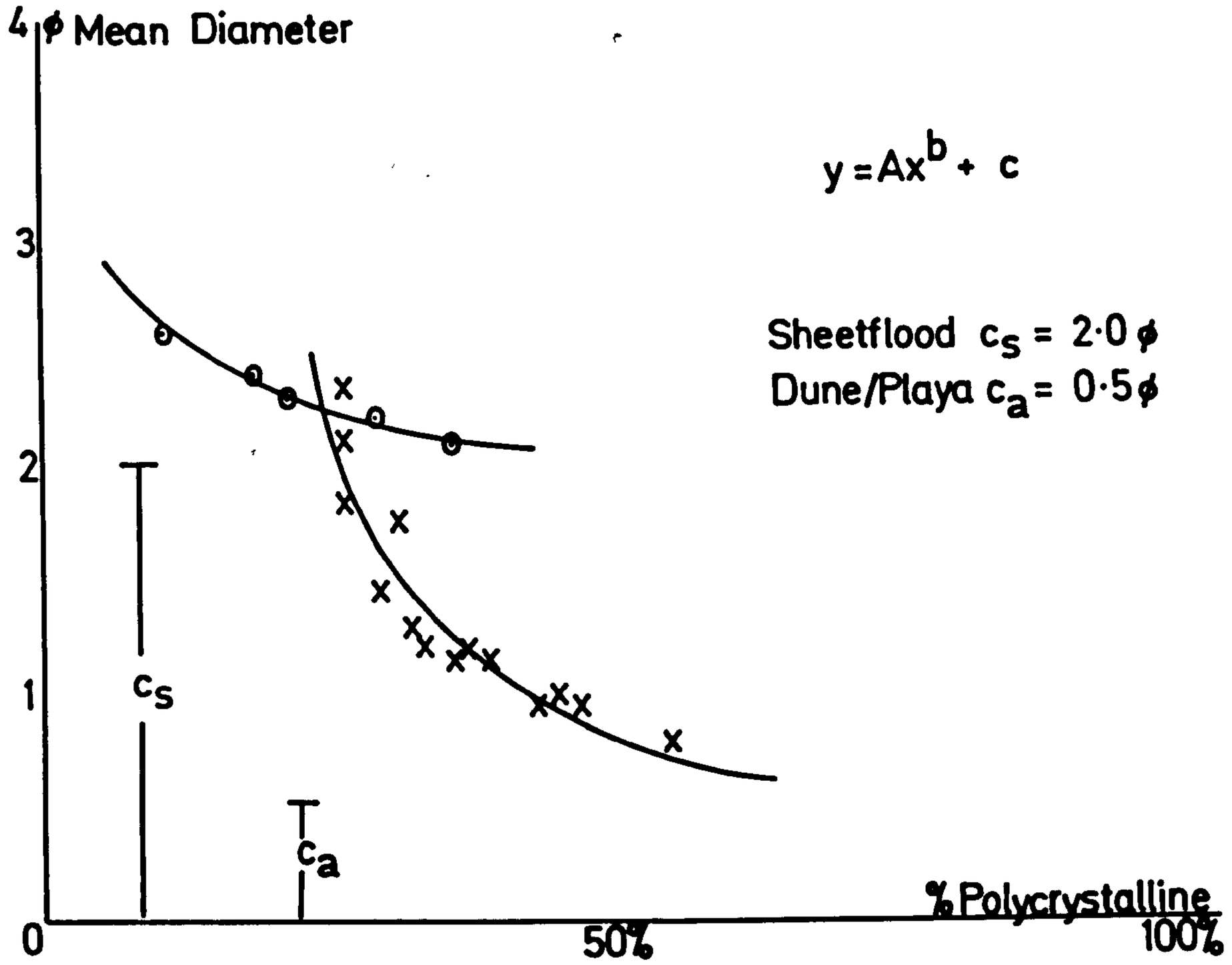

Fig. 6.5. Percentage of polycrystalline quartz plotted against mean diameter.

As the playa and aeolian deposits plot on the same curve, this would support the theory that the playa sediments are basically reworked dune sediments.

It is therefore concluded that the aeolian/playa and sheetflood were derived from two different sources and therefore their detrital components are discussed separately.

SHEETFLOOD DEPOSITS (Plate 6.1A)

Unstrained quartz

These consist of a single unicrystalline crystal and show the simplest structures of the three types of quartz. Most of the unstrained quartz exhibit some form of inclusion within the grain although these inclusions are relatively minor in volume. The most common type of inclusion are a series of minute black blebs which may be randomly distributed or aligned along distinct lineations. Where the inclusions are aligned, they are either subparallel or bisect each other at 60 degrees. Grains with small colourless cavities are also common, these representing small gas or fluid inclusions.

The following are also found:

(a) Grains with randomly orientated rutile needles

(b) Grains with inclusions of mica derived from quartz granulites

(c) Square and hexagonal inclusions

(d) Fractured quartz grains with iron oxide concentrated along the fractures indicating probable derivation from the Old Red Sandstone.

The percentage of unstrained quartz varies from 1-28 per cent, the low percentage being a reflection of the dominantly metamorphic source.

Strained quartz

Strained quartz varies from 45-72 per cent of the total quartz. Three main types of strained quartz can be identified although the divisions are gradational. Some grains exhibit a relatively low degree of straining and only require a rotation of 1-10 degrees to achieve complete extinction over the whole grain. These grains were probably derived from low grade metamorphic

and igneous rocks. Other strained grains require a rotation of 10-45 degrees to achieve complete extinction, these probably being derived from higher grade metamorphic rocks. Fractured quartz grains also show a moderate degree of straining along the vicinity of shatter zones where they can be identified by the distinct alignment of the shattered quartz.

Polycrystalline quartz

Polycrystalline quartz grains display the greatest complexity of all the quartz grain types. They represent between 20-50 per cent of the total quartz present but this is to a certain extent governed by the grain size of the individual sample, i.e. the larger the mean grain size, the higher the percentage of polycrystalline quartz grains.

The greater percentage of the polycrystalline quartz appears to be metamorphic in origin; two main types can be distinguished although gradations exist between the two types;

1. High grade metamorphic polycrystalline quartz grains can be recognised by the highly welded nature between the unit contacts; these contacts are highly sutured suggesting a high degree of pressure solution at the contacts of quartz grains. They display a schistose structure, particularly in the coarse grains and are characterised by sutured and strained boundaries between the units. These elongated units can be equated with the strained quartz which require a rotation of 30-50 degrees to achieve complete extinction.
2. Low grade metamorphic polycrystalline quartz grains exhibit a smaller degree of straining and lack the schistosity of the high grade metamorphic quartz. These units, both coarse and fine, tend to be globular in outline but still display the characteristic sutured contacts between the units. Each quartz unit has a different optical orientation.

Other types of polycrystalline quartz include;

3. Rare fragments of myrmekitic quartz, which possibly implies derivation from a granite.

NUMBER	Strained	Unstrained	Polycrystalline
CH9	69.6%	0	30.4
CH10	72.0	0	28.0
CH11	53.6	0.7	45.7
CH12A	59.5	1.3	39.2
CH12B	65.9	6.5	27.6
CH13	51.5	2.5	46.0
E24	53.6	18.2	28.3
E25	58.3	11.8	29.9
E26	58.7	13.2	28.1
E27	64.4	12.4	23.2
E28	61.5	10.1	28.4
E29	67.1	7.8	25.1
E30	62.6	14.8	22.6
E31	45.8	29.5	34.7
E32	50.5	22.0	27.5
E33	55.3	14.8	29.9
E34	56.0	15.5	28.5
E35A	60.0	18.7	21.3
E35B	64.9	14.6	20.5
H60	59.0	17.9	23.1
H64	62.3	11.5	26.3
H65	69.1	11.3	19.6
H66	69.0	7.7	23.3
H70	52.7	6.8	40.5

TABLE 6.3 Ratio of Quartz types in the Hopeman Sandstone

4. Chert is frequently present and is normally stained by iron oxides; in some cases the microcrystalline quartz is seen to replace the micritic grade calcite. These chert fragments are therefore thought to represent derived fragments of silicified Old Red Sandstone cornstones which are exposed locally to the south of Elgin. Chertified sandstones are also probably Old Red Sandstone in origin.

Feldspar

Feldspar constitutes between 3-8 per cent of the total detrital components in the sheetflood deposits. Microcline is the most common feldspar and represents 80-90 per cent of the total feldspar. It is normally relatively unaltered although sericitisation may occasionally occur. Orthoclase makes up the remaining 10-20 per cent of the feldspar content; it appears to be more susceptible to weathering than the microcline and occurs as highly weathered, iron stained, cloudy feldspars. The total absence of plagioclase feldspar is probably due to the garnet grade metamorphism.

Rock fragments

Rock fragments constitute 4-35 per cent of the total detrital components of the sheetflood deposits. The percentage is again related to the grain size of the sample. This is because the rock fragments are dominantly quartz granulites so when they disaggregate to fine grain fragments, they are represented by single strained quartz and mica.

Quartz granulites can be recognised by their schistose strained quartz with sutured contacts and accessory mica. Some granulites also contain up to 10 per cent feldspar, the feldspar usually being microcline.

Rarely myrmekitic quartz and microcline rock fragments are present indicating derivation from a granitic source. Extremely rare cornstone and friable angular sandstones showing no pressure solution indicate derivation from the Old Red Sandstone.

Mica and clays

Mica constitutes up to 1 per cent of the detrital components of the

sheetflood deposits; muscovite is the only mica which has been identified and occurs in a highly weathered condition.

Clays are often associated with the micas, but they are normally stained by iron oxides and therefore difficult to identify in thin section.

Heavy minerals

Mackie (1925), Dunham (1952) and Peacock (1968) have made extensive studies of the heavy minerals in the Permo-Triassic sandstones of the Elgin district. A restudy of them was therefore not undertaken and the results of these authors are discussed in the following section together with some additional observations made by the author. These results also apply to the basal H2 barchan phase at Quarry Wood which were derived from the sheetflood deposits.

Zircon is the commonest heavy mineral and represents up to 50-60 per cent of the total heavy minerals present. Garnet and tourmaline are also relatively abundant although less abundant than in the underlying Old Red Sandstone. Monazite is present throughout. Mackie (1925) noted that hornblende topaz and anatase were present in all the samples studied whereas augite, enstatite and corundum were only present in some horizons.

The most common heavy minerals appear to be similar to those found in the Old Red Sandstone of the Elgin area (Mackie 1925). Although Mackie thought that the differences were relevant, close study shows that only the more easily weathered and less abundant heavy minerals are absent in the sheetflood deposits when compared to the Old Red Sandstone (Hornblende, epidote and augite). This would be expected as the heavy minerals are second cycle. Apatite appears to be uncommon in both sets of rocks.

AEOLIAN (Plate 6.1B) AND PLAYA DEPOSITS (Plate 6.1C)

Peacock (1968) noted the similarities between the sandstones of Quarry Wood and those exposed along the coast. Environmental studies suggest that the deposits are in part contemporaneous although the sandstones at Quarry Wood were deposited closer to the source area. Thus, although the aeolian sandstones of both localities show a similar petrology, the sheetflood and the

aeolian sandstones were derived from two different sources and show slightly different characteristics. These differences however are not great so this section will concentrate on the anomalies of these differing petrological characteristics.

Unstrained/strained quartz from both source areas show similar characteristics although there are minor differences. Myrmekitic quartz is completely absent from the aeolian sandstones whereas zoned quartz (probably from hydrothermal quartz veins) is only present in the aeolian deposits.

Polycrystalline grains from the aeolian sandstones show similar types to those of the sheetflood deposits. However, statistical analyses of the main types show that different percentages of each type are present.

	High Grade	Low Grade	Old Red Sandstone	
	Metamorphic		Chert	Fragments
Sheetfloods	63%	8%	17%	12%
Aeolian	33%	27%	25%	10%
Playa	46%	26%	16%	10%
Basal Barchan Dune	62%	18%	14%	6%

From this table, it can be seen that two different end members are present, these being the products of two different sources;

(a) Sheetfloods characterised by a large percentage of high grade metamorphic quartz and relatively low chert and low grade metamorphic quartz, and

(b) Aeolian deposits represented by equal amounts of high grade and low grade metamorphic quartz and relatively high chert content. Thus the importance of the high grade metamorphic rocks appears to have diminished in the source area of the aeolian deposits.

The values of the playa and basal barchan dune deposits appear to reflect intermediate values and were therefore presumably influenced by both sources as suggested in previous chapters.

Rock fragments also show marginally different properties in both deposits. In the aeolian sandstones, micaceous quartz granulites dominate the

rock fragment types; these are characterised by iron staining suggesting derivation from the Old Red Sandstone. Chertified arkosic sandstones are also much commoner than seen in the sheetflood deposits. Quartz feldspathic granulites are rarely present.

Feldspars are again dominantly microcline with subsiduary orthoclase. Little or no mica is present even in the playa deposits but when present it is always muscovite; there is thus a relative deficiency of mica compared to the sheetflood deposits.

Clay is completely absent from the aeolian deposits except where dune deposits have been contaminated by the overlying playa deposits; clays are present in the playa deposits in the form of silt galls but are not generally present in the matrix as is the case in the sheetflood deposits. These clays are characterised by iron oxide staining and minute fragments of angular quartz. Smallrhombs, which may be dolomite, are also present but the high degree of iron staining precludes any optical determinations.

Heavy minerals are much less common in the aeolian deposits compared to the sheetflood deposits. Dunham (1952) notes the common occurrence of zircon and tourmaline and more rarely rutile, garnet, anatase, leucoxene, magnetite, haemetite, corundum, kyanite and amphibole. Monazite appears to be the only relatively common heavy mineral not found in the aeolian deposits but found in the sheetflood deposits.

Thus, although there is not a great difference in the types of detrital components from each source, the relative percentage of each type does serve as an indication of the environment. Thus, mica and clay are almost completely absent from the aeolian deposits and they are also characterised by a much lower percentage of high grade metamorphic polycrystalline quartz and a higher percentage of micaceous quartz granulites.

ROUNDNESS AND SPHERICITY

Different environments stamp their individual properties of roundness on quartz grains. Sorby (1880)was probably the first to suggest that roundness

and sphericity could be useful in environmental interpretation. It is well known that beach sands are relatively less rounded than dune sands and that glacial sands are characterised by angular splinters of quartz. However, although these properties hold for grains of primary origin, grains of secondary origin may show two different characters or only characters of their primary origin. Thus, fluvial sands derived from aeolian sands may show totally uncharacteristic highly rounded grains. As the Hopeman Sandstones are thought to be partially derived from the Old Red Sandstone, this problem of secondary derivation is therefore particularly relevant.

Quantitive evaluation of the roundness and sphericity of quartz grains is however very difficult. One must also differentiate between sphericity and roundness, i.e. a quartz grain may be well rounded but have a low sphericity. Riley (1942) proposed a method of measuring sphericity by measuring the diameters of the inscribed and circumscribed circles. As sphericity is a measure of the approach to a spherical body, this equation was thought to be appropriate and was used to measure the sphericity for the Hopeman Sandstone;

$$\text{Sphericity} = \text{square root of } \frac{d_1}{d_2}$$

Where d_1 = diameter of inscribed circle

d_2 = diameter of circumscribed circle

Roundness is a measure of the curvature of the corners and the edges expressed as a ratio to the average curvature of the particle. Krumbein (1941) and Wadell (1932) proposed a method for measuring the roundness by drawing an image at a standard magnification and determining the radii of the inscribed circle and of the edges and corners of the image.

However the method is extremely tedious and time consuming considering the relevance of roundness as an environmental indicator. Powers (1953) devised a visual method in which he proposed six roundness classes ranging from very angular to well rounded. He also divided these into those showing high sphericity and those showing low sphericity.

A Roundness Scale (after Powers, 1953)

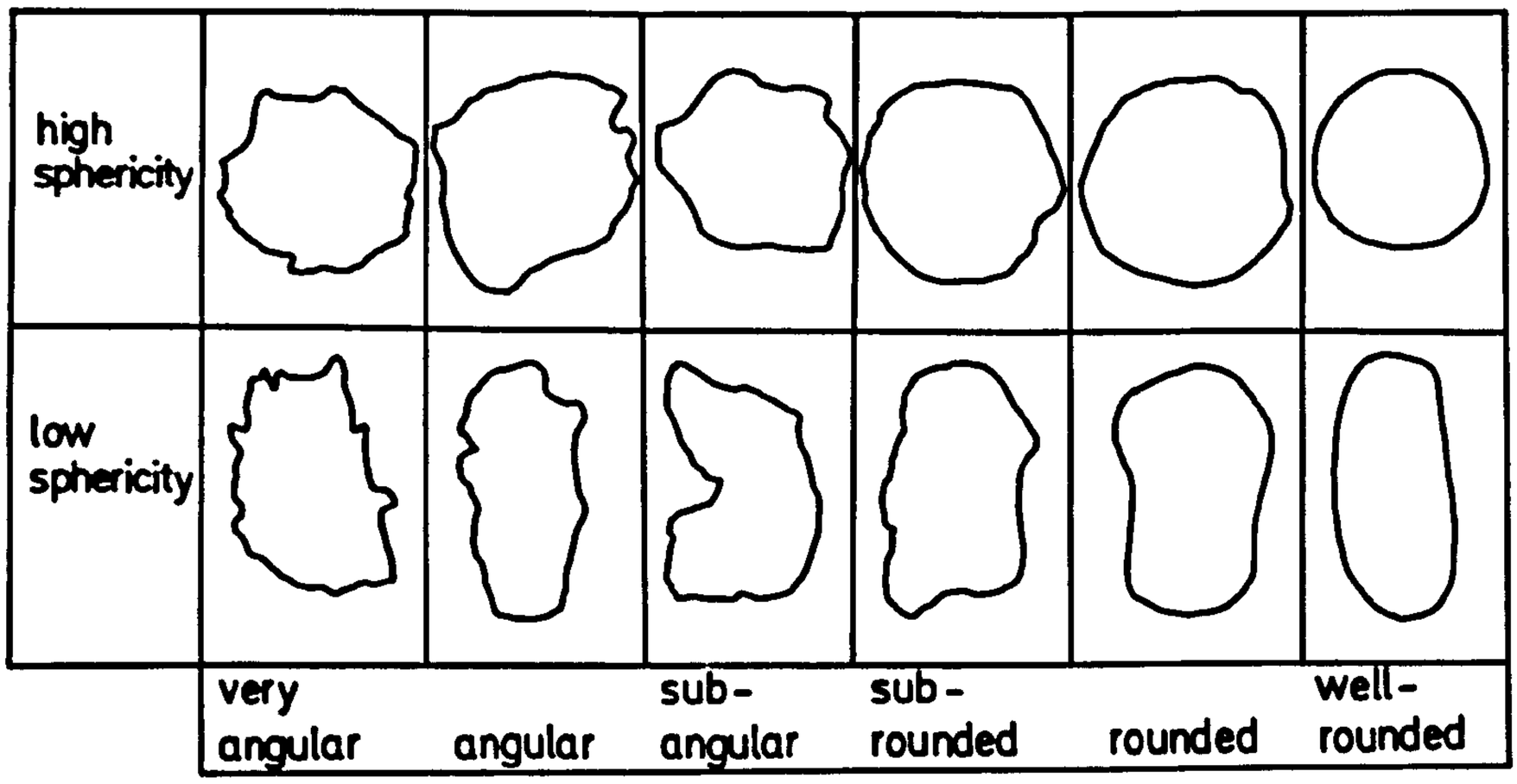

B Sphericity (after Riley, 1942)

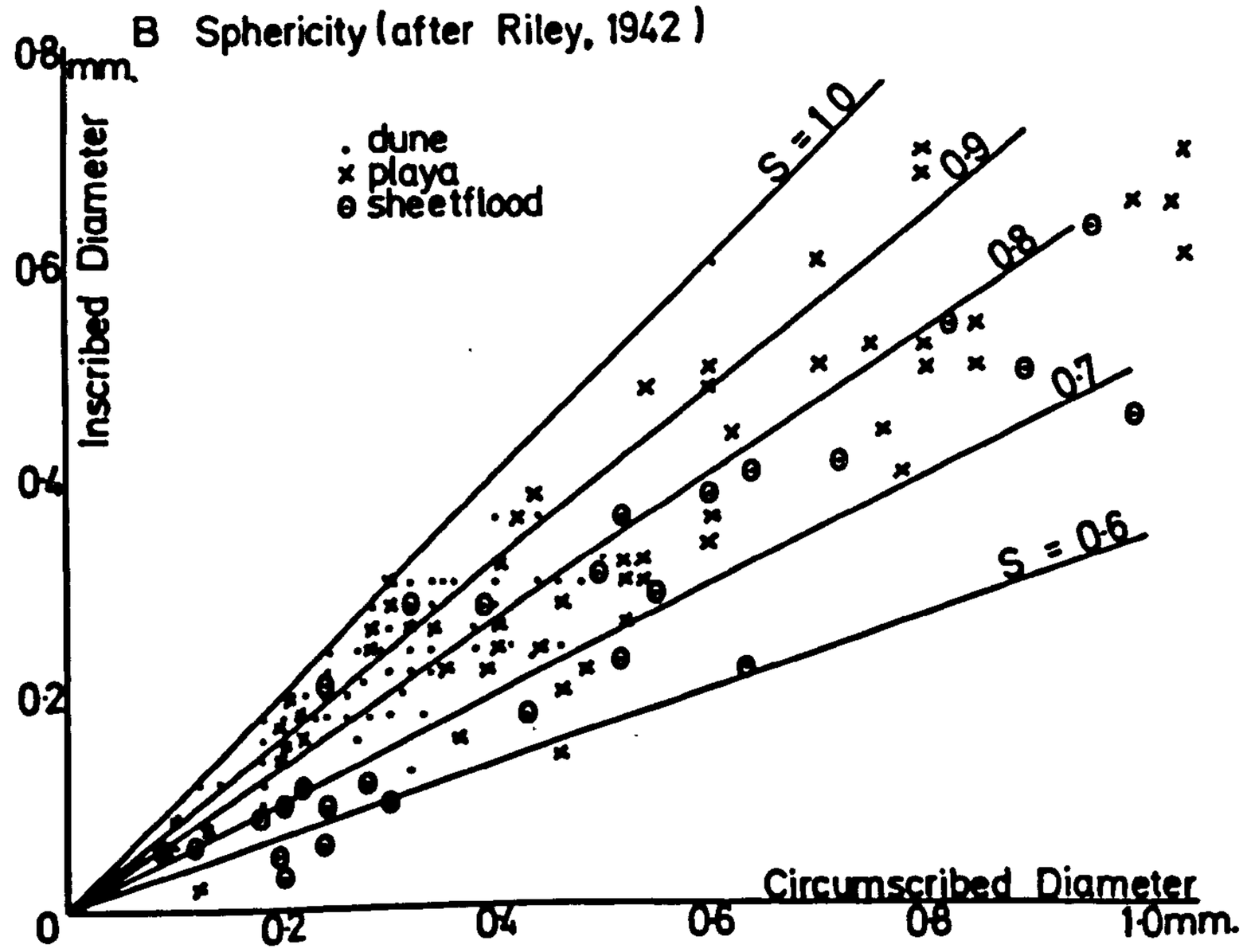

Fig. 6.6. Roundness and sphericity.

Fig. 6.6 shows the various sphericity values for aeolian, playa and sheetflood deposits of the Hopeman Sandstone. No readings below a grain size of 0·05 mm were used as Kuenen (1960) notes that below this size, the grains increase in angularity. Two hundred grains were studied for each environment using the standard point count technique and then each grain placed in a roundness class according to Powers (1953).

Aeolian sandstones range from sub rounded to well rounded but are dominantly in the rounded class. The sphericity is also extremely high as seen in Fig. 6.6. Playa deposits show both high sphericity and low sphericity grains and were dominantly sub rounded, although they range from sub angular to rounded. They are thought to have been mainly derived from the aeolian sandstones but abrasion during transport may have lowered their roundness; this low roundness value may also be due to contamination by some sheetflood grains.

Sheetflood deposits vary enormously in their roundness and sphericity properties. Many grains are well rounded and of a high sphericity whereas others are highly angular and of low sphericity, (Fig. 6.6). Contamination by aeolian grains may explain the high sphericity but it is thought to be more likely that the high sphericity is due to their second cycle origin.

GRAIN SIZE ANALYSIS

The relevance of grain size analysis to define the textural attributes characterising sedimentary rocks was first discovered by Trask (1932). Since that time, many authors have objected to the use of the Trask coefficients on theoretical grounds with the result that two new methods of calculating grain size results have been introduced; these are the phi method of Inman (1952) and the inclusive graphic method of Folk and Ward (1957). These methods are based on the geometry of the normal curve and, on theoretical grounds, should more adequately describe the characteristics of sediments than the coefficients of Trask.

In recent years, various sedimentologists have published conflicting opinions on the environmental sensitivity of the textural parameters relating to grain size analysis (mean diameter, standard deviation, skewness and kurtosis). To take an example, it is generally acknowledged that inland dunes are characterised by a positive skewness; however, if the source area of the dunes is characterised by sediments with a dominantly negative skewness and the dunes are local in origin, the dunes may also have a negative skewness. Thus, although the textural parameters are effective in differentiating environments in general, too much emphasis must not be placed solely on these results. However, if the importance of the provenance, mode of deposition and diagenesis of the sandstones is taken in conjunction with the results from grain size analysis, grain size textural parameters may be taken as environmental indicators.

Method

The samples were first of all treated with concentrated Hydrochloric Acid to remove any possible calcium carbonate cement in the samples. Sandstones which were cemented by fluorite and barytes were not used in the grain size analyses. The samples were then dried in ovens for 24 hours prior to sieving. The samples were analysed at quarter phi intervals using an automatic siever.

The weight percentages of the phi distributions were then calculated and plotted as a cumulative curve. The 5th, 16th, 25th, 50th, 75th, 84th and 95th percentiles were then read from the cumulative curve and used to calculate the standard deviation, mean diameter, skewness and kurtosis from the following formulae of Folk and Ward (1957). These formulae were preferred as the inclusion of the 5th and 95th percentiles provided greater accuracy:

$$\text{Mean Diameter (M.D.)} = \frac{p_{16} + p_{50} + p_{84}}{3}$$

$$\text{Standard Deviation (S.D.)} = \frac{p_{84} - p_{16}}{4} + \frac{p_{95} - p_5}{6{\cdot}6}$$

$$\text{Skewness (Sk.)} = \frac{p_{16} + p_{84} - 2p_{50}}{2(p_{84} - p_{16})} + \frac{p_5 + p_{95} - 2p_{50}}{2(p_{95} - p_5)}$$

$$\text{Kurtosis (kg.)} = \frac{p_{95} - p_5}{2{\cdot}44(p_{75} - p_{25})}$$

$$\text{Kg'} = \frac{\text{Kg}}{\text{Kg} + 1}$$

where p_5, p_{16}, etc., are the grain sizes in phi units ($-\text{Log}_2$ of grain size in millimetres) corresponding to the 5th and 16th percentiles on the cumulative curve of the grain size distribution. Folk and Ward (1957) have also modified Inman's (1952) sorting classification which is used here.

INTERVAL		SORTING DESIGNATION
Less than	0·35	Very well sorted
	0·35–0·50	Well sorted
	0·50–1·00	Moderately sorted
	1·00–2·00	Poorly sorted
	2·00–4·00	Very poorly sorted
Greater than	4·00	Extremely poorly sorted

Sheetflood deposits

The mean diameter of the sheetflood deposits varies from -2·5 phi to 2·15 phi (Fig. 6.7 and Table 6.4A) and is dependent on the proportion of the gravel fraction present in the sample. The highly variable nature can clearly be seen in Fig. 6.8 where the grain size ranges from -7 to +4 phi (Plate 6.1A). This variability is also seen in the standard deviation which indicates that the sheetflood deposits are poorly to very poorly sorted. This is a reflection of the high sediment water ratio which does not favour good sorting of the sediment. Skewness is generally negative indicating the

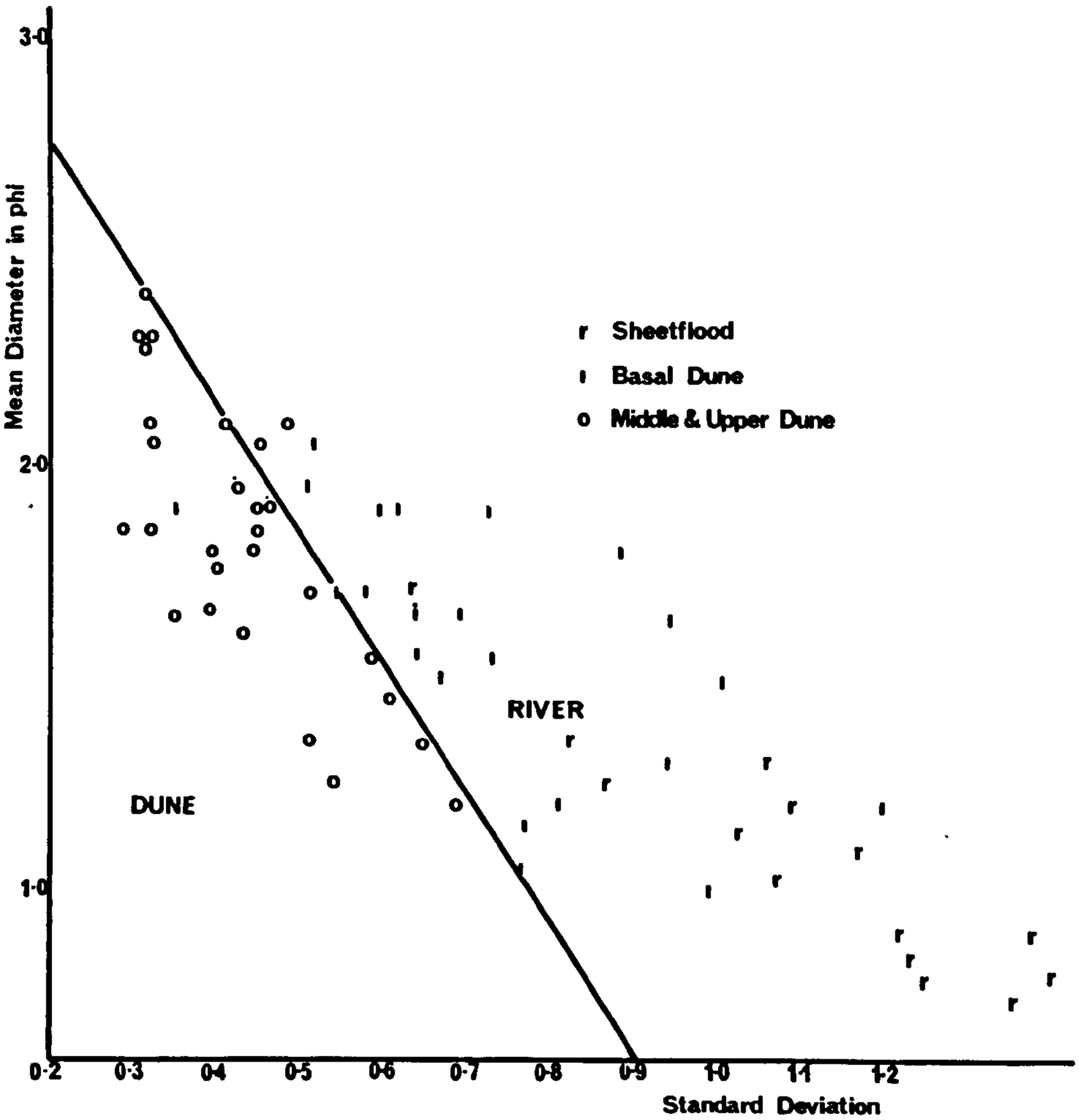

Fig. 6.7. Standard deviation plotted against the mean diameter for the barchan dunes and the sheetflood deposits of the Hopeman Sandstone.

Number	phi percentiles 5th	16th	25th	50th	75th	84th	95th	St.D.	Sk.	Kg'.	Mean Diam.
Sheetfloods											
RQ2-3	0.5	1.25	1.70	2.30	2.70	2.90	3.30	0.84	-0.28	0.55	2.15
RQ2-4A	-2.75	-1.50	0.50	2.45	2.65	2.90	3.50	2.05	-0.73	0.54	1.30
RQ2-4B	-7.00	-6.50	-6.00	-3.50	2.40	2.45	2.90	3.75	+0.32	0.53	-2.50
QW2-6	-0.90	0.10	0.70	1.60	2.35	2.50	3.20	1.22	-0.23	0.51	1.40
QW2-2	-4.50	-3.50	-2.50	2.20	2.50	2.65	3.25	2.81	-0.79	0.39	0.40
H2 Basal Barchan Dune											
H1F28	-1.50	-0.50	0.10	1.20	2.10	2.35	3.10	1.41	-0.36	0.49	1.00
H1F42	-0.80	-0.63	0.85	1.30	1.90	2.30	2.65	0.94	-0.03	0.57	1.00
H1F23	0.10	0.55	0.80	1.70	2.40	2.80	3.60	1.10	+0.03	0.39	1.70
H1F47	-5.00	-4.00	-3.00	-1.00	0.80	2.00	3.10	2.70	+0.06	0.47	-1.00
H1F26	-0.25	0.10	0.20	0.50	1.10	2.00	4.10	1.05	+0.52	0.66	0.90
H1F27	-0.90	0.10	0.70	1.15	1.75	2.30	3.25	1.20	+0.03	0.62	1.20

TABLE 6.4A. Grain size analyses of the sheetflood and basal H2 barchan dune deposits.

Number	phi percentiles 5th	16th	25th	50th	75th	84th	95th	St.D.	Sk.	Kg.	Mean Diam.
Playa											
H2F36C	-1.45	-0.25	1.25	2.10	3.00	3.45	5.30	1.95	-0.16	0.61	1.90
H2F36D	0.05	0.50	1.05	1.80	2.60	2.95	3.75	1.08	+0.07	0.49	1.75
H2F36B	0.10	0.80	1.30	1.90	2.70	3.30	4.80	1.34	+0.17	0.58	2.00
H2F36A	0.80	1.20	1.35	1.70	2.10	2.40	3.25	0.67	+0.25	0.58	1.50
H2F37A	0.20	0.75	1.00	1.50	2.35	3.20	5.00	1.34	+0.62	0.59	1.85
H2F37B	0.40	0.80	0.95	1.25	2.05	2.45	3.30	0.85	+0.41	0.52	1.35

TABLE 6.4B. Grain size analyses of the playa deposits (upper H2 phase).

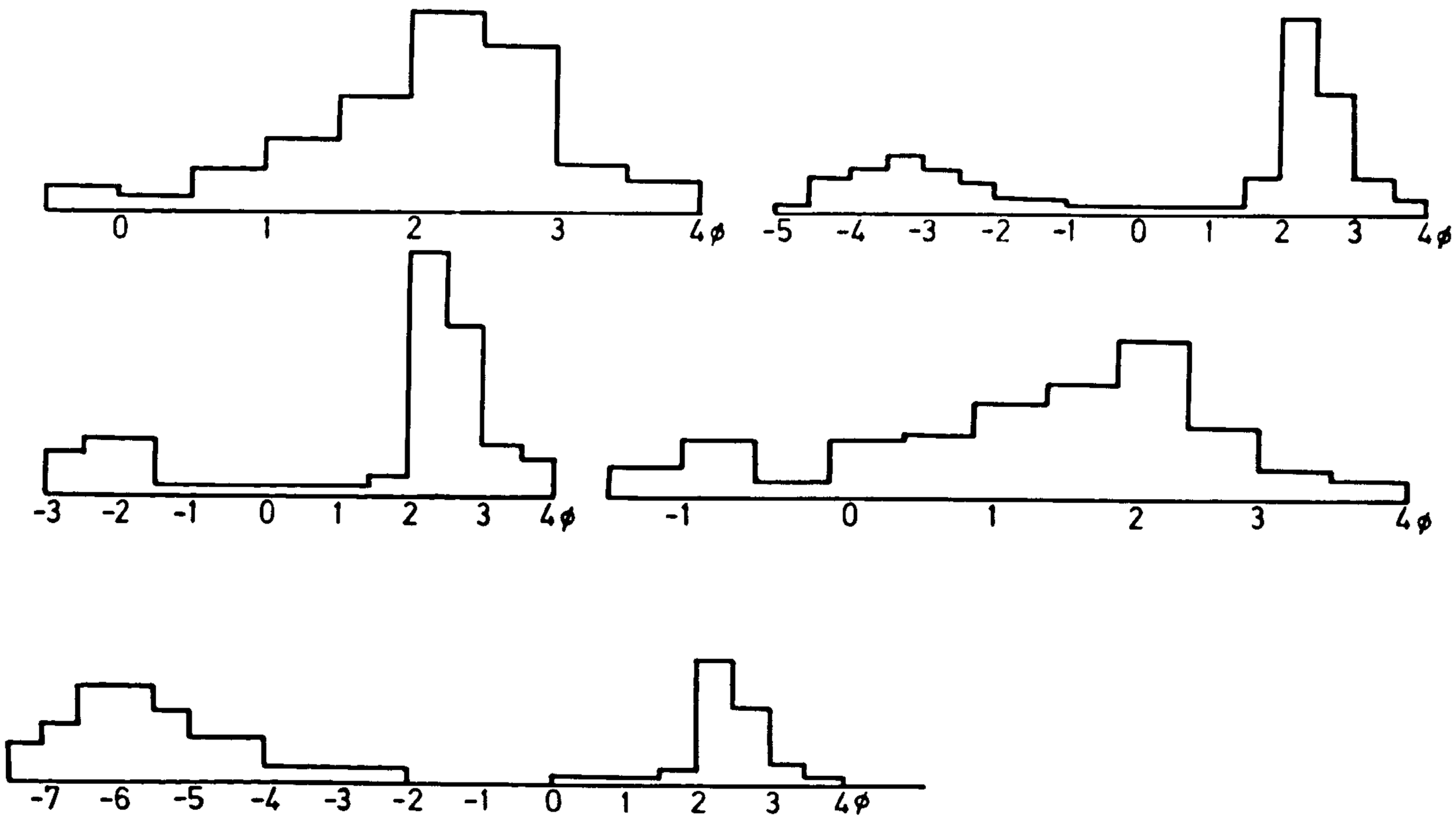

Fig. 6.8. Grain size histograms of the H1 sheetflood deposits.

large amount of and range of fine material in the sediments. One sample however is markedly positive indicating a concentration of coarse material in the sediments and a relative deficiency of fine material.

Histograms show that the sheetflood sediments possess a bimodal character; the finer mode remains constant between 2·0-2·5 phi whereas the coarser mode is highly variable but is generally in the gravel mode. The fine mode approximately corresponds to the mode seen in the unimodal dune sandstones and may represent reworked dune sands incorporated into the sheetflood deposits. The coarse material is brought into the area by the sheetfloods from the source area to the south, the variable coarse mode being dependent on the amount of coarse material present in the sample.

Extremely coarse sandstones seen in the basal deposits of the H2 barchan dunes at Covesea have similar grain size characteristics as the sheetflood deposits (Fig. 6.7). They are unusually poorly sorted for dune sediments and their bimodal nature is similar to deflation sediments described by Folk (1968). Folk suggests that these sediments may be deposited in periodic sheetfloods in the inter-dune areas. The similarity of the two deposits can thus be explained by postulating that the basal dune deposits of the H2 phase are relic inter dune deposits derived from the sheetflood deposits.

Playa deposits

Grain size analyses (Table 6.4B) of the playa lake deposits show a remarkable similarity to those of the dune sandstones. This is seen in Fig. 6.9 when skewness is plotted against the median diameter. The two grain size analyses can however be differentiated by their standard deviation, this being a reflection of the larger grain size limits seen in the playa lake deposits. The poorer sorting is due to the additional fine material brought in from the source area by the sheetfloods and the coarse inter dune material. However the greater percentage of the playa sediments appear to be aeolian derived material which were incorporated into the floodwaters.

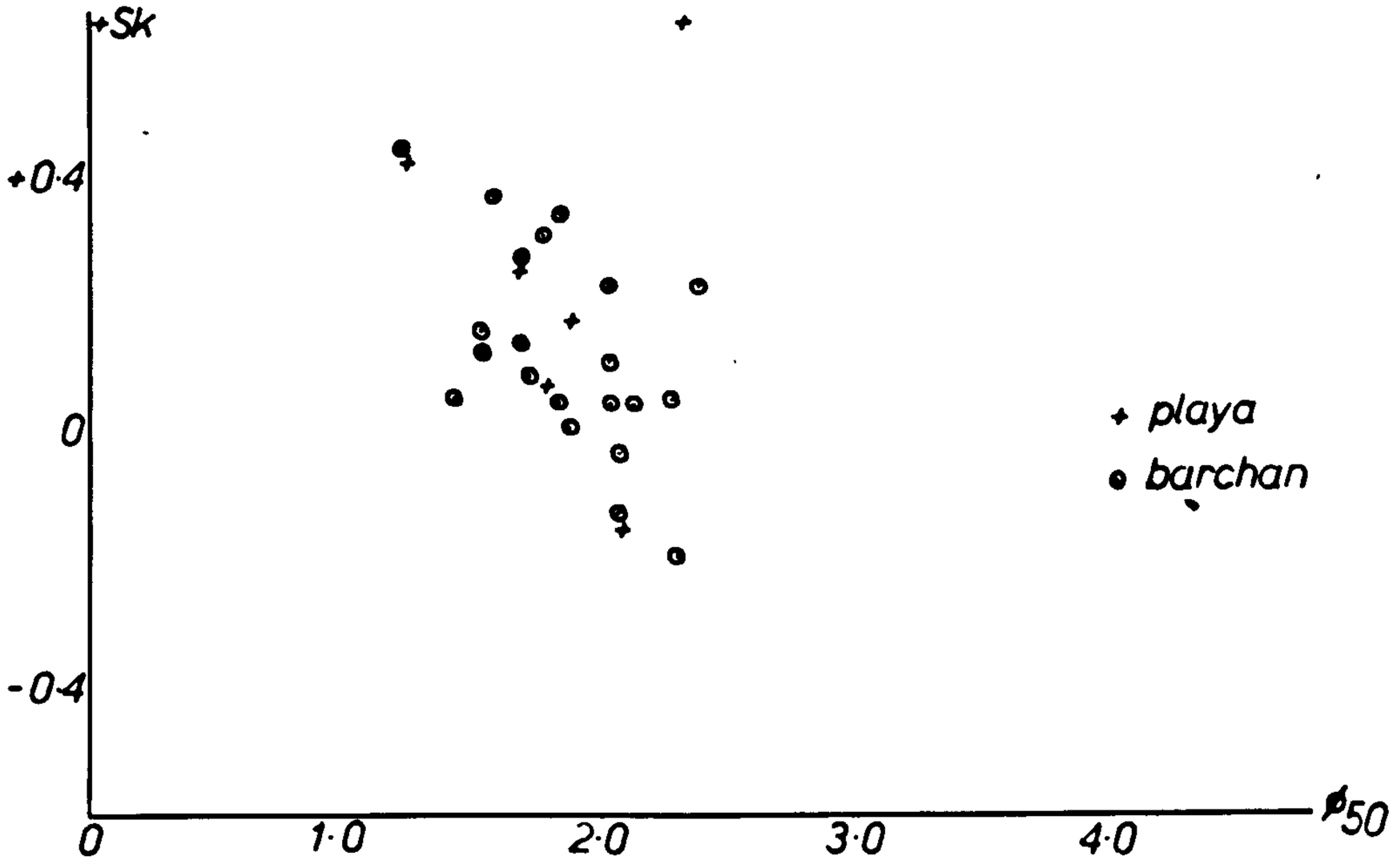

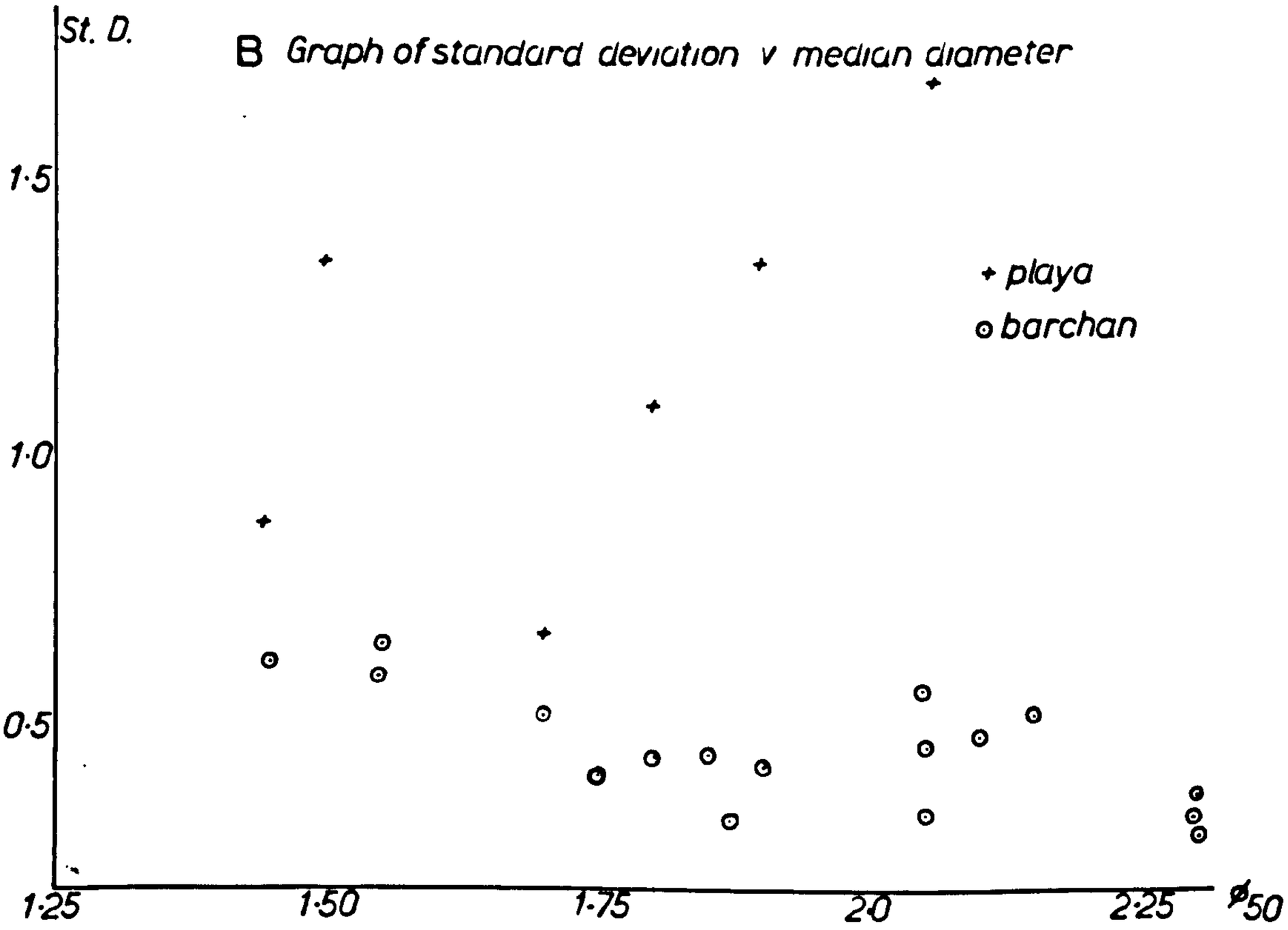

Fig. 6.9. Comparison of the playa and barchan dune deposits of the Hopeman Sandstone.

Number	5th	16th	25th	50th	75th	84th	95th	St.D.	Sk.	Kg.	Mean Diam.
Seif Dunes											
H1C18	0.80	1.15	1.30	1.75	2.25	2.45	2.90	0.64	+0.09	0.48	1.8
H1S35	1.60	1.65	1.70	1.85	2.05	2.20	2.45	0.27	+0.30	0.51	1.9
H1C1	0.12	0.20	0.70	1.45	2.15	2.40	3.10	0.89	-0.02	0.46	1.35
H1S2	1.50	1.65	1.70	1.90	2.30	2.50	3.10	0.45	+0.38	0.52	1.95
H1S3	1.75	1.95	2.10	2.30	2.50	2.60	2.75	0.31	-0.14	0.50	2.30
H1S12	1.25	1.45	1.60	1.80	1.95	2.10	2.75	0.39	+0.09	0.64	1.80
H1S13	1.40	1.60	1.70	1.90	2.30	2.40	3.00	0.46	+0.24	0.52	1.95
H1S11	1.50	1.80	1.90	2.10	2.15	2.35	2.70	0.32	-0.04	0.67	2.10
H1S9	1.20	1.70	1.85	2.15	2.35	2.50	2.90	0.46	+0.12	0.58	2.15
H1C16	0.25	0.75	1.00	1.45	1.90	2.15	2.45	0.68	-0.04	0.50	1.45
H1S8	1.55	1.80	1.90	2.10	2.45	2.70	2.85	0.42	+0.30	0.50	2.20

TABLE 6.5. Grain Size Analysis of H1 Seif Dunes.

This interpretation is substantiated by the similarity of the median grain size and the positive skewness of the playa deposits, normally a characteristic of aeolian sands. Sorting is however much poorer than in aeolian deposits, the playa sediments being moderately to poorly sorted. This is a reflection of the poorer sorting qualities of water compared to wind and also the broader grain size range of the playa deposits. (Plate 6.1C).

Seif Dunes

Table 6.5 shows the grain size analyses obtained from the H1 seif dune sediments. Mean grain size of the seif dunes varies between 1.45 and 2.3 phi but is generally near to 2.0 phi. Standard Deviation indicates that the sediments are normally very well sorted to well sorted, although where contorting has occurred, the sediments may only be moderately sorted. Well sorted laminae of different mean grain sizes are mixed together to form a less well sorted sediment. Kurtosis is highly variable but is normally meso-kurtic to lepto-kurtic.

Comparison of the results with those of modern day seif dunes described by McKee and Tibbitts (1964) shows that the majority of the samples from the Hopeman Sandstone seif dunes represent the high angle strata rather than the low angle strata, i.e. foresets deposited close to the crest of the seif dune rather than the flank of the seif dune (Fig. 6.10). Similar seif dunes described by Folk (1971) from the Australian deserts also suggests that these deposits of the H1 seif dunes exposed at the present day represent the crest of the dune rather than the flank. This interpretation is substantiated by the sedimentary structures. Sorting is generally better on the crests of the dunes and the grain size also tends to be coarser (Fig. 6.11). The positive skewness so characteristic of aeolian dune deposits is due to the removal of the fine fraction in suspension by the wind.

Barchan Dunes

The three main units (Lower, Middle and Upper) of the barchan dunes which were recognised by means of their sedimentary structures can also be differentiated by grain size analysis (Figs. 6.13, 6.14, Table 6.6).

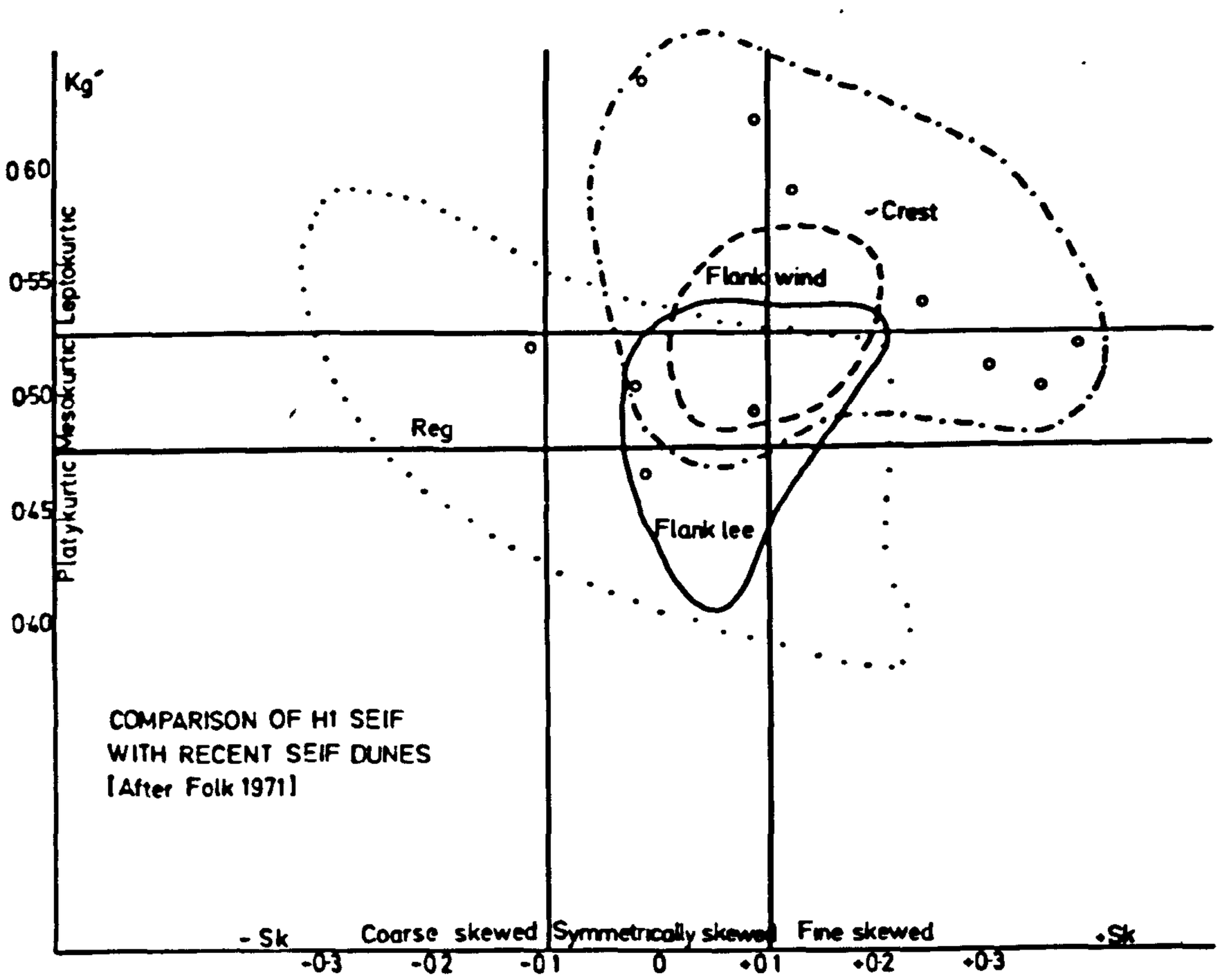

Fig. 6.10. Comparison of the grain size characteristics of the H1 seif dunes with recent seif dunes from Australia.

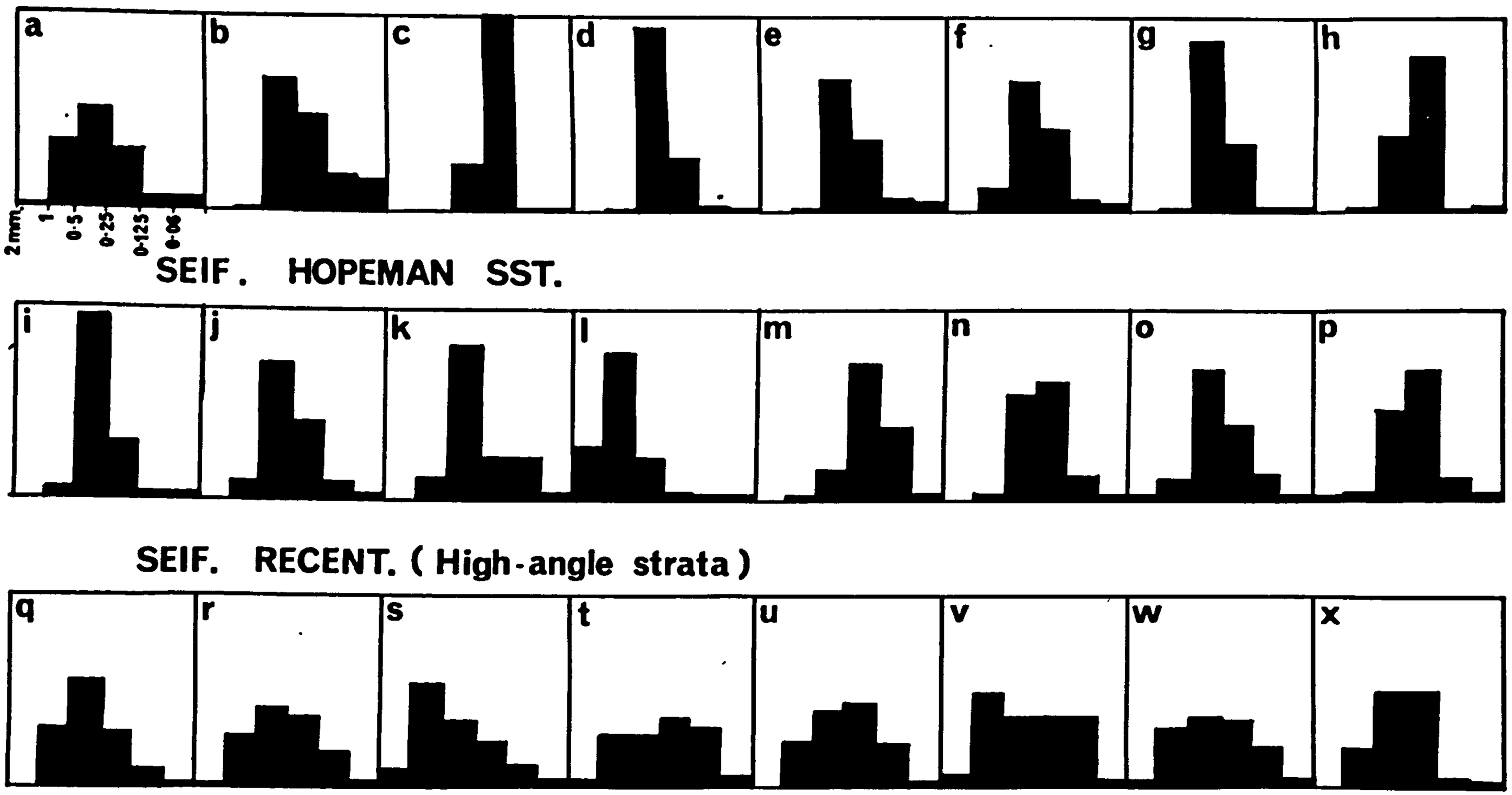

Fig. 6.11. Comparison of the grain size characteristics of the H1 seif dunes with recent seif dunes from Libya described by McKee and Tibbitts(1962).

Number	phi percentiles 5th	16th	25th	50th	75th	84th	95th	St.D.	Sk.	Kg.
Upper Barchan Unit										
H2P29	0.80	1.20	1.30	1.70	2.05	2.20	2.70	0.54	+0.03	0.51
H2P48	1.10	1.35	1.55	1.95	2.35	2.45	2.65	0.51	-0.19	0.44
H2P1	1.50	1.80	1.90	2.10	2.15	2.35	2.70	0.32	-0.04	0.67
H2P3	0.60	0.85	1.10	1.40	2.00	2.20	2.60	0.64	+0.19	0.47
H2P4	1.30	1.60	1.70	1.90	2.20	2.30	2.45	0.35	+0.05	0.48
H2P5	1.65	1.95	2.05	2.30	2.55	2.65	2.85	0.32	+0.04	0.49
Middle Barchan Unit										
H2B9	2.05	2.10	2.20	2.40	2.50	2.70	3.30	0.34	+0.22	0.59
H2B10	1.20	1.55	1.80	2.05	2.40	2.65	3.10	0.56	+0.10	0.58
H3B4	1.40	1.70	1.75	2.05	2.25	2.35	2.50	0.33	-0.13	0.47
H3B34	1.50	1.60	1.70	1.85	2.15	2.25	2.60	0.33	+0.34	0.50
H3B35	1.45	1.70	1.75	2.05	2.40	2.60	3.00	0.46	+0.22	0.49
H3B9	1.20	1.55	1.60	1.85	2.15	2.35	2.85	0.45	+0.05	0.55

TABLE 6.6. Grain Size Analysis of Barchan Dunes.

Number	phi percentiles 5th	16th	25th	50th	75th	84th	95th	St.D.	Sk.	Kg.
Middle Barchan Dune (continued)										
H3B47	1.15	1.55	1.60	1.80	2.05	2.30	3.00	0.44	+0.31	0.63
H3B48	1.65	1.95	2.05	2.30	2.45	2.50	2.80	0.31	-0.20	0.54
H3B50	1.10	1.30	1.40	1.70	2.10	2.30	2.90	0.52	+0.26	0.51
H3B52	1.10	1.40	1.50	1.75	2.05	2.20	2.45	0.40	+0.08	0.50
H3B53	1.35	1.60	1.80	2.10	2.40	2.45	3.10	0.48	-0.02	0.54
H3B54	1.35	1.60	1.85	2.15	2.45	2.60	3.10	0.52	+0.02	0.54
H2B49	1.10	1.40	1.45	1.65	1.95	2.10	2.55	0.39	+0.36	0.54
H2B51	0.60	0.85	1.00	1.45	1.90	2.10	2.55	0.62	+0.05	0.48
H2B52	0.65	0.95	1.15	1.55	2.00	2.35	2.65	0.65	+0.12	0.49
H2B53	0.75	1.05	1.20	1.55	1.90	2.25	2.65	0.59	+0.16	0.53
H4B-9	1.70	2.00	2.10	2.35	2.50	2.70	3.10	0.38	+0.04	0.58
H2B-5	1.65	1.95	2.05	2.30	2.55	2.65	2.85	0.32	+0.04	0.49
Lower Barchan Dune										
H2P36	0.60	0.90	1.10	1.55	2.00	2.20	2.65	0.64	+0.06	0.48
H2P37	0.45	0.80	1.05	1.55	2.00	2.15	2.55	0.73	-0.08	0.48
H4P10	0.30	0.95	1.50	1.65	2.55	2.80	3.45	0.94	+0.02	0.55

TABLE 6.6 (continued). Grain Size Analysis of Barchan Dunes.

Number	phi percentiles 5th	16th	25th	50th	75th	84th	95th	St.D.	Sk.	Kg.
Lower Barchan Dune (continued)										
H3P12	0.60	0.95	1.15	1.90	2.35	2.50	2.80	0.73	+0.012	0.43
H3P13	1.10	1.30	1.45	1.70	2.10	2.40	3.10	0.58	+0.34	0.55
H2P7	-0.65	-0.05	0.30	1.00	1.60	1.90	2.65	0.99	-0.04	0.51
H2P32	0.40	0.65	0.85	1.80	2.20	2.45	3.25	0.88	-0.13	0.45
H2P43	0.90	1.10	1.20	1.65	2.15	2.40	2.85	0.63	+0.17	0.46
H2P44	0.90	1.30	1.50	1.90	2.25	2.45	2.90	0.59	+0.02	0.52
H2P45	0.60	0.95	1.10	1.65	2.10	2.35	2.75	0.68	+0.01	0.47
H2P46	1.00	1.30	1.45	1.90	2.35	2.45	2.65	0.51	-0.19	0.44
H2P47	0.20	0.55	0.70	1.15	1.75	2.05	2.85	0.74	+0.24	0.51
H3P48	0.15	0.55	0.75	1.50	2.40	2.70	3.25	1.01	+0.12	0.42
H3P10	0.25	0.65	0.85	1.20	1.95	2.35	2.90	0.83	+0.32	0.50
H3P11	0.90	1.45	1.65	2.05	2.35	2.45	2.70	0.52	-0.23	0.39
H3P51	0.35	0.60	0.75	1.05	1.80	2.20	2.75	0.76	+0.33	0.47
H2P1	0.12	0.20	0.70	1.45	2.15	2.40	3.10	0.89	-0.02	0.46

TABLE 6.6 (continued). Grain Size Analysis of Barchan Dunes.

Number	phi percentiles 5th	16th	25th	50th	75th	84th	95th	St.D.	Sk.	Kg.
Contorted Barchan Dunes										
H2C27	0.15	0.45	0.80	1.20	1.75	1.90	2.30	0.69	-0.07	0.48
H2C30	1.20	1.60	1.70	1.95	2.25	2.40	2.70	0.43	+0.06	0.53
H2C25	0.10	0.55	0.95	2.15	2.25	2.45	3.00	0.92	-0.08	0.47
H2C18	0.60	0.95	1.05	1.35	1.75	1.95	2.40	0.52	+0.18	0.51
H2C19	0.60	0.80	0.90	1.25	1.65	1.90	2.35	0.54	+0.22	0.49
H2C20	1.00	1.30	1.40	1.65	1.85	1.95	2.35	0.35	+0.02	0.55
H2C22	1.00	1.20	1.35	1.60	1.90	2.05	2.45	0.43	+0.12	0.50
H2C42	0.30	0.70	1.05	1.45	1.85	2.00	2.45	0.66	-0.11	0.53
H2C50	0.60	0.85	1.05	1.35	1.90	2.20	2.70	0.65	+0.29	0.50
H2C41	0.90	1.20	1.40	1.70	2.05	2.35	3.05	0.61	+0.19	0.58
H2C21	0.60	0.80	0.90	1.25	1.80	2.30	3.05	0.76	+0.42	0.53
H2C32	-0.25	0.50	0.80	1.40	2.50	3.10	4.80	1.39	+0.32	0.55
H2C44	0.20	0.75	1.10	1.70	2.50	2.95	3.50	1.05	+0.11	0.49

Fig. 6.7. Grain Size Analyses of the H2 Barchan Contorted Dunes.

EXPLANATION OF PLATE 6.1.

PETROGRAPHY OF THE HOPEMAN SANDSTONE

A. Sheetflood deposits illustrating the poor sorting and angular nature of the detrital grains. Only poor evidence of quartz overgrowths is present but perfect overgrowths occur on the detrital feldspars. Clays are frequently present in the matrix together with rare micas. Crossed nicols.

B. Barchan dune sandstone illustrating the good sorting and relatively more rounded nature of the detrital grains. Overgrowths on both quartz and feldspar are common but there is little evidence of micas or clays being present. Unimodal quartz is more abundant than in the sheetflood deposits. Crossed nicols.

C. Playa deposits showing all the characteristic features of dune sandstones but also showing the presence of mica and clay in the groundmass. Crossed nicols.



A

1mm.

0

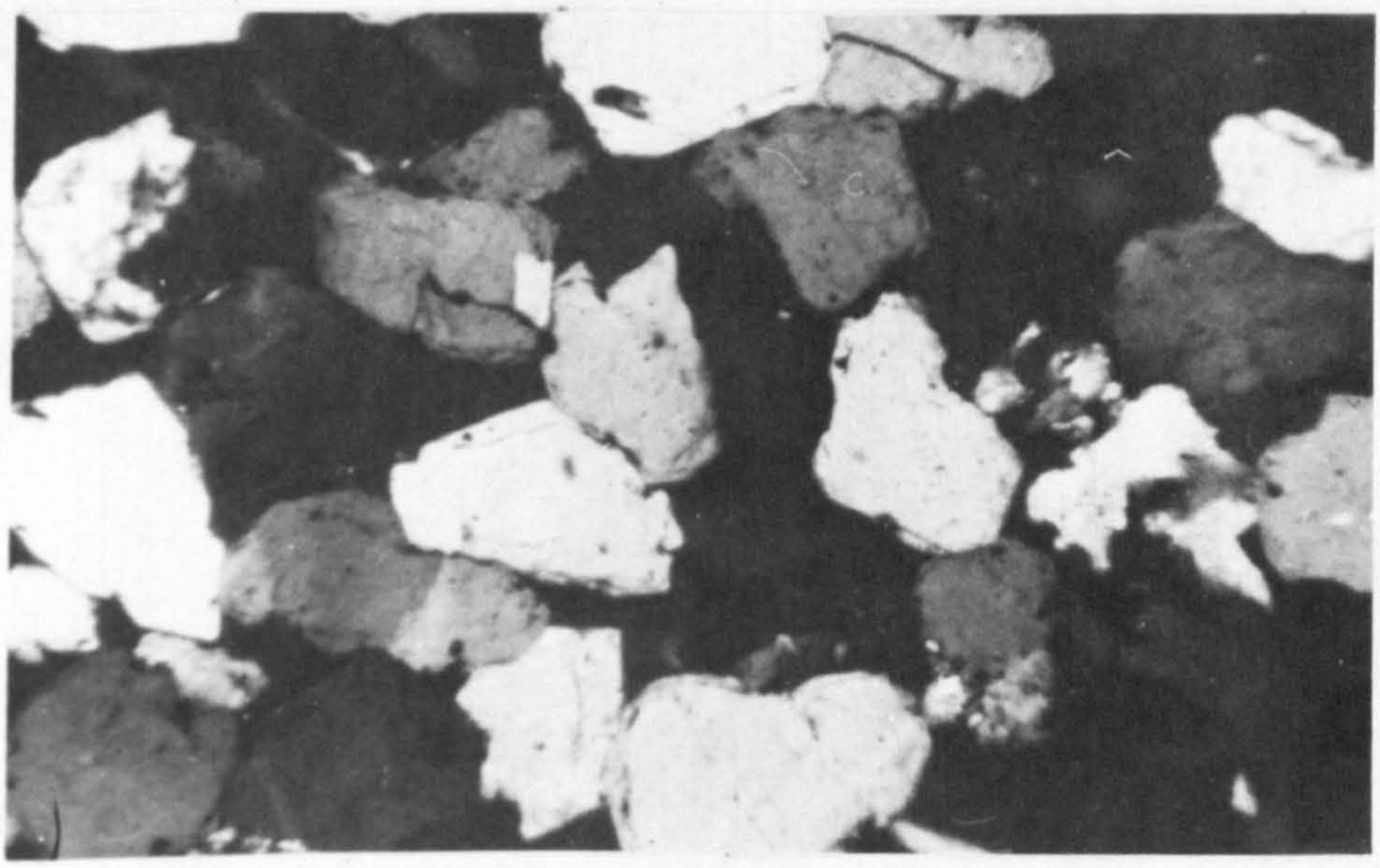

B

1mm.

0

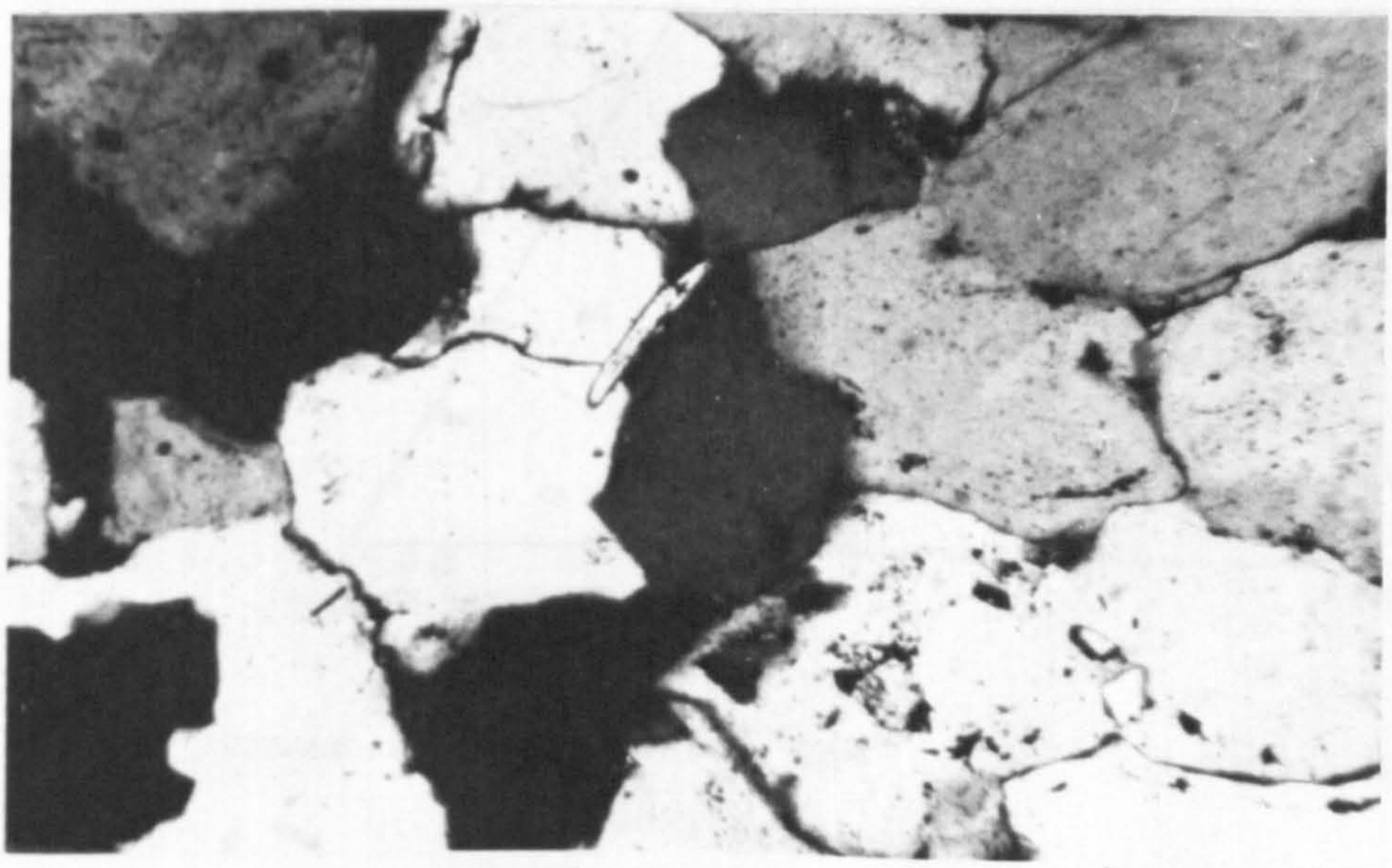

C

1mm.

0

PLATE 6·I

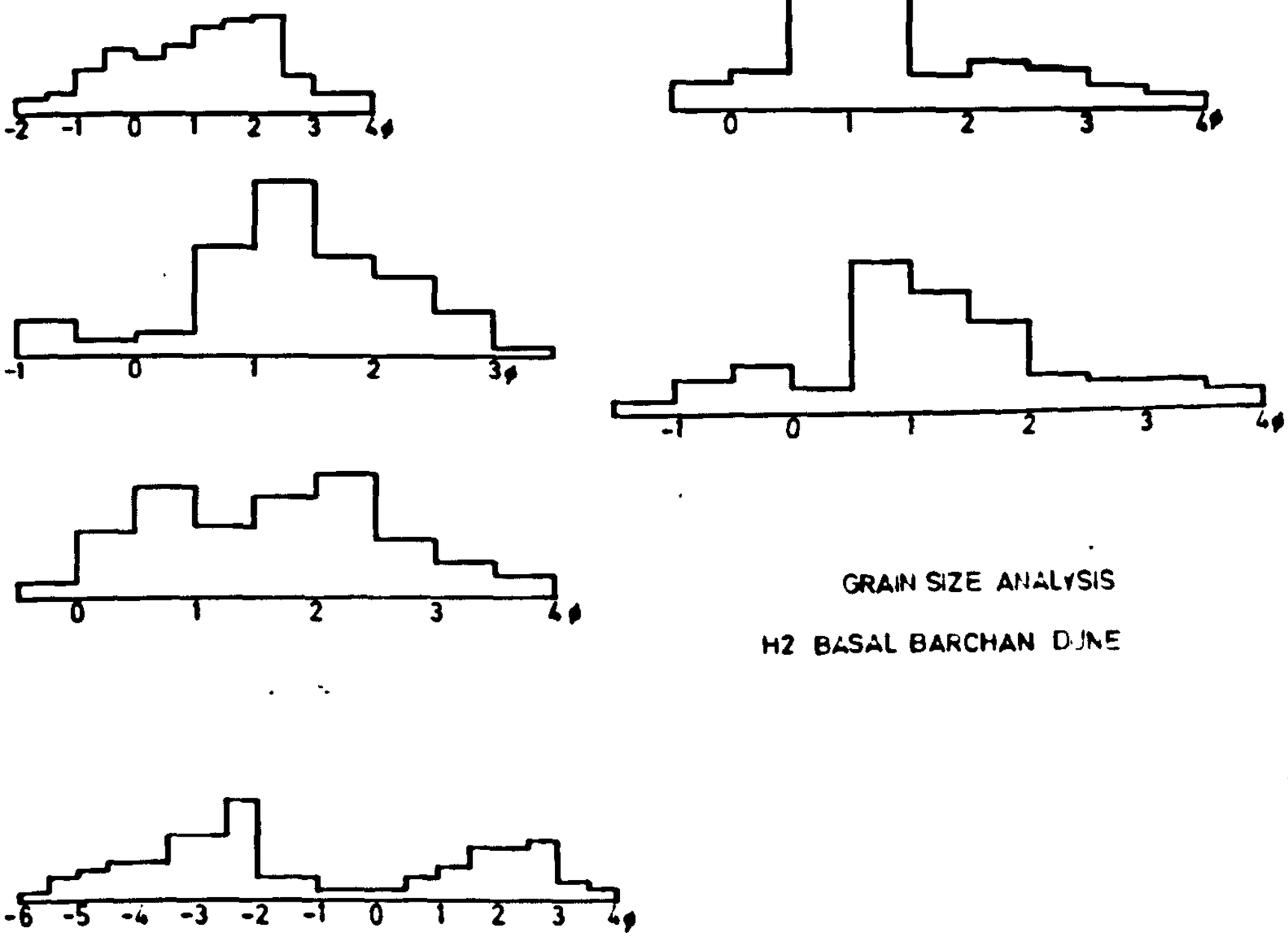

Fig. 6.12. Grain size characteristics of the basal barchan dune.

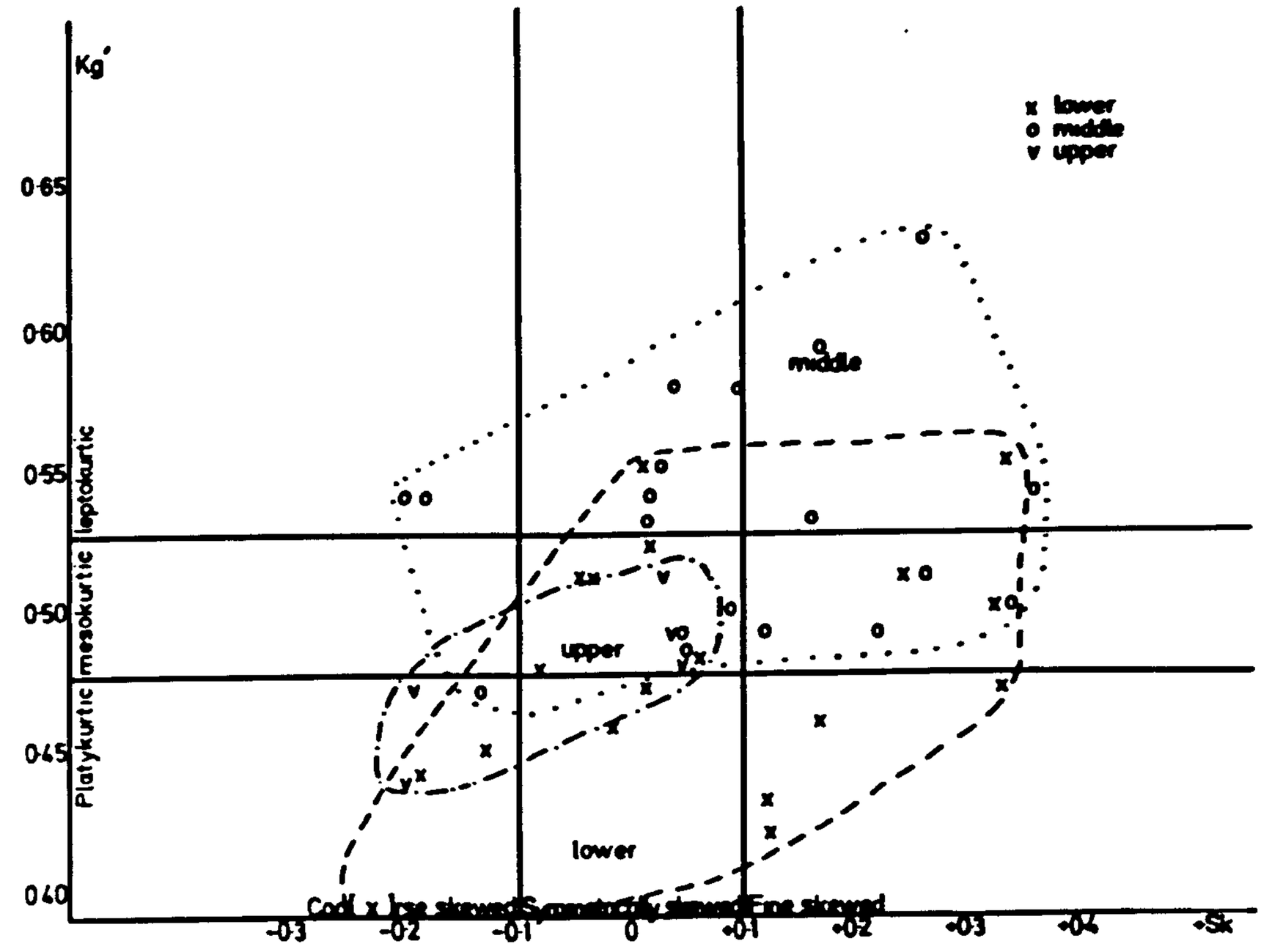

A. Kurtosis v Skewness

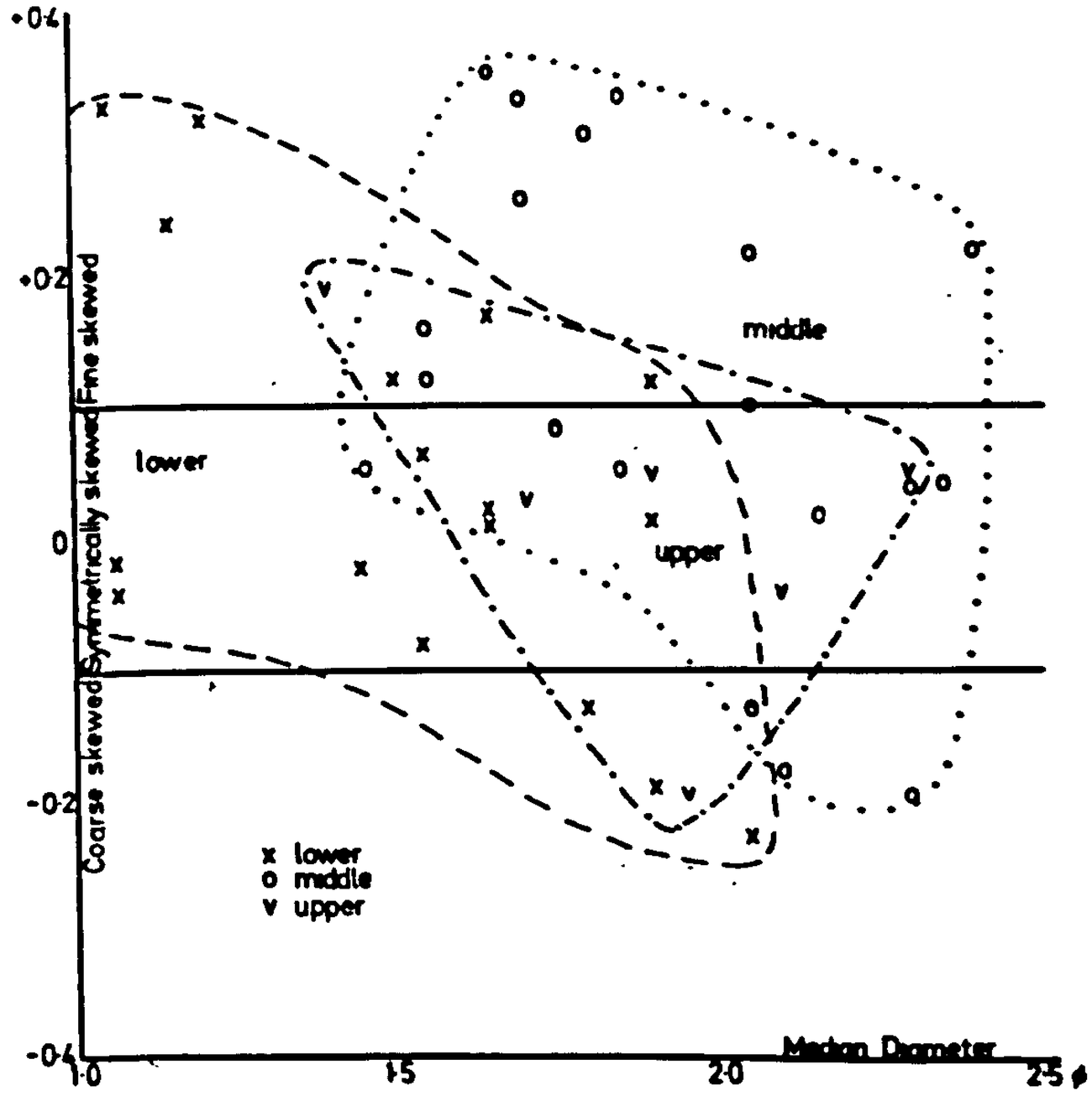

B. Skewness v Median diameter

Fig. 6.13. Differentiation of the three barchan dune units.

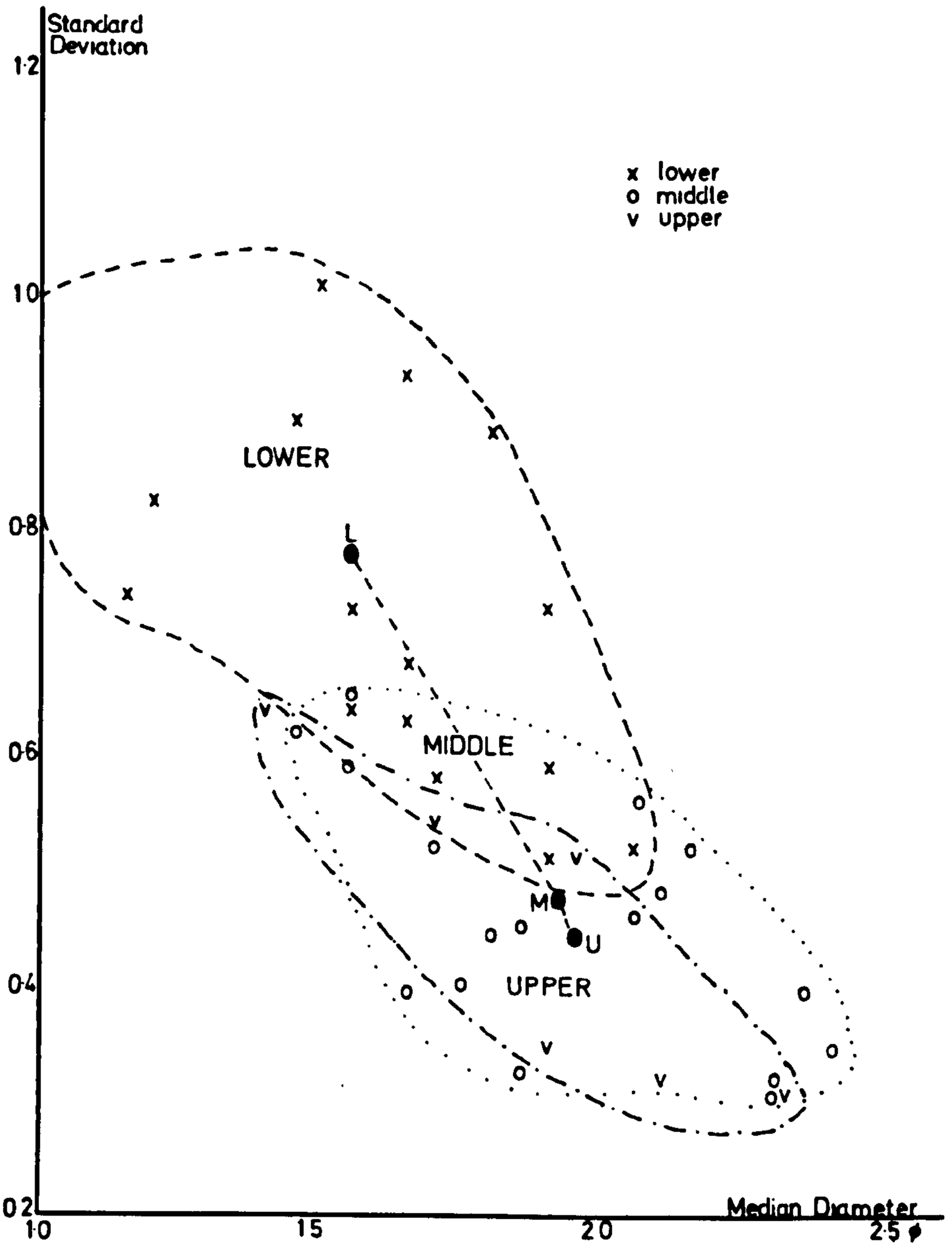

Fig. 6.14. Standard deviation plotted against median diameter to differentiate the three barchan dune units.

From the base of the dune to the crest, a general decrease in mean grain size takes place together with an increase in the sorting coefficient (standard deviation). The lower dune unit is relatively poorly sorted compared to the middle and upper dune units and also displays a much coarser mean grain size. The lower dune unit probably represents resorting of the inter-dune areas, and also appears to represent the reworked flood deposits which produced the underlying contortions. Fig. 6.12 shows the close relationship between the grain size characteristics of the basal dune sediments and the playa sediments when compared to the middle and upper dune units. The coarser grain size is therefore the results of coarse material brought in by the floodwaters rather than aeolian grains.

Fig. 6.13 shows the relationships of skewness in the various dune units. There is a tendency for the lower dune unit to be negatively skewed, a characteristic not normally seen in aeolian sediments. Folk (1971) recognises the frequent occurrence of negative skewness in inter dune areas and this may explain the negative skewness of the basal dune unit. The middle and upper dune units display the characteristic positive skewness of aeolian sandstones due to the removal of the fine fraction in suspension by the wind.

Kurtosis is variable but there is again a tendency for the lower dune unit to be different from the middle and upper dune units. The basal dune units are platykurtic to mesokurtic, a characteristic once again seen in inter dune sediments due to the removal of the intermediate grain sizes. The middle and upper dune units however are dominantly mesokurtic to leptokurtic showing the prevalence of the intermediate grain sizes (Plate 6.1B).

It is also interesting to note that there is a general decrease in grain size from H2 to H4 (Fig. 6.15B). This may represent recession of the source area although this is unlikely. A more probable theory is that there was a decrease in the strength of the wind so that this prevented coarser modes being transported.

Fig. 6.15A. Comparison of the grain size and sorting of the contorted and barchan dunes

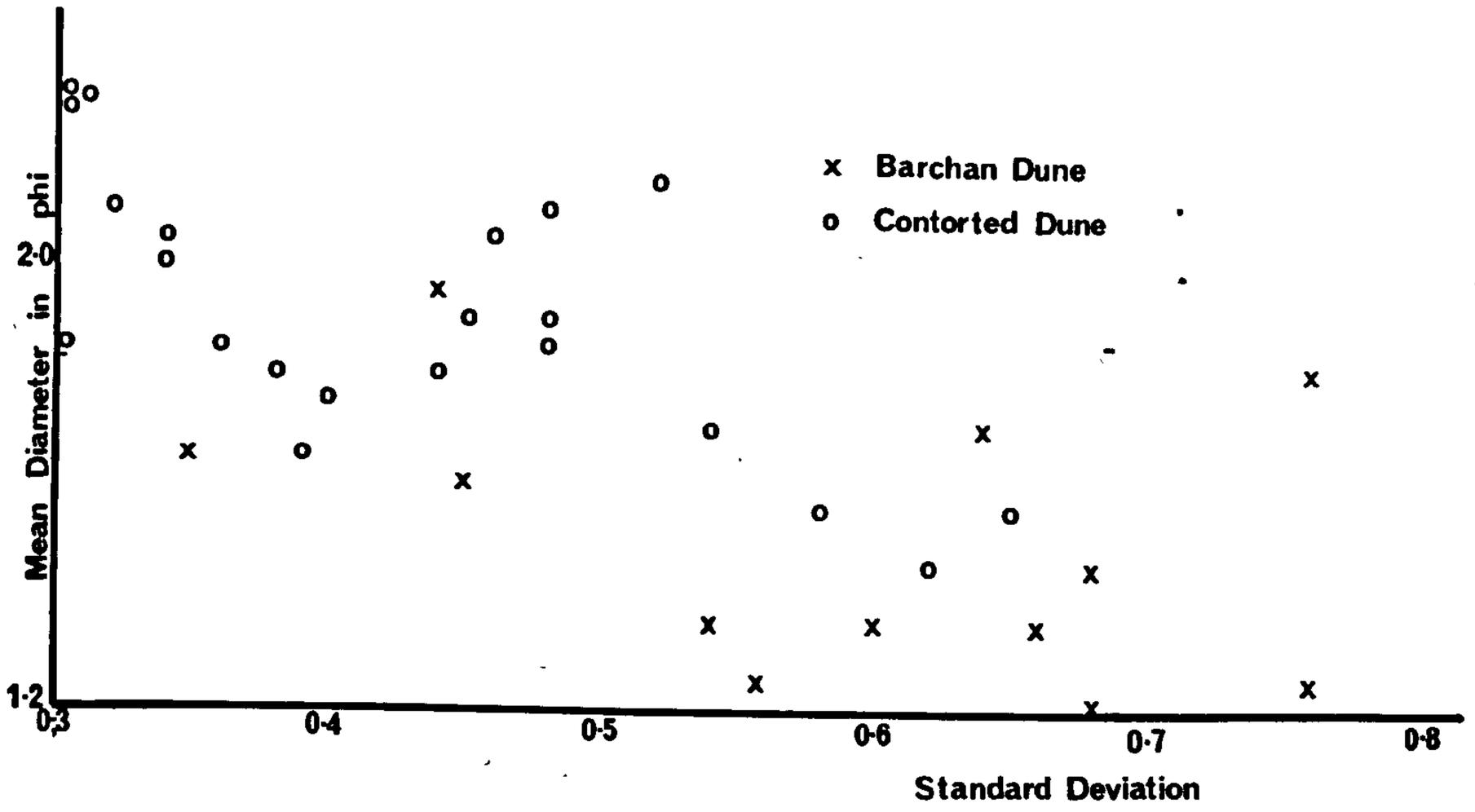

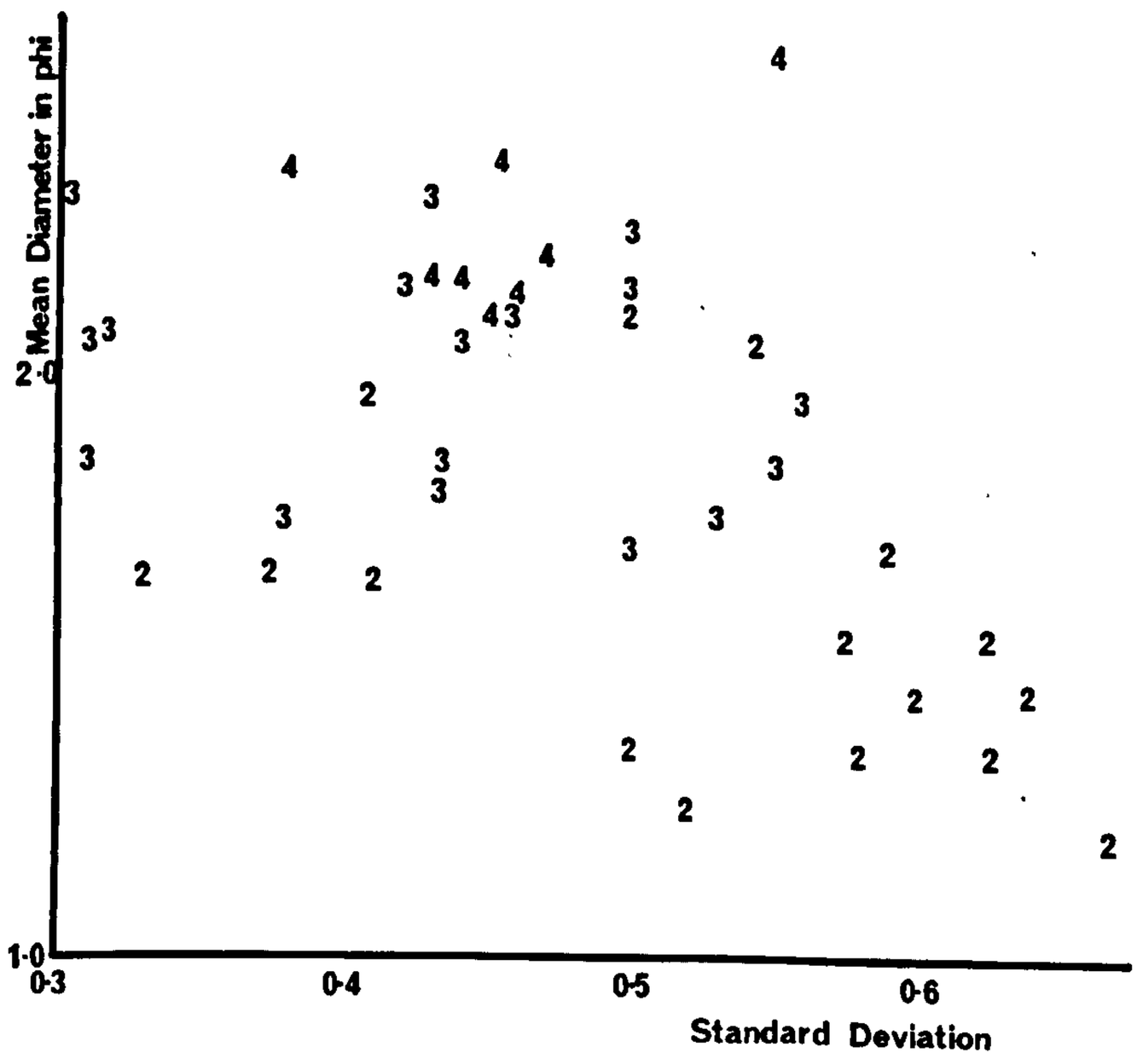

Fig.6.15B. Variation in grain size characteristics in the three barchan dune phases of the Hopeman Sandstone.

Contorted Dunes

The contorted dunes represent deformation in the upper dune by periodic floodwaters. Fig. 6.16B shows the relationship between the mean grain size and the standard deviation. Although several analyses are comparable, the other results are more akin to the basal dune unit and the playa deposits, i.e. high standard deviation and coarser median grain size. (Fig. 6.16A). This can be partially explained by mixing several well sorted laminae; however it is thought that although the different laminae have differing mean grain sizes, the difference would not be great enough to produce such a large standard deviation. The close resemblance with the lower dune unit and the playa sediments may however mean that the contorted dunes are in part dune deposits contaminated by the playa sediments. The high silt and clay content in many of the contorted horizons tends to substantiate this hypothesis.

Skewness shows the characteristic positive value characteristic of dune sediments; the kurtosis tends to be mesokurtic to leptokurtic.

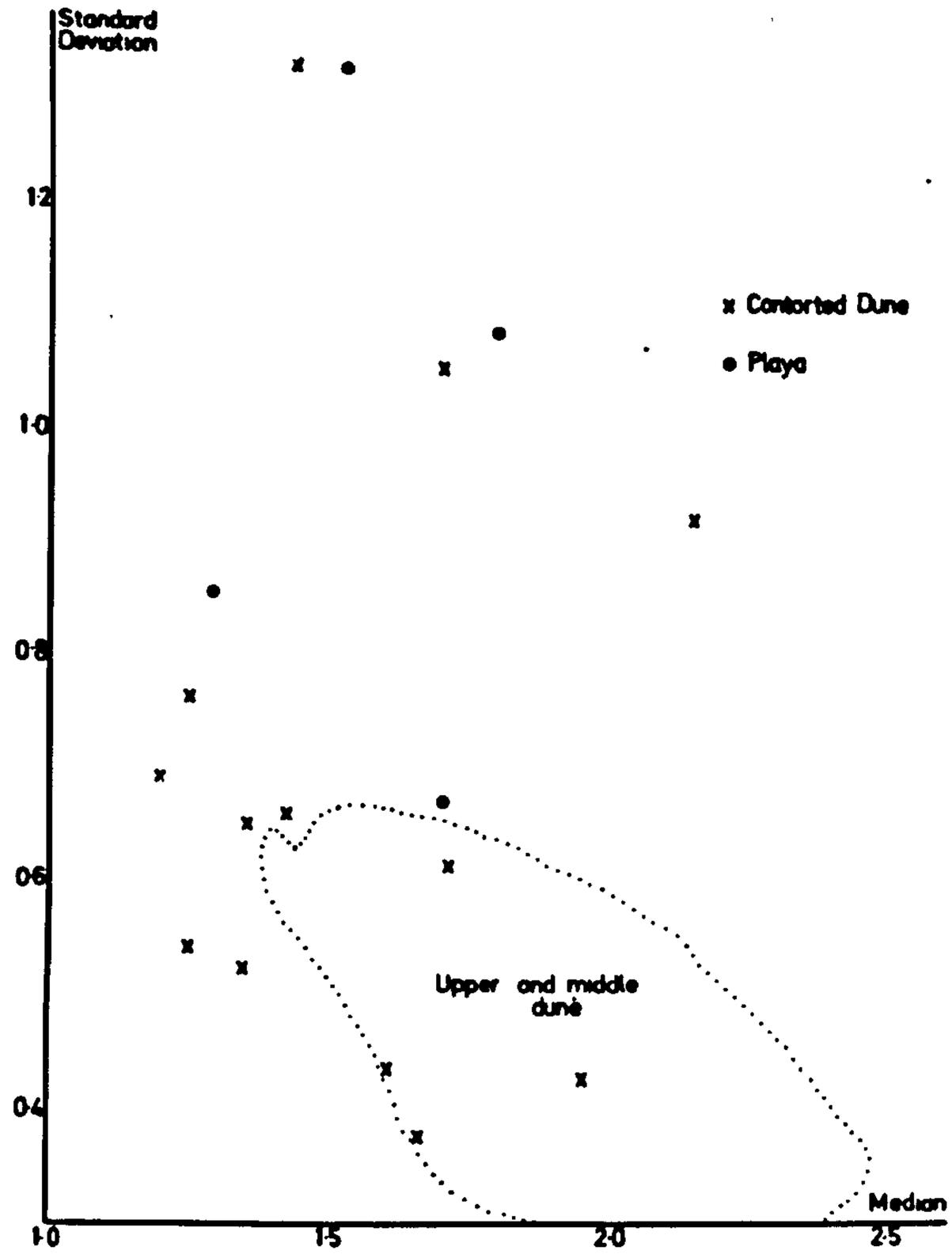

Fig. 6.16A. Comparison of contorted dunes and playa deposits.

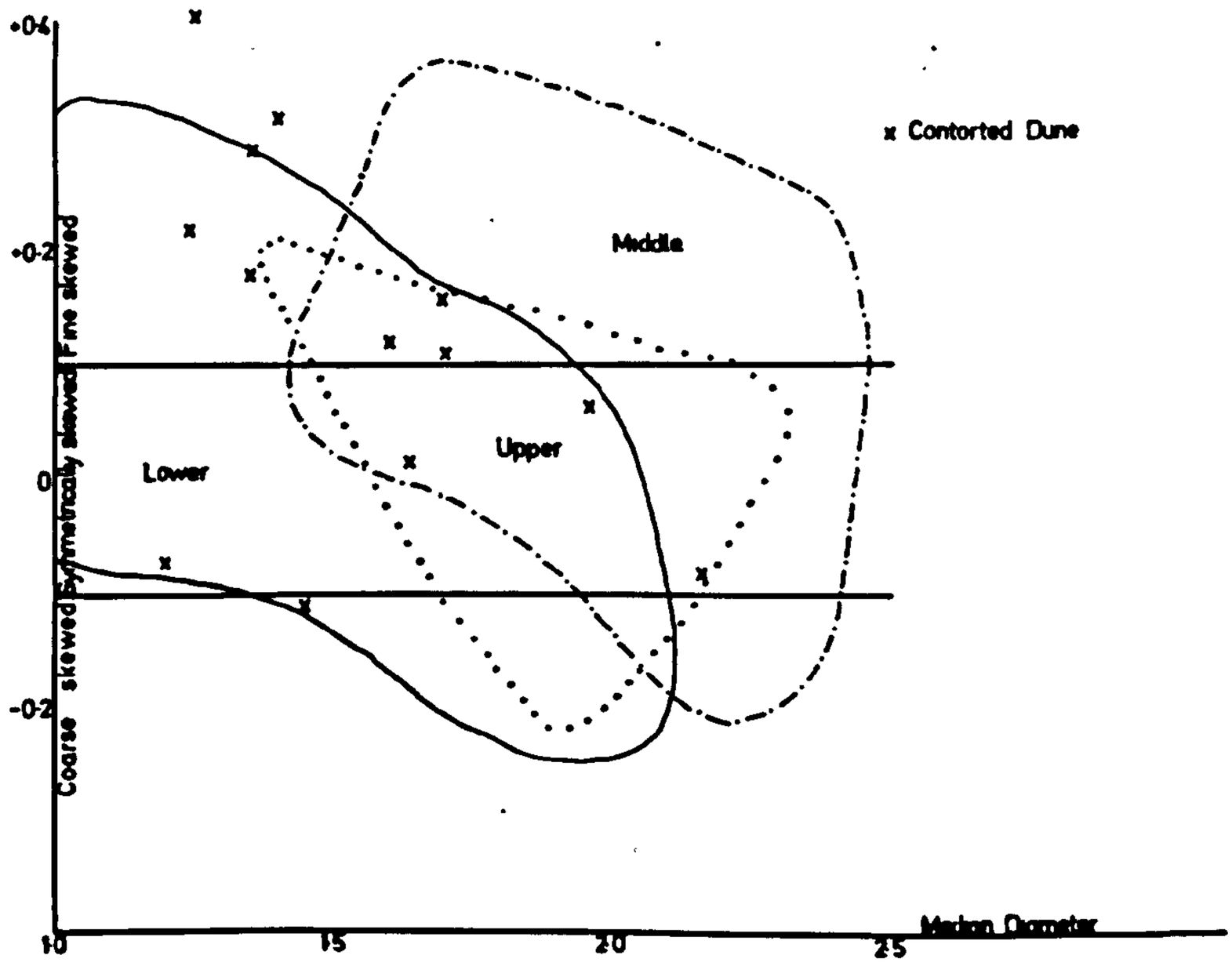

Fig. 6.16B. Comparison of the contorted dunes with the three barchan dune units.

CHAPTER 7

BURGHEAD BEDS : POINT BAR DEPOSITS

The Burghead Beds are exposed to the west of the Elgin district in the vicinity of Burghead, Cummingstown and Roseisle (Fig. 1.3). Field relationships discussed in Chapter 3 suggest that the fluviatile Burghead Beds are laterally equivalent to the aeolian Lossiemouth Sandstones outcropping in the eastern part of the Elgin district.

The Burghead Beds consist of a series of pebbly sandstones, sandstones and silts, and were regarded by Peacock (1968) to be dominantly fluviatile in origin, probably floodplain deposits. Detailed surface mapping and a study of the vertical sequence of stratification types shows that the Burghead Beds can in fact be divided into floodplain and point bar deposits. This Chapter will deal solely with the point bar deposits, the floodplain deposits being discussed in the following Chapter.

As the name would suggest, the point bar deposits are well exposed in the Burghead area both in cliff sections and along the foreshore. At Burghead Harbour, 3-4 metres of silts and pebbly sandstones are exposed as part of the harbour wall (10856908, Fig. 7.9). To the west of Burghead, the cliffs adjacent to the coastguard station display the best vertical and lateral successions of stratification types in the area. A maximum of 4 cycles of point bar deposition is seen in the cliffs, and many of the horizons can be traced along the complete cliff exposure (10766909 to 10806921). A maximum of 2 metres of point bar deposits are also exposed along the stairway leading to the "old Roman Well" in Burghead village (11026915).

The point bar deposits are next seen along the foreshore from the north east of the coastguard station (10836913) to the foreshore north west of Masonshaugh Quarries where they are faulted against the Hopeman Sandstones. This section is invaluable in that the horizons can be traced laterally for large distances although the vertical sequence of stratification types is poorly exposed. Trough and foreset cross stratification is particularly well seen. At the faulted contact with the Hopeman Sandstone, the point bar deposits are overlain by 6 metres of bimodal sandstones which are extremely reminiscent of the Sago Pudding Sandstones.

The contact between the Hopeman Sandstone and the point bar deposits is again seen in the old railway cutting north of Masonshaugh Quarry (11276911) and in a small quarry to the west of the main quarry. East of Masonshaugh Quarry, the shore section is composed entirely of Hopeman Sandstone but small outcrops

to the south of the fault do occur at Roddoch Wells (132692), the adjacent railway cutting and also in the post glacial cliffs of Cabrach How (100 metres to the east of Roddoch Bow). These exposures are fairly small but show excellent examples of trough and foreset cross bedding.

At Clarkly Hill, 400 metres south east of the Transmitting Station (125686), four old quarries display a maximum of 4 metres of point bar deposits. This is also the site of the important borehole sunk by the Institute of Geological Sciences (Table 3.1).

At Gallows Hill (147685), the main quarry at the summit exposes 5-6 metres of Sago Pudding Sandstones and Lossiemouth Sandstones. However, at a lower level (14516838), a few metres of pebbly sandstones and horizontally laminated sandstones can be equated with the point bar deposits. This locality is an example of the interdigitation of the point bar deposits with the Lossiemouth Sandstones.

On the south side of the Hill of Roseisle (1516690), a small overgrown quarry exposes typical pebbly sandstones of the point bar deposits.

COMPARISON OF THE BURGHEAD BEDS WITH MODERN DAY POINT BARS

Standard fluvial point bar systems normally display an upward fining sequence and a vertical succession of stratification from high to low energy stream power (Bernard and Major, 1963, Allen, 1965 and Frazier and Osanik, 1968). However, McGowen and Garner, (1970) described a point bar model in which no systematic change in grain size was apparent and a vertical sequence of stratification types which did not correspond to the standard point bar model.

Study of the Burghead Beds indicates that they can be compared to the modern day Colorado and Amite rivers described by McGowen and Garner (1970). The Colorado and Amite rivers were found to conform to bed load streams characterised by relatively low sinuosity and high gradient, bank stabilisation by vegetation and short duration peak discharge. Flow in the Colorado was found to be less that 5,000 cubic feet per second for 95% of the time with high discharge rates of 150,000 cubic feet per second for 5% of the time.

The general physiographic features of this type of point bar can be seen in Figs. 7.1 and 7.2. The sections indicate that four major units are present:

1. Scour Pools are formed in the deeper parts of the river adjacent to the concave bank and are characterised by trough cross stratification.
2. The Lower Point Bar occupies an intermediate position between the Scour Pool and the Upper Point Bar. Trough, trough and foreset cross stratification, parallel lamination and ripple marked sandstones and silts are generally formed under more tranquil conditions than the other units.

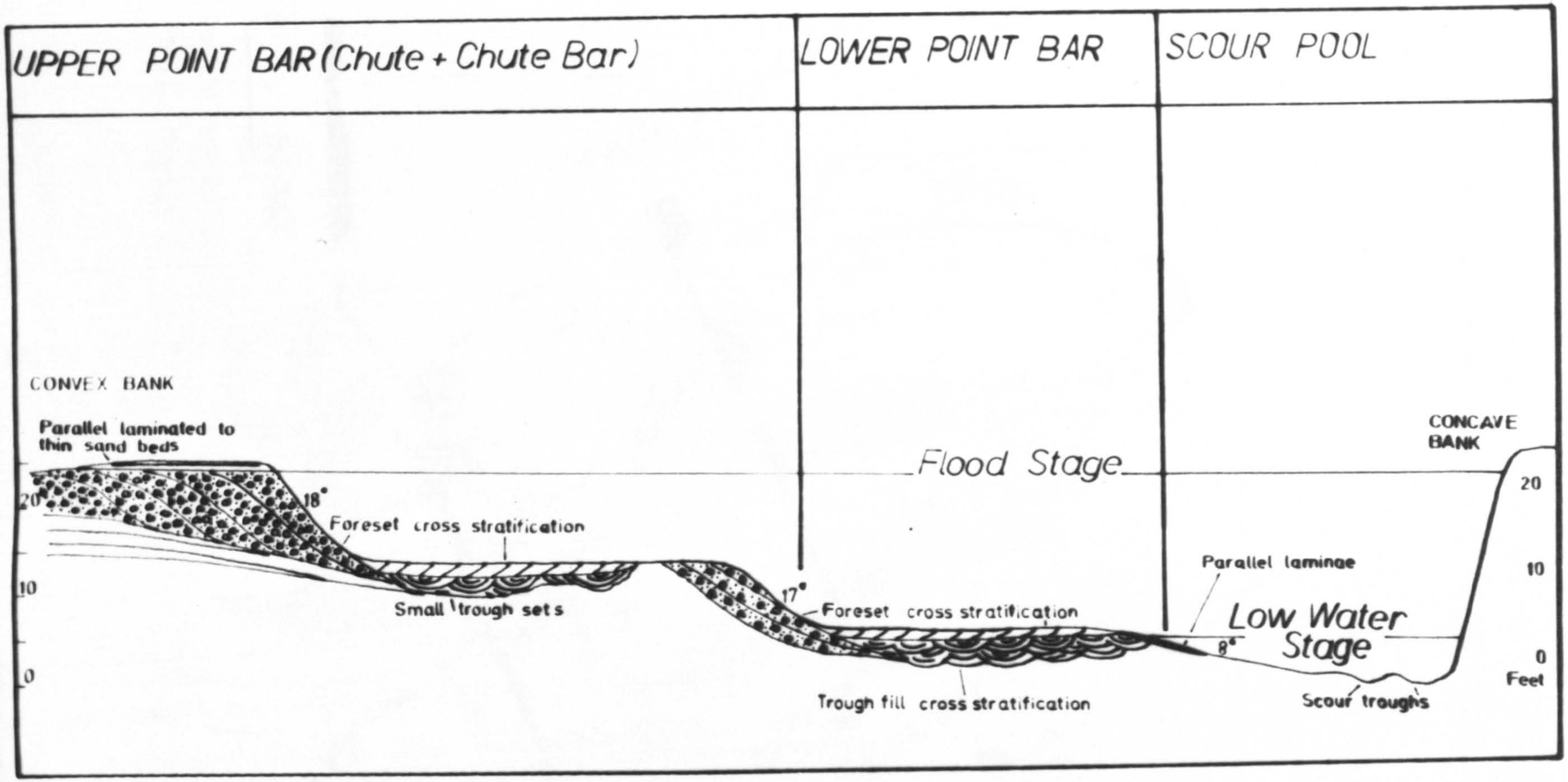

Fig. 7.1. Physiographic features of modern day coarse grained point bar deposits(after McGowen and Garner,1970).

Fig. 7.2. Sketch sections of the modern day Colorado River illustrated by McGowen and Garner(1970).



3. Upper Point Bar deposits are characterised by large scale foreset cross stratification and are developed during periods of flooding.
4. Floodplain deposits.

The point bars are therefore developed during the flood water stage of the river when there is a high water:sediment ratio. The water level falls rapidly and the river becomes choked with sediment, thereby producing a braided river system during the low water stage. Thus, there is no contradiction in terms as the point bars and the braids are produced by different load:discharge ratios.

Comparison with the Burghead Beds reveals that similar features to those described above can be recognised. In the Burghead Beds, an ideal sequence (Fig. 7.3) from flood to low water stage is often present and it is this sequence which is discussed in the following section. The ideal cycle represents 30-40% of the cycles present although often in the non-ideal cycles, only a minor unit is absent. The thickness of the cycle is generally between 3 and 6 metres.

THE IDEAL CYCLE

Fig. 7.3 shows the vertical sequence of stratification types of the ideal cycle. The cycle is divided into the four major units described in the preceding section; the floodplain deposits will however be discussed in the next chapter as they are normally poorly exposed where they are associated with the point bar deposits.

Scour Pool Unit

Scour Pool deposits form in the deeper parts of the river adjacent to the concave bank during the flood stage and are characterised by trough cross stratification. They are therefore present as the lowest unit of the ideal cycle and rest unconformably on the preceding cycle (Fig. 7.4 and Plate 7.1).

The sediments are generally coarse pebbly sandstones although the lithology is clearly dependent on the current velocity during the period of flooding. However, the high velocity and the high bed load of the river is clearly evidenced by the degree of erosion into the preceding cycle. This is generally between 0.5-1.0 metres but may reach up to 1.5 metres into the underlying cycle. The scour troughs reach a maximum thickness of 1.75 metres and are generally 1-2 metres in width.

The cause of the initiation of the scour troughs is uncertain although McGowen and Garner (1970) note that they are commonly developed downstream from large trees. The presence of large trees in the Burghead Beds is unlikely as no evidence of any flora has been found in the deposits. However, it is suggested that the process could develop around a similar object e.g. large

Fig. 7.3. An ideal cycle for the coarse grained point bar deposits of the Burghead Beds.The cycle is generally 3-6 metres in thickness.

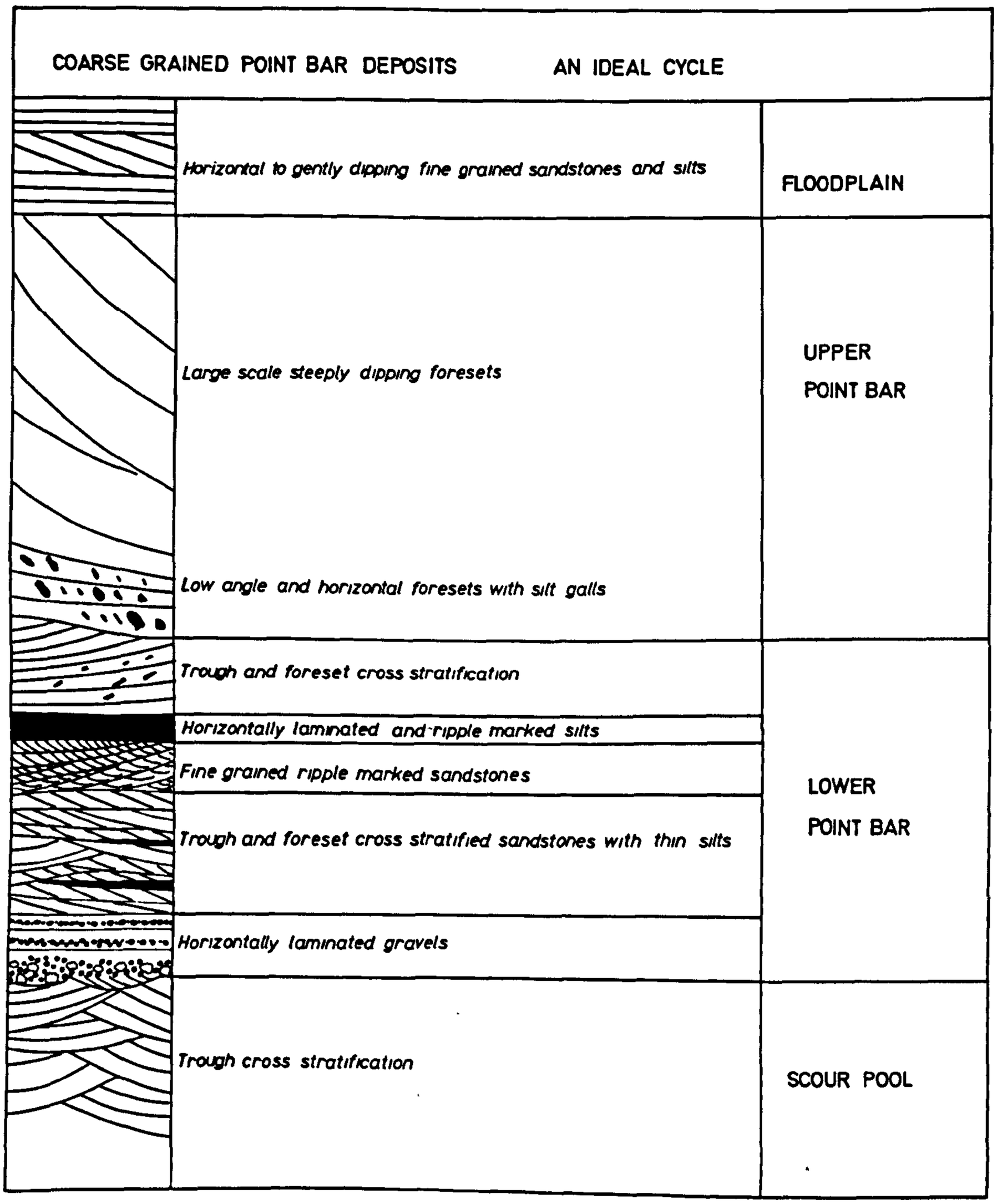

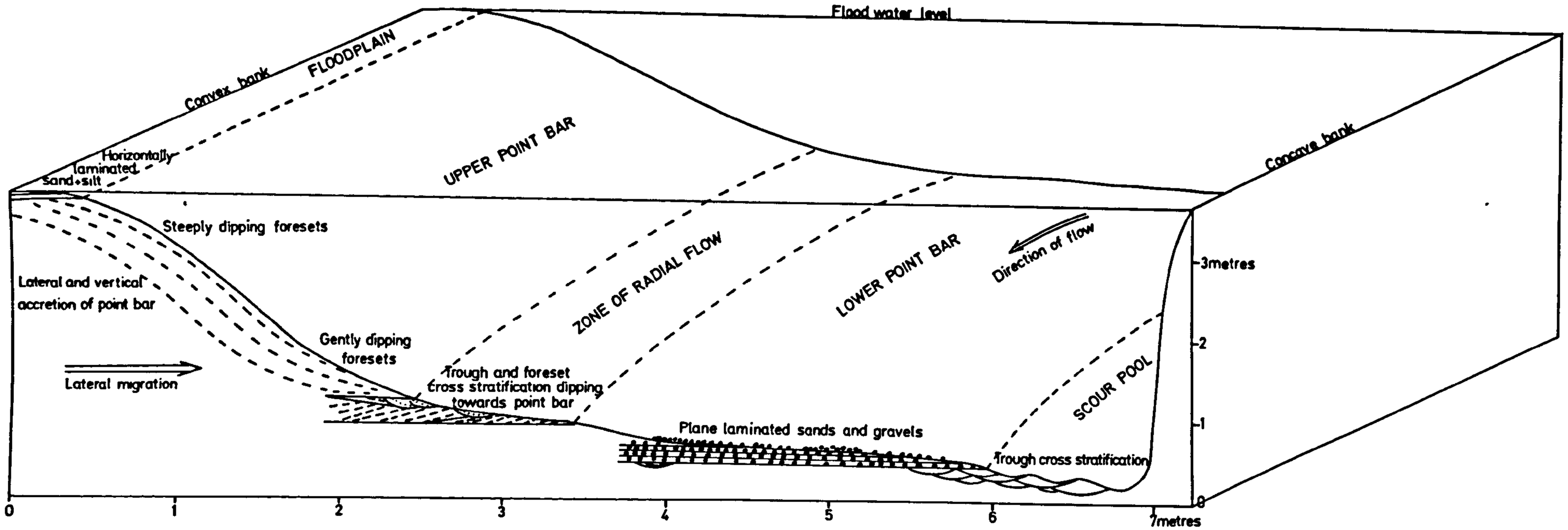

Fig. 7.4. Diagrammatic representation of the flood stage of the river channel.

pebbles lying on the stream bed would provide a nucleus around which the high velocity flood waters could initiate a scour. The scour, once developed, would be subsequently infilled to produce the characteristic trough cross stratification of the Scour Pool unit (Fig. 7.5).

Lower Point Bar Unit

The Lower Point Bar deposits represent a complete sequence from the flood stage of the river through to the low water stage and finally to complete desiccation. From flood stage, the velocity and depth of water continues to decrease, shown in the Lower Point Bar deposits by an upward decrease in grain size and stratification types characteristic of more tranquil conditions. However, where renewed flooding occurs before complete desiccation, two or more fining upwards cycles may be present, but this is extremely rare.

Plane laminated horizons are normally found at the base of the Lower Point Bar sequence and may reach 0.5 metres in thickness although they are generally nearer to 0.25 metres. Their lithology is represented by gravels and sandy gravels; pebbles may reach up to 100 mm in diameter. This, together with their basal position in the Lower Point Bar, suggests that they were deposited during the flood stage or at intermediate time between flood and low water stage.

Little or no erosion occurs on to the underlying Scour Pool deposits although, rarely, small trough infills are present but these never reach more than 0.1 metre in depth (Plate 7.2D). This suggests that the horizon was not erosional but probably infilled irregularities in the underlying surface. At the classic locality of Burghead harbour (107689128), the horizon is floored by 0.1 metres of unsorted gravels which grade up into 0.4 metres of parallel laminated sandy gravels. The pebbles are often concentrated in specific horizons giving the impression of grading. Rarely, the beds show gently dipping foresets with values never greater than 5 degrees but they are not laterally extensive.

The plane laminations of this horizon appear to be similar in nature to those seen in experimental flume studies at high stream velocity (Guy et.al., 1966). This theory is supported by the next stage in the cycle which represents a decrease in stream velocity and water depth.

The next unit is represented by trough and foreset cross stratification, a type of cross stratification which is extremely common and may reach up to 1 metre in thickness. Detailed examination of the trough and foreset cross stratification reveals that it is similar to deposits described by Williams and Rust (1969) from braided rivers. Thus, as the water depth decreases, the channel becomes choked with sediment and braiding occurs (Fig. 7.6).

Foreset cross stratification was probably formed by transverse bars which characterise braided rivers. Migration of the transverse bars takes place

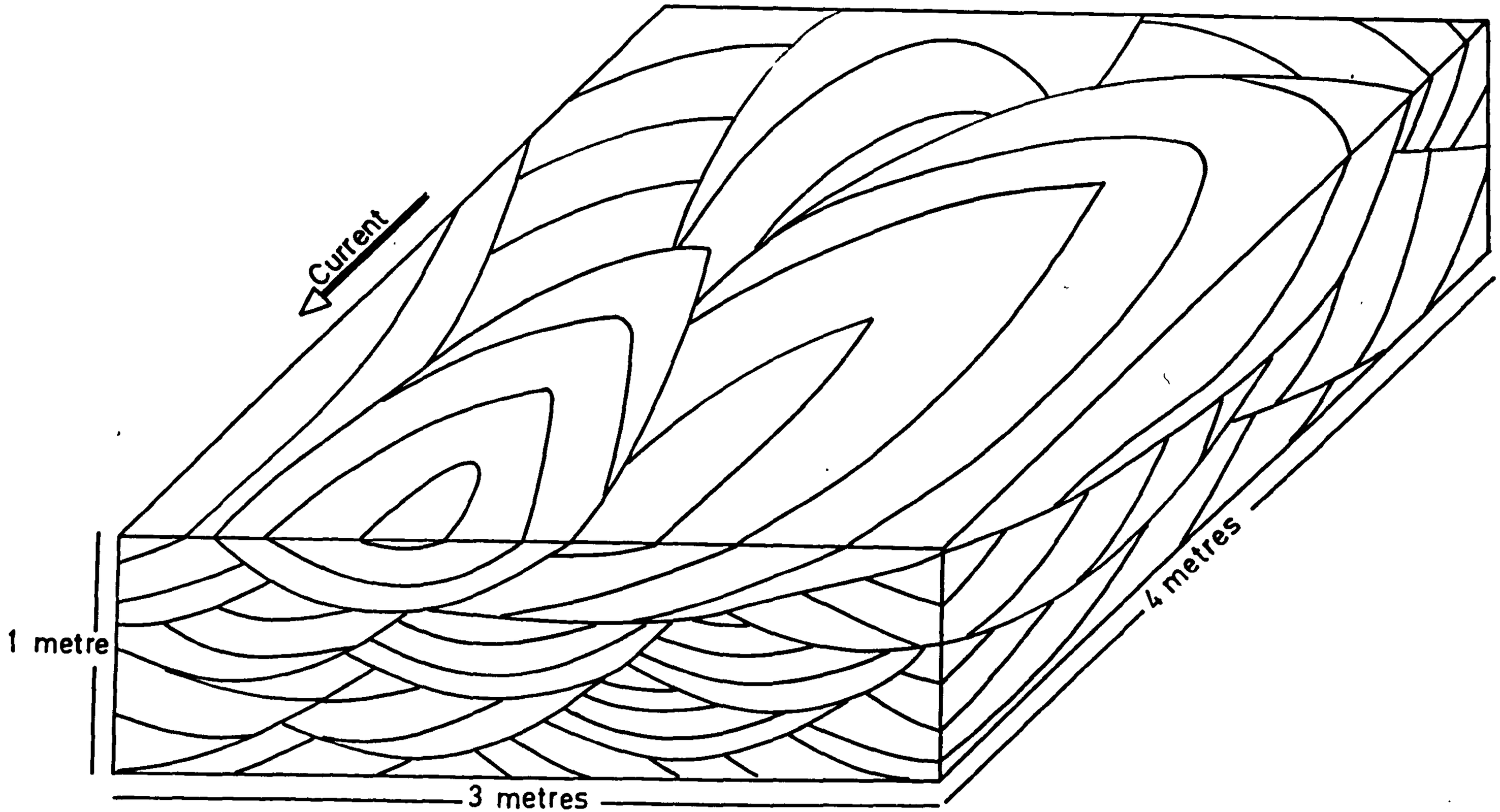

Fig. 7.5. Trough cross stratification of the Scour Pool unit.

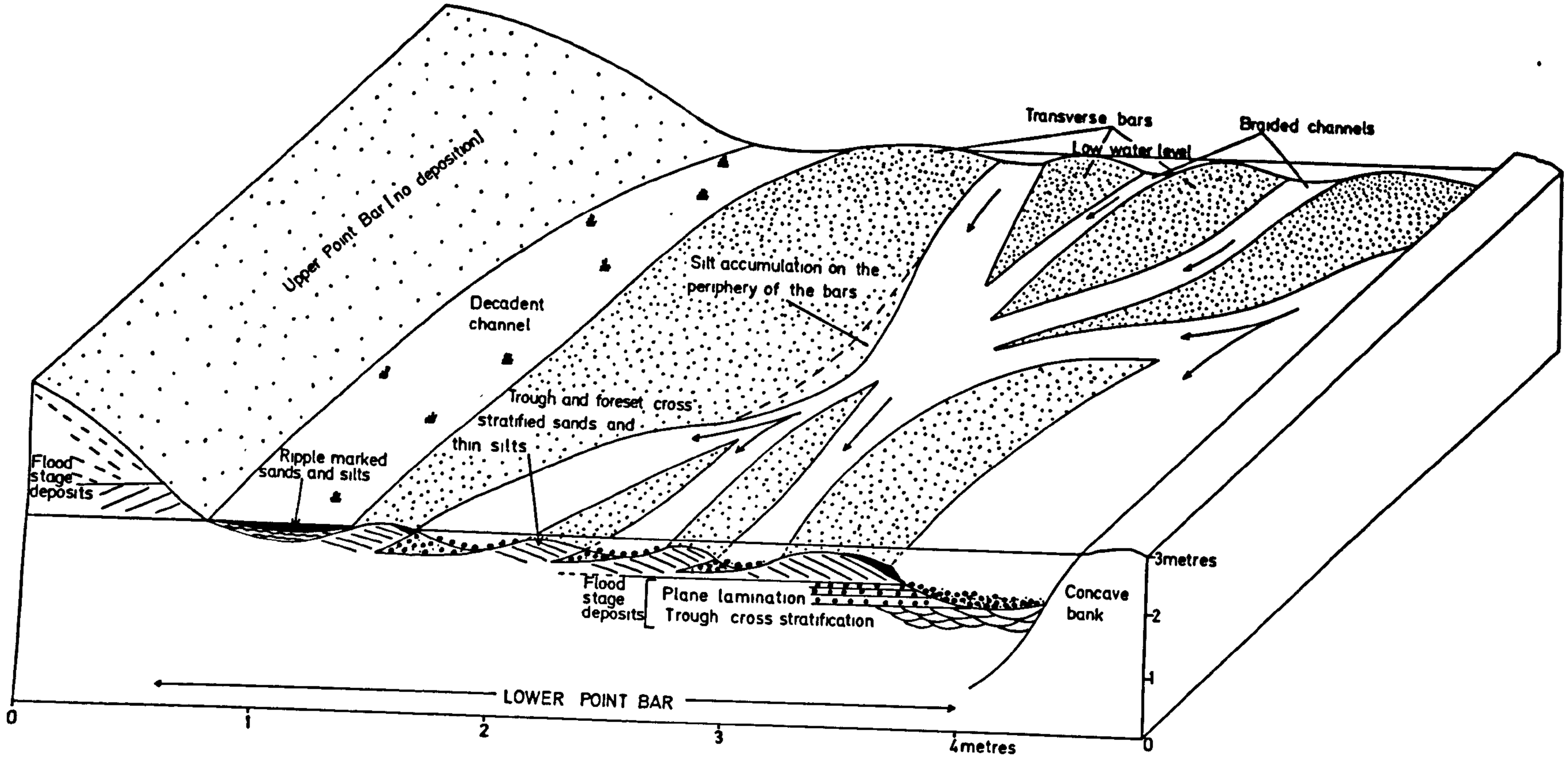

Fig. 7.6. Diagrammatic representation of the low water stage of the river channel.

EXPLANATION OF PLATE 7.1

SCOUR POOL DEPOSITS: BURGHEAD HARBOUR

A. Scour channel cutting down into the Upper Point Bar deposits (Cliffs north of the harbour, 10766910).

B. A series of scour troughs eroding up to 2 metres into the underlying Upper Point Bar deposits (Cliffs north of the harbour, 10766910).

C. Trough cross stratification with palaeocurrent running from left to right (Cliffs north of the harbour, 10766910).

D. Trough cross stratification with the section at right angles to the palaeocurrent direction (Cliffs below the Coastguard Station, 10776912).

PLATE 7·1

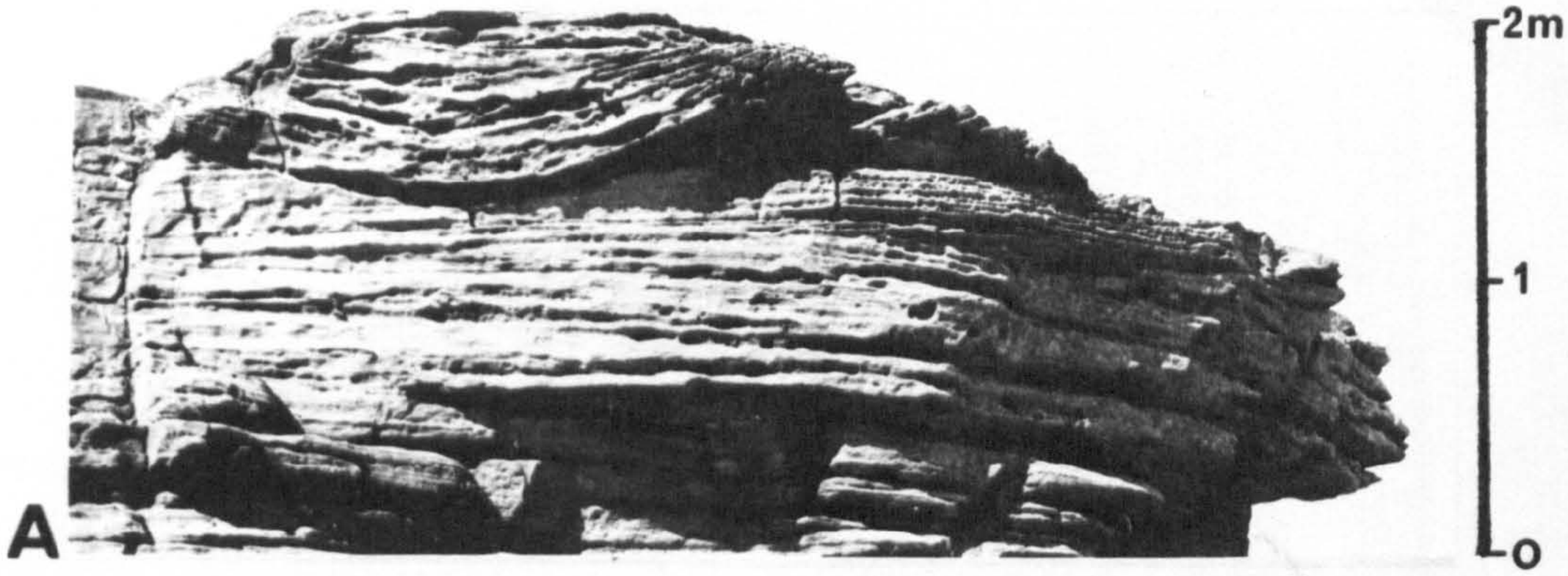

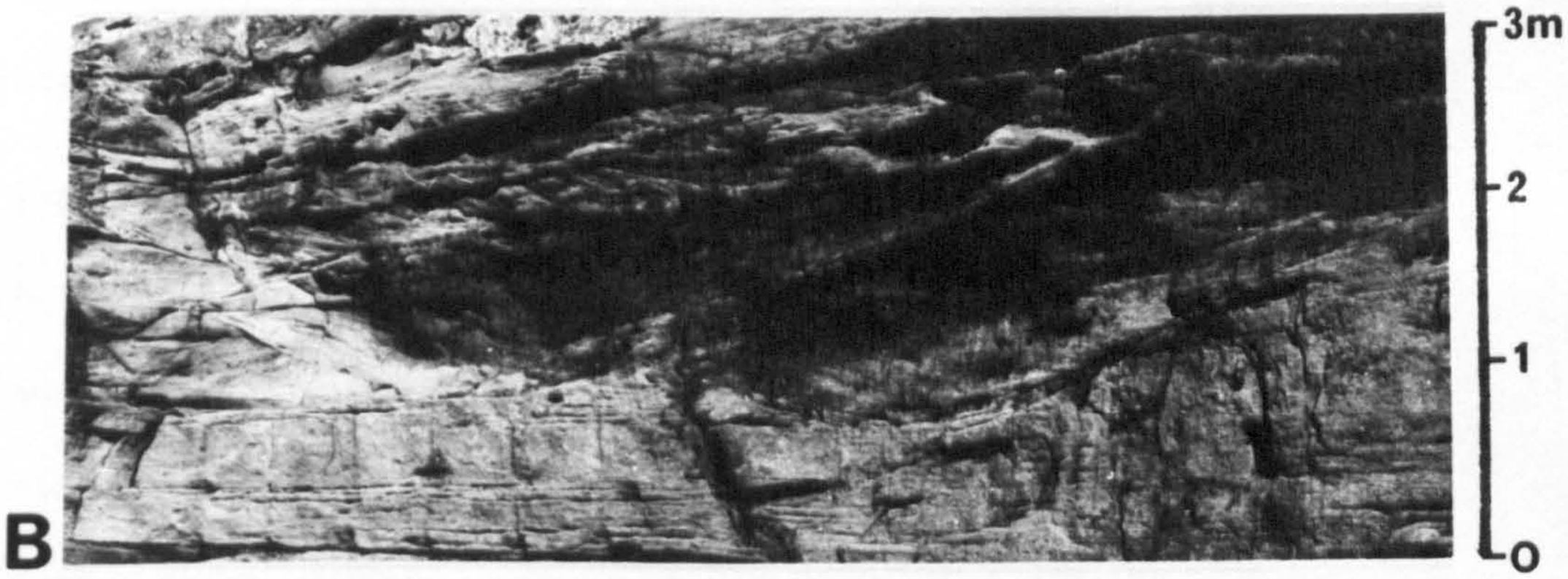

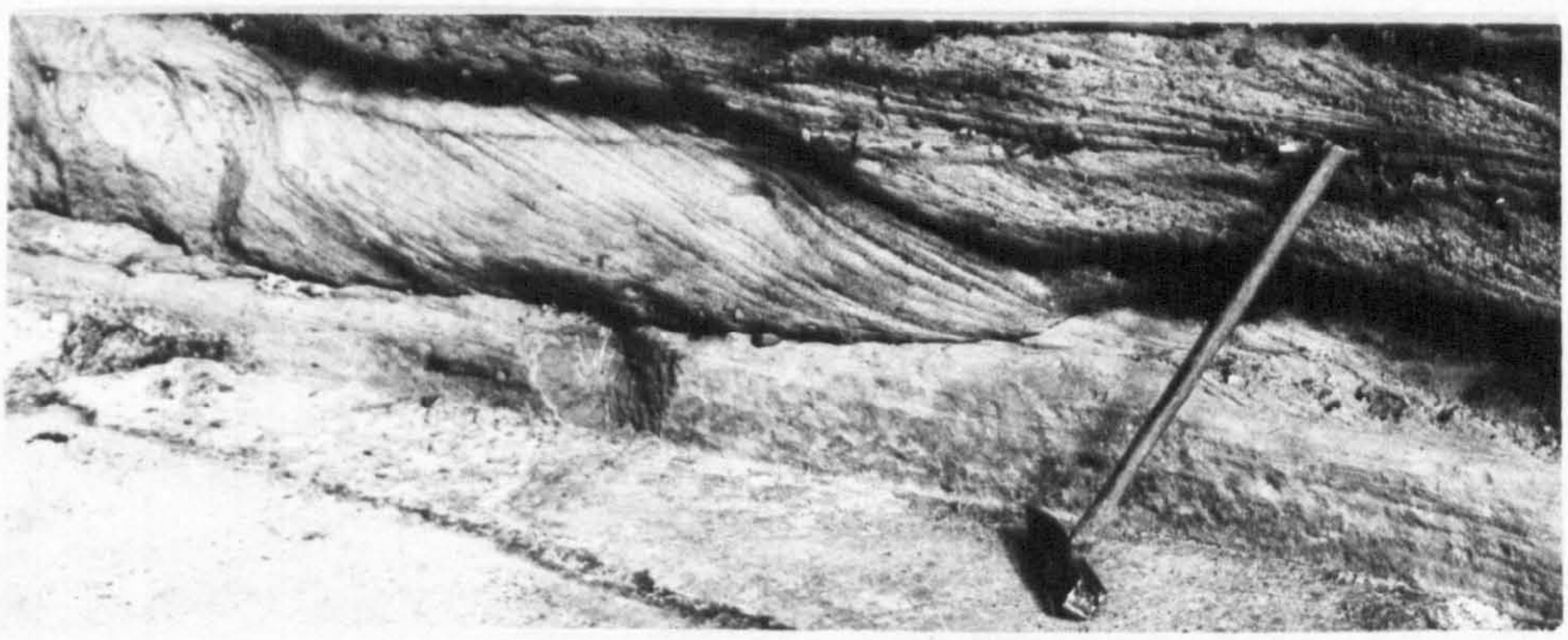

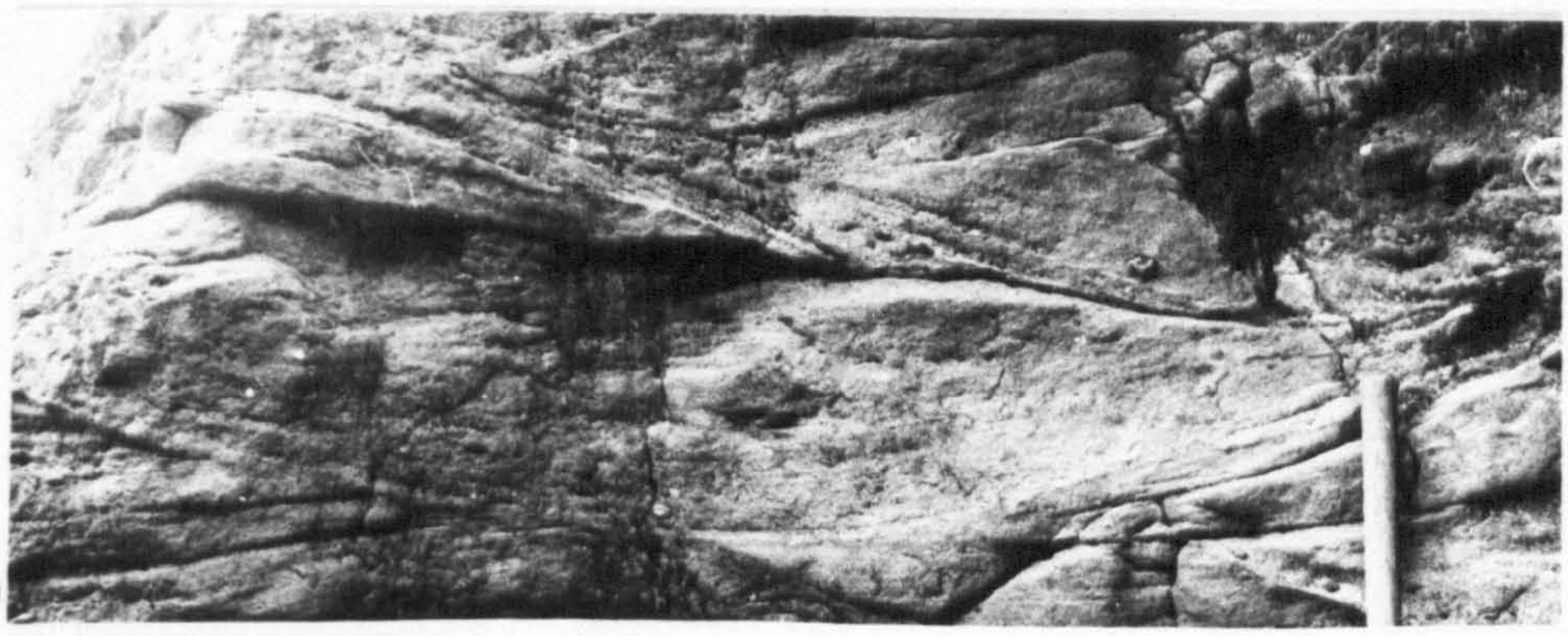

EXPLANATION OF PLATE 7.2

LOWER POINT BAR DEPOSITS

A. Plane laminated gravels of the Lower Point Bar, Burghead Harbour (10766910).

B. Plane laminated gravels of the Lower Point Bar at Burghead Harbour (10766910).

C. Plane laminated gravels overlain by trough and foreset cross stratification and ripple marked silts. The Lower Point Bar deposits are eroded by steeply dipping foresets of the Upper Point Bar and underlain by low angle Scour Pool deposits, (Clarkly Hill, 125686).

D. Small prograded channel at the junction of the Scour Pool deposits and the plane laminated gravels of the Lower Point Bar (Clarkly Hill, 125686).

PLATE 7·2

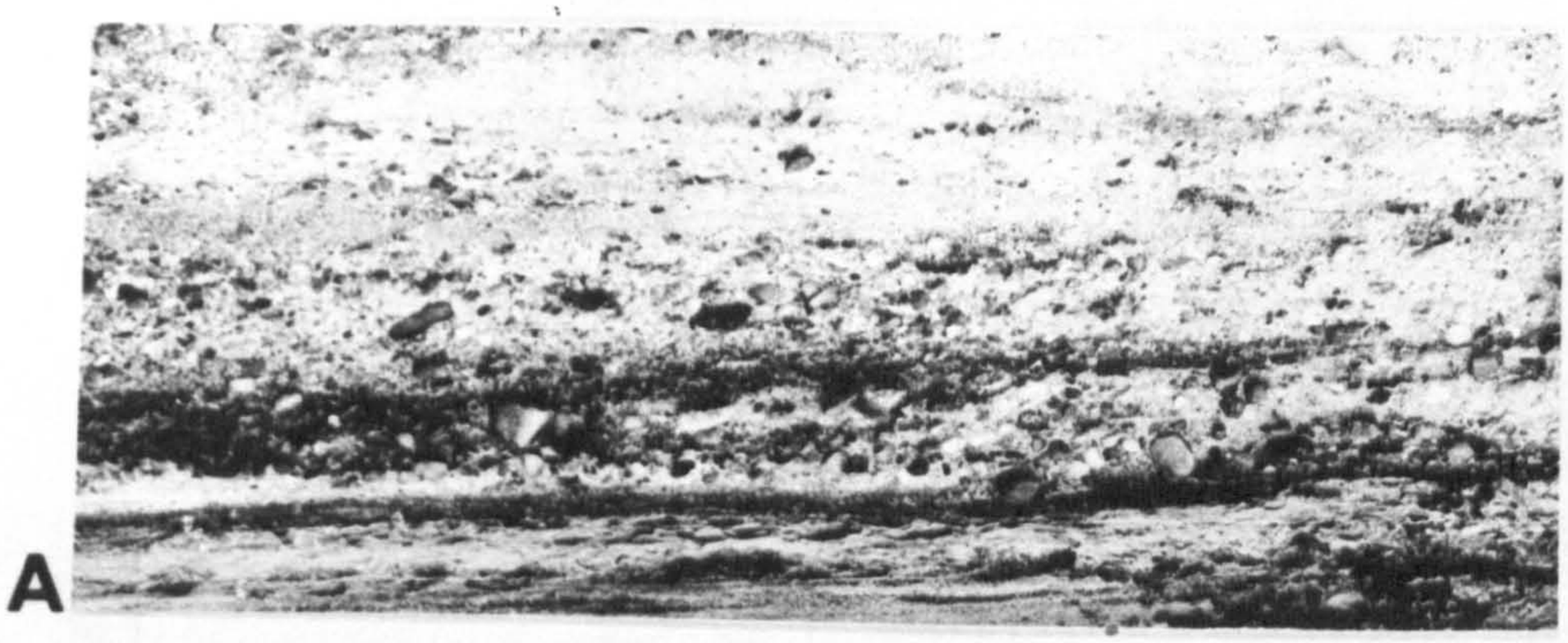



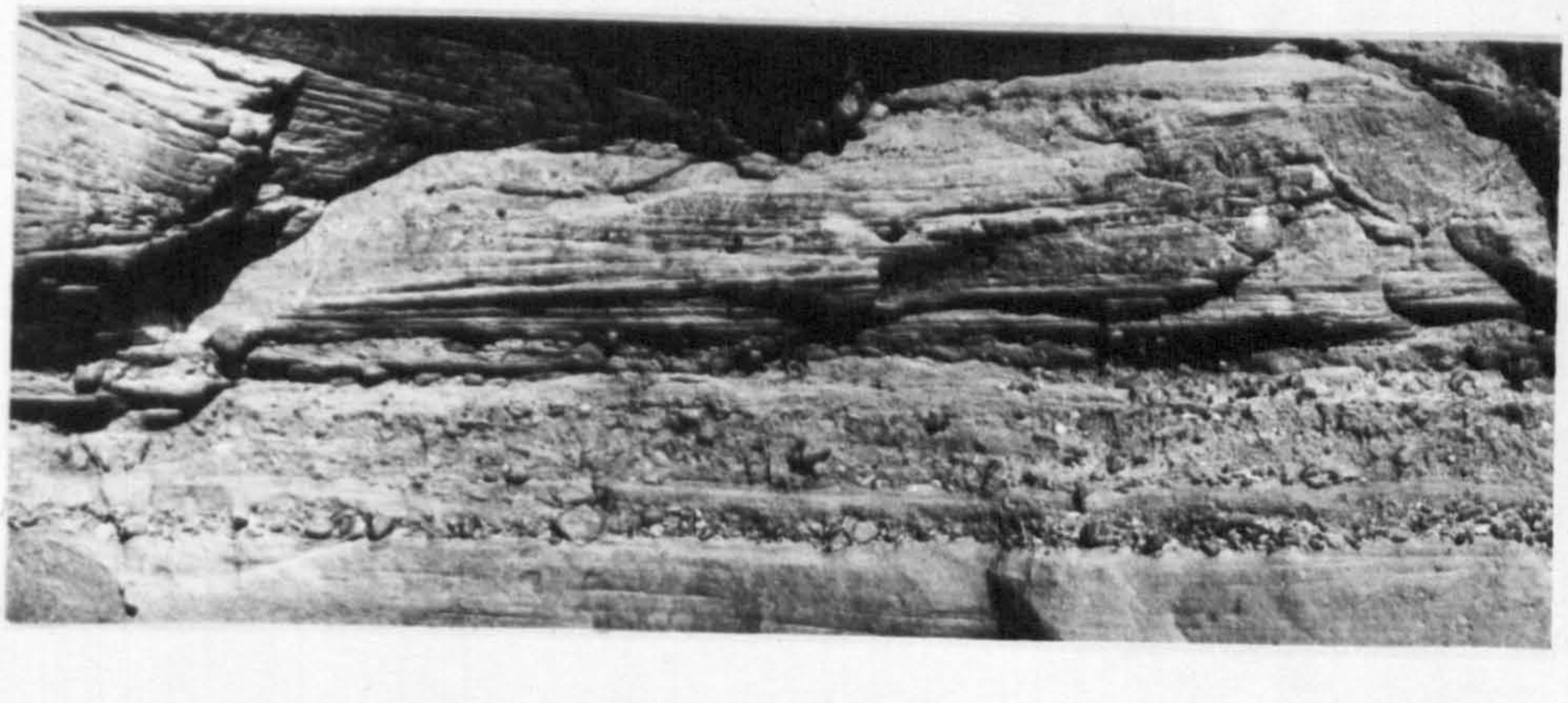

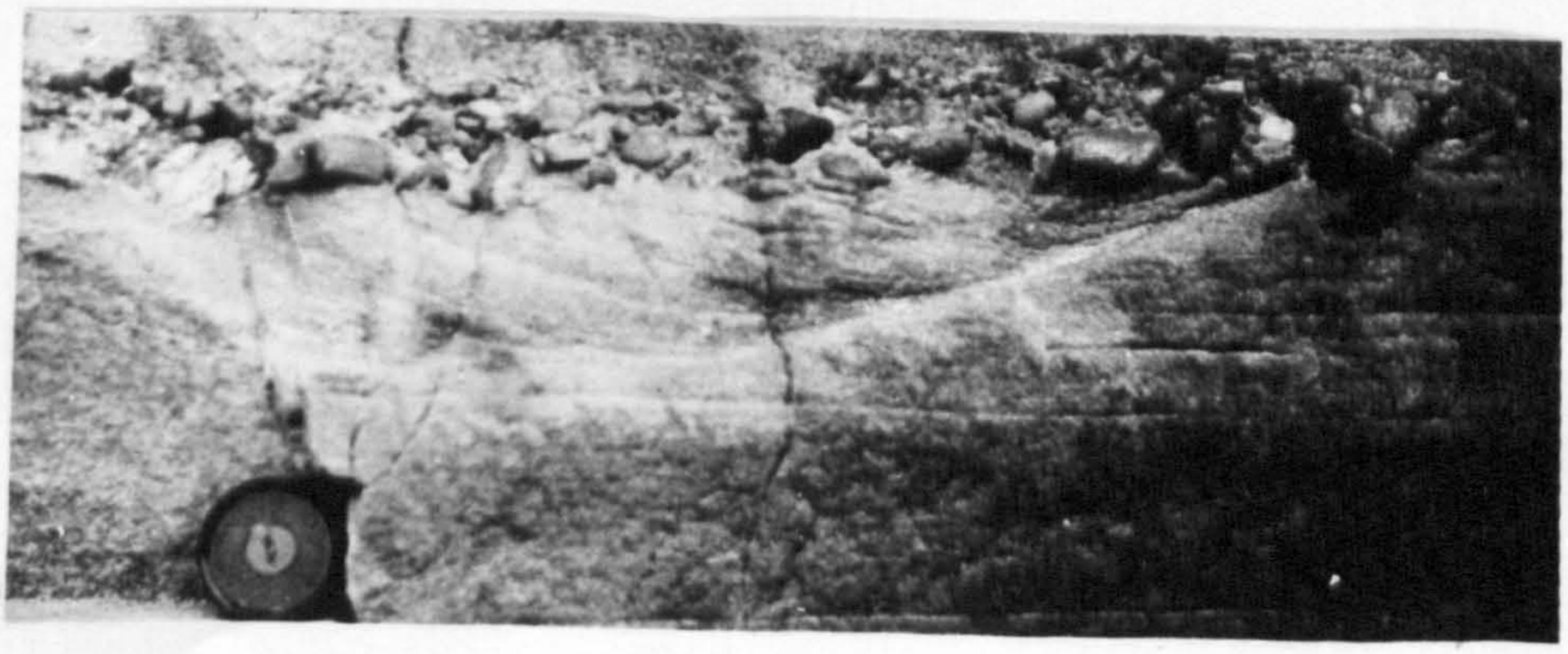

EXPLANATION OF PLATE 7.3

LOWER POINT BAR DEPOSITS

A. Mega rippled medium grained sandstones (Cliffs below Burghead Coastguard station, 10806920).

B. Ripple marked and plane laminated silts overlying trough and foreset cross bedded sandstones. A lens of medium grained sandstone in the silt horizon represents renewed flooding into a decadent channel (10806920).

C. Ripple marked silts (1086920).

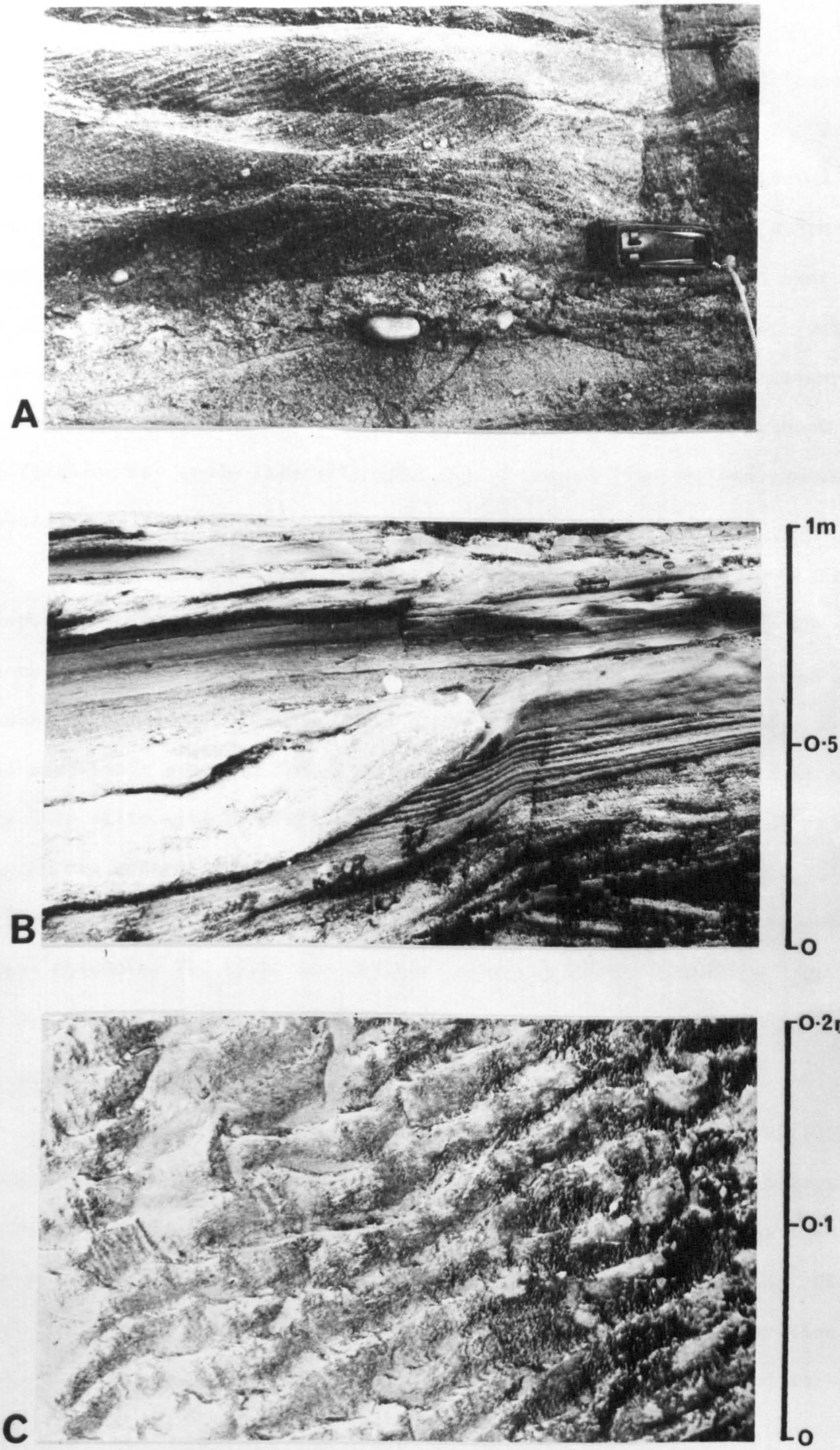

PLATE 7·3

both laterally and downstream so that the foreset cross stratification migrates over the trough cross stratification formed in the braided channels. This forms the characteristic trough and foreset cross stratification (Fig. 7.7). Troughs are normally 0.1 metres in depth and 0.3 metres in width whereas the foresets are rarely thicker than 0.2 metres but are laterally more extensive. The transverse bars are normally coarse sands or sandy gravels, but sometimes silts may form on the tops of the bars although they are seldom preserved. The silts are often eroded by the braid channels to form pellet conglomerates. Where channels are cut off from the main channel, the trough and foreset cross stratification may grade laterally into ripple marked fine grained sandstones and silts; rarely mud cracks may be present.

A further decrease in velocity and depth of water is marked by the development of ripple marked sandstones and silts over a wide area; these horizons have been traced for more than 150 metres and therefore appear to represent uniform conditions over the whole of the river channel. The ripple marked sandstones grade up into ripple marked silts and laminated silts and rarely into silts with evidence of mud cracks. The ripples are migratory in character and generally have an amplitude from 10-30 mm and a wavelength of 100-150 mm. The ripples are assymetrical and migrate in the direction of the dominant channels. The silts are frequently eroded by the overlying Upper Point Bar unit where they are often seen as pellet conglomerates.

Upper Point Bar Unit

The Upper Point Bars are equivalent to the chute bars described by McGowen and Garner (1970) and are products of both lateral and vertical accretion. The height of the bar is controlled by the height of the flood waters as the chute bars only form under conditions of extreme flood. Chute bars of the Burghead Beds are directly comparable to the simple accretion sequence of stratification types seen in the modern day Colorado and Amite rivers.

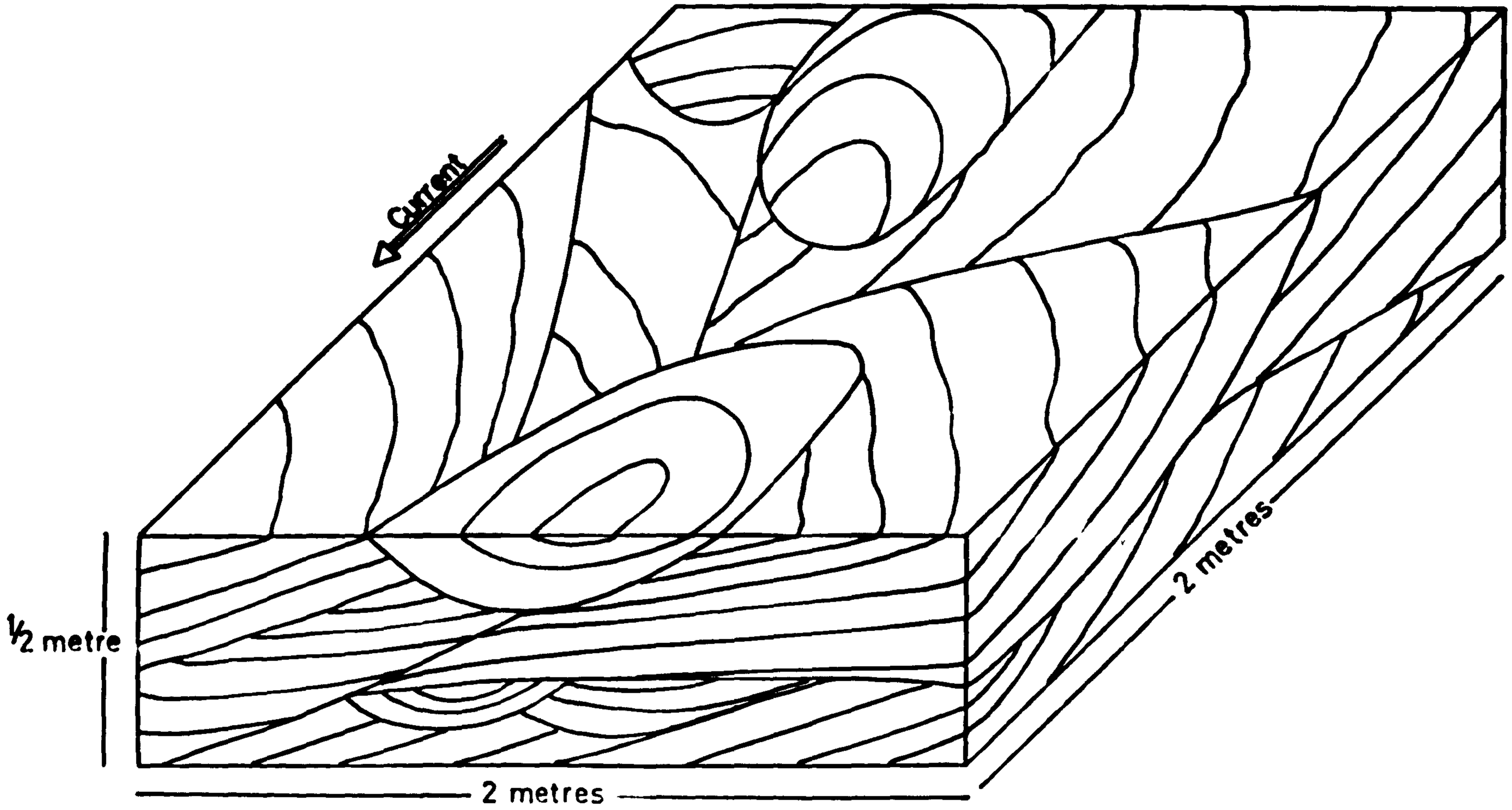

Fig. 7.7. Trough and foreset cross stratification of the Lower Point Bar unit.

At the base, a transitionary sequence of trough fill cross stratification dipping in the opposite direction to the main foresets of the point bar is seen, together with small scale foreset cross strata also dipping away from the main point bar. Thin pebbly sandstone lenses are also common. These deposits appear to represent the depressions lateral to the main chute bar described by McGowen and Garner (1970). Boersma et al. (1968) describe a similar phenomena due to the backflow at the base of chute bar. It is suggested that these deposits arise where radial flow takes place in the bend of the meandering river.

The main part of the chute bar is represented by large scale foresets dipping at angles between 10-30 degrees (Plate 7.4, Fig. 7.8). These illustrate the lateral and vertical accretion of the chute bar and may reach 3-4 metres in height. At the base, horizontal laminae are common but these grade up into the large scale foresets. More than one accretionary event may occur in the Upper Point Bar unit. They are often separated by small scour troughs eroding into the silts of the first accretionary event. These silts show similar features to the floodplain deposits.

Grain size varies from coarse sands to sandy gravels and is dependent on the strength of the flood phase. Small clay galls may be present at the base due to erosion of the underlying Lower Point Bar silts; these silts are often contorted due to the force of erosion of the chute bars. The Upper Point Bar deposits are overlain by horizontally laminated to gently inclined foreset bedding of the floodplain deposits.

LOCALITY DESCRIPTIONS

To avoid repetition only the four localities which illustrate the most complete vertical sequence of stratification types are described below. These localities display all the features of the coarse grained point bar deposits.

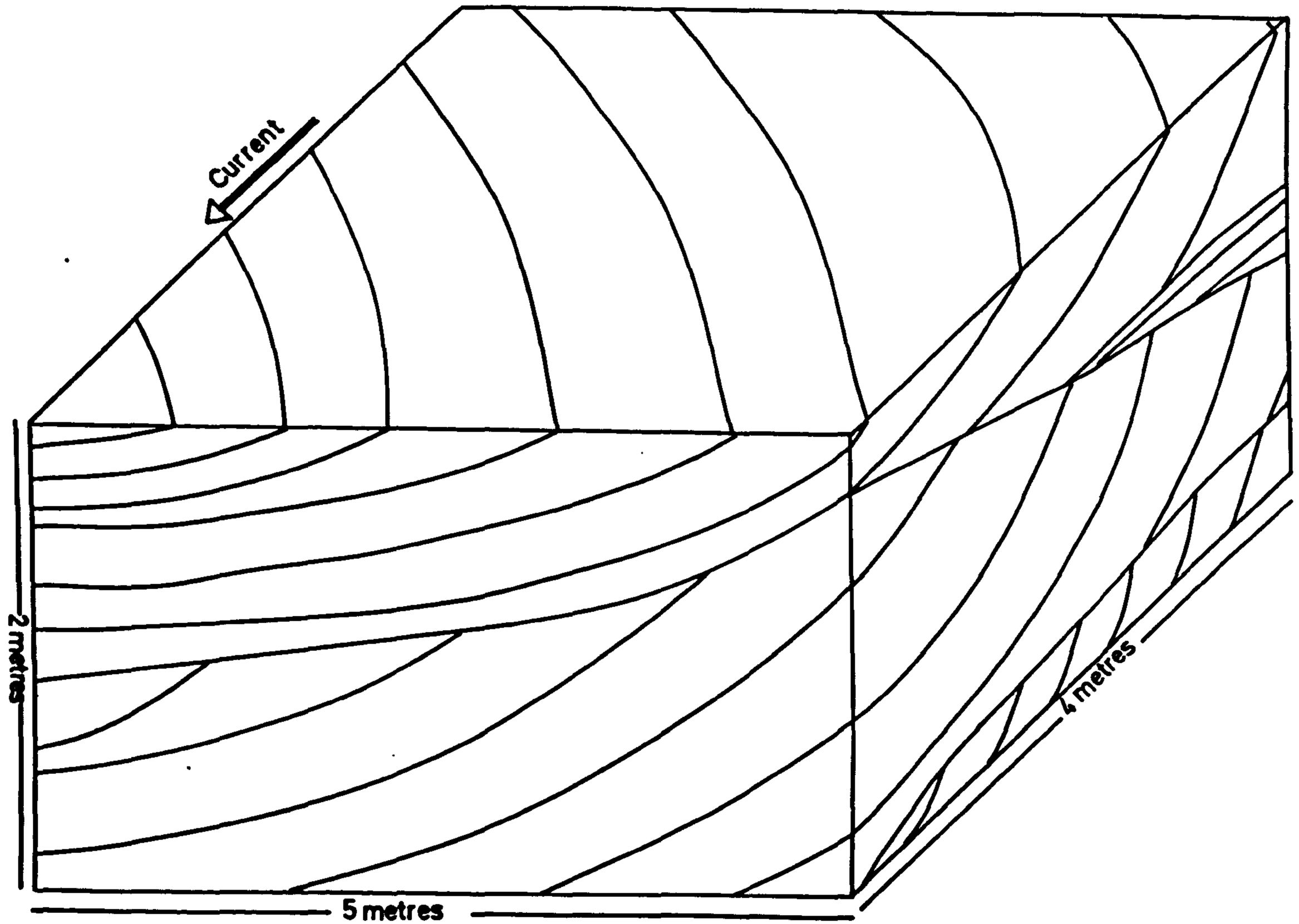

Fig. 7.8. Large scale foreset cross stratification of the Upper Point Bar unit.

EXPLANATION OF PLATE 7.4

UPPER POINT BAR DEPOSITS

A. Steeply dipping foresets of the Upper Point Bar (Clarkly Hill, 125686).

B. Several stages of Upper Point Bar development can be recognised by the different grain sizes of different sets of foresets. They overlie Lower Point Bar and Scour Pool deposits (Clarkly Hill, 125686).

PLATE 7·4

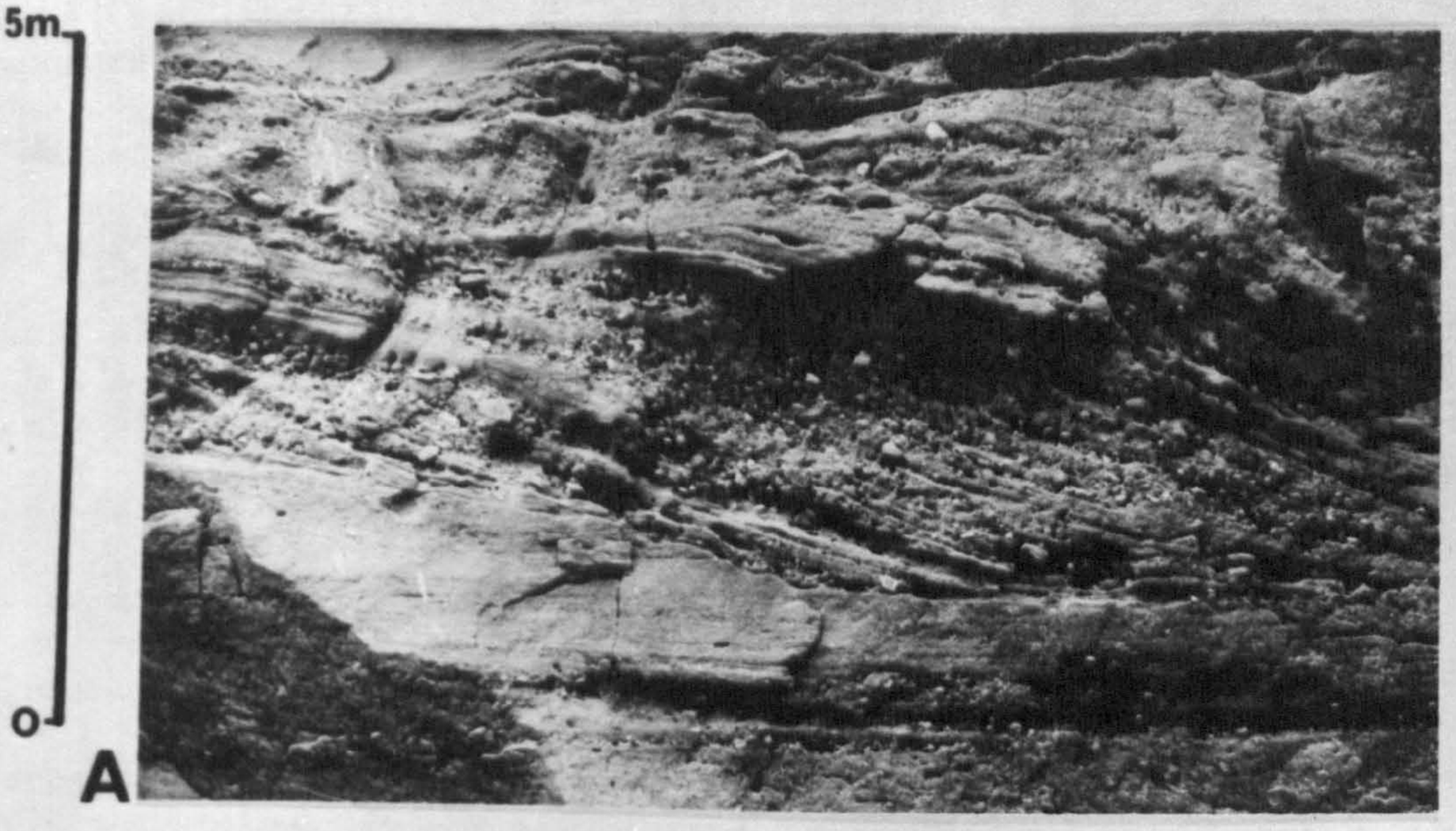



Burghead Harbour (1087569062)

A wall exposed along the edge of the harbour at Burghead incorporates an exposure of 2-2½ metres of point bar deposits. The succession is floored by a series of parallel laminated gravels and sandy gravels representing the flood stage deposits of the Lower Point Bar unit (Fig. 7.9). The pebbles are normally aligned in horizontal bands between more sandy units but pebbles are randomly distributed throughout the sandy layers. The plane laminated gravels are overlain by trough and foreset cross bedded sandstones of the low water stage of the Lower Point Bar. These deposits are approximately 0.3 metres in thickness. Foreset cross stratification dominates the unit and is characterised by foresets dipping at approximately 10 degrees. Small trough sets with current directions at right angles to the foreset bedding are sometimes seen. Lithologically they are slightly coarser than the foreset units. The troughs are normally 100-200 mm in depth and 0.75 metres in width.

The trough and foreset cross stratification is succeeded by a series of silts which display both ripple marks and horizontal laminations. This locality therefore shows the ideal cycle of Lower Point Bar deposits. The silts are up to 100 mm in thickness but this is highly variable owing to erosion by the overlying Upper Point Bar deposits.

The Upper Point Bar deposits reach a maximum of 1.5 metres in thickness; however, this thickness is variable as they cut down into the underlying deposits by as much as 0.5 metres (Fig. 7.9). At the base, the large-scale foresets are horizontal to low angled but they grade upwards into foresets dipping at 18-25 degrees. The lithology is dominantly coarse sandstones with pebbles being fairly common. A silt which is present in the middle of the Upper Point Bar deposits represents the division between two stages of Upper Point Bar development. The silt can be equated with floodplain deposits of the point bar. During a succeeding period of flooding, another point bar was developed to a greater height and therefore overlies the floodplain deposits.

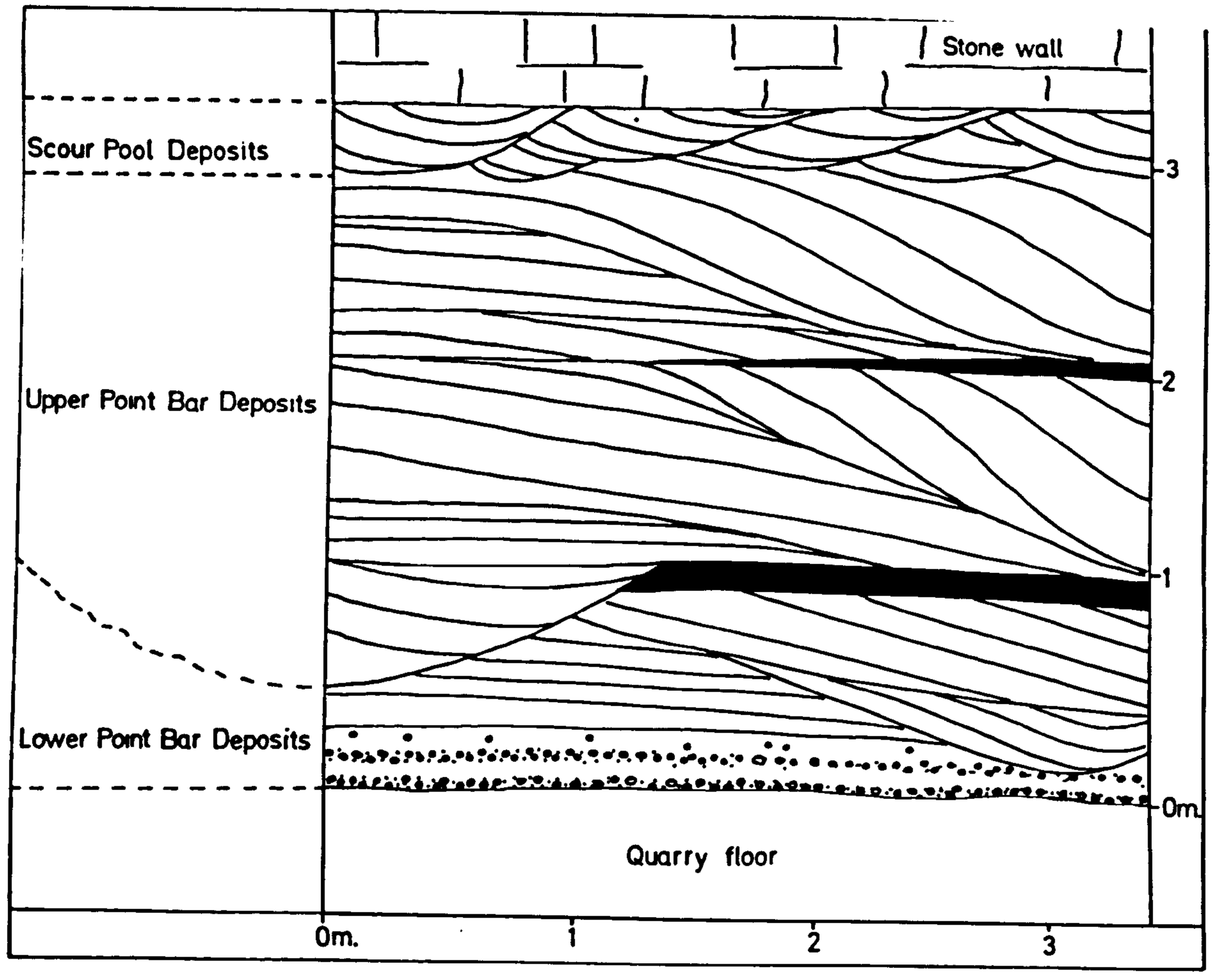

Fig. 7.9. Sequence of stratification types at Burghead Harbour(1087569062).

The uppermost horizon at this locality comprise the characteristic trough cross bedding of the Scour Pool unit cutting down on to the Upper Point Bar deposits. The lithology is represented by coarse grained pebbly sandstones which reach 0.5 metres in thickness.

Burghead Harbour (1076869128)

A small cliff facing southwards towards the harbour represents the best exposed and the most accessible succession of point bar deposits in the area (Fig. 7.10). Although the ideal succession is not present at this locality, only one unit is absent, but if the cycle is traced northwards along the cliffs, a full succession may be seen.

The sequence starts with a series of trough cross bedded sandstones of the Scour Pool unit. The cross bedding exposed here is parallel to the main current direction and therefore typical festoon bedding is not seen (Plate 7.1C). However, cliff sections at right angles to this locality do show typical festoon bedding at the same horizon (Plate 7.1D). The lithology varies from gravels to coarse sandstones; the angle of dip of the foresets reaches a maximum at the top of the trough of 20-25 degrees but these grade into more gently dipping units at the base.

This horizon is overlain by the plane laminated gravels and sands of the flood stage of the Lower Point Bar (Plate 7.2A, 7.2B). At the base, poorly sorted gravels overlie the trough cross bedded sandstones but little or no erosion has taken place into the underlying unit. The poorly sorted gravels are overlain by horizontally laminated sands and gravels which appear to be graded. There are at least three graded units present. Occasionally, the beds may form extremely shallow troughs towards the top of the unit but these units seldom exceed a dip of greater than 5 degrees.

The next horizon is a series of ripple marked and horizontally laminated silts, suggesting that the area was rapidly cut off from the main channel at low water stage, i.e. the trough and foreset cross bedded unit is

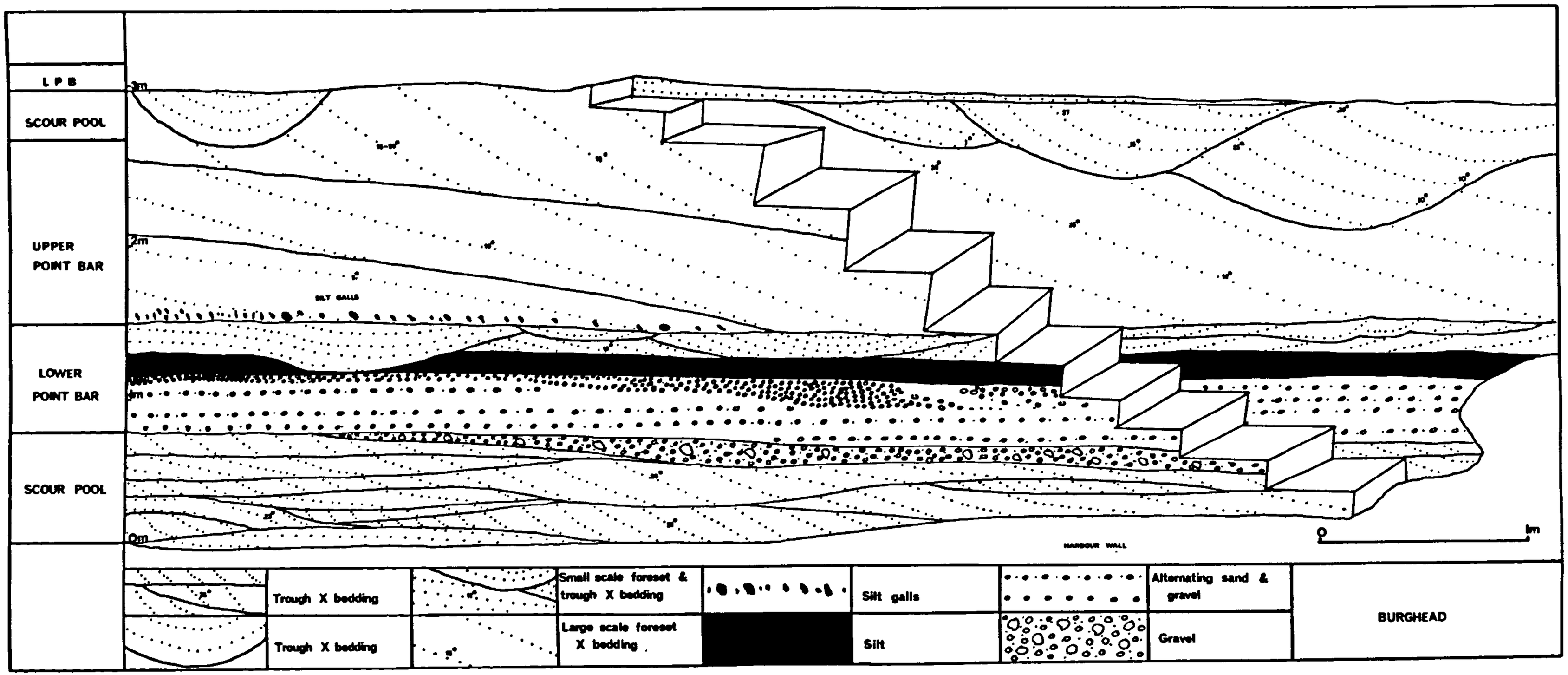

Fig. 7.10. Sequence of stratification types at Burghead Harbour(1076869128).

absent. The amplitude of the ripples is 10-20 mm. These grade up into horizontally laminated silts suggesting even more tranquil conditions. The thickness of the silt horizon varies but reaches a maximum of 25 cm although it may be completely absent owing to erosion by the Upper Point Bar.

The silts are overlain and have been eroded by a series of coarse pebbly sandstones displaying trough and foreset cross stratification. They dip at approximately 15-20 degrees in the opposite direction to the foresets of the overlying Upper Point Bar unit. At the base, climbing ripple laminae separate the silts from the trough and foreset cross bedding. These beds represent the zone of radial flow which occurs as a zone of backflow on meanders. These beds are overlain by and grade into the Upper Point Bar unit.

The Upper Point Bar unit is characterised by large scale foreset bedding, 1-2 metres in thickness. At the base the foresets are gently dipping to horizontal but these grade up into foresets dipping at 15-25 degrees. Lithologically they are composed of pebbly sandstones although silt galls are common towards the base.

The Upper Point Bar deposits are overlain by Scour Pool trough cross stratification of the succeeding cycle. The troughs are exceedingly large and cut down as much as a metre into the underlying Upper Point Bar. They are also composed of coarse pebbly sandstones. In this section, the troughs represent a section at approximately 45 degrees to the main current direction (Plate 7.1A, 7.1B).

Clarkly Hill (13036838)

Fig. 7.11 illustrates the vertical and lateral sequences of stratification types seen in the main Clarkly Hill Quarry. The lowest horizon is a horizontally laminated, medium grained sandstone which shows evidence of ripple marks on the upper surface. The lithology, stratification and position in the vertical sequence all suggest that this horizon is a floodplain deposit.

CLARKLY HILL QUARRY	FLOODPLAIN	3d	a&c Horizontally bedded sst b Low angled foresets - sst
	UPPER POINT-BAR	3c	High angled foresets - pebbly grit
	FLOODPLAIN	3d	SHR
	UPPER POINT BAR	3c	High angled foresets - pebbly grit
	LOWER POINT BAR	3b	a Gravel b Low angled foresets - sst c SHR
	SCOUR POOL	3a	Trough bedded sst
	FLOODPLAIN	1d	Horizontally bedded sst

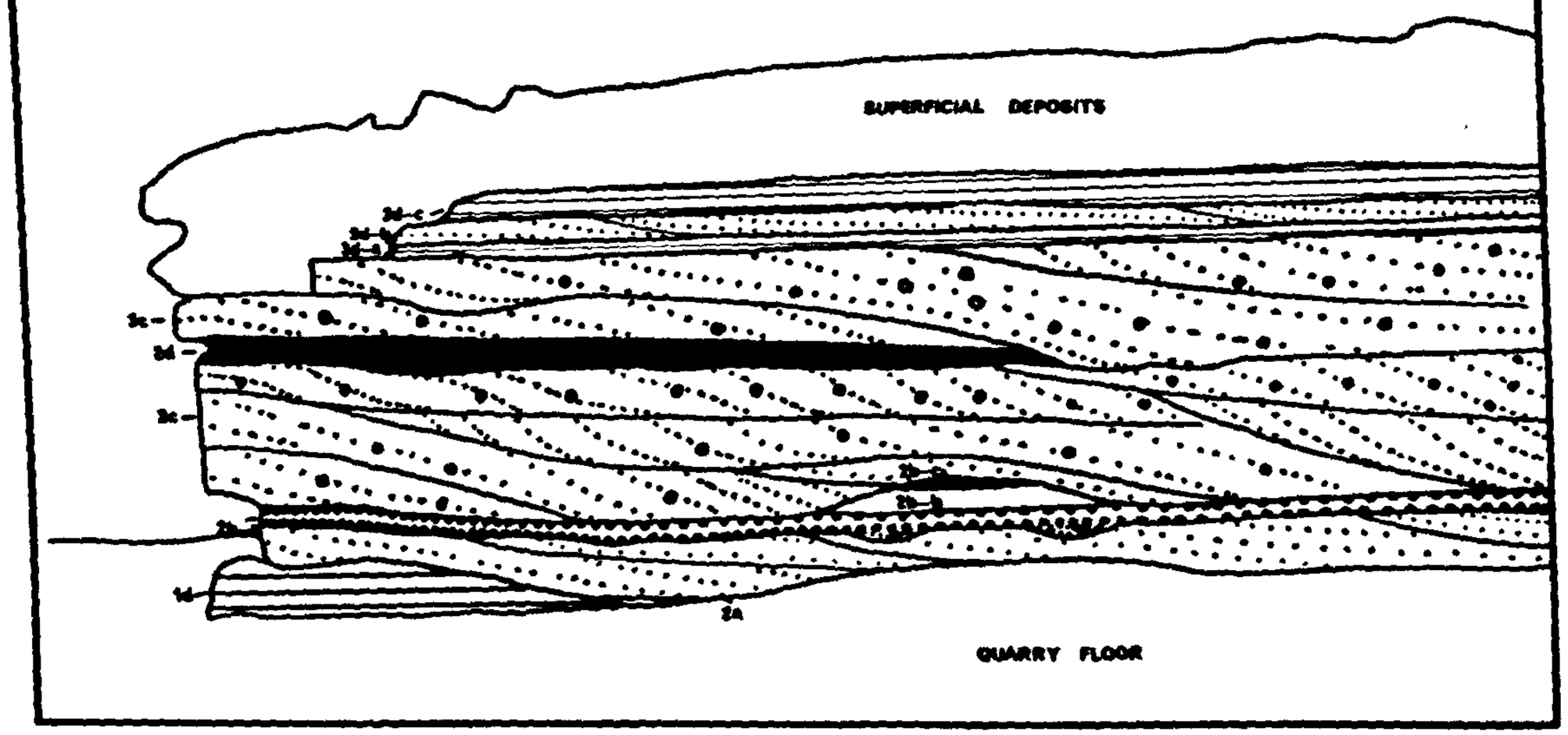

Fig. 7.11. Sequence of stratification types at Clarkly Hill Quarry(125686).

This horizon is overlain by trough cross stratified Scour Pool deposits representing the lowest unit of the next cycle. Although the main quarry face only displays sections parallel to the current, others display the characteristic festoon bedding. The lithology is dominantly coarse sandstones with isolated pebbles.

Plane laminated beds of the Lower Point Bar unit follow this horizon but show little or no erosion into the underlying beds. The only sign of erosion is seen by a small prograded channel cutting down a maximum of 100 mm (Plate 7.2C, 7.2D). The unit is characterised by three graded units deposited as horizontal laminations and varying from gravels to coarse sands; the coarse sandstones may show gently inclined bedding towards the top of the unit. In places only two graded units are present but the horizon can be traced laterally for at least 30 metres.

Foreset cross stratified coarse to medium grained sands may follow the plane laminated horizon although it is frequently absent owing to erosion by the Upper Point Bar. However, to the west of the quarry, these deposits are well exposed. Here, they display low angle foreset bedding dipping at 5-10 degrees with occasional trough bedded channel fills. Thin impersistent silts may also be present. These beds grade up into ripple marked sandstones, a few centimetres in thickness, and finally into ripple marked silts. From the base of the foreset bedded sands to the top of the silts is a thickness of 30-40 cm. The silts are often contorted owing to erosion by the overlying Upper Point Bar deposits.

The Upper Point Bar unit reaches a maximum thickness of 3 metres, this being divided into two main units. The lower unit is highly variable in lithology varying from coarse sands to gravel, each lithology probably representing different flood stages. The angles of deposition are also highly variable, varying from 0-30 degrees. The foresets tend to dip more steeply at the top of the unit, each unit eroding the previous unit. Silts which are present in in the middle of the Upper Point Bar deposits illustrate the maximum height of

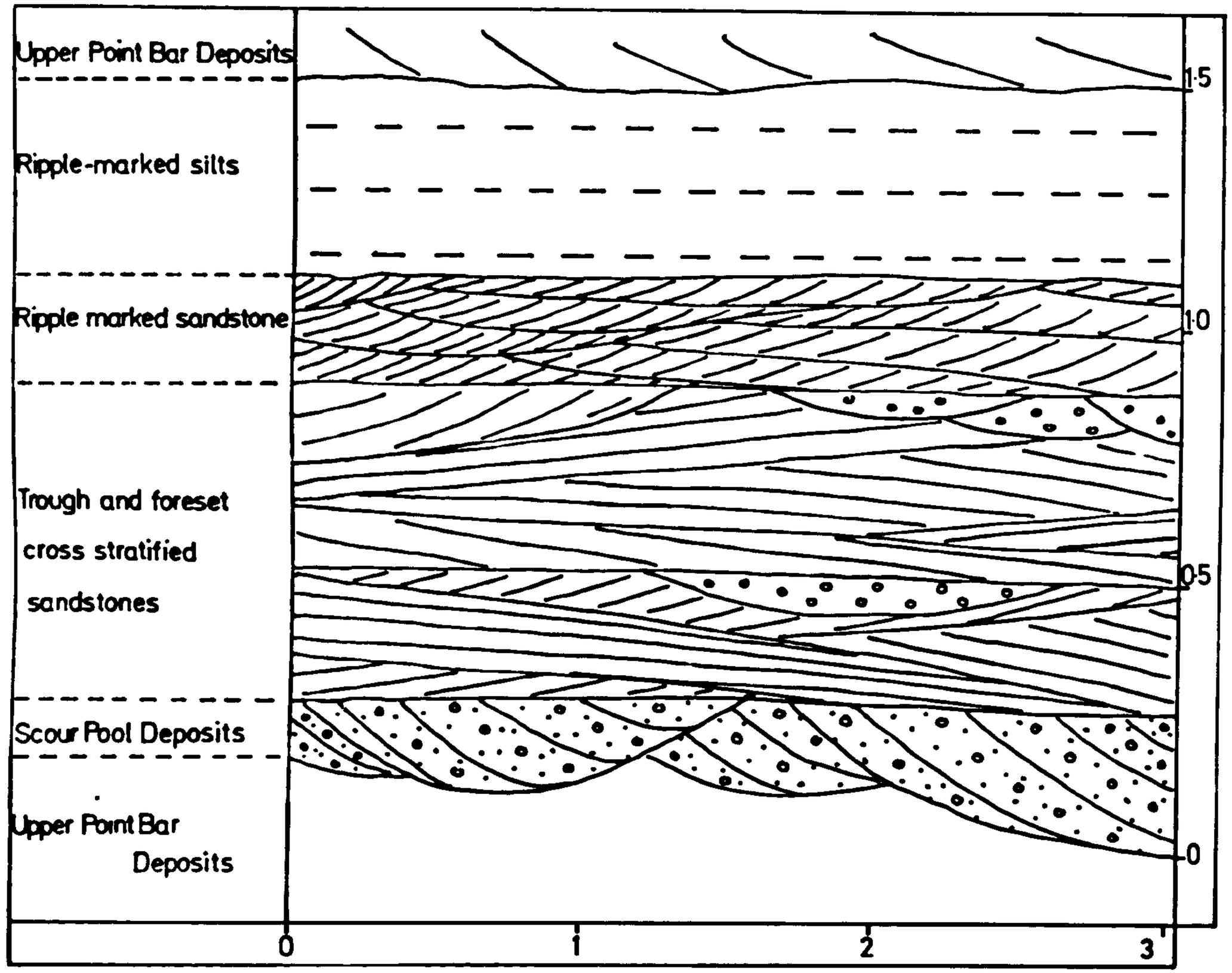

Fig. 7.12. Section of Lower Point Bar deposits at 10746912,west of Burghead Coastguard Station.

the first stage of flooding and are equivalent to floodplain deposits. However, a succeeding phase of flooding attained a greater height. Thus the point bar is built by both vertical and lateral accretion (Plates 7.4A and 7.4B).

The Upper Point Bar deposits are overlain by low angle to horizontal coarse to medium grained floodplain deposits.

Cliffs west of Burghead Coastguard Station (10746912 to 10756930)

Sections of the Lower Point Bar deposits are exposed extremely well at this locality. Fig. 7.12 illustrates the Lower Point Bar unit from trough and foreset cross stratified beds through to ripple marked sandstones and silts. These beds are overlain by Upper Point Bar deposits and underlain by the Scour Pool (Plate 7.3).

Fig. 7.13A shows a thickness of 1 metre of Lower Point Bar deposits with more than one phase of flooding. The lowest horizon is a thick silt with ripple marks which is overlain by trough and foreset cross stratified sandstones indicating renewed flooding. The sequence is terminated by a series of alternating ripple marked sandstones and silts suggesting tranquil conditions which are periodically disturbed by fresh incursions from the main channel.

Figs. 7.13B and 7.13C illustrate the equivalent horizons 10 and 20 metres to the south of the exposure at 7.13A. The lateral extent of the thicker silts is well seen indicating that complete desiccation occurred over the whole channel at the same time. The thinner silts however are not laterally persistent and represent drying up in decadent channels rather than drying up of the main channel.

PALAEOCURRENT ANALYSIS AND PROVENANCE

Fig. 7.14 shows palaeocurrent data measured from pebble orientations and measurement of the trough cross stratification of the Scour Pool unit. Results from the transverse bars of the Lower Point Bar and the chute bars were not included as the directions are generally perpendicular to or at an obtuse angle to the main current direction. The results were obtained from the upper parts of the Burghead Beds.

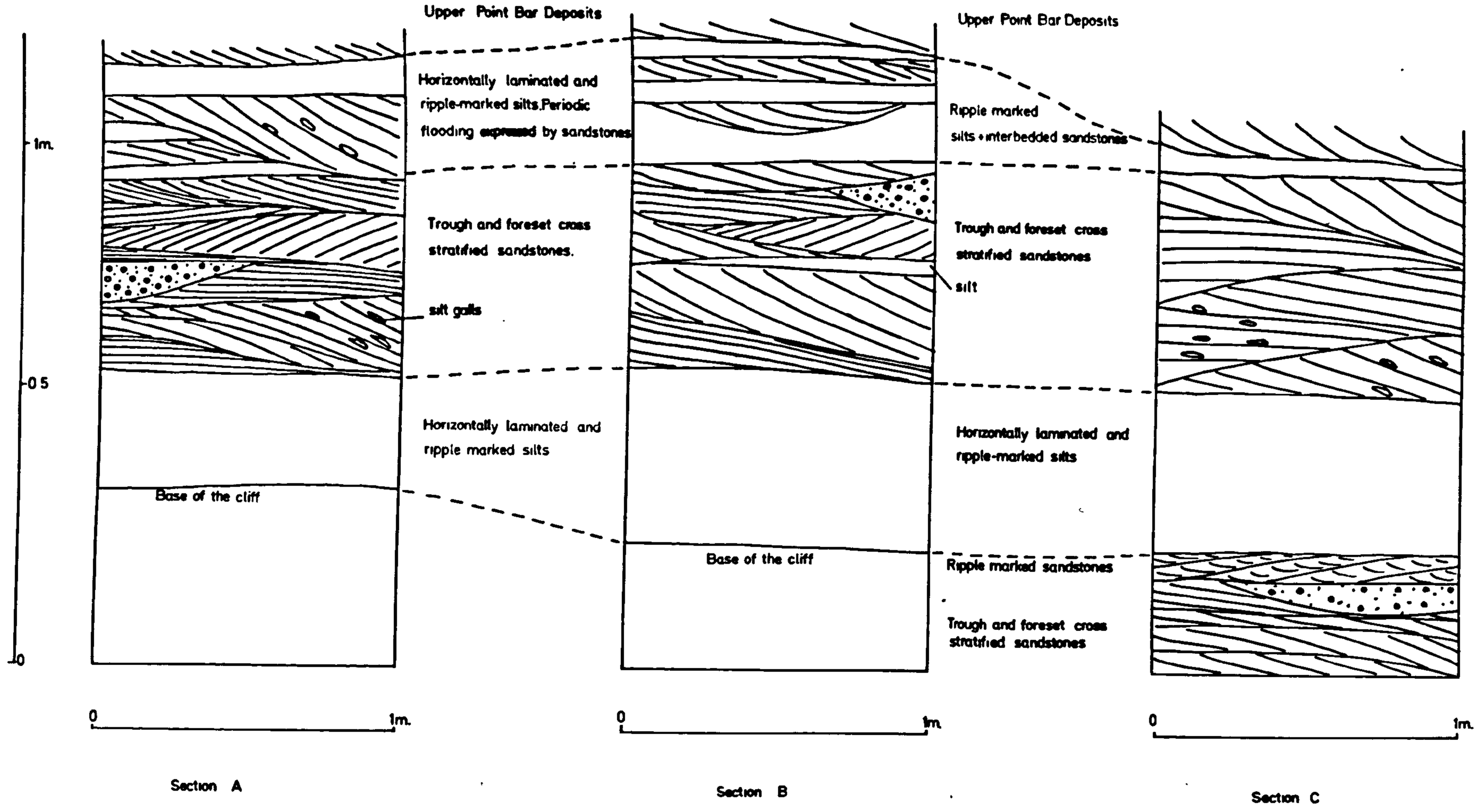

Fig. 7.13. Three sections of Lower Point Bar deposits exposed at grid reference 10756930.

Individual mean directions show variation from a north west to easterly direction; the dispersion is relatively small and probably reflects the low sinuosity of the river. In the vicinity of Burghead, the mean direction gives a fairly uniform easterly to east north easterly direction. However, to the east of Burghead, values are more northerly in direction. The mean direction of all the readings is N77E.

Although the number of readings is relatively large, the accuracy of the mean direction is somewhat in doubt owing to the marked bias of readings from the Burghead area. Over 90 per cent of the readings are from the Burghead district and although these give a fairly constant value, areas to the east of Burghead show a more northerly direction. If more exposures were present to the east, it is suggested that the mean direction would be more north easterly. This is supported by the assymetrical distribution around the arithmetical mean value. Theoretically the results should have a symmetrical skewness in which case the mean value would be towards the north east.

This evidence is also substantiated by the results obtained from drilling in the Moray Firth; these suggest that the centre of the New Red Sandstone Elgin Basin lay to the north and north east of the Elgin area. Thus, although the analyses give an approximate indication of the palaeocurrent, too much emphasis should not be placed on these results.

Study of the present distribution of strata to the south west shows that the area is dominantly Dalradian and Moinian with minor Old Red Sandstone exposures. Thirty kilometres to the south west, a series of Caledonian granites are exposed near to Loch Moy.

Pebble analyses of the Burghead Beds give the following results:

Moinian and Dalradian detritus		Old Red Sandstone detritus	
Aplite	5%	Cornstones	1.6%
Vein Quartz	8.3%	Sandstones	10%
Metaquartzite	10%	Feldspathic Grits	1%
Quartzite	11.6%		
Psammitic Granulite	35%		
Quartz Feldspathic Granulite	19%		

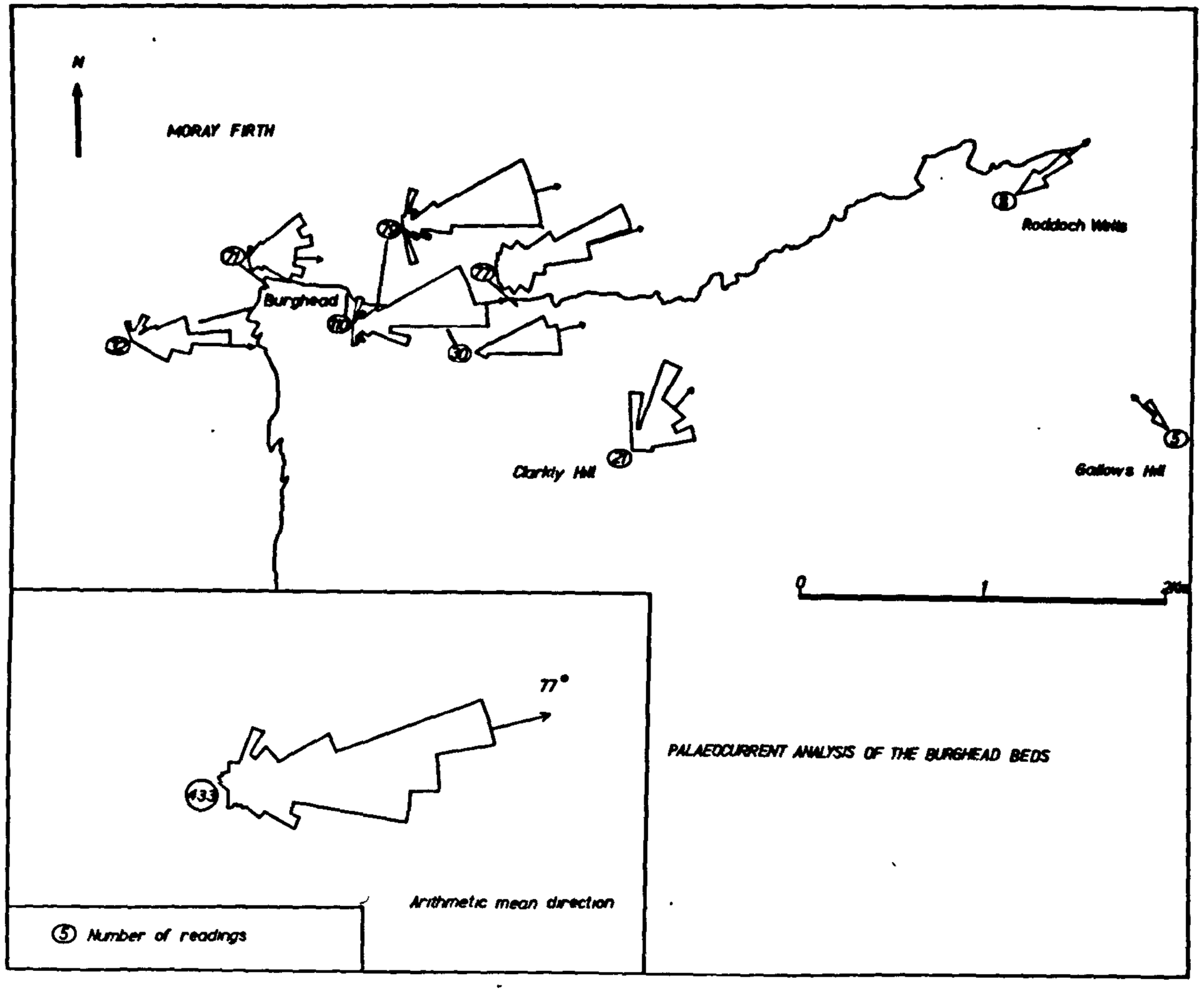

Fig. 7.14. Palaeocurrent analysis of the coarse grained point bar deposits of the Burghead Beds.

There is no evidence of granitic pebbles being present in the Burghead Beds which would suggest that either the granites were not exposed, pebbles were not present, or that the source area was nearer to Burghead. There is evidence of granitic pebbles being present in the Old Red Sandstone (Peacock 1968) although these are often in a highly weathered state. It is therefore unlikely they would be preserved if they were retransported. Extremely rare fragments of myrmekitic quartz supposedly indicating a granitic source are found in the Burghead Beds.

The pebble analysis would suggest that the detritus of the Burghead Beds was dominantly derived from the Moinian and Dalradian rocks. Comparison of the pebbles in the Middle Old Red Sandstone described by Peacock (1968) does indicate close similarities with those seen in the Burghead Beds although the proportions are different. It is thus thought very probable that the Old Red Sandstone played a more important role in the source area of the Burghead Beds than is suggested by the pebble analyses, i.e. the Burghead Beds are probably dicyclic in origin.

The source area of the Burghead Beds was therefore in a south westerly direction and made up of Old Red Sandstone cornstones and sandstones and Moinian and Dalradian metaquartzites and granulites.

GRAIN SIZE ANALYSES

Table 7.1 shows the results of grain size analyses of the Burghead Beds point bar deposits calculated using the method of Folk and Ward (1957). In the case of the point bar deposits, samples were sieved after disaggregation using $\frac{1}{4}$ phi intervals.

The median grain size of the Scour Pool deposits is highly variable and to a certain extent dependent on the amount of pebbles in the sample; they vary from 0.1 to 1.75 phi in mean diameter. Standard deviation is also high showing the large grain size range present in the samples. The standard deviation indicates the poorly sorted nature of the sediments. Skewness is generally positive due to the deficiency of the fine material in the sediments; this is

because the fines are held in suspension owing to the high velocity of the stream. Kurtosis is near to the norm of 0.50, this illustrating the presence of the intermediate grain sizes.

The Lower Point Bar deposits show an upward fining sequence in response to a decrease in velocity of the stream and corresponding decrease in depth of the water. The plane laminated horizons have a grain size normally in the range 1.25-1.5 phi, a range which is extremely similar to that of the Scour Pool deposits. The standard deviation which reflects the poor sorting of the sediments is also similar to that of the Scour Pool deposits. Skewness is approximately symmetrical whilst the kurtosis reflects the lack of intermediate grain sizes in the horizon.

The transverse bars indicate a decrease in mean grain sizeand an increase in sorting from the horizon below. Standard deviation shows the sediments to be moderately sorted. Skewness is positive reflecting the deficiency of fine material but the kurtosis again approximates to the norm indicating the presence of the intermediate grain sizes. The ripple marked sandstones and silts again indicate a decrease in the mean grain size but the decrease in standard deviation, which would be expected, is not seen.
The horizons show moderate to poor sorting owing to contamination of the sediments by flooding into the isolated channels. Skewness and kurtosis are highly variable owing to this fact.

The median grain size of the Upper Point Bar deposits ranges from 0.8-2.9 phi and is controlled by the amount of silt galls and pebbles in the sample; the matrix is essentially one of coarse sand which appears to remain fairly constant. Generally, the mean grain size ranges from 1.2-1.5 phi, extremely similar to that of the Scour Pool deposits and the plane laminations of the Lower Point Bar. Standard deviation indicates that the sediments are generally moderately sorted but some samples are poorly sorted to very poorly sorted. Skewness is generally negative showing an excess of fines due to the high position of the Upper Point Bar in the stream. Kurtosis is high variable but often less than 0.50.

Fig. 7.15. Grain size analysis of the coarse grained point bar deposits of the Burghead Beds.

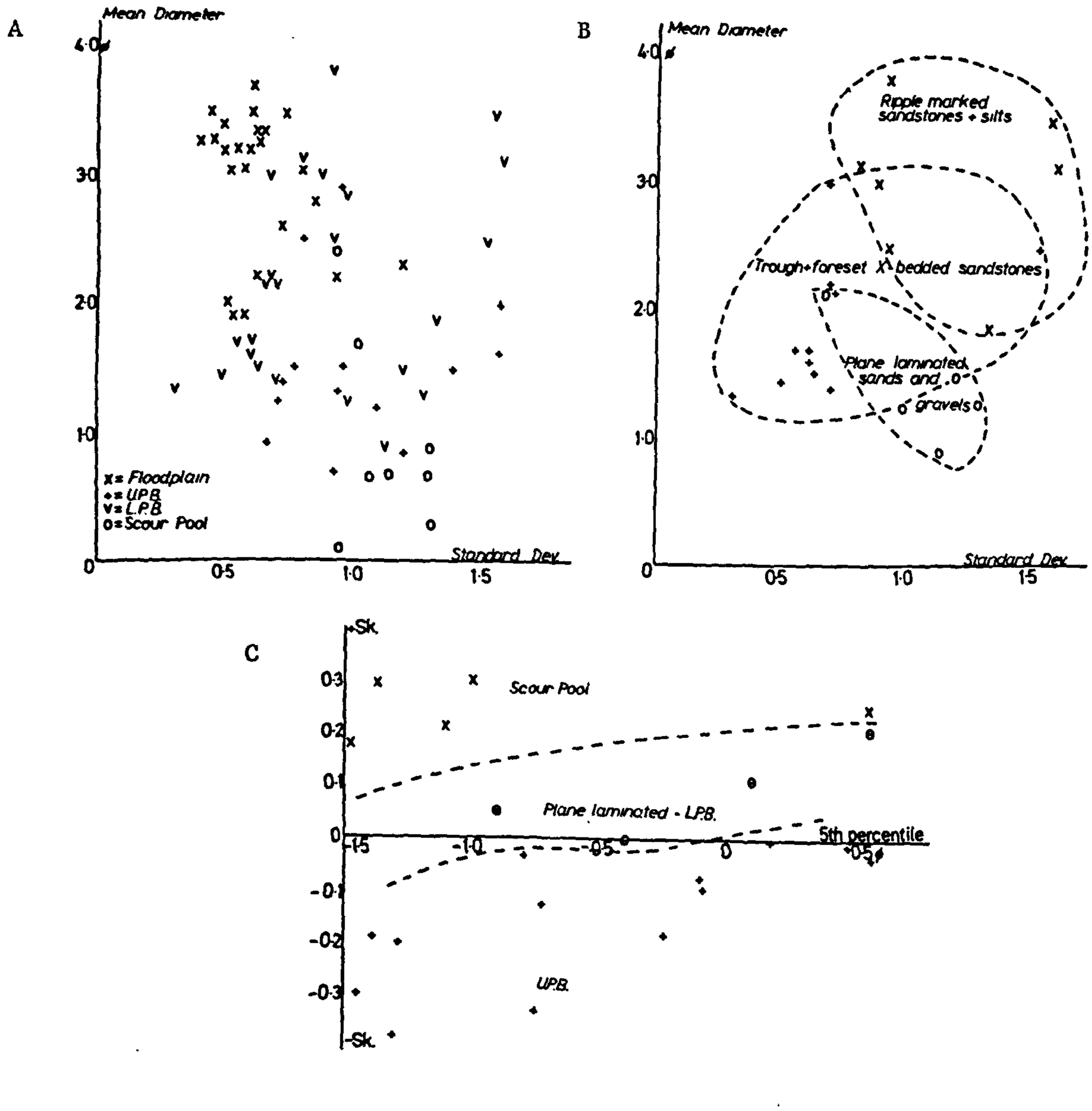

Facies	Number	5th	16th	25th	50th	75th	84th	95th	St.D,	Sk.	Kg'
Scour Pool											
	B178	0.55	0.90	1.10	1.75	2.55	3.00	3.90	1.04	+0.24	0.49
	CH3	-1.55	-0.70	-0.20	0.30	1,55	2.00	2.60	1.30	+0.19	0.50
	CH6	-1:10	-0.45	-0.10	0.90	1.90	2.20	3.20	1.31	+0.02	0.47
	CHQ6	-1.00	-0.50	-0.30	0.10	0.90	1.40	2.15	0.95	+0.33	0.52
Lower Point Bar; Gravels											
	CHQ2	-0.85	0.20	0.60	1.30	2.10	2.30	2.85	0.60	+0.05	0.51
	CHQ3	-0.40	0.35	0.70	1.25	1.80	2.00	3.20	0.98	-0.04	0.58
	B179	-0.50	0.65	1.00	1.50	2.05	2.30	3.50	1.17	-0.03	0.61
Lower Point Bar; Sands											
	BH1E2	0.70	1.15	1.30	1.70	2.10	2.30	2.85	0.60	+0.05	0.52
	E52	0.25	0.80	1.00	1.45	2.00	2.25	2.60	0.70	+0.10	0.54
	CHB1	-0.90	1.10	1.15	1.35	1.60	1.80	2.10	0.35	+0.25	0.48
	CHB4	0.90	1.05	1.20	1.45	1.85	2.05	2.40	0.50	+0.20	0.48
	B209	1.20	1.60	1.80	2.15	2.60	3.00	3.40	0.68	+0.18	0.53
	B211	0.60	1.00	1.10	1.60	2.05	2.15	2.65	0.60	-0.01	0.47
	B468	1.35	1.75	1.95	2.20	2.60	2.95	3.95	0.69	+0.39	0.62
	B469	2.00	2.35	2.60	3.00	3.50	3.85	4.35	0.73	+0.23	0.52
	B210	0.60	1.20	1.30	1.70	2.05	2.20	2.60	0.55	+0.10	0.52
	CH2	0.40	1.00	1.05	1.55	2.00	2.25	2.55	0.61	+0.03	0.48
Lower Point Bar; Silts											
	BC4	0.00	0.70	1.10	1.85	2.60	3.35	4.40	1.33	+0.07	0.54
	BH2A-3	1.15	2.05	2.30	2.85	3.65	3.90	4.50	0.98	-0.02	0.50
	BH3-1	1.75	2.10	2.20	3.00	3.40	3.80	4.70	0.87	+0.03	0.51
	BC10	1.80	2.50	2.75	3.15	3.60	4.00	4.65	0.80	+0.015	0.58
	B212	0.75	1.75	2.05	2.50	3.05	3.40	4.10	0.92	-0.015	0.61
	B185	0.60	1.75	2.20	3.15	4.45	5.10	6.10	1.66	+0.11	0.45
	B182	-1.00	2.20	2.65	3.50	4.25	4.60	5.50	1.58	-0.31	0.62
	B193	1.55	2.50	3.00	3.80	4.20	4.25	4.75	0.92	-0.16	0.52
	B197	0.70	1.30	1.70	2.50	3.50	4,85	5.50	1.64	0.30	0.53

TABLE 7.1. Grain Size Analyses.

Facies	Number	5th	16th	25th	50th	75th	84th	95th	St.D.	Sk.	Kg'
Upper Point Bar											
	BH1A4	1.65	2.25	2.45	2.90	3.50	4.00	4.90	0.95	+0.24	0.56
	E50	0.13	0.70	1.00	1.50	2.00	2.20	2.60	0.75	+0.11	0.51
	E57	0.17	0.70	0.90	1.25	1.65	1.90	2.50	0.70	+0.02	0.55
	E53	-0.75	0.40	0.80	1.47	2.00	2.20	2.60	0.95	-0.36	0.47
	E54	-0.10	0.25	0.50	0.92	1.25	1.50	2.20	0.66	-0.10	0.56
	E70	-0.80	0.60	0.85	1.30	1.90	2.30	2.65	0.94	-0.03	0.57
	CHB2	-1.35	-0.60	0.20	1.20	1.80	2.00	2.45	1.10	-0.47	0.42
	CHB3	-1.35	-0.70	-0.15	0.85	1.60	1.90	2.50	1.20	-0.20	0.47
	B187	-4.50	-0.50	1.00	2.05	2.85	3.50	5.50	2.50	-0.30	0.69
	B153	1.10	1.75	2.05	2.50	2.95	3.25	3.90	0.80	0.00	0.57
	B470	-1.40	-1.25	-1.10	0.70	1.40	1.75	2.60	0.92	-0.18	0.39
	B471	-0.13	0.70	1.00	1.40	1.90	2.15	2.50	0.72	-0.07	0.52
	B472	-0.25	0.40	0.90	1.65	2.20	2.45	3.40	1.60	-0.17	0.53
	B473	-0.75	-0.25	0.40	1.50	2.35	2.65	3.55	1.40	-0.12	0.47

TABLE 7.1 (continued)

Number	Rock Fragments	Quartz	Matrix
CH1A	8.5	91.5	0
CH1B	6.9	91.3	1.3
CH2A	6.25	87.5	6.25
CH2B	6.75	91.0	1.25
CH2D	7.8	90.2	2.0
CH3A	4.8	93.6	1.6
CH3B	9.75	85.0	5.25
CH4B	7.4	92.6	0
CH5	6.6	93.4	0
CH6	8.3	91.3	0.4
CH7	5.8	94.0	0.2
CH8	5.6	94.0	0.4
E466	7.2	92.8	0
E467	9.15	90.5	0.35
E468	14.2	85.5	0.30
E469	13.9	85.8	0.30
E470	5.9	91.3	2.40
E471	8.4	90.1	1.50
E472	6.7	92.6	0.70
E473	4.6	94.3	0.70
E474	5.4	94.6	0
E475	18.0	68.4	13.65
E51	0.6	99.2	0.20
E52	4.6	94.6	0.80
E53	5.0	94.2	0.80
E54	5.6	94.4	0
E56	5.0	94.7	0.30
E75	3.5	96.5	0
E76	7.2	92.8	0
B185	6.1	93.9	0
B210	9.05	50.5	40.5
B209	6.8	90.1	2.1
B211	5.0	85.5	9.5
B178	8.4	90.1	1.5

TABLE 7.2. Sandstone Classification Results (after Pettijohn 1954)

Number	Rock Fragments	Quartz	Matrix
B184	4.8	86.0	9.2
B179	7.8	76.1	16.1
B212	6.1	88.7	5.2
B212	11.0	75.0	14.0
B196	4.2	28.4	67.4
B184-2	6.2	80.0	13.8
B197	5.6	69.4	25.0
B182	5.0	45.0	50.0
B187	6.8	76.7	16.5

TABLE 7.2. (continued)

Number	Unimodal Quartz	Others	Clay and Mica
CH1A	42,5	57.5	0
CH1B	52.0	46.7	1.3
CH2A	48.8	44.95	6.25
CH2B	44.75	54.0	1.25
CH2D	38.4	59.6	2.0
CH3A	36.8	61.6	1.6
CH3B	31.0	63.75	5.25
CH4B	47.2	52.8	0
CH5	45.0	55.0	0
CH6	39.4	60.2	0.4
CH7	46.2	53.6	0.2
CH8	48.0	51.6	0.4
E466	65.4	34.6	0
E467	67.3	32.5	0.35
E468	72.6	27.1	0.3
E469	71.3	28.4	0.3
E470	59.0	38.6	2.4
E471	64.7	33.8	1.5
E472	42.5	56.8	0.7
E473	74.0	25.3	0.7
E474	58.6	41.4	0
E475	69.2	17.2	13.65
E51	27.6	71.2	0.2
E52	45.4	53.8	0.8
E53	51.2	48.0	0.8
E54	48.3	51.7	0
E56	37.6	62.1	0.3
E75	29.6	70.4	0
E76	41.0	59.0	0
B185	28.3	71.8	0
B210	33.9	25.6	40.5
B209	58.7	39.2	2.1
B211	47.6	42.9	9.5

TABLE 7.3. Sandstone Classification Results (after Williams 1972)

Number	Unimodal Quartz	Others	Clay and Mica
B211	47.0	51.5	1.5
B178	53.0	37.8	9.2
B184	65.4	18.5	16.1
B179	36.0	58.8	5.2
B212	53.0	33.0	14.0
B196	22.0	10.6	67.4
B184-2	58.0	28.3	13.8
B197	59.2	15.8	25.0
B182	38.0	12.0	50.0
B187	60.3	23.2	16.5

TABLE 7.3. (continued)

Fig. 7.15A shows the results of mean grain size plotted against standard deviation for all the coarse grained point bar deposits. It can clearly be seen that no upward fining sequence is present as in the more normal fine grained point bar deposits. Statistical parameters vary enormously but the following section will show that these parameters are related to the depth of water in which they were deposited.

Thus, if the deposits are compared relative to their time of deposition in the cycle, some relevant statistical comparisons can be made. At the flood stage, Scour Pool, plane laminations of the Lower Point Bar and Upper Point Bar sediments are deposited. If skewness is plotted against grain size (for convenience the 5th percentile has been used) a general trend relative to the depth of water in which the sediments were deposited can be seen. Fig. 7.15C shows that the deeper water deposits of the Scour Pool tend to be positively skewed whereas those of the Upper Point Bar tend to be negatively skewed. Thus the Scour Pool deposits are relatively deficient in fines whereas the Upper Point Bars have a relative excess. This can be explained by the fine material being held in suspension during the high velocity flooding except where the velocity decreased on the periphery of the channel.

Fig. 7.15B shows the relationship of the grain size and standard deviation of the Lower Point Bar deposits. The coarsest material is seen at the base of the unit in the form of the plane laminated horizon of sands and gravels. A decrease in size is seen in the trough and foreset cross stratified sandstones and again in the ripple marked sandstones and silts. This reflects the decrease in velocity and water depth of the stream. An upward increase in sorting is also seen although it is not carried on into the highest units owing to contamination by the overlying sediments and by flooding.

PETROLOGICAL CLASSIFICATION OF THE POINT BAR DEPOSITS

The various classification schemes were discussed in the previous chapter with reference to the Hopeman Sandstone. It was concluded that the sandstones deposited in desert environments were a special case and that two

classifications were necessary to adequately classify the sandstones. The first classification was a method by which the sandstones could be compared relative to other arenaceous deposits; the classification of Pettijohn (1954) was used. The parameters are also able to differentiate various environments by comparing the maturity, provenance and fluidity (Pettijohn, 1954). The second classification proposed by the author attempts to classify the sandstone within desert sandstones by choosing the most relevant parameters applicable to their genesis in that environment.

Tables 7.2 and 7.3 show the results of standard point count techniques using the parameters of Pettijohn (1954) and the revised classification proposed by author in the previous chapter. Fig. 7.16 illustrates these values plotted on triangular diagrams. The classification of McBride (1963) is again included for comparative reasons.

Fig. 7.16A indicates that the point bar deposits generally fall into the orthoquartzite and subarkosic clans. Rarely fine grained silts containing a high percentage of clay can be included in the greywacke clan of Pettijohn (1954). However, the second classification (Fig. 7.16C) illustrates that the variation in the values of the vaious parameters is to a certain extent related to the grain size. The coarse grained flood stage deposits are characterised by a high percentage of polycrystalline quartz and rock fragments and a relatively low percentage of clay minerals and micas. In comparison with the flood stage deposits, those of the low water stage show an increase in clay content and decrease in rock fragments and polycrystalline quartz. The variations are however more relevant when applied to the descriptive and genetic properties of maturity, provenance and fluidity proposed by Pettijohn (1954).

The maturity indices quartz:feldspar and quartz and chert:feldspar and rock fragments for the point bar deposits are 17:1 and 13:1 respectively. However, it is felt that these ratios are deceptively high due to the dominantly metaquartzite source which gives an anomalous deficiency of rock fragments.

Fig. 7.16. Classification of the coarse grained point bar deposits.

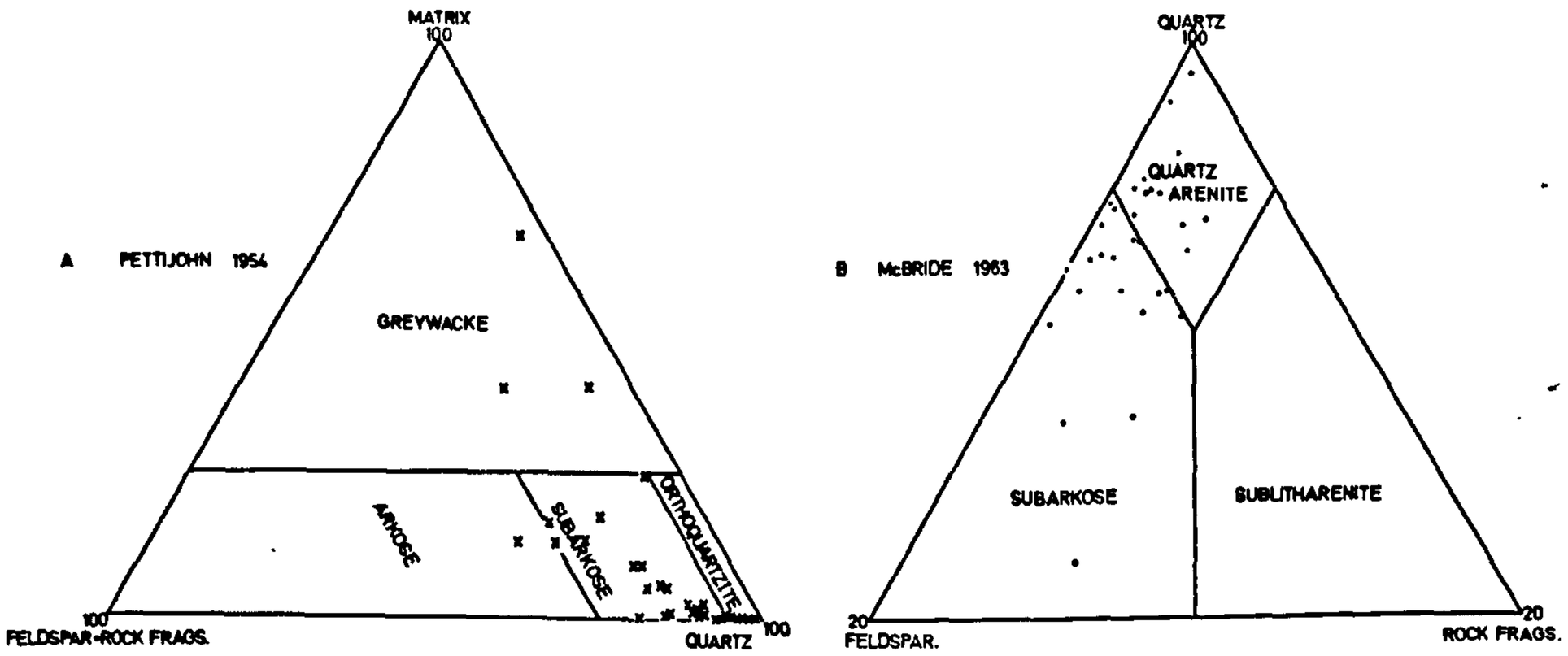

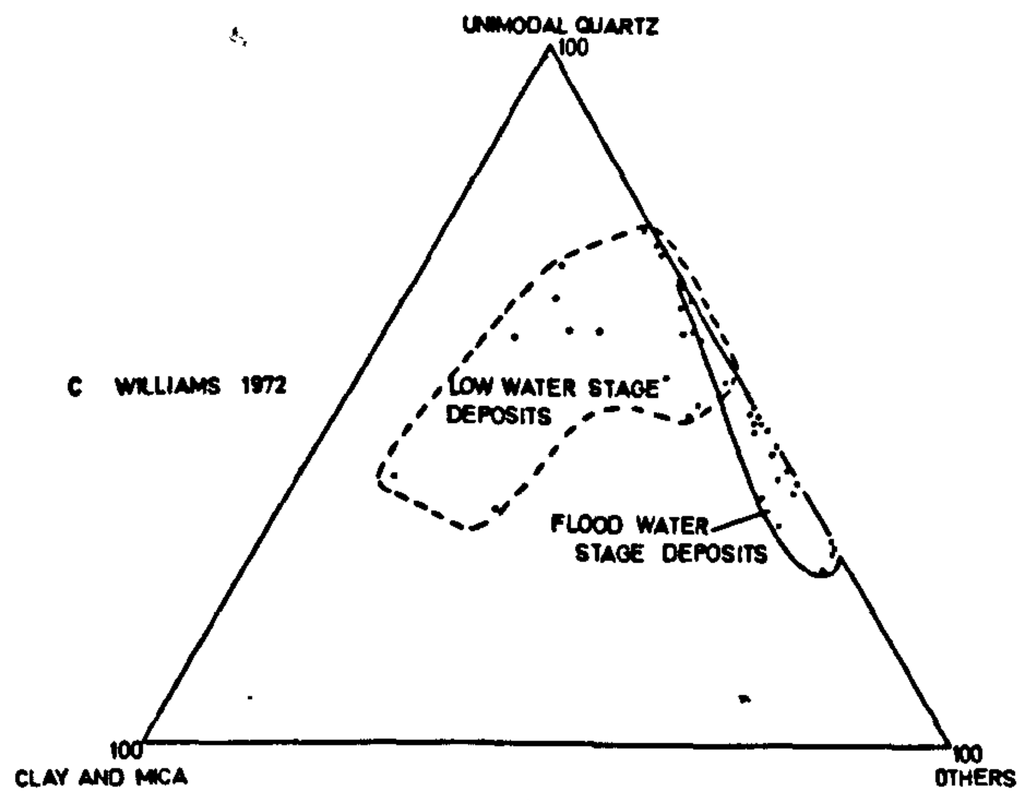

Number	Strained	Unstrained	Polycrystalline
CH1A	53.1	5.5	41.4
CH2B	57.4	2.4	40.2
CH2A	57.4	3.8	38.8
CH2B	52.0	4.1	43.9
CH2D	44.5	2.3	53.2
CH3A	40.8	3.5	55.7
CH3B	38.3	0.3	61.4
CH4	60.7	4.7	34.6
CH5	62.3	4.5	33.2
CH6	55.5	3.3	41.3
CH7	63.7	1.9	34.4
CH8	41.4	7.0	41.6
E53	66.5	17.9	15.6
E54	56.8	11.0	32.1
E56	46.9	10.0	43.1
E68	72.6	15.0	12.4
E71	64.7	8.3	27.0
E75A	69.2	28.5	12.3
E73	74.0	6.3	19.7
E74	44.8	36.0	19.2
E75	41.8	30.5	27.7
E76	59.4	28.6	12.0

TABLE 7.4. Relative Percentage of the three main types of quartz.

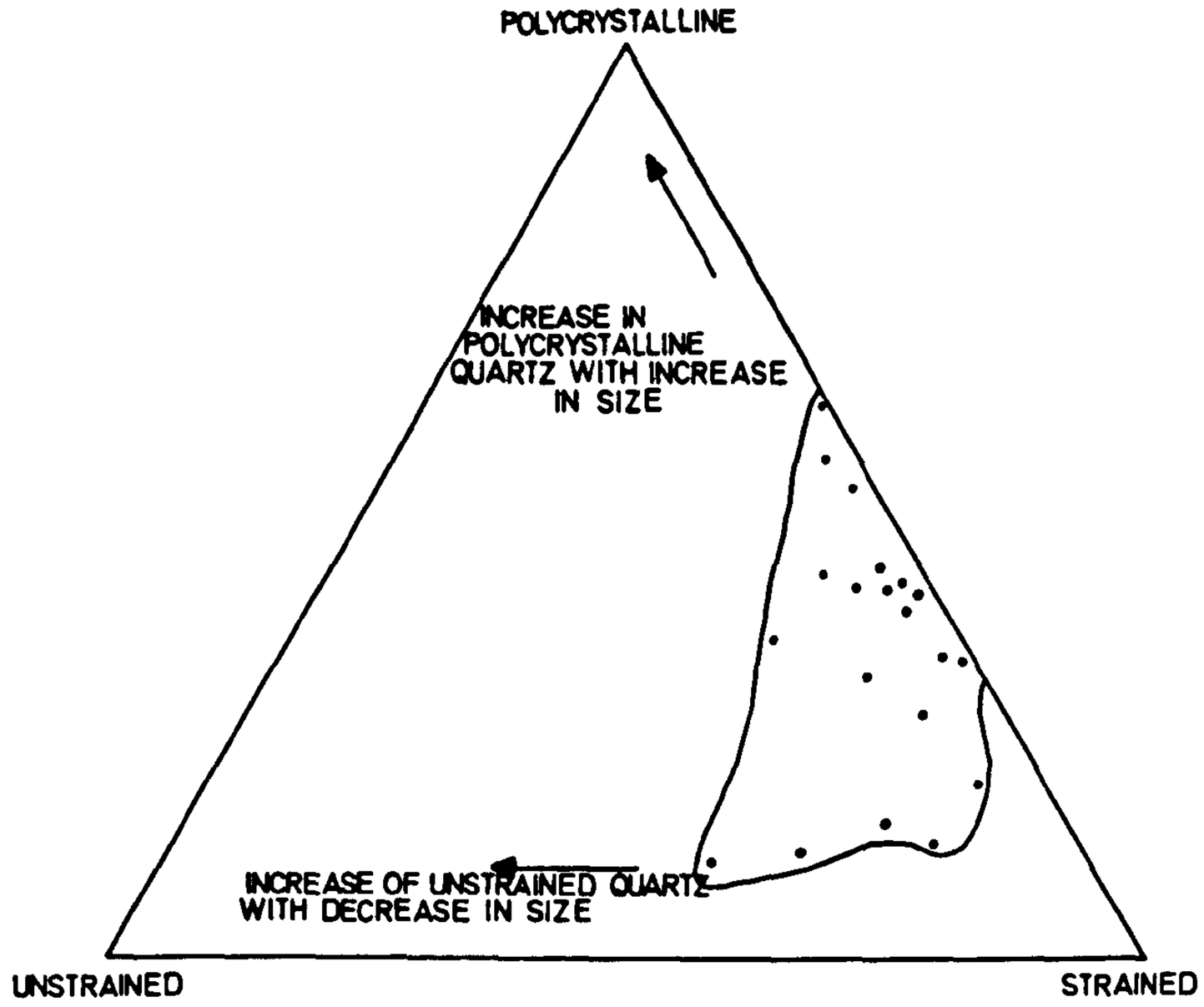

Fig. 7.17. Ratio of quartz types.

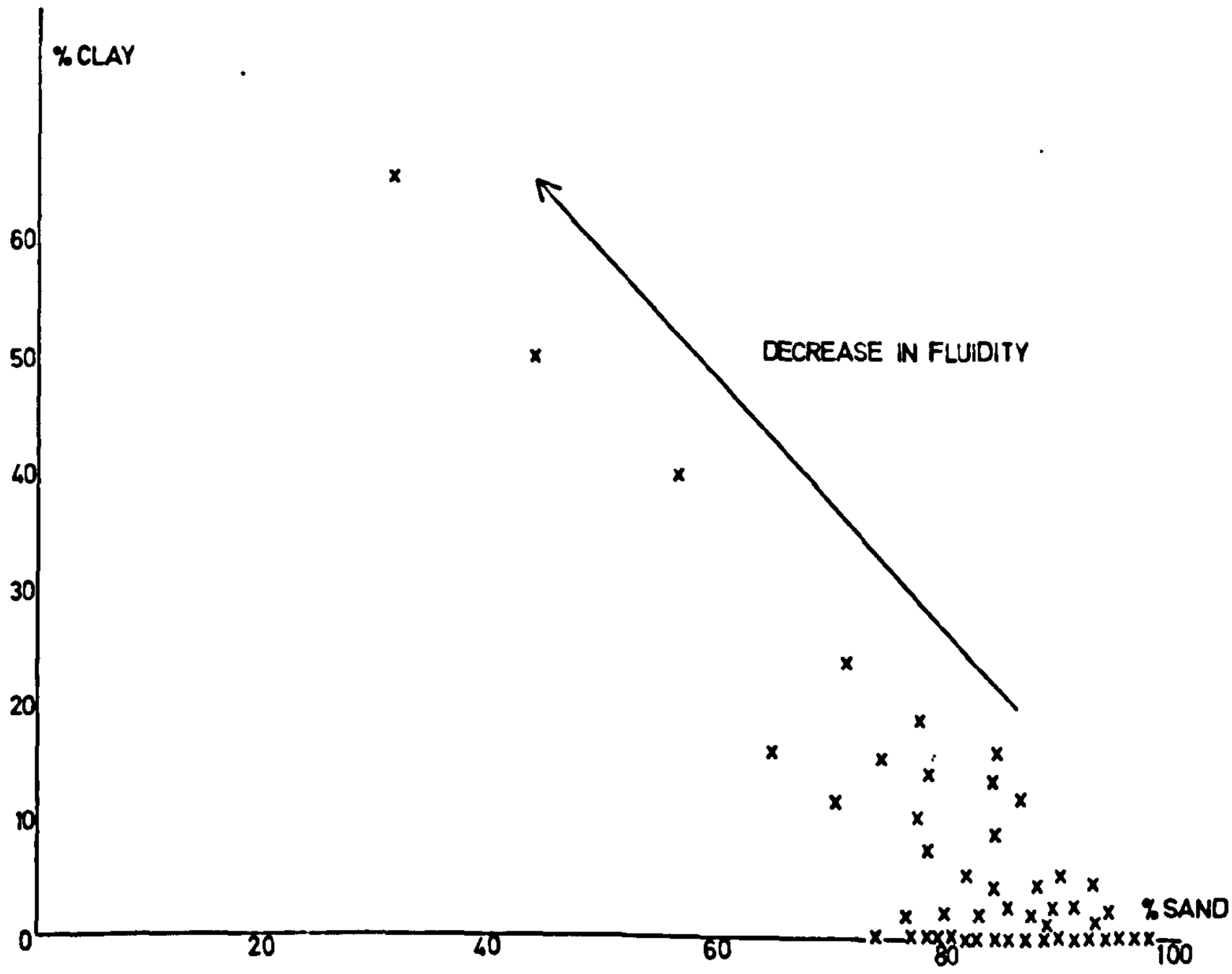

Fig. 7.18. Fluidity decreases from flood to low water stage.

The provenance ratio of feldspar:rock fragments is 3:1 suggesting that the source area was dominantly plutonic in origin. However, pebble analyses suggest a dominantly supracrustal source. This can once again be explained by the paucity of rock fragments due to the quartzitic source. The fluidity of the depositing medium (sand:clay, Pettijohn, 1954) is highly variable as the sediments were laid down in both flood and low water stages. Fig. 7.18 shows that the fluidity is greatest during the flood stage and progressively decreases to the low water stage, i.e. the silts of the low water stage have a fluidity of less than 1.

DETRITAL COMPONENTS OF THE POINT BAR DEPOSITS

Quartz

Table 7.4 illustrates the relative percentage of the three main types of quartz present in the point bar deposits of the Burghead Beds.

Unstrained quartz:

The percentage of unstrained quartz varies from 0-30 per cent but is generally nearer to 2-10 per cent. Samples with the higher percentages of unstrained quartz are generally fine grained, (Fig. 7.17). It is suggested that this is due to the breakdown of larger strained grains. It may also be noted that the percentage of unstrained quartz is inversely proportional to the percentage of polycrystalline quartz, again indicating that the percentage of unstrained quartz is related to the finer grain size. The types of unstrained quartz recognised in the point bar deposits show the familiar inclusions which were described in detail in the Hopeman Sandstone. Unstrained quartz with randomly orientated rutile needles does however appear to be more common..

Strained quartz:

Strained quartz constitutes between 30-75 per cent of the total quartz present although this value is generally nearer 40-55 per cent. Various types of strained quartz can be recognised by the degree of straining which they illustrate. However, these can once again be divided into the two main

groups derived from high and low grade metamorphic granulites and meta-quartzites as distinguished in the previous chapter, i.e. the higher the degree of straining, the higher probability that the grains were derived from high grade metamorphic sources.

Polycrystalline quartz

The percentage of polycrystalline quartz grains is to a certain extent dependent on the mean grain size of the sample, i.e. the larger the mean grain size, the higher the percentage of polycrystalline grains. This may be seen in Fig. 7.19 where the mean grain size is plotted against the percentage of polycrystalline quartz. It will be noted that the results suggest that the Hopeman Sandstones were derived from a similar source to that of the Burghead Beds, i.e. Old Red Sandstone, Moinian and Dalradian.

The most common type of polycrystalline quartz present belong to the high grade metaquartzites. These grains are highly strained and normally exhibit a marked schistosity. Contacts between the grains are highly sutured, reflecting the high pressure under which they were formed. Low grade meta-quartzite fragments exhibit less straining, little or no schistosity, a more globular outline and less pressure solution at the contacts, i.e. although they are closely welded, the degree of suturing is not as great as in the higher grade metamorphic quartz. These two types of quartz represent 80-90 per cent of the total polycrystalline quartz grains present.

Old Red Sandstone grains are less frequently present but how much this is due to their more friable nature is very difficult to tell. They show no pressure solution, and are however often stained by iron oxides, making their identification very easy. Moinian and Dalradian metaquartzites may also exhibit the iron staining reflecting their second cycle nature. Chertified sandstones are also present together with chertified metaquartzites. These are probably derived from Old Red Sandstone caliche horizons which are frequently replaced by chert.

Myrmekitic quartz is rarely present but suggests derivation from granitic rocks; vein quartz and mylonitic quartz are also rarely seen.

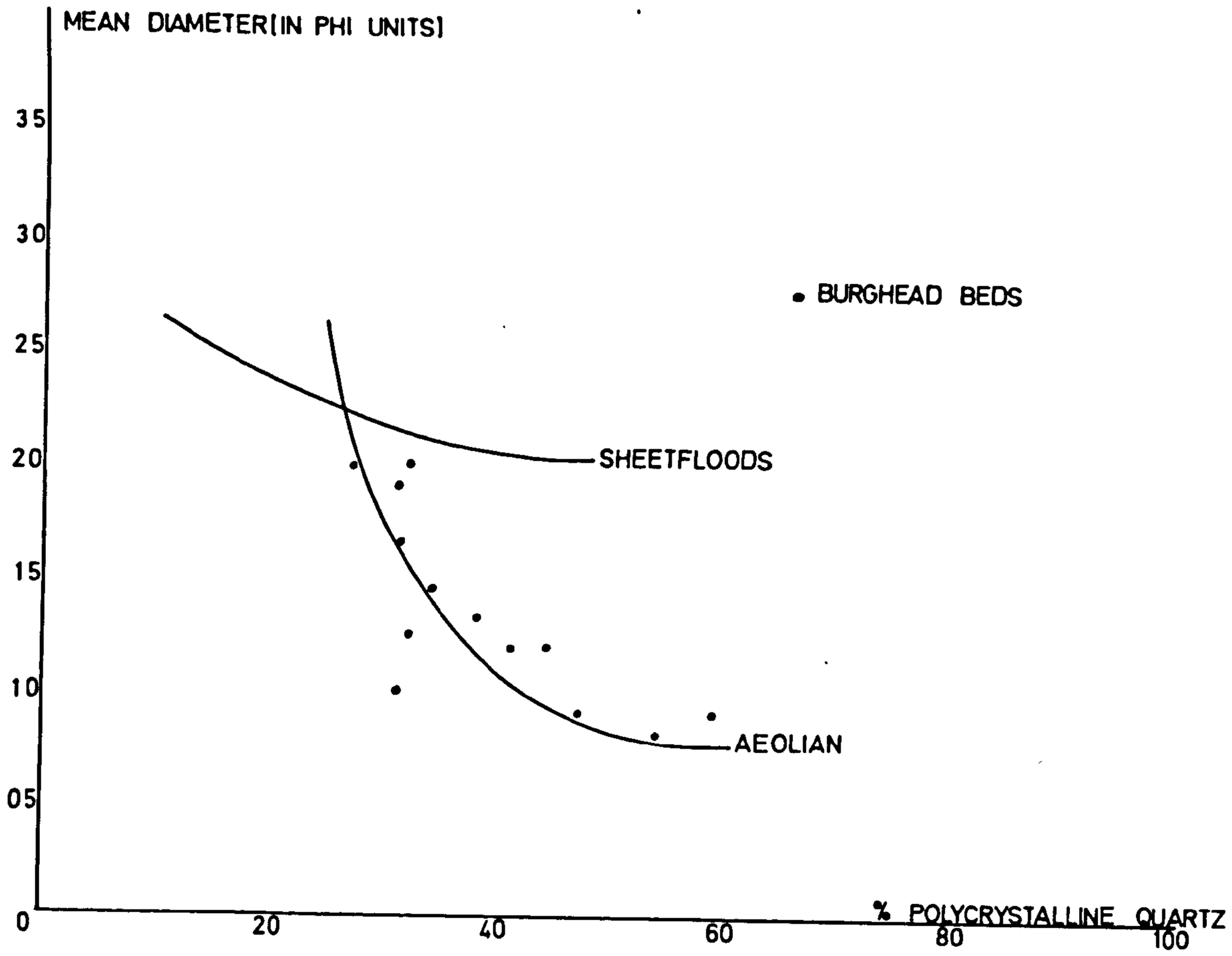

Fig. 7.19. Graph of mean diameter against the percentage of polycrystalline quartz.

Rock Fragments

The rock fragments can be generally equated with the results of the pebble analyses which were discussed earlier, i.e. dominantly Moinian and Dalradian with subsiduary Old Red Sandstone rock fragments.

Moinian and Dalradian granulite rock fragments are most common. Quartz granulites, showing high grade metamorphic sutured contacts and strained quartz, together with their characteristic muscovite, are the most common type of granulite represented. They sometimes show concentrations of heavy minerals, normally in the form of zircon, although tourmaline and apatite are sometimes present. The other type of granulite present is quartz feldspathic granulite, the feldspar being microcline.

Old Red Sandstone rock fragments are less common owing to their friable nature, but they can often be recognised by their iron staining and lack of pressure solution. Feldspathic grits are also present and are probably derived fragments of calcareous cemented sandstones which sometimes have microline present. Cornstones in various stages of alteration are however quite common. The cornstones rarely exhibit their original microcrystalline calcite as this is more often than not replaced by chert.

Other rock fragments are extremely rare although fragments of rhyolite and hornfels are sometimes seen.

Feldspar

Feldspar may constitute up to 15 per cent of the total detrital components of the point bar sediments although the percentage tends to be highest in the fine grained sediments. The feldspars are dominantly microline, which accounts for 90-95 per cent of the total feldspar. Clouded untwinned alkali feldspar also occurs but the degree of weathering and iron staining precludes any positive identification.

The absence of plagioclase and the prevalence of alkali feldspars is explained by their derivation from a predominantly high grade metamorphic source.

Heavy Minerals

Heavy minerals are far more common in the Burghead Beds than in the aeolian Hopeman Sandstone and may represent up to 4.3 per cent of the total detrital components, although they are generally less that $1\frac{1}{2}$ per cent.

Zircon is the commonest species present and constitutes over 80 per cent of the heavy minerals. Brown and green tourmaline are also common and were present in every sample studied. Seen to a lesser extent and in only a few of the samples are rutile, apatite, sphene, spinel, epidote and garnet. Leucoxene and magnetite are rare.

Clays and Micas

Muscovite is the normal mica present in the Burghead Beds; highly altered biotite is rare. Clay minerals are only common in the low water stage silts.

CHAPTER 8

BURGHEAD BEDS : FLOODPLAIN DEPOSITS

The floodplain deposits were formed when the coarse grained point bar river system overflowed its bank during periods of flooding. They reached a maximum distance of 5 kilometres from the main channel indicating the gentle relief of the plains surrounding the river. The deposits are only seen on the easterly side of the river channel at the present day owing to the lack of exposure to the west of Burghead.

Floodplain deposits are exposed beneath the main Lossiemouth Quarries (23547062) where they rest unconformably on the Old Red Sandstone. It appears that they have been brought up by a small fault, as the beds at the equivalent horizon to the east are represented by the aeolian Lossiemouth Sandstone. The sediments are overlain by the Lossiemouth Sandstone from which they can be differentiated by their more friable nature. The individual horizons range from coarse grained sandstones to silts and are yellow, grey or red-brown in colour. A maximum thickness of 8 metres is seen at the present day.

At Spynie Quarry (22286559), a Geological Survey Borehole indicates that the Lossiemouth Sandstone is underlain by 8 metres of silts and sandstones of floodplain origin (see Table 3.2). They illustrate similar sedimentary structures to the floodplain deposits at Lossiemouth and again rest unconformably on the Old Red Sandstone. The deposits range from siltstones to coarse grained sandstones and vary in colour from grey, pink, yellow to orange-brown.

The main quarry at Findrassie displays 5 metres of Triassic strata faulted against coarse pebbly sandstones of the Old Red Sandstone. The Triassic is dominantly aeolian in character but at the base of the quarry, coarse grained sandstones and silts show a remarkable similarity to the floodplain deposits at Lossiemouth and Spynie. It is therefore thought that the junction of the Lossiemouth Sandstone and the floodplain deposits occurs at the base of this quarry.

A quarry (20756416), 100 metres north east of Spynie Hospital, exposes less than a metre of silty Triassic sandstones overlying the Old Red Sandstone. The horizon is also thought to represent the floodplain deposits, an interpretation which is substantiated by thin section evidence. The following section is taken from the Elgin memoir (Peacock, 1968 p.50);

Sand and rubble ..... 0.66 metres

Weathered, yellow, flaggy, calcareous and dolomitic sandstone, brown weathering. Triassic ..... 0.66 metres.

Reddish brown, variably weathered, slightly micaceous, flaggy siltstone with thin strips of pale yellow green sand. Some carbonate cement. Old Red Sandstone ..... 1.3 metres

Hard pebbly sandstone. Old Red Sandstone ..... 5 metres

In the Clarkly Hill Borehole, the Burghead Beds are divided into two main units as seen in Table 3.1. The uppermost horizon has previously been discussed in Chapter 7 and was shown to represent coarse grained point bar deposits. In comparison, details from the borehole log (Peacock, 1970, personal communication of a detailed description of the borehole log) of the lower horizon indicate that the sediments are almost completely devoid of pebbles. Grain size varies from coarse sandstone to siltstones and are comparatively well sorted. Sedimentary structures are confined to low angled foresets and horizontal lamination. Their relative environmental position, sedimentary structures and petrography all indicate that these sediments are floodplain in origin. Although the sediments are slightly coarser than those at Spynie and Lossiemouth, this can be explained by their closer proximity to the main channel.

McKee et al (1967) describe a modern floodplain sequence from low angle to horizontally laminated sandstones through to ripple marked sandstones

and silts. The floodplain deposits of the Burghead Beds resemble this cycle in all aspects but an additional coarse grained scour unit is also recognised at the base.

FLOOPLAIN CYCLE

Studies of the floodplain cycle are based on the exposures at the Lossiemouth Quarries (23547062), as it is here that the most continuous sequence is seen. The cycles are also seen at the other localities but the limited data available renders their analyses statistically invalid. Table 8.1 illustrates three successions from this locality from which the following idealised cycle is taken (Fig. 8.1).

Base:

Unit A Coarse grained sandstones containing silts and pebbles cut down into the preceding cycle.

Unit B The coarse sandstones grade up into low angled foreset bedded, medium grained sandstones, succeeded by horizontally laminated sandstones. These separate units are included together owing to the difficulty of identification in unweathered sections.

Unit C Ripple marked sandstones, fine grained.

Unit D Ripple marked silts and structureless silts where sedimentary structures are obliterated by weathering. (Possibly horizontally laminated silts or silts with mud cracks as seen in other floodplain cycles).

Top:

The cycle is a fining upward cycle (Fig. 8.2), the coefficient of sorting also increasing upwards. The full cycle is not always present, the relative composition of individual cycles being:

ABCD (Ideal cycle) = 39 per cent

BCD = 27.5 per cent

AB = 22 per cent

ABC = 5.5 per cent

BC = 5.5 per cent

Fig. 8.1. Ideal cycle for the floodplain deposits of the Burghead Beds.

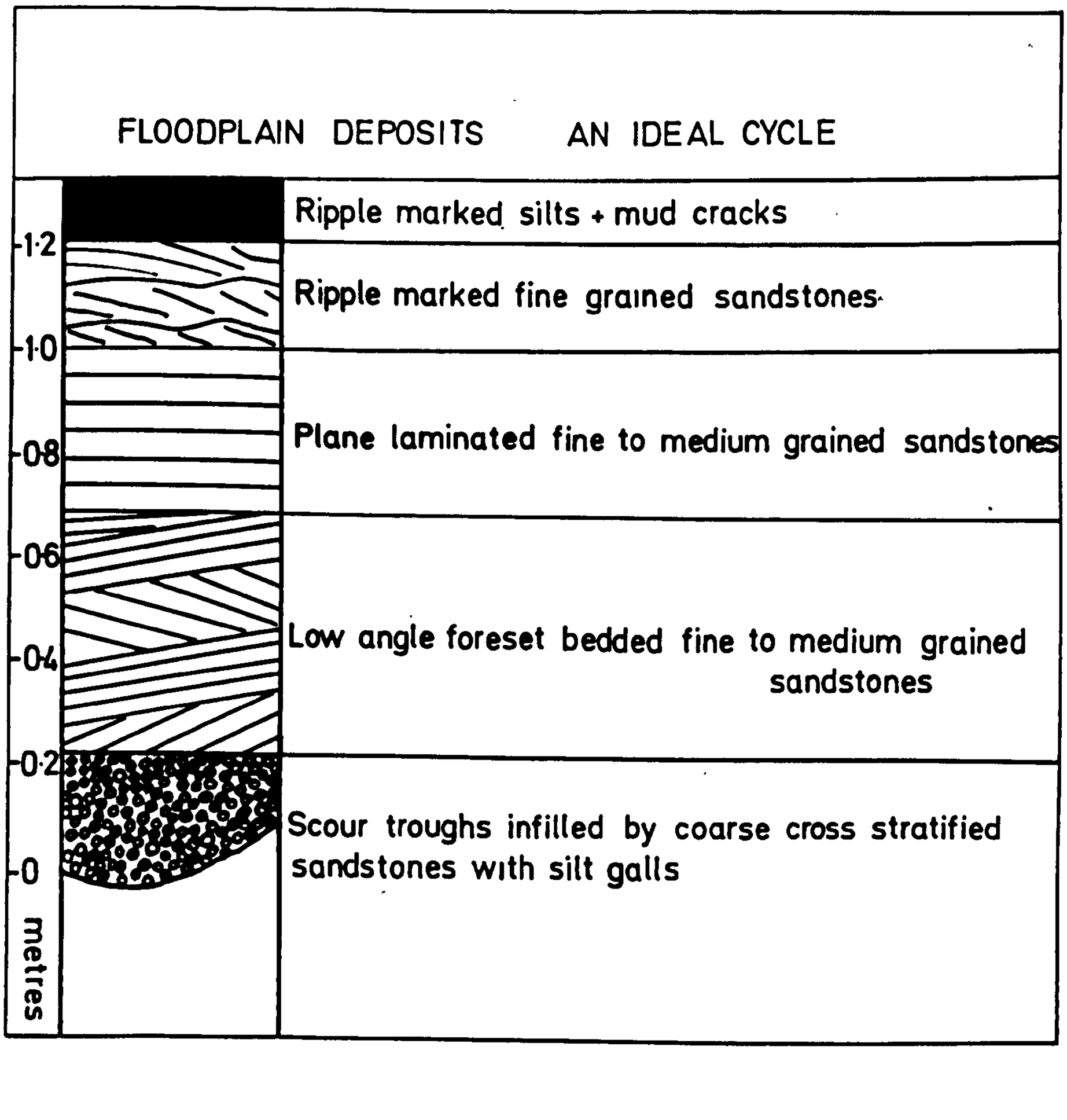

Section 1

Top		
Ripple marked sandstones	5 mm	
Low angled foreset bedding	75 mm	= 80 mm
---------- EROSION		
Silt	5 mm	
Ripple marked sandstone	15 mm	= 70 mm
Massive horizontally laminated sandstone	50 mm	
---------- EROSION		
Ripple marked sandstone	100 mm	= 140 mm
Massive sandstone	40 mm	
---------- EROSION		
Silt	10 mm	
Ripple marked sandstone	20 mm	
Horizontally laminated sandstone	100 mm	= 150 mm
Massive sandstone with silt galls	20 mm	
---------- EROSION		
Silt	10 mm	
Ripple marked silt	90 mm	
Ripple marked sandstone	50 mm	= 180 mm
Horizontally laminated sandstone	30 mm	
---------- EROSION		
Ripple marked silt	5 mm	
Ripple marked sandstone	5 mm	
Low angled foreset and horizontally laminated sandstone	100 mm	= 160 mm
Medium to coarse sandstone with silt galls	50 mm	
---------- EROSION		
Silt	50 mm	
Ripple marked sandstone	150 mm	= 280 mm
Low angled foreset bedding	80 mm	
---------- EROSION		
Ripple marked sandstones and silts	5 mm	
Low angle foreset bedded sandstone	95 mm	= 200 mm
Coarse channel scour sandstone with silts	100 mm	
---------- EROSION		

TABLE 8.1. Floodplain sequences at Lossiemouth Quarries (23547062)

Ripple marked sandstone with silt	100 mm	
Massive sandstone	50 mm	= 200 mm
Scour channel	50 mm	
---------- EROSION		
Ripple marked sandstones and silts	10 mm	
Low angled foreset bedding	70 mm	= 80 mm
---------- EROSION		
Ripple marked sandstone and silt	20 mm	
Horizontally laminated sandstone	50 mm	= 70 mm
---------- EROSION		
Ripple marked sandstone	120 mm	
Horizontally laminated sandstone	20 mm	= 160 mm
Low angled foreset bedded sandstone	20 mm	
---------- EROSION		
Ripple marked sandstone and silt	10 mm	= 10 mm

Section 2

Low angled foreset bedded sandstone	250 mm	
Coarse scour channel sandstone	50 mm	= 300 mm
---------- EROSION		
Silt	30 mm	
Ripple marked sandstone	30 mm	= 160 mm
Low angled foreset bedded sandstone	100 mm	
---------- EROSION		
Silt	5 mm	
Low angled foreset bedded sandstone	80 mm	= 85 mm
---------- EROSION		
Ripple marked sandstone	30 mm	
Low angled foreset bedded sandstone	220 mm	= 250 mm
---------- EROSION		
Ripple marked sandstone	50 mm	= 50 mm

TABLE 8.1. (continued)

Section 3

Ripple marked sandstone and silts	50 mm	
Low angled foreset bedded sandstone	150 mm	= 210 mm
Coarse channel scour sandstone	10 mm	
---------- EROSION		
Ripple marked sandstone	10 mm	
Low angled foreset bedded sandstone	150 mm	= 160 mm
---------- EROSION		
Ripple marked sandstone	50 mm	
Low angled foreset bedded sandstone	300 mm	= 450 mm
Coarse channel scour sandstone	100 mm	
---------- EROSION		
Ripple marked sandstone and contorted silts	50 mm	
Low angled foreset bedded sandstone	150 mm	= 210 mm
Coarse channel scour sandstone and silt galls	10 mm	
---------- EROSION		
Low angled foreset bedded sandstone	100 mm	
Coarse channel scour sandstone	50 mm	= 150 mm
---------- EROSION		
Silt	50 mm	= 50 mm

TABLE 8.1. (continued)

EXPLANATION OF PLATE 8.1

FLOODPLAIN DEPOSITS, QUARRY ROAD, LOSSIEMOUTH

A. Ripple marked sandstones overlying horizontally laminated sandstones.

B. Complete floodplain cycle. Coarse sandstones (0.1 m) cut down into the underlying silts of the preceding cycle and are overlain by foreset cross bedded sandstones (0.2 m), horizontally laminated sandstones (0.1 m) and ripple marked sandstones and silts (0.1 m).

C. Coarse trough bedded sandstones scour down into foreset cross bedded sandstones of the preceding cycle.

a

b

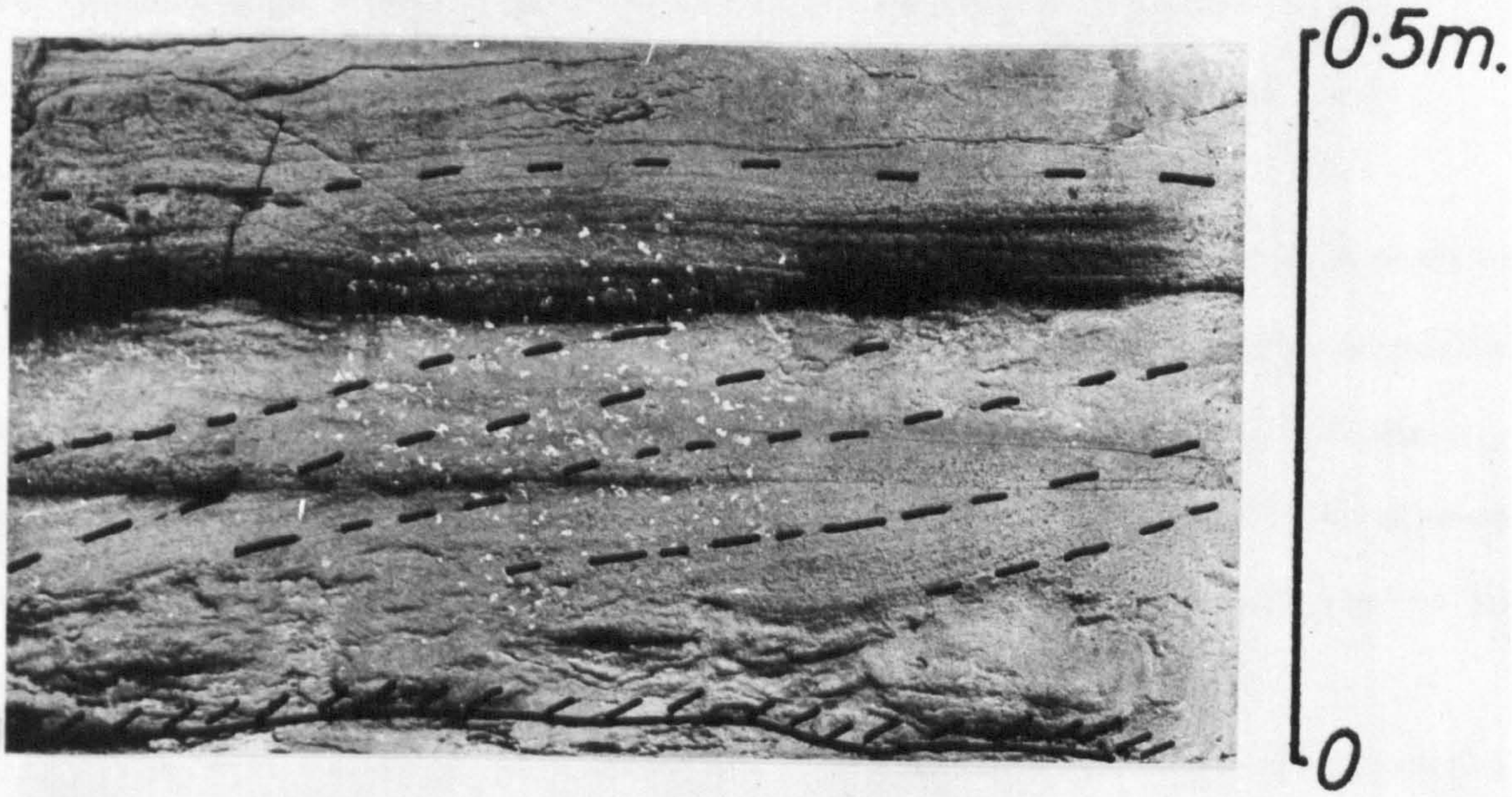

c

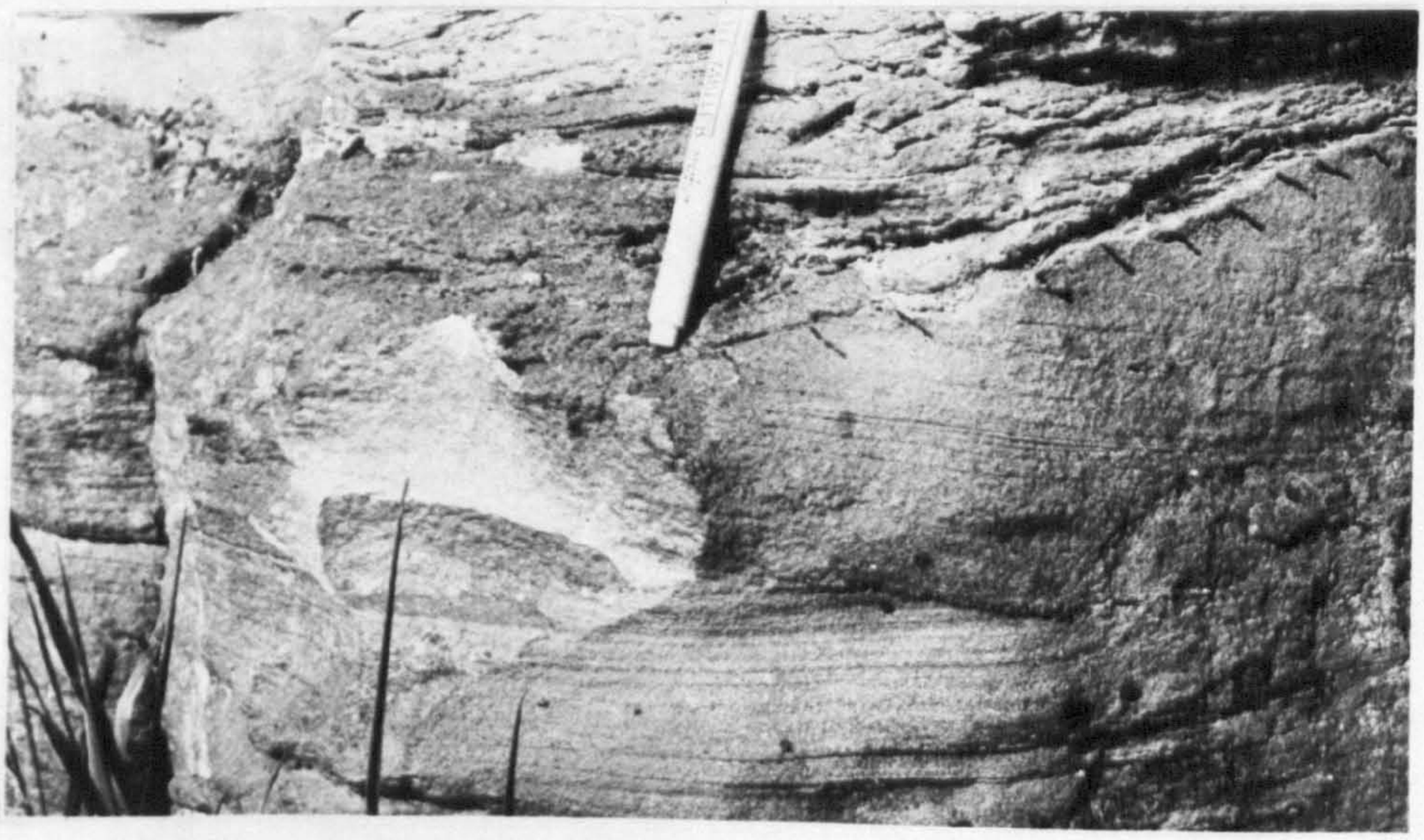

PLATE 8·1

Erosion of the upper and lower units of the cycle is clearly the main reason for absence of the full cycle. The upper unit D is often absent due to erosion of the silts by the overlying scour unit or by deflation soon after deposition. The scour unit A may be absent if the period of flooding is weak.

Unit A

Unit A consists of coarse to medium grained sandstones which cut down into the preceding cycle. The sandstones sometime contain pebbles up to 20 mm in diameter. Scours are usually in the form of channels which are generally less than a metre in width and less than 100 mm in depth; the sandstone frequently contain silt galls eroded from the preceding cycle (Plate 8.1C).

The unit represents the first stage of flooding with the subsequent deposition of the coarsest material. High velocity and the maximum amount of sediment enable the flood waters to cut down into the upper units of the preceding cycle. Palaeocurrent directions of the channel scours give a mean direction of 337 degrees; this direction is approximately at right angles to the mean palaeocurrent direction of the point bar deposits.

The well cemented nature of the sandstones eliminated the possibility of grain size analysis by sieve methods; however, thin sections were made and the grain size measured using a Humphries Micrometer Screw Gauge eyepiece; no allowance was made for experimental error of the thin section method as the results were not compared with grain size analyses by other methods. The statistics are documented in Table 8.2 using the method of Folk and Ward (1957). This method was used, as the 5th and 95th percentiles were necessary to differentiate the units.

The mean grain size of unit A is highly variable and depends on the amount of silt eroded from the preceding cycle and the coarseness of the incoming sediment. Periods of large scale flooding bring in coarser material as the velocity, and therefore the momentum, is higher. The skewness is similarly

dependent on the amount of silt eroded from the preceding cycle. Normally one would expect a deficiency in fines as these are still held in suspension at the higher velocity; in this case, there would be a positive skewness. However, the large amount of silty material from the underlying silts is inclined to make this unit have a negative skewness. This is the case in over 70 per cent of unit A occurence, but where there is no evidence of silt galls, the unit displays a high positive skewness.

Standard deviation is also higher than in any of the other units; this is a reflection of the large range of grain size from pebbles to silt galls. This gives a moderate to poor sorting of the sediment, the standard deviation ranging from 0.56 to 1.35 (Plate 8.2A).

Unit B

The coarse channel scour deposits are succeeded by low angle foreset bedded sandstones which grade up into horizontally laminated sandstones. Foreset bedded sandstones are formed where the water is deep and unable to maintain massive sand transport over a flat surface (McKee et al 1967). Thus, during deposition of the foreset bedding, current activity was still strong but it was depositional rather than erosional as in the previous unit. The foresets, which represent migration of small transverse sand bars, dip between 0 and 10 degrees. The foreset unit is usually the thickest of any of the units and may reach up to 300 mm in thickness.

These beds grade up into horizontally bedded laminations which are a product of the lower flow regime (McKee et al 1967). They represent a transition between the transverse bars and the ripple marked sandstones. They may be absent, but are normally present in the thicker cycles (Plate 8.1B).

Grain size analysis shows a remarkably uniform nature in all the Unit B samples analysed. The mean grain size ranges from 3.05 to 3.45 phi; the 5th and 95th percentiles also exhibit uniform values. The skewness varies from +0.13 to -0.28 but is generally negative. This is because much of the finer material which was held in suspension during the initial stages of flooding

was now deposited. Standard deviation ranges from 0.74 to 0.38 but generally reflect moderate to well sorted sediments (Plate 8.2B).

Comparison of grain size parameters of the floodplain samples from Clarkly Hill (Table 8.1) with grain size analyses obtained from this unit would suggest that the samples are extremely similar. These views are substantiated by the low angle to horizontal bedding seen in the Clarkly Hill floodplain samples. However, the mean grain size varies from 1.9 to 2.2 phi which is far coarser than equivalent samples of the same unit from Lossiemouth, Spynie or Findrassie. This appears to be a reflection of the proximity of Clarkly Hill to the main river channel compared to the other localities which are clearly on the periphery of the floodplain.

Unit C/D

The horizontally laminated sandstones grade up into ripple marked sandstones and finally into silts. Ripples are formed due to overloading of the water with sediment as the velocity falls (McKee et al 1967). Ripple wavelength varies between 25 to 60 mm and the amplitude is generally less than 20 mm. The thickness of the ripple unit itself may be up to 100 mm but the silts are generally only a few centimetres in thickness. The ripples tend to be sinusoidal in form (Plate 8.1A).

The current directions of the ripples is to the north east which is approximately parallel to the direction of the main channel of the coarse grained point bar system. The ripples may however be due to the wind blowing on the surface of the floodwaters generating ripple marks in the underlying sediments when the water becomes shallow. This theory is supported by the south west to north east palaeo-wind direction of the Lossiemouth Sandstone.

The ripple marked sandstones grade up into silts. Due to their highly weathered nature, the silts do not show any internal structures at the present day but, by analogy with modern day deposits, they would probably have at one time shown ripple marks and mud cracks. The silts are extremely thin, which is partially due to deflation after desiccation, and partially due

No.	phi percentiles									
	5	16	25	50	75	84	95	St.D.	Sk.	Kg'
Unit A										
1.	0.50	1.05	1.70	2.40	2.85	3.00	3.25	0.91	+0.21	0.49
2.	-0.50	0.35	0.60	1.60	2.15	2.40	2.95	1.06	-0.26	0.48
3.	1.75	2.45	2.65	3.05	3.30	3.45	3.85	0.56	-0.26	0.57
4.	2.30	2.75	3.05	3.45	3.80	4.00	4.15	0.59	-0.18	0.44
5.	1.10	2.25	2.55	3.00	3.40	3.60	4.00	0.77	-0.21	0.59
6.	2.00	2.60	2.85	3.25	3.60	3.75	4.20	0.62	-0.14	0.56
7.	-0.65	-0.25	0.05	0.90	2.60	2.80	3.10	1.35	-0.20	0.40
8.	0.85	1.90	2.35	2.80	3.45	3.75	4.40	1.01	-0.03	0.58
9.	-0.45	-0.10	0.10	0.75	2.05	2.35	2.85	1.12	+0.33	0.40
Unit B										
10.	2.35	2.75	3.00	3.45	3.90	4.05	4.20	0.60	-0.17	0.47
11.	1.45	2.40	2.75	3.30	3.65	3.80	4.10	0.74	-0.28	0.56
12.	2.45	2.75	2.90	3.25	3.60	3.75	4.10	0.50	+0.02	0.53
13.	2.05	2.55	2.80	3.20	3.60	3.75	4.00	0.59	0	0.40
14.	2.50	2.70	2.85	3.15	3.60	3.75	4.00	0.47	+0.13	0.45
15.	2.75	3.10	3.20	3.45	3.70	3.80	4.00	0.38	-0.06	0.50
16.	2.20	2.55	2.70	3.05	3.35	3.55	3.95	0.51	+0.01	0.53
17.	2.45	2.75	2.90	3.25	3.55	3.70	3.95	0.55	-0.06	0.49
18.	2.25	2.85	3.00	3.40	3.75	4.00	4.25	0.58	-0.06	0.53
Unit C/D										
19.	2.75	3.15	3.25	3.55	3.85	4.00	4.35	0.45	+0.03	0.48
20.	2.45	2.85	3.00	3.35	3.65	3.80	4.10	0.48	-0.07	0.52
21.	2.75	3.20	3.40	3.70	4.10	4.25	4.60	0.53	+0.01	0.52
22.	2.40	2.85	3.10	3.50	3.80	4.00	4.25	0.56	-0.15	0.52
23.	2.65	2.95	3.15	3.45	3.85	4.00	4.40	0.50	+0.05	0.52
Floodplain deposits of the Clarkly Hill borehole										
24.	1.10	1.40	1.60	1.90	2.25	2.45	2.95	0.54	+0.10	0.54
25.	1.10	1.40	1.60	2.00	2.40	2.55	2.75	0.51	+0.08	0.46
26.	1.20	1.40	1.65	2.20	2.55	2.70	3.15	0.62	-0.13	0.47
27.	1.00	1.20	1.40	1.90	2.00	2.45	2.70	0.57	-0.10	0.43

TABLE 8.2. Grain size analysis of the floodplain deposits, Lossiemouth.

	SILT	FINE SAND	MEDIUM AND COARSE SAND
Ripple marked sandstones	9.5	89	1.5
	9.5	86.5	4
	16.5	80	3.5
	30.0	69	1.0
	16.0	82.5	1.5
Foreset and horizontally laminated sandstone	4.0	95.5	0.5
	4.5	87.5	8
	21.5	75	3.5
	14.0	81.5	4.5
	7.5	80	12.5
	5.5	92.5	2
	7.0	91.5	1.5
	5.5	86.5	8
Channel sandstones	0	21.5	78.5
	0	58	42
	0	18.5	81.5
	0	34	66
	5.5	78	16.5
	15.5	81.5	4
	2.0	86.5	11.5
	4.0	89.5	6.5
	11.5	67	21.5

TABLE 8.3. Percentage of silt, fine sand and medium/coarse sand in the floodplain deposits, Lossiemouth.

EXPLANATION OF PLATE 8.2

FLOODPLAIN DEPOSITS, IN THIN SECTION

A. Coarse channel scour sandstones. Unit A.

B. Medium grained foreset bedded sandstones. Unit B and C.

C. Fine grained ripple marked sandstones. Unit D.

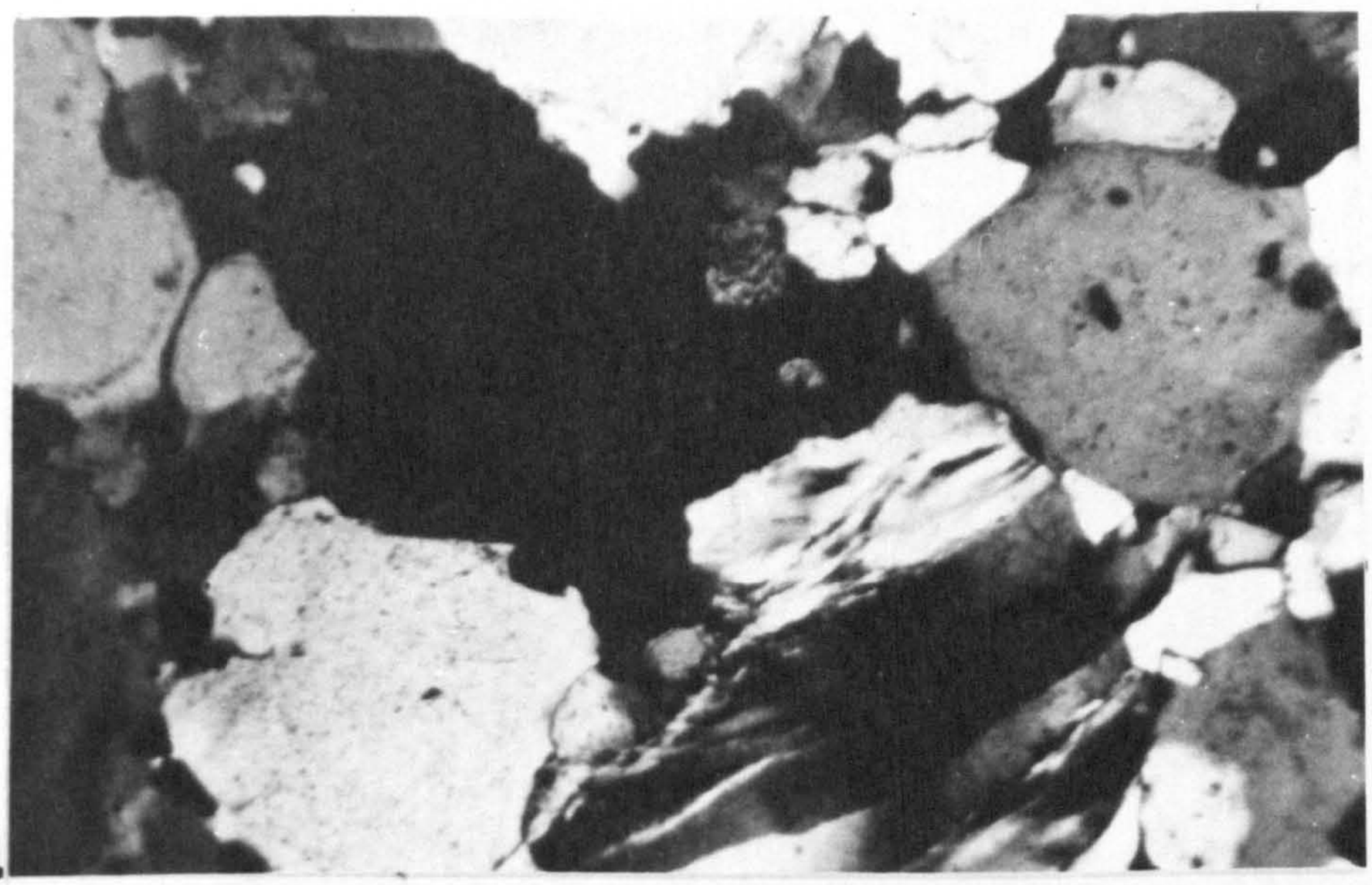

a

1mm.

0

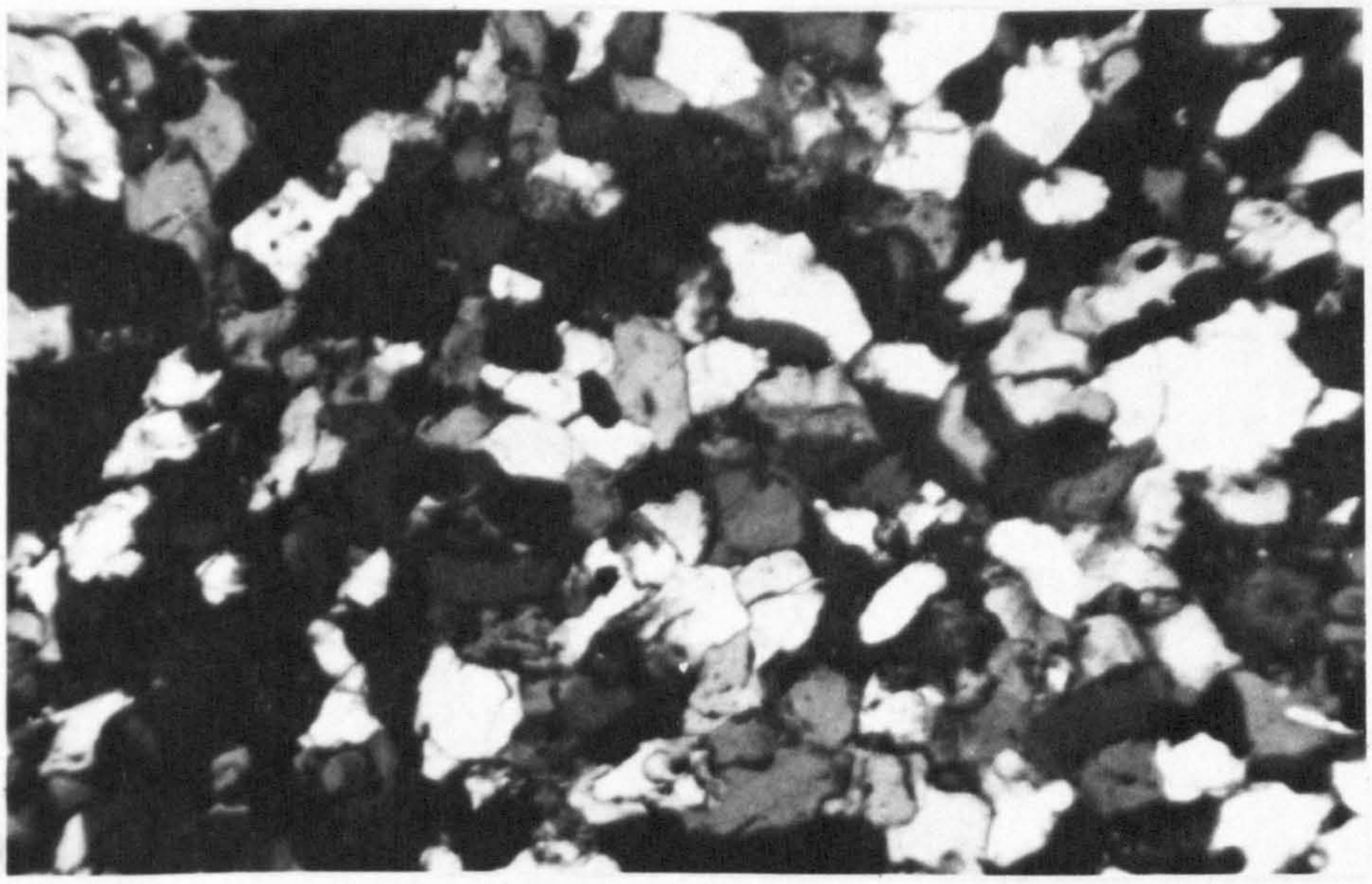

b

1mm.

0

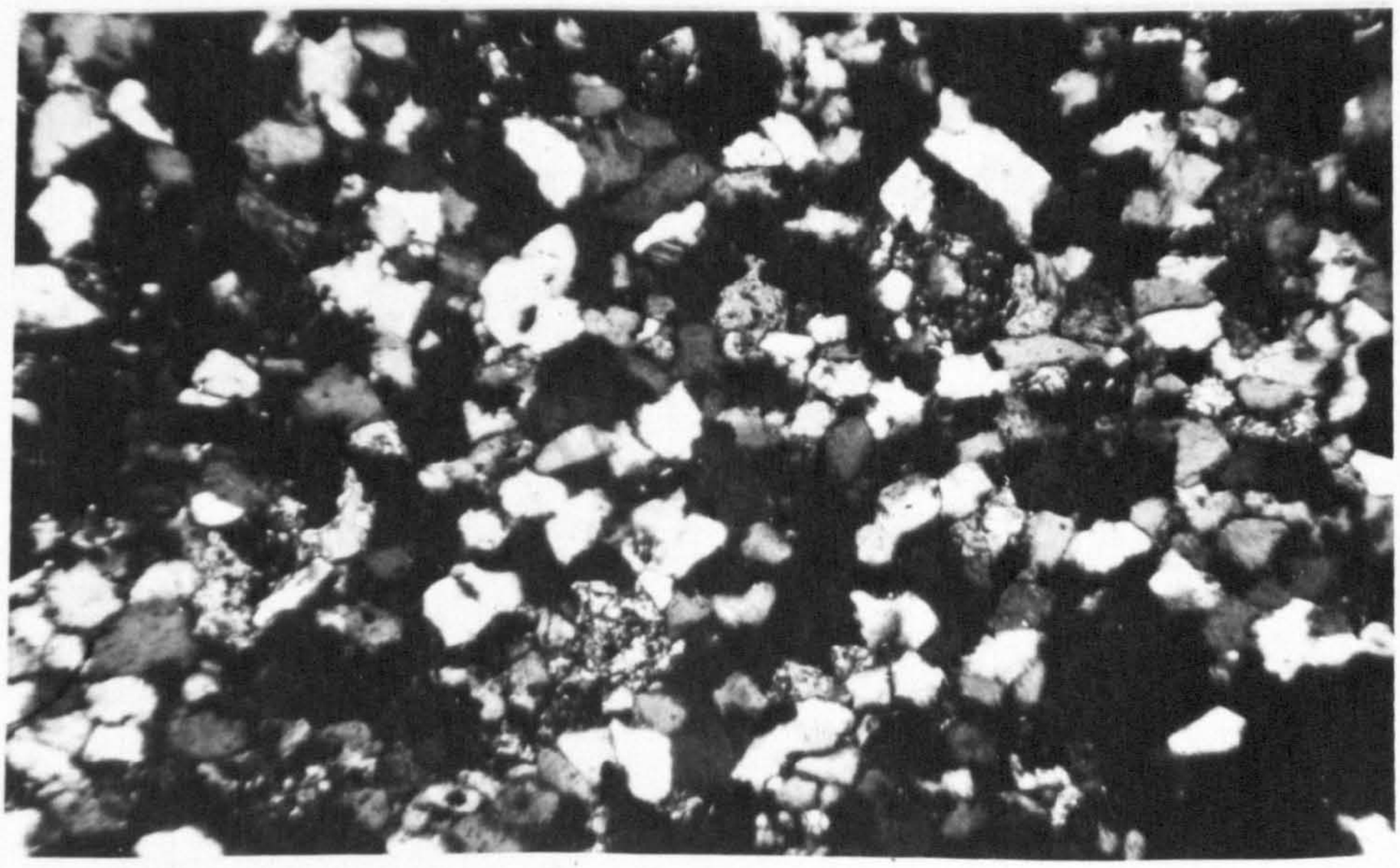

C

1mm

0

PLATE 8·2

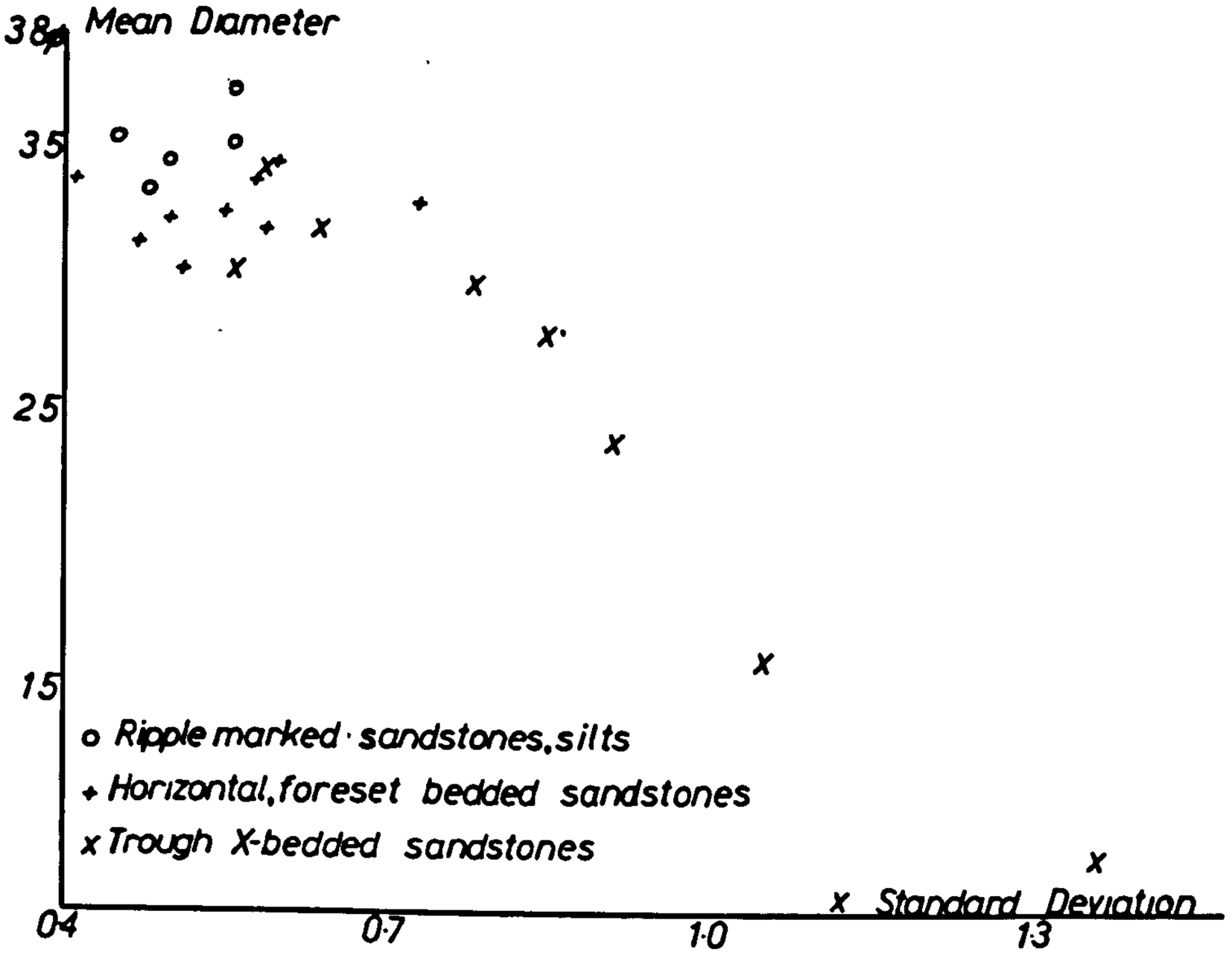

Fig. 8.2. Mean diameter plotted against standard deviation to illustrate the increase in sorting with decrease in size.

to erosion by the succeeding cycle. The succeeding cycle may also contort the underlying silts due to the force of the channel scour during flooding.

Grain size analysis has only been possible with the fine grained sandstones and silty sandstones as the silts were too soft to be impregnated in thin section. Grain size analysis again shows the effect of the fining upwards cycle. The mean grain size is finer than in any of the previous units and ranges from 3.35 to 3.7 phi (Plate 8.2C). Skewness tends to be symmetrical. The unit is well sorted as shown by the standard deviation which ranges from 0.56 to 0.45. Fig. 8.2 illustrates the comparison between standard deviation and mean diameter in the floodplain cycle, indicating the fining upwards nature, together with an increase in sorting. Kurtosis is variable but there is a tendency towards the norm (0.50-) as one goes up the cycle.

The floodplain cycle is therefore a fining upward cycle and represents a sequence from flooding to desiccation in the plains surrounding the main river channel.

CHAPTER 9

LOSSIEMOUTH SANDSTONE

The aeolian Lossiemouth Sandstones are exposed to the east of the Elgin district in the vicinity of Lossiemouth, Hill of Spynie and Findrassie. They are laterally equivalent to the fluviatile Burghead Beds (Peacock, 1968) and have been dated by Walker (1961) as Upper Triassic in age. The sediments vary from fine to coarse grained sandstones and are siliceous at the top but become progressively more calcareous towards the base. As a result of the extensive silicification, the aeolian foreset bedding is often absent at the top of the Lossiemouth Sandstone but becomes increasingly clear in the more easily weathered calcareous sandstones at the base.

The main sections of the Lossiemouth Sandstone are exposed in the vicinity of Lossiemouth, along the foreshore and in a series of quarries to the south of the town. In the post glacial cliffs, south of Stotfield Golf Course, the Lossiemouth Sandstone is overlain by the Sago Pudding Sandstone at 22457047, 22537053, 22577062, 22637065 and 22687069. A maximum thickness of only 2 metres of the Lossiemouth Sandstone can be recognised here by its unimodal nature. No traces of aeolian cross bedding can be seen owing to the intense silicification.

The Lossiemouth Sandstones are also exposed along the foreshore to the north of Lossiemouth from Maggie's Crag to 440 metres to the north east. At the former locality they are faulted against the Old Red Sandstone and are intensely silicified due to later mineralisation. Where the aeolian sandstones grade up into the Sago Pudding Sandstone, the sandstone is again silicified, but becomes more calcareous away from this junction. East of Lossiemouth Harbour, they again grade up into the Sago Pudding Sandstone and show similar features.

On the south side of Lossiemouth, the aeolian sandstones were previously quarried west of School Brae. Although they are still documented in the recent Elgin memoir, the quarry has since been infilled and only 3 metres of Lossiemouth Sandstones are exposed at the present day. The sandstones are

highly friable and calcareous, and thus probably represent the lowermost horizons. Peacock (1968) noted the presence of a joint system at this quarry with main west north west joints, subsidiary north north east joints and an associated barytes/fluorite mineralisation.

To the east of School Brae, old quarries are exposed for 450 metres along Quarry Road to the old Lossiemouth Railway Station. 400 metres west south west of the old railway station, 25 metres of fine grained, friable to siliceous aeolian sandstones overlie the soft friable floodplain deposits described in the previous chapter. However, the sandstones are highly jointed and traces of cross bedding are rarely present. To the west of this locality a small fault throws to the south so that the quarry floor approximates to the contact of the of the aeolian sandstones with the floodplain deposits. 15-20 metres of hard siliceous sandstones are exposed in the quarry face, the top 1-2 metres being the Sago Pudding Sandstone. The Lossiemouth Sandstone is therefore represented by a maximum thickness of 18 metres at this locality. Detailed studies of the aeolian cross bedding, which can only be seen at isolated localities, suggests that the quarry face represents a single unit of cross bedding with foresets dipping uniformly to the north and north east at angles varying from 20-30 degrees.

At the Hill of Spynie, the Lossiemouth Sandstone is present at five separate localities. The most westerly quarry is exposed to the east of a bend in the main Elgin-Lossiemouth road and displays 5 metres of fine to coarse grained grey sandstones. The friable nature of the sandstones and the coarseness of the laminae all suggest that the exposures are in the lower parts of the sequence. Two to three metres of a unit of cross bedding have foresets dipping uniformly to the north east at angles between 25-30 degrees. Hyperodapedon is thought to have been recovered from this quarry (Peacock, 1968, p.68).

The Lossiemouth Sandstone is again exposed at a quarry centred on 22066557, from which Leptopleuron has been recorded. The quarry is at present 12-15 metres in depth but it is clearly a remnant of a much larger quarry as

the base is now obscured. At the present base, alternating coarse and fine laminae gradually pass up with a series of fine grained sandstones; here, the cross bedding dips towards the north east. Unfortunately, the vertical faces of the quarry do notlend themselves to more extensive studies.

To the east and north of this quarry, a number of shallow quarries illustrate the hard and siliceous upper parts of the Lossiemouth Sandstone. A series of joints trend towards the north west and have an associated fluorite, calcite and galena mineralisation. To the east, the Lossiemouth Sandstones finally grade up into the bimodal Sago Pudding Sandstone. Little or no trace of cross bedding is seen.

Further to the east, the main quarry of Spynie Hill (22256565) displays a maximum of 20 metres of Lossiemouth Sandstones. The sandstones are highly siliceous at the top but grade down into more calcareous cemented sandstones. The top of the quarry face exposes a series of sandstones containing cavities and joints with associated galena and fluorite. The presence of the Cherty Rock in isolated outcrops in the plantation above the quarry clearly indicates that the tip of the quarry is the contact of the Lossiemouth Sandstone with the Cherty Rock, the intervening Sago Pudding Sandstone often being absent at Spynie. No traces of cross bedding have been found. Table 3.1 (Peacock, 1968) shows the Geological Survey borehole at this locality and illustrates the increase of calcite cement with depth.

At Findrassie, three small overgrown quarries centred on grid reference 20456510 show isolated exposures of hard, fine to medium grained aeolian sandstones. Although the Elgin memoir indicates that 6 metres of Lossiemouth Sandstone are present, these quarries are now infilled and only reveal one metre of the rock, grading up into one metre of the Sago Pudding Sandstone. A quarry to the south of these small quarries shows 3 metres of the Lossiemouth Sandstone overlying the floodplain sediments of the Burghead Beds. They are faulted against the Old Red Sandstone. The quarry clearly represents the lower part of the Lossiemouth Sandstone. Stagonolepsis has been recorded from this locality.

A borehole at Saint Peter's Well, Duffus has yielded the following information, (Peacock, 1968, p.64):

Cherty Rock	2 metres
Sago Pudding Sandstone	8 metres
Lossiemouth Sandstone	4.25 metres
Burghead Beds	base not seen

The Lossiemouth Sandstone here consists of fine grained, brown to grey sandstones; at the base, quartz pebbles up to 20-30 mm in diameter are found in thin bands and probably represent reworking of the underlying point bar deposits.

Similar successions are seen at Gallows Hill and Inverugie House where 4 metres of hard, siliceous, massive red sandstones underlie the Sago Pudding Sandstone and overlie the Burghead Beds.

Foreset analysis

Aeolian cross bedding is only seen at isolated exposures at Lossiemouth and the Hill of Spynie, as the structures have been obliterated by later silicification in most of the Lossiemouth Sandstone. However, the uniform grain size and the cross bedding which is present, all suggest that the Lossiemouth Sandstones represent fossil aeolian dune sandstones. The foresets dip at angles between 15-30 degrees and are concave upwards in form. The angle of foreset dip decreases from the top to the base. They reach a maximum of 15 metres in thickness and 33 metres in length. Individual laminae are extremely well sorted.

Fig. 9.1 displays the results of all foreset measurements taken at Lossiemouth and Spynie. A mean direction of north 51 degrees east indicates that the dunes were laid down by a prevailing south westerly wind. The rose diagram clearly indicates deposition by a unidirectional wind but the lack of sections other than vertical cliff sections makes the overall morphology of the dunes difficult to interpret. However, the uniformity of the cross bedding at any one exposure is extremely reminiscent of the middle units of the Hopeman Sandstone barchan dunes. Thus, although they are on a much smaller scale than

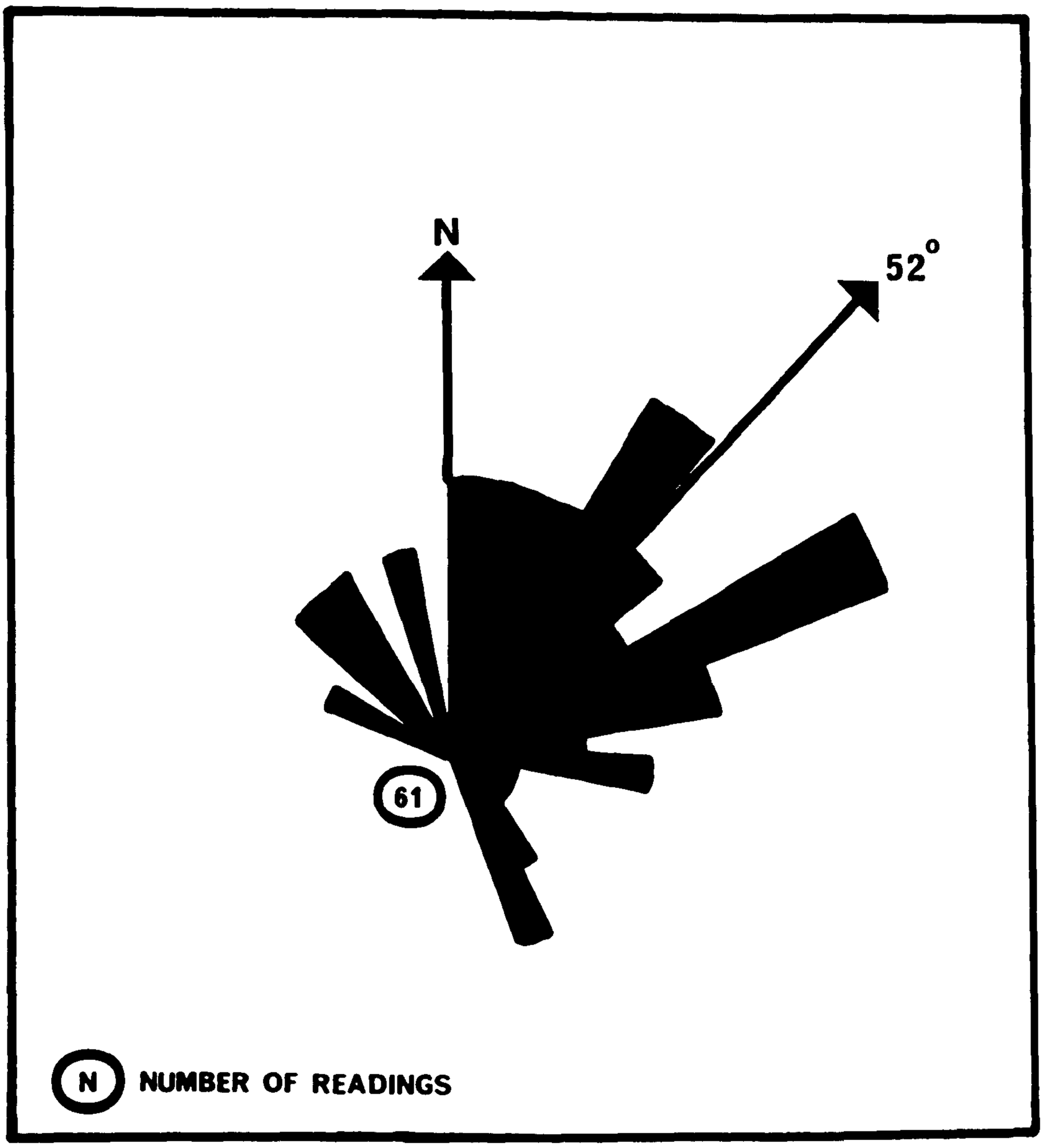

Fig. 9.1. Foreset analysis of the Lossiemouth Sandstone.

in the Hopeman Sandstone the aeolian Lossiemouth Sandstones are interpreted as barchan dunes.

Grain size analysis

Table 9.1 illustrates the grain size characteristics of the Lossiemouth Sandstone. The results were obtained using a Humphries Micrometer Eyepiece on thin sections. Sieve analysis could not be used owing to the problems of disaggregation.

The Lossiemouth Sandstones are generally fine to medium grained, although coarse grained sandstones are sometimes present at the base. The median diameter is generally between 2.4 to 2.8 phi but the main mode is normally much finer. If the mode is compared with the mean diameter of the Burghead Beds floodplain deposits, it will be noted that there is a remarkable similarity.

Standard deviation is generally between 0.50 to 0.65 indicating moderate sorting. However, when compared to most aeolian dune sandstones described in the literature, they are exceedingly poorly sorted. Kurtosis is generally mesokurtic.

Aeolian sandstones are generally positively skewed owing to the removal of the fine material in suspension by the wind. The Lossiemouth Sandstones however are generally negatively skewed although not markedly so. Thus, there is an excess of fine material in the Lossiemouth Sandstone when compared to most other dune sandstones.

Origin of the Lossiemouth Sandstone

The aeolian sandstones are intimately associated with both the floodplain deposits and the point bars of the Burghead Beds. At Lossiemouth, the aeolian sandstones rest directly on floodplain deposits whereas to the west at Gallows Hill, they rest on the point bar deposits. It is more usual for the point bar deposits to grade laterally into the floodplain deposits, which in turn grade into the aeolian sandstones. However, in some cases, the floodplain deposits are clearly absent, the aeolian sandstones resting directly on the point bar deposits.

NUMBER	MODE 1	MODE 2	MEDIAN	Standard Deviation	Skewness	Kurtosis
1	2.0	3.05	2.50	0.68	-0.05	0.46
2	---	2.95	2.70	0.53	-0.05	0.57
3	---	2.90	2.75	0.52	+0.05	0.48
4	---	3.15	2.95	0.50	-0.14	0.58
5	---	3.15	2.45	0.83	-0.05	0.47
6	---	1.80	1.90	0.68	+0.04	0.46
7	---	3.15	2.85	0.51	-0.20	0.56
8	---	3.20	2.85	0.63	-0.20	0.46
9	---	3.15	2.70	0.57	+0.16	0.55
10	---	3.15	2.70	0.60	+0.01	0.55
11	---	3.10	2.75	0.57	+0.10	0.53
12	---	2.25	2.25	0.50	-0.01	0.52
13	2.25	2.80	2.20	0.79	-0.15	0.57
14	---	3.00	2.65	0.52	-0.04	0.49
15	---	2.50	2.45	0.61	-0.04	0.58
16	2.60	3.00	2.40	0.62	+0.07	0.50

TABLE 9.1. Grain size characteristics of the Lossiemouth Sandstone (in phi)

The remarkable similarity between the grain size of the Lossiemouth Sandstones and that of the floodplain deposits is explained by the dunes being derived from the floodplain deposits by reworking of these sediments. The anomalies in grain size characteristics can thus be explained by removal of some of the fine material by the wind. However, the minimal distance of transport of the aeolian grains still enabled much of the fine material to be retained in the dunes, as is implied by their negative skewness. The dunes are therefore essentially local in origin and derived from the nearby floodplain deposits. A similar phenomena is described in the Trias of Cheshire by Thompson (1969).

The dunes achieved a maximum height of approximately 20 metres and were formed on the periphery of the floodplain. However, when complete desiccation occurred, the dunes were able to migrate across the surface of the floodplain only to be replaced by successive phases of flooding. This explains why the floodplain deposits are sometimes absent between the point bar and aeolian deposits. Aeolian deposition was finally terminated by a large scale flooding which led to the formation of the Sago Pudding Sandstone. The Sago Pudding was also reworked by the wind but retains qualities of both the aeolian and floodplain deposits.

The reptilian remains of the Lossiemouth Sandstone are normally found near the contact with the floodplain deposits and have been described by Walker (1962). Walker noted the remarkably good articulation in the remains and concluded that they had been preserved near to their life environment. There are many diverse forms amongst the reptiles but they can be divided into two main types. The first type, Walker concluded, lived on sand dunes, whereas the second type was herbivorous and able to dig. Personal communications with Walker (1971) indicate that the two types are consistent with reptiles living on a floodplain and adjacent dunes.

CHAPTER 10

SAGO PUDDING SANDSTONE

The Sago Pudding Sandstones represent a variable thickness of silicified and calcareous sandstones which overlie the aeolian Lossiemouth Sandstone and underlie the Cherty Rock. As its name so aptly suggests, it is characterised by isolated coarse quartz grains in a fine grained matrix, giving the appearance of a sago pudding.

The Sago Pudding Sandstone is exposed in the post glacial cliffs to the south of Stotfield Golf Course, the outcrops occurring in the gardens of several large houses at 22457047, 22537053, 22577062, 22637065 and 22687069. The horizon reaches a maximum thickness of 3 metres and grades down into the Lossiemouth Sandstone, which it would resemble if the coarse mode was absent. The sandstones are highly silicified, and chalcedonic cavities at the top of the exposures indicate the proximity to the Cherty Rock. The coarse mode constitutes less than 5 per cent of the total volume in most occurrences and is randomly distributed throughout the sample. Rarely, the coarse grains may constitute up to 50 per cent of the volume and in two cases, channels consisting of only coarse detrital components have been recognised. The channels were up to 1 metre in width and 0.25 metres in depth. They resembled the scour channel unit of the floodplain deposits of the Burghead Beds in all respects.

The Sago Pudding Sandstones are also exposed along the foreshore to the north of Lossiemouth (22657098). Here, they are downfaulted against the Old Red Sandstone and are overlain by the Cherty Rock. The beds become increasingly silicified towards the contact with the Cherty Rock until the presence of chalcedonic/opaline structures and sandy limestones indicate that the Cherty Rock has been reached. The upper contact is again seen at varying points along the foreshore (233713, 23807125, 240712) and, more rarely, the contact with the underlying Lossiemouth Sandstone (229711).

To the south of Lossiemouth (23557068), silicified bimodal sandstones are exposed overlying the Lossiemouth Sandstones. Plate 10.1B shows

a channel present at this locality. The channel is 2 metres wide and 80 mm in depth and is composed totally of coarse grained detrital components. Above the channel there is evidence of low angled foreset bedding which then grades up into massive sandstones. Other areas display high concentrations of the coarse mode. The horizon reaches a maximum thickness of 5 metres at Lossiemouth.

At Spynie Hill, the bimodal sandstones are not so well developed but are seen to reach a maximum thickness of 2 metres. They are well displayed at 22146561 and 22176564 where they are associated with silicified joints, fluorspar, calcite and galena. Evidence of coarse sandstones, sometimes bimodal, is seen at the highest horizon in the main quarry (22706567) but it is often absent at this locality.

The Sago Pudding Sandstone is again exposed to the east at Findrassie in a small overgrown quarry (20726524) 400 metres south of Lochside (207656). It is also exposed at 20486510 and 60 and 120 metres south of the previous quarry. At all these localities, it is highly silicified and typically bimodal.

A borehole at St. Peter's Well, Duffus (Peacock, 1968 p.64) indicates that the Sago Pudding here is nearly 8 metres thick. Just south of the summit at Gallows Hill (147685), a quarry face exposes nearly 7 metres of hard red massive fine grained sandstones. The 7 metres can be sub-divided into the bimodal Sago Pudding Sandstone in the top 3 metres underlain by 4 metres of Lossiemouth Sandstone. A few quarries immediately to the west show a maximum thickness of 2 metres of bimodal sandstones.

Overgrown quarries in the grounds of Inverugie House (15526855) give the following succession:

Chertified limestones 4 m	Cherty Rock
Red massive silicified sandstones 1.5 m	Sago Pudding Sandstone
Bimodal massive silicified sandstone 2 m	
Red massive silicified sandstone 4 m	Lossiemouth Sandstone
Laminated sandstones and pebbly sandstones (in landscape garden and gardener's coal shed)	Burghead Beds

EXPLANATION OF PLATE 10.1

SAGO PUDDING SANDSTONE

A. The Sago Pudding Sandstone illustrating the bimodal character of the sandstone. The high degree of silicification owing to the formation of quartz overgrowths during the early stages of caliche development is well seen. Crossed nicols.

B. The Sago Pudding Sandstone, Quarry Road, Lossiemouth (23557068). (X) illustrates a shallow channel extremely reminiscent of channels in the floodplain deposits of the Burghead Beds. (Y) illustrates feint traces of low angle foreset bedded sandstones grading into the massive bimodal Sago Pudding Sandstone (Z).

A

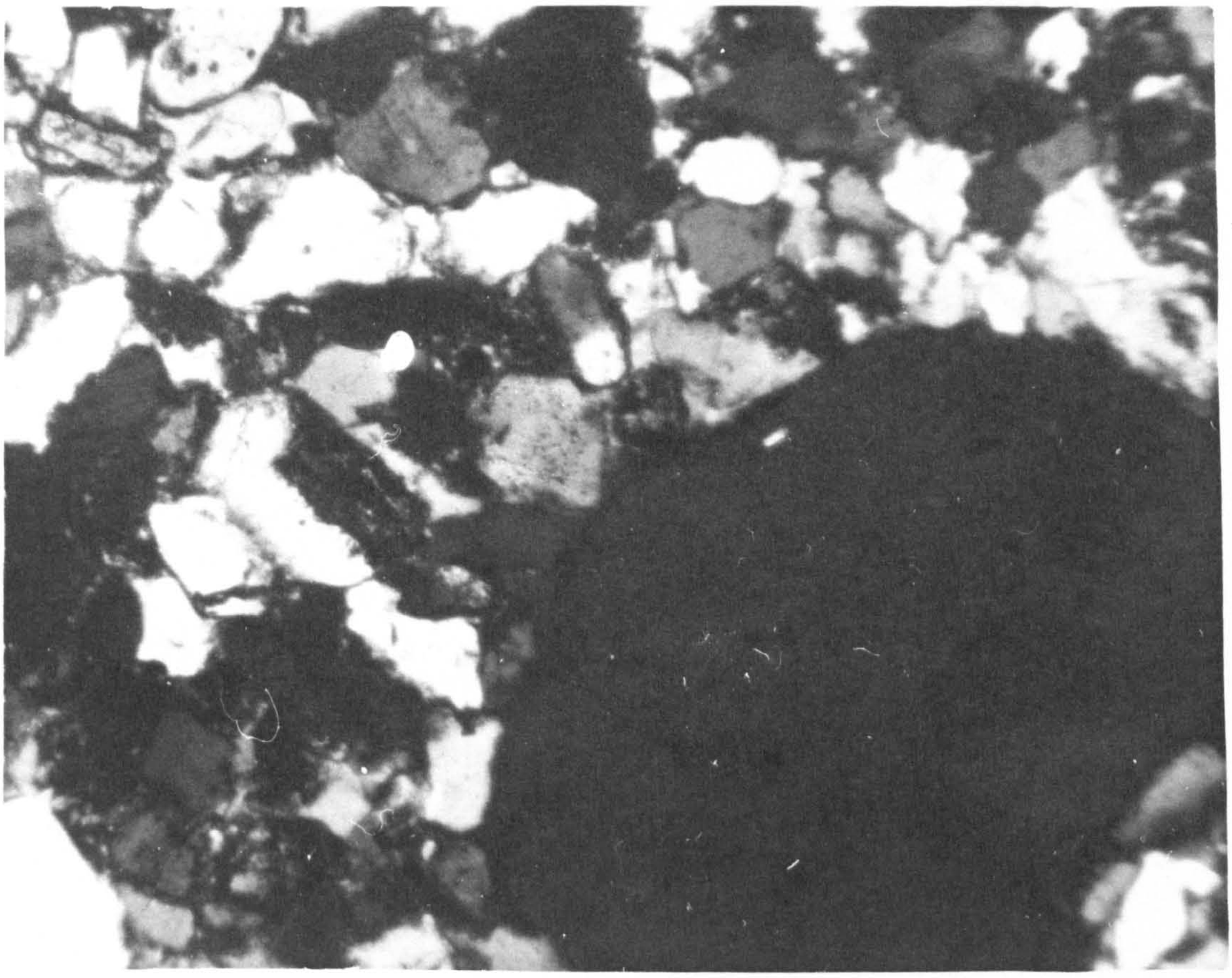

B

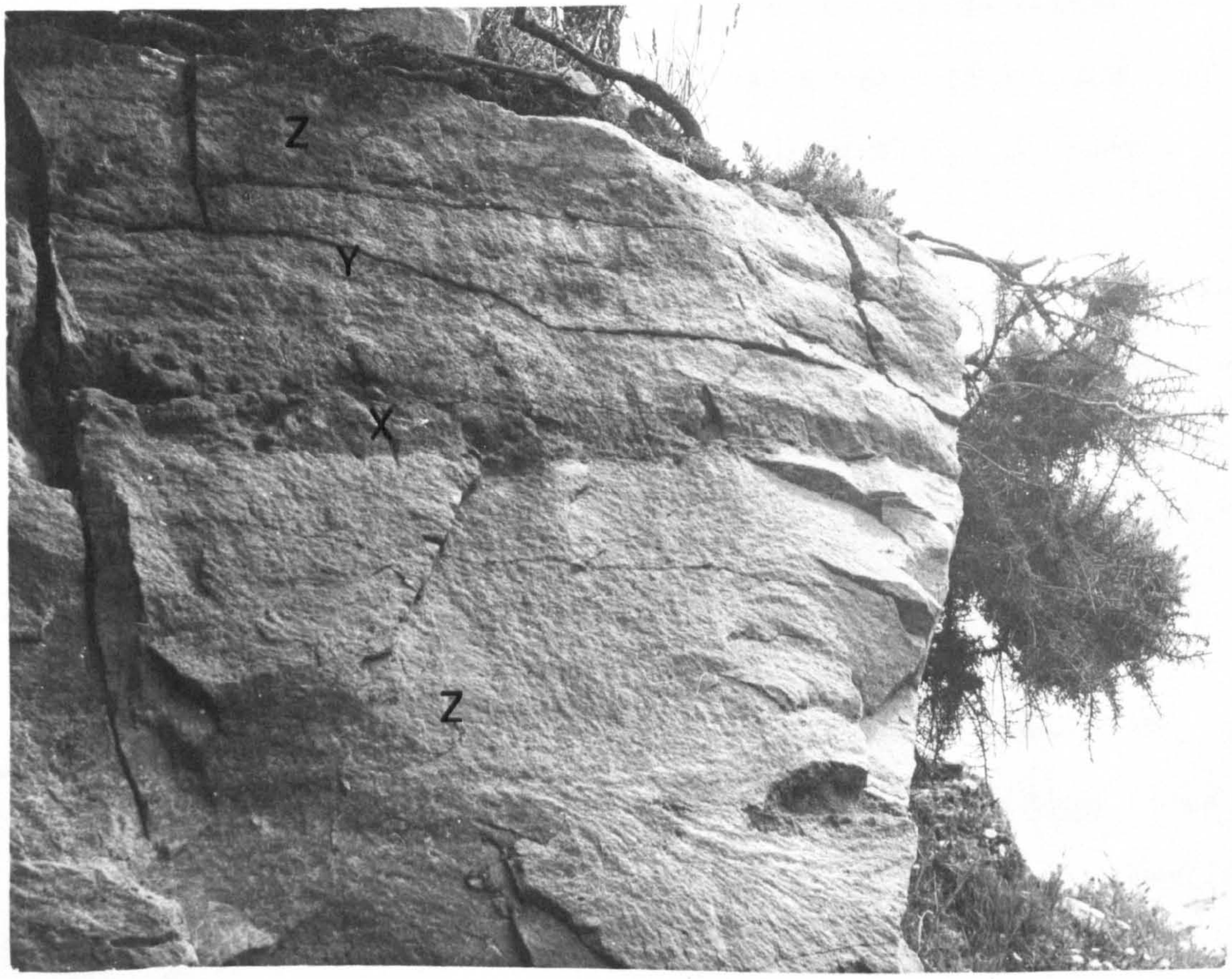

PLATE 10·1

A small overgrown quarry to the east of Clarkly Hill displays a thickness of 2 metres of bimodal sandstones which are interpreted as being the Sago Pudding Sandstone. Chalcedony cavity infilling at the top indicates the incoming of the Cherty Rock.

On the foreshore, north east of Masonshaugh Quarries, a bimodal sandstone overlies the pebbly sandstones of the Burghead Beds. Although the quartz grains are coarser than normal and the sandstone is cemented by calcite, the horizon is thought to be equivalent to the Sago Pudding Sandstone.

GRAIN SIZE ANALYSIS

Table 10.1 illustrates the grain size characteristics of the Sago Pudding Sandstones which were obtained using a Humphries Micrometer Eyepiece on thin sections.

The mean grain size is highly variable and ranges from 0.75 to 3.45 phi; this being a reflection of the large grain size range. Standard deviation varies from 0.58 to 1.70 indicating a poor to moderate sorting coefficient. The poor sorting and variation in mean grain size is clearly due to excessive amounts of coarse or fine material as the matrix appears to be fairly uniform. Skewness is normally negative although positive skewness occurs when there is a high percentage of the coarse mode present. Kurtosis is variable.

The Sago Pudding Sandstones are invariably bimodal and sometimes polymodal. It is therefore difficult to compare grain size characteristics with unimodal sandstones. However, if the various modes are measured separately, these can sometimes be compared to the unimodal sandstones associated with them. This is because many bimodal sandstones are deposited in a state of disequilibrium and are normally derived from more stable environments (Folk, 1968).

A mode between 2.85 and 3.35 phi is constant throughout the sandstones and represents the main matrix of the sandstones. Secondary modes often occur in the coarse and fine modes. However, in the channel sandstones (see Table 10.2, Nos. 15, 16 and 19) the main mode is generally nearer to 0.5 phi

No.	5%	16%	25%	50%	75%	84%	95%	St.D	Sk	Kg	Mean
1	0.40	1.20	1.60	2.40	2.90	3.10	3.65	0.98	-0.09	0.49	2.2
2	1.90	2.25	2.45	2.90	3.20	3.40	3.75	0.58	-0.16	0.50	2.85
3	1.30	1.70	1.95	2.40	2.85	3.00	3.40	0.64	-0.06	0.55	2.4
4	-0.15	2.65	2.80	3.00	3.40	3.70	4.20	0.92	-0.06	0.67	3.1
5	1.80	2.00	2.25	2.85	3.40	4.20	5.50	1.11	+0.27	0.55	3.0
6	-0.10	2.40	2.65	3.05	3.35	3.50	3.80	0.87	-0.29	0.68	3.0
7	0.65	1.75	2.55	3.45	4.50	5.15	6.00	1.70	-0.03	0.53	3.45
8	0.20	0.90	2.00	2.80	3.60	4.00	5.00	1.50	-0.23	0.55	2.6
9	1.40	2.10	2.25	2.60	2.95	3.20	3.55	0.58	-0.01	0.55	2.6
10	1.70	2.15	2.35	2.60	4.25	4.60	5.50	1.70	+0.63	0.45	3.1
11	1.85	2.35	2.60	2.95	3.30	3.50	3.75	0.58	-0.01	0.53	2.9
12	1.60	2.15	2.35	2.90	3.35	3.45	3.80	0.66	-0.17	0.48	2.8
13	1.70	2.55	2.80	3.15	3.55	3.70	4.00	0.63	-0.14	0.56	3.1
14	1.00	2.10	2.35	2.75	3.15	3.35	3.90	0.75	-0.12	0.60	2.7
15	-0.45	-0.10	0.10	0.75	2.05	2.35	2.85	1.12	+0.33	0.40	1.0
16	1.90	2.30	2.45	2.90	3.30	3.60	4.15	0.65	+0.07	0.52	2.9
17	1.15	1.90	2.10	2.50	2.85	3.05	3.60	0.64	-0.07	0.56	2.5
18	0	0.60	1.15	2.00	2.50	2.70	2.90	0.96	-0.34	0.47	1.75
19	1.65	1.90	2.05	2.45	2.90	3.05	3.65	0.59	+0.12	0.49	2.5
20	1.50	2.15	2.30	2.70	3.20	3.35	3.65	0.63	-0.02	0.50	2.7
21	1.10	2.30	2.50	2.80	3.25	3.40	3.75	0.68	+0.29	0.53	2.8
22	0.10	2.15	2.40	2.75	3.10	3.25	3.45	0.78	+0.22	0.66	2.75
23	1.10	2.25	2.55	2.95	3.35	3.50	3.85	0.73	+0.23	0.47	2.90
24	0.90	1.35	1.65	2.45	3.10	3.30	4.10	0.82	-0.05	0.47	2.4

TABLE 10.1. Grain size analysis of the Sago Pudding Sandstone

	No.	1st	2nd	3rd	4th	5th
1.	191A		3.1			
2.	159		3.1	-0.1		
3.	191B	5.0	3.1			
4.	E75		3.2			
5.	157		3.35	0		
6.	E17	4.5	3.2	1.1		
7.	E16	4.5	3.1	0.6		
8.	E74		3.1			
9.	E76		2.85			
10.	176	4.5	3.1			
11.	L5		3.25	2.7	1.0	
12.	155		3.3	2.8	0.5	
13.	L6		3.25	1.75	-0.5	
14.	L7		3.0	1.6	0.5	
15.	QR2		2.5	1.3	0.3	
16.	199			0.5		
17.	F3		3.0	2.5	0.5	
18.	SQ6		3.15			
19.	S4-3	4.5	2.8	-1.0		
20.	S4-2		2.9	1.75	0.75	0.25
21.	S4-1	4.5	3.1	2.5	1.25	
22.	46867		3.1	1.0		
23.	46868		3.2	0		
24.	46869		3.25	1.5		

TABLE 10.2. Analysis of the modes of the Sago Pudding Sandstone

Masonshaugh foreshore

1.	1.84, 1.60, 1.44, 1.00, 0.96	
2.	1.50, 0.70, 1.92, 1.60, 1.30	Average 1.27 mm
3.	1.00, 1.40, 1.40, 0.60, 2.12	
4.	1.48, 1.20, 1.04, 0.90, 0.70	

Gallows Hill

1.	1.52, 1.04, 0.70, 0.96, 0.76	
2.	0.80, 1.20, 0.84, 0.76, 1.04	
3.	0.90, 0.80, 0.82, 1.10, 0.70	Average 0.93 mm
4.	0.90, 1.04, 0.96, 1.20, 0.80	
5.	1.70, 0.80, 1.30, 0.94, 0.94	

Clarkly Hill East

1.	1.14, 0.80, 1.06, 1.00, 0.90	Average 1.00 mm
2.	0.84, 1.14, 1.16, 0.96, 1.00	

Findrassie

1.	0.94, 0.60, 0.56, 0.64, 0.58	Average 0.64 mm
2.	0.64, 0.50, 0.60, 0.70, 0.64	

Inverugie

1.	1.00, 1.24, 0.94, 0.96, 0.96	
2.	0.88, 1.20, 1.06, 0.94, 0.92	Average 0.94 mm
3.	0.94, 1.16, 1.20, 0.94, 0.90	
4.	0.80, 0.96, 1.10, 0.76, 0.70	

Lossiemouth

1.	1.00, 0.70, 0.88, 1.10, 0.80	
2.	0.80, 0.70, 0.76, 0.82, 0.96	
3.	0.76, 0.84, 0.96, 0.88, 0.84	Average 0.84 mm
4.	0.90, 0.84, 0.86, 1.00, 1.04	
5.	0.70, 0.80, 0.60, 0.84, 0.96	

Spynie Hill

1.	0.70, 0.70, 0.80, 0.66, 0.80	
2.	0.70, 0.80, 0.84, 0.62, 0.60	
3.	0.70, 0.80, 0.90, 0.60, 0.66	Average 0.72 mm
4.	0.72, 0.84, 0.74, 0.56, 0.74	
5.	0.64, 0.80, 0.60, 0.60, 0.70	

St. Peter's Well, Duffus

1.	0.80, 0.70, 0.56, 0.70, 0.60	
2.	0.48, 0.50, 0.70, 0.50, 0.50	
3.	0.44, 1.10, 1.10, 0.70, 0.72	Average 0.72 mm
4.	0.90, 0.74, 0.60, 0.64, 0.60	

TABLE 10.3. Grain Size Analysis of the coarse mode of the Sago Pudding Sandstone (in mm)

which is similar to the secondary mode in the bimodal sandstones. Fig. 11.1 illustrates the similarity in grain size between the Lossiemouth Sandstone, floodplain deposits and the Sago Pudding Sandstones. It is suggested that the Sago Pudding Sandstones are floodplain deposits which have since been partially reworked by the wind. They are therefore a transitional stage between the aeolian Lossiemouth Sandstone and the floodplain deposits (Fig. 11.3).

The main matrix of the Sago Pudding Sandstones, which is similar to the Lossiemouth Sandstone, is probably derived from the low angled foreset and horizontally laminated horizons which constitute the greatest percentage of the floodplain deposits. The coarse mode is probably derived from the re-working of the scour channel of the floodplain. Sago Pudding Sandstones with fine modes, although present, are extremely rare presumably due to the removal of the silty material in suspension by the wind; these were clearly derived from the ripple marked and silty horizons of the floodplain deposits.

Thus, after deposition of the Lossiemouth Sandstone, the floodplain deposits were deposited over the aeolian dunes. The waters then dried up and the floodplain deposits were reworked by the wind mixing the coarse, medium and fine grained sandstones to produce the Sago Pudding Sandstone. Further reworking would have produced an aeolian sandstone but the process was terminated by the formation of the Cherty Rock.

The size of the grains which the floodwaters can carry is directly related to the velocity of the water which deposits them. As the velocity decreases away from the main river channel, the size of the grains should get progressively finer.

The size of the five coarsest grains was measured in several random thin sections from many localities. The average grain size of the coarse mode was then calculated (Table 10.3). When the results are superimposed on to the base map (Fig. 10.1) it can be seen that the contours run parallel to the mean palaeocurrent direction of the fluvial channel. This indicates that the grain size of the sediments does decrease uniformly away from the main channel and supports the theory that the Sago Pudding Sandstones were derived originally from the floodplain deposits.

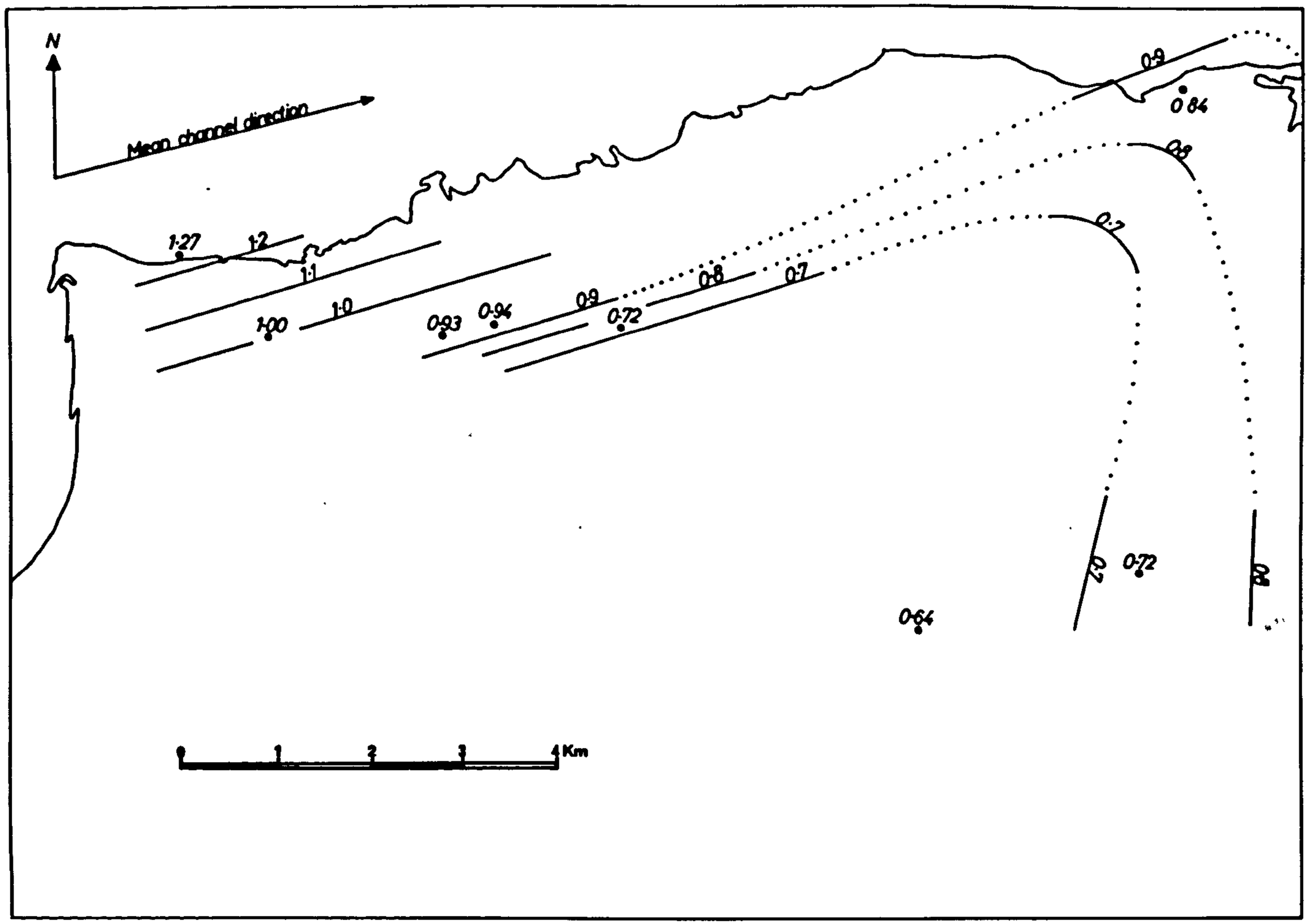

Fig. 10.1. Distribution of the average coarse mode of the Sago Pudding Sandstone.

CHAPTER 11

PETROGRAPHY OF THE LOSSIEMOUTH SANDSTONE, SAGO PUDDING SANDSTONE AND THE FLOODPLAIN DEPOSITS OF THE BURGHEAD BEDS

It has been suggested in previous chapters that the Sago Pudding Sandstone and the Lossiemouth Sandstone represent various stages in the reworking of the floodplain deposits. If this interpretation is correct, the petrography of the sandstones should indicate a common source with only minor variation due to the environmental controls of the depositing media.

GRAIN SIZE COMPARISON

Grain size characteristics have already been discussed in the relevant chapters. Fig. 11.1 summarises the major differences between the three sandstones.

(a) The floodplain deposits show a general increase in sorting with decrease in grain size, clearly reflecting the progressive increase in sorting in the fining upwards cycle.

(b) Most of the floodplain deposits have a mean grain size of between 3.0 to 3.5 phi whereas the mean of the aeolian Lossiemouth Sandstone varies between 2.0 to 3.0 phi. Thisis explained by the removal of the fine material in suspension by the wind, thus giving a coarser mean grain size to the Lossiemouth Sandstone.

(c) The Sago Pudding Sandstone only reflects a partial reworking of the floodplain deposits and thus has characteristics of both the floodplain and the aeolian deposits. Where the floodplain deposits have only been partially reworked, the fine and coarse material from the floodplain deposits have been mixed together giving the same mean grain size but a much poorer coefficient of sorting. Progressive reworking is reflected by an increase in the sorting coefficient until sorting is the same as in the Lossiemouth Sandstone.

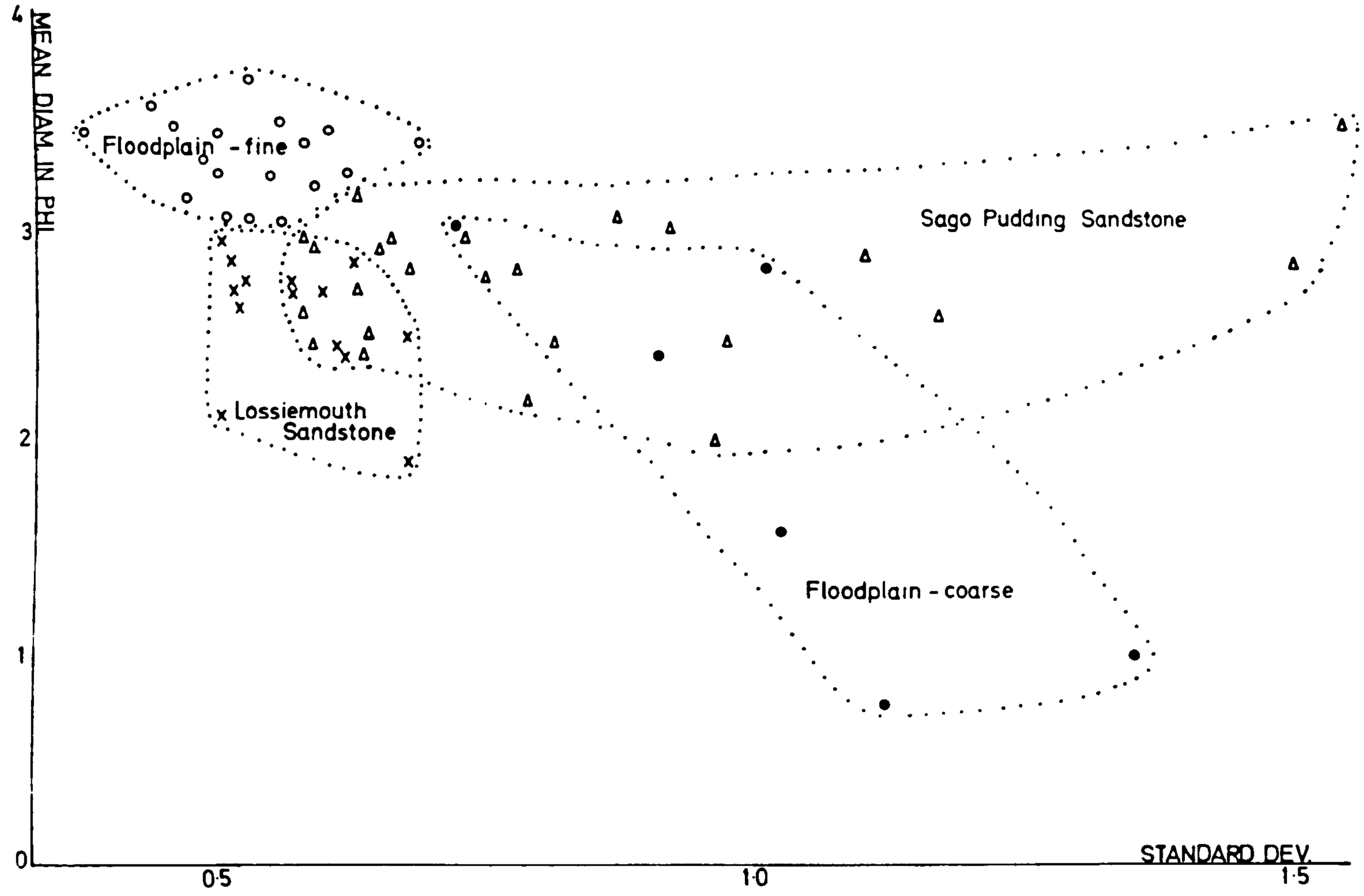

Fig. 11.1. Comparison of the grain size characteristics of the Sago Pudding Sandstone, Lossiemouth Sandstone and the floodplain deposits of the Burghead Beds.

Number	Quartz	Feldspar/Rock Fragments	Matrix
Lossiemouth Sandstone			
S1	90.2	9.8	0
S2	90.0	10.0	0
S3	86.9	13.1	0
S5	96.5	3.5	0
S7	90.0	10.0	0
S9	82.0	18.0	0
S10	94.7	5.3	0
S11	89.9	10.1	0
S12	91.4	8.6	0
L5	86.0	14.0	0
Floodplain			
C2	76.0	16.0	8.0
C3	86.5	13.0	0.5
QR3	84.5	12.0	3.5
FB	85.0	11.0	4.0
FC	75.0	16.0	9.0
FA	84.0	14.0	2.0
FD	79.0	14.0	7.0
RC	60.0	19.0	21.0
RB	81.0	12.5	6.5
RA	69.0	11.0	21.0
Sago Pudding Sandstone			
159	89.5	10.5	0
155	84.5	13.5	2.0
S4-1	76.5	11.0	12.5
E74	89.5	9.5	1.0
E76	94.0	6.0	0
199	89.5	10.0	0.5
QR2	95.0	5.0	0
Qr2-1	88.5	8.5	3.0
E16	88.5	11.5	0
E19	78.0	15.0	7.0
L7	92.0	6.5	1.5
E75	90.5	9.5	0
157	88.5	11.5	0
F3	94.5	5.5	0
191B	89.0	11.0	0

TABLE 11.1. Classification parameters of Pettijohn (1954)

Number	Quartz	Feldspar	Rock Fragments
Lossiemouth Sandstone			
S1	90.1	8.2	1.6
S2	90.0	8.0	2.0
S3	86.8	8.7	4.4
S5	96.5	3.5	---
S7	90.0	9.0	1.0
S9	82.1	9.0	9.0
S10	94.2	5.3	---
S11	89.6	6.7	3.4
S12	91.3	8.6	---
L5	86.0	7.5	6.5
Floodplain			
C2	82.0	7.0	11.0
C3	87.0	10.0	3.0
QR3	88.0	7.5	4.5
FB	89.0	5.0	6.0
FC	84.0	8.5	7.5
FA	86.0	9.0	5.0
FD	85.5	5.0	9.5
RC	75.0	12.0	13.0
RB	87.0	5.5	7.5
RA	87.0	6.5	6.5
Sago Pudding Sandstone			
159	90.0	9.0	1.0
155	86.5	11.5	2.0
S4-1	88.5	7.5	4.0
E74	90.0	7.5	2.0
E76	93.0	7.0	---
199	89.5	7.0	3.0
QR2	95.0	3.5	1.5
Qr2-1	91.0	7.5	1.0
E16	88.0	6.5	5.0
E19	85.0	7.5	7.5
L7	93.5	3.5	3.0
E75	90.8	6.0	3.5
157	88.5	8.0	3.5
F3	94.0	4.5	1.0
191B	89.0	9.0	2.0

TABLE 11.2. Classification parameters of McBride (1963)

Number	Unimodal Quartz	Clay and Mica	Polyx. Qtz. Feldspar, Chert and Rock Fragments
Lossiemouth Sandstone			
S1	73.7	0	26.3
S2	73.0	0	27.0
S3	72.4	0	27.4
S5	83.5	0	16.5
S7	70.0	0	30.0
S9	74.6	0	25.4
S10	80.1	0	19.9
S11	77.5	0	22.5
S12	73.0	0	27.0
L5	70.0	0	30.0
Floodplain			
C2	58.0	13.0	29.0
C3	73.5	0.5	26.0
QR3	65.5	4.0	30.5
FB	74.0	6.0	20.0
FC	64.0	11.0	25.0
FA	63.0	3.0	36.0
FD	62.0	10.0	28.0
RC	51.0	30.0	19.0
RB	69.0	11.5	19.5
RA	54.0	22.0	24.0
Sago Pudding Sandstone			
159	75.0	1.0	24.0
155	70.5	3.0	26.5
S4-1	67.5	13.5	19.0
E74	77.0	1.0	22.0
E76	79.5	0	20.5
199	78.5	2.5	19.0
QR2	62.5	0	37.5
Qr2-1	67.5	3.0	29.5
E16	76.0	2.5	21.5
E19	66.0	9.0	25.0
L7	72.0	3.0	25.0
E75	81.3	0	18.7
157	78.0	1.0	21.0
F3	79.0	1.0	20.0
191B	79.0	1.0	20.0

TABLE 11.3. Classification parameters of Williams (1972)

		Burghead Beds Floodplain	Lossiemouth Sandstone	Sago Pudding Sandstone
	(a) Quartz:Feldspar	11:1	25:2	13:1
MATURITY				
	(b) Quartz+Chert:Feldspar +Rock Fragments	7:1	9:1	19:2
PROVENANCE	(c) Feldspar:Rock Fragments	2:1	3:1	5:2
FLUIDITY	(d) Sand:Clay	Variable	Infinity	Variable

TABLE 11.4. Comparison of the Maturity, Provenance and Fluidity ratios proposed by Pettijohn (1954)

CLASSIFICATION

The dual classification suggested in Chapter 5 is used once again together with the classification of McBride (1963). Figs. 11.2A, 11.2B and 11.2C, illustrate the results recorded in Tables 11.1, 11.2 and 11.3 plotted on triangular diagrams. The classification of McBride (1963) indicates that the sandstones belong to the quartzarenite, subarkose and sublitharenite clans. However, this scheme fails to differentiate between the three major facies types represented by these analyses. It therefore fails as a genetic classification.

Fig. 11.2A, the classification of Pettijohn (1954), although showing a preferential grouping in the subarkose clan, does however reveal a higher degree of environmental differentiation. This is due essentially to the inclusion of matrix as a major parameter. As previously stated, the floodplain deposits probably represent the source from which both the Lossiemouth Sandstone and the Sago Pudding Sandstone were derived. Thus, when the Lossiemouth Sandstone is compared to the floodplain deposits, it is seen that there is a complete absence of matrix in aeolian sandstones. This can be readily explained by the removal of the fine material in suspension. The Sago Pudding Sandstones plot at intermediate values betweem the floodplain deposits and the Lossiemouth Sandstones and reflects the partial re-sorting of the floodplain deposits by the wind giving them characteristics of both environments (Fig. 11.3).

Fig. 11.2C again illustrates the removal of clays from the Lossiemouth Sandstone and also the lack of mica compared to the waterlain sandstones. It also indicates that in the floodplain deposits, the percentage of clay is inversely proportional to the percentage of unimodal quartz, indicating that the increase in clay is due to decrease in grain size.

Table 11.4 illustrates the genetic and descriptive properties of maturity, provenance and fluidity proposed by Pettijohn (1954). It indicates the close similarity between the maturity and provenance values substantiating

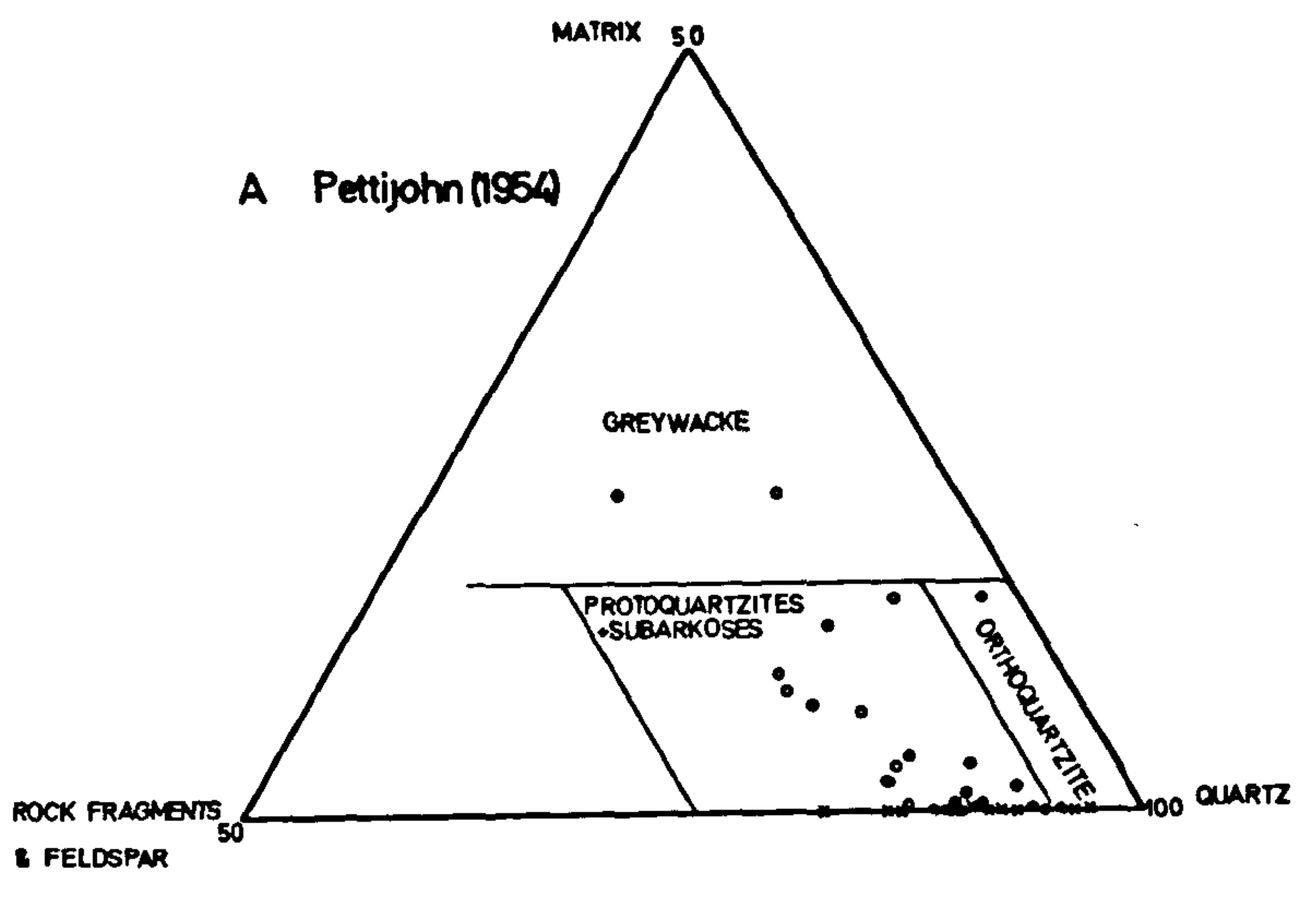

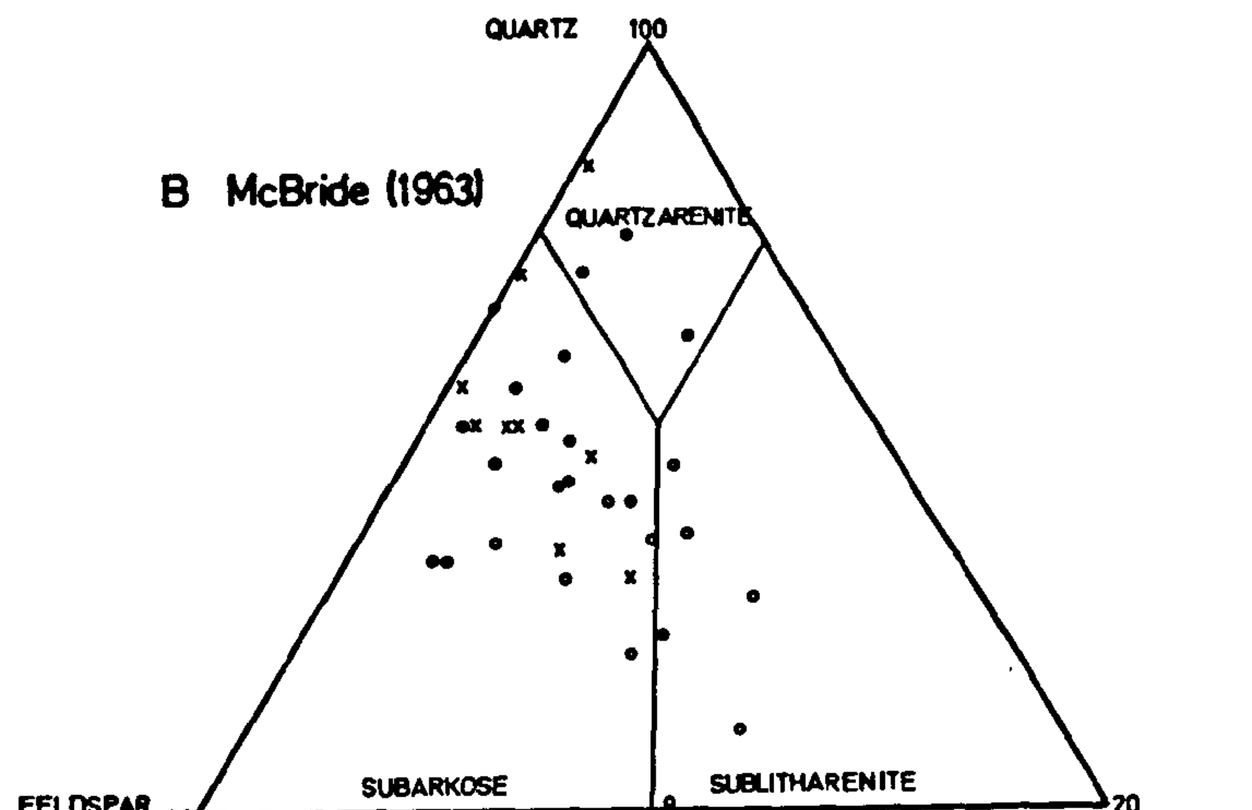

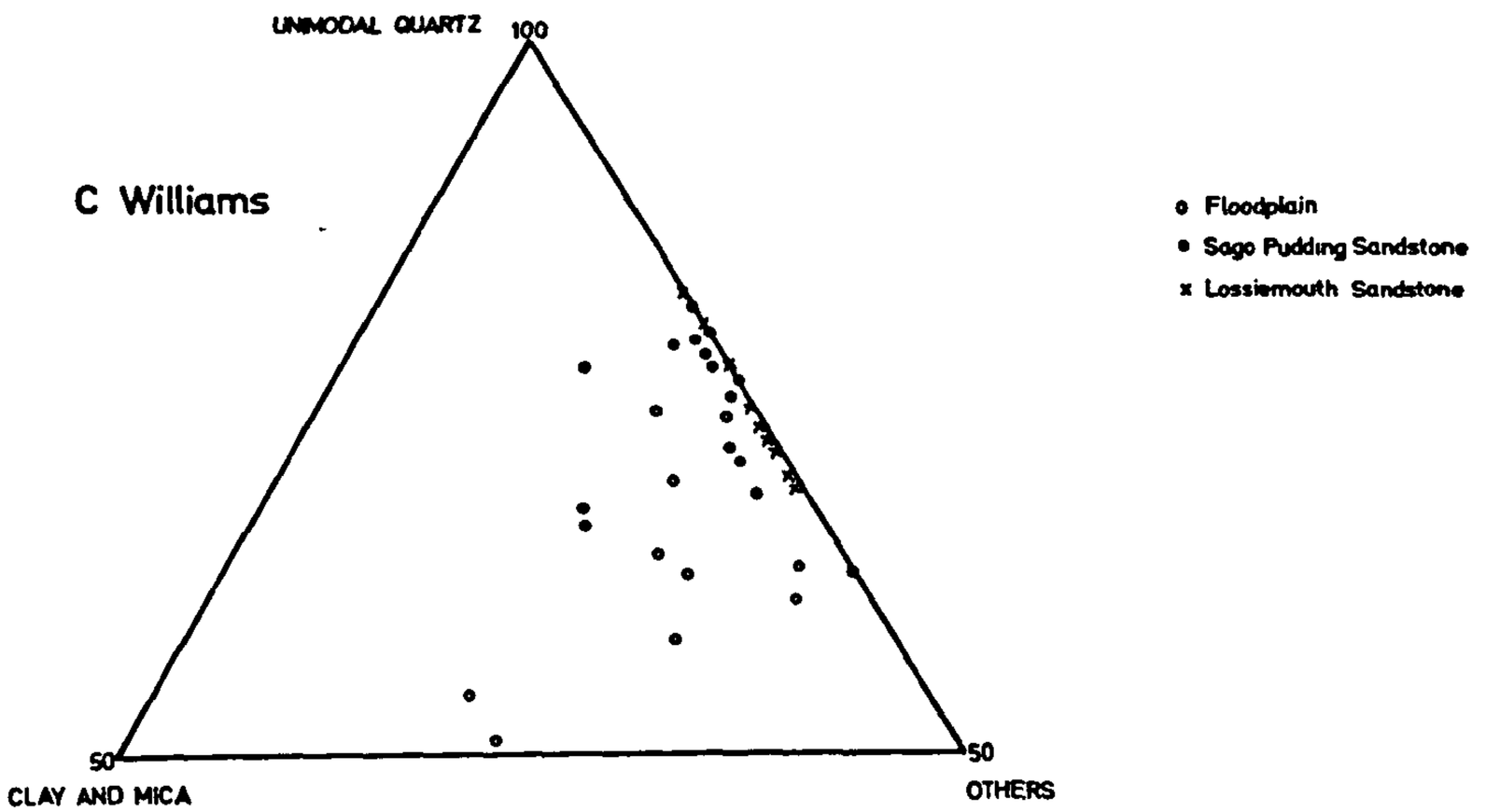

Fig. 11.2. Classification of the Sago Pudding Sandstone, Lossiemouth Sandstone and floodplain deposits.

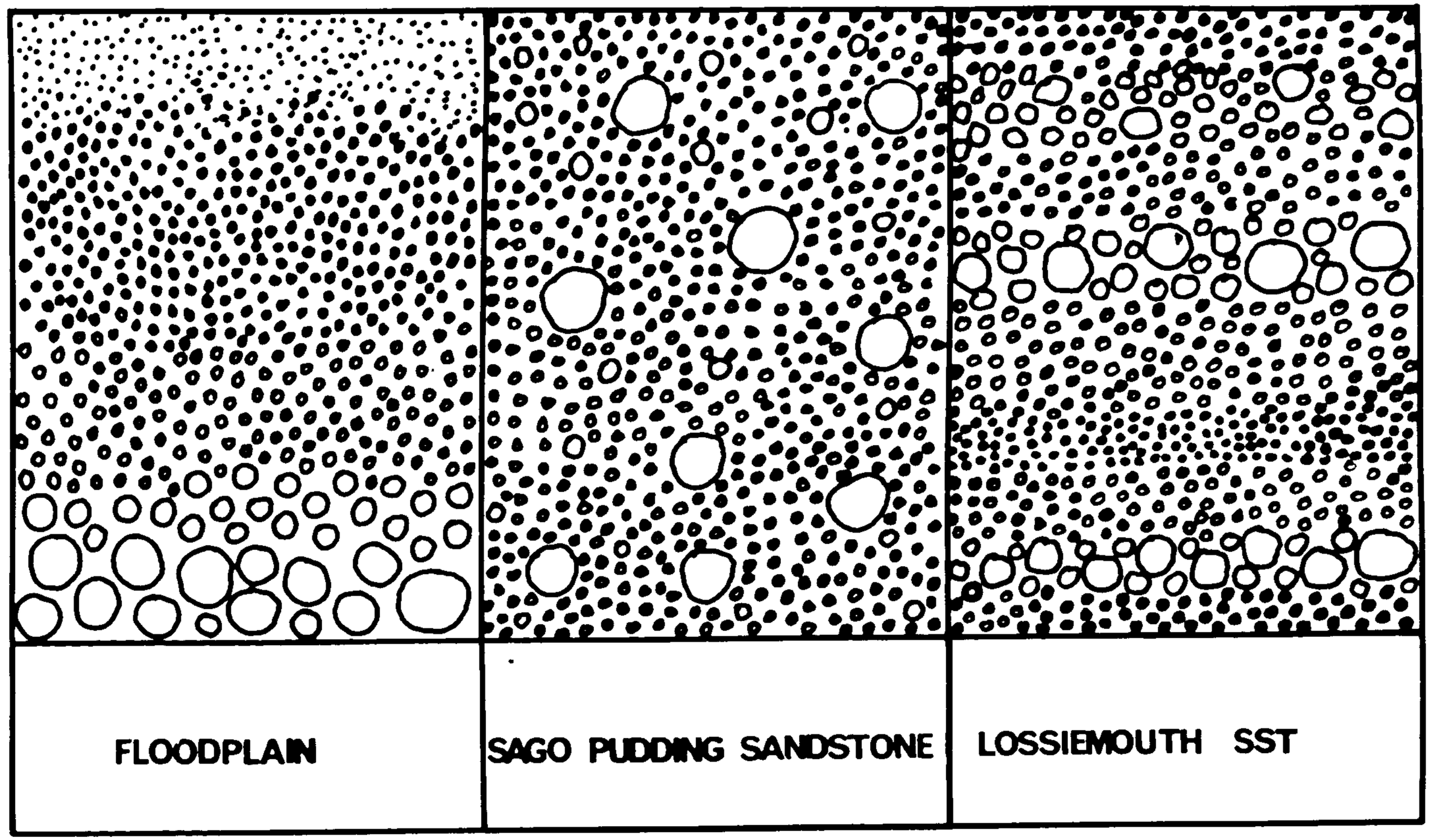

Fig. 11.3. Reworking of the floodplain deposits by the wind to produce the Sago Pudding Sandstone(transition) and the Lossiemouth Sandstone(aeolian).

the interpretation that the three sandstones were from the same source but were laid down by different depositing media (fluidity).

DETRITAL COMPONENTS

Analysis of the detrital components of the three facies indicates that they are similar to those found in the coarse grained point bar deposits of the Burghead Beds. This is to be expected as the floodplain deposits are from the same fluviatile source. However, the fine grained nature of most of the deposits makes grain type recognition more difficult with the result that only the more easily recognised components were identified.

The three basic types of quartz can once again be recognised and are used here.

Unstrained Quartz

Unstrained quartz represents 20-30 per cent of the unicrystalline quartz present in the sandstones. All the types listed below have been recognised from all three sandstone facies.

The most common type of unstrained quartz are those with aligned black dust particles although rarely the dust particles may be randomly orientated. Unstrained quartz with inclusions are also common; these are normally in the form of bubbles, but hexagonal and cubic shaped inclusions have also been recognised.

In the floodplain deposits, unstrained quartz with randomly distributed rutile needles have also been identified.

Strained Quartz

The two types of strained quartz which were present in the point bar deposits can similarly be recognised. Highly strained quartz requiring a rotation of between 20-40 degrees before complete extinction is achieved are thought to be derived from high grade metaquartzites and granulites. Strained quartz requiring a rotation of less than 20 degrees can often be compared to rock fragments derived from lower grade metamorphic rocks.

Strained quartz is frequently recognised in the vicinity of faults and fractures in the Lossiemouth Sandstone; the quartz grains are themselves fractured and require a rotation of 5-10 degrees to achieve complete extinction.

Polycrystalline Quartz

Polycrystalline quartz represents between 6-30 per cent of the total detrital quartz grains, the percentage being directly related to the grain size, i.e. the coarser the mean grain size, the higher the percentage of polycrystalline grains. Fig. 11.4 shows a graph of mean grain size plotted against the percentage of polycrystalline quartz. The floodplain deposits plot on the fine grained extension of the graph for the point bar deposits reflecting the same source area. The aeolian Lossiemouth Sandstone however plots on a separate line from that of the Sago Pudding Sandstone and the floodplain deposits. The gradient of the graphs are however the same, the difference being the coarser mean grain size of the Lossiemouth Sandstone. The aeolian deposits therefore possess a relative deficiency of fine material compared to the floodplain deposits.

The most common type of polycrystalline quartz is represented by fragments of high grade metamorphic quartz. These show highly sutured contacts on the grain boundaries, the individual quartz grains often requiring a rotation of up to 40 degrees to achieve complete extinction. The grains often show a distinct schistosity, a feature which is most evident in the larger grains of quartz. Metaquartzite fragments derived from lower grade metamorphic rocks can also be recognised although these are less common. They show tangential contacts between the quartz units and the degree of straining is less marked. Some of these metaquartzite fragments are stained by iron oxides suggesting that they are derived from pebbles in the Old Red Sandstone.

Cherts may represent between 1-5 per cent of the total detrital components. These are secondary cherts which have replaced Old Red Sandstone cornstones although little or no evidence of calcite may be present. Rarely

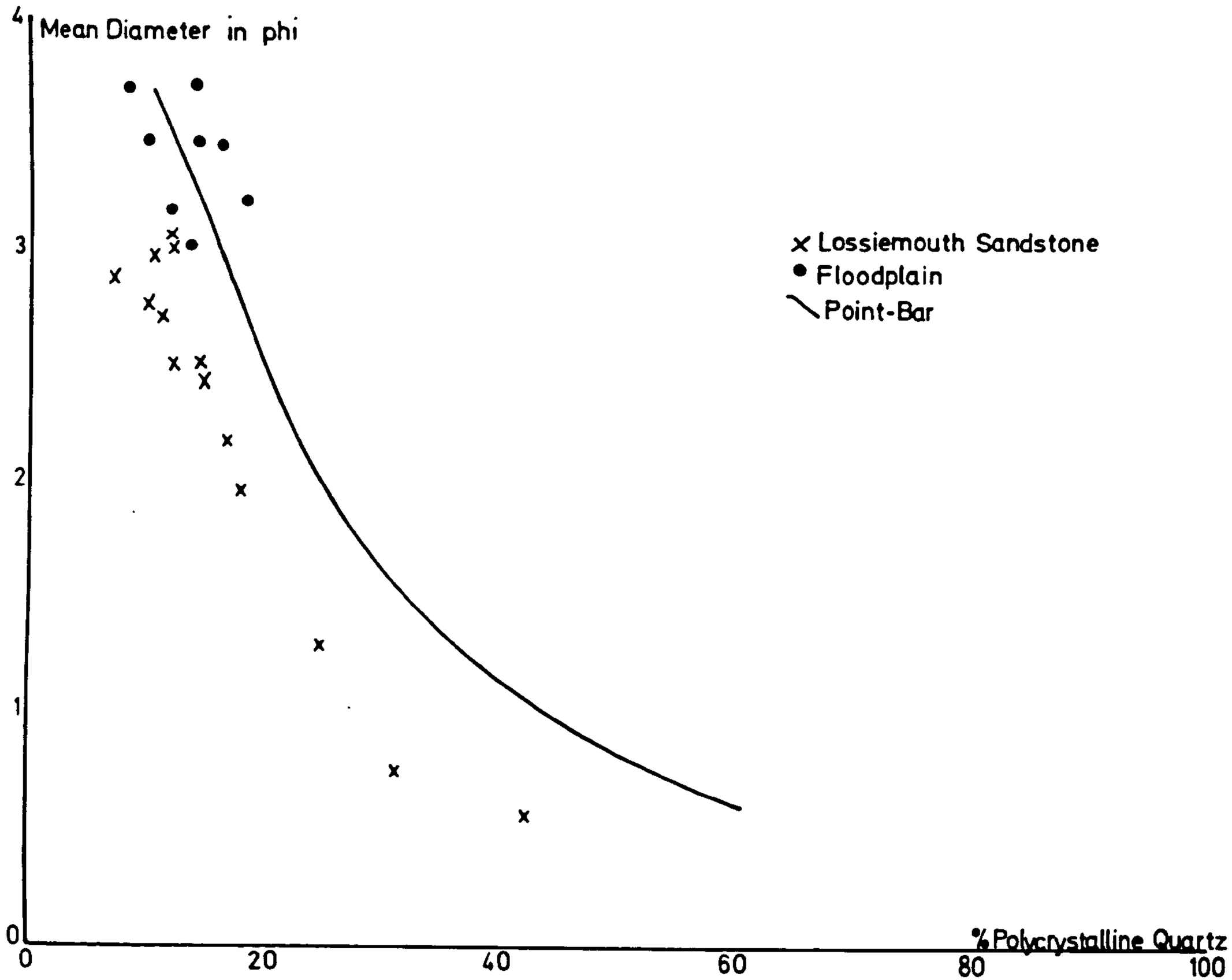

Fig. 11.4. Mean diameter plotted against the percentage of polycrystalline quartz.

chertified sandstones are also present. Sandstones of the Old Red Sandstone are rarely preserved owing to their highly friable nature which leads to disaggregation prior to consolidation.

Rock Fragments

Rock fragments represent a maximum of 3 per cent of the total detrital constituents. The rock fragments are generally derived from the metamorphic Moinian and Dalradian.

Quartz granulites are the most common type of rock, these being characterized by quartz with subsidiary muscovite. Rarely concentrations of heavy minerals are present, these being normally zircon or apatite. Quartz feldspathic granulites are rarely seen in these sandstones.

Little or no evidence of Old Red Sandstone rock fragments is seen although many of metamorphic fragments are stained by iron oxides and have clearly been derived from the Old Red Sandstone. Chert replacing cornstones and feldspathic sandstones are however sometimes present.

Feldspar

Feldspars represent between 3.5-11.5 per cent of the total detrital grains but generally between 6-9 per cent.

Tabular microcline is the most common type of feldspar present although cloudy orthoclase may also be present. The microcline is characteristically fresh whereas the orthoclase is often stained by iron oxides or shows traces of sericitisation. No plagioclase feldspars have been recognised in any of the sandstones.

Heavy minerals

Between 0-2.5 per cent of the total detrital grains are represented by heavy minerals. In the floodplain deposits this percentage is generally between 1.5-2.5 per cent but in the Lossiemouth Sandstone they are rare or completely absent. The Sago Pudding Sandstone has variable amounts of heavy minerals dependent on the influence of the aeolian agencies.

The following table represents the relative percentage of heavy minerals which were identified from five thin sections of the floodplain deposits:

Zircon	32%
Garnet	18%
Tourmaline	14%
Apatite	14%
Rutile	8%
Spinel	8%
Hornblende	4%
Topaz	2%

Where the Sago Pudding Sandstone displays characteristics of water-lain sandstones, there is a high concentration of heavy minerals but those showing aeolian characteristics are deficient in heavy minerals. Zircon, tourmaline, apatite and garnet are most common although rutile, topaz and biotite are sometimes present.

In the Lossiemouth Sandstone, the sediments show only rare occurrences of heavy minerals. Zircon and garnet are the most common although tourmaline, amphibole, apatite and monazite are sometimes present. It will be noted that these are the commonest heavy minerals found in the floodplain deposits.

Micas

Micas are common in the floodplain deposits and may represent up to 6 per cent of the total detrital grains in some of the finer grained sediments. They generally constitute between 1-2 per cent.

In the aeolian Lossiemouth Sandstone, as expected, micas are rare. In the Sago Pudding Sandstone, mica is frequently present in the preserved waterlain horizons but is rare in sediments redeposited by the wind.

Muscovite constitutes the greater percentage of micas and is probably derived from the quartz granulites. Biotite is rarely present, and always is highly altered.

CHAPTER 12

CHERTY ROCK (ELGIN) : A CALICHE HORIZON

The Cherty Rock contains various rock types ranging from calcareous sandstones and cherts through to limestones. These are thought to represent various stages in the alteration and formation of an original caliche horizon which was developed as the final phase of New Red Sandstone sedimentation in the Elgin district. The horizon overlies the Lossiemouth and Sago Pudding Sandstones to the east whereas to the west, it overlies the Burghead Beds. The presence of Liassic marls overlying the Cherty Rock would suggest that the caliche was late Triassic in age.

The horizon has been compared to the superficial chalcedony of arid regions by Watson and Hickling (1914), while Peacock (1968) noted their resemblance to modern day caliche deposits. However, Peacock thought that the abnormally high content of silica was foreign to this rock type. Petrological studies have now shown that the silica is mainly replacing the original carbonate, indicating that the horizon was indeed originally a caliche soil.

This chapter compares the Cherty Rock with modern day caliche from the New Mexico and Texas areas and shows that all features that are present in the modern deposits can also be recognised in the Cherty Rock. The replacement features of the Cherty Rock are discussed in Chapter 13.

LOCALITY DESCRIPTIONS

At Lossiemouth, the Cherty Rock rests directly on the Sago Pudding Sandstone. Where this sandstone is highly silicified, the contact with the Cherty Rock is often gradational, but in those cases where the original carbonate sediment of the Cherty Rock can be seen, there is usually a sharp contact between the two horizons. However, the degree of quartz replacement in the Cherty Rock is extremely high and only rarely can the original form of the caliche horizon be recognised.

The Cherty Rock outcrops in the post glacial cliffs to the south of Stotfield Golf Course, the exposures being in the gardens of several large houses at 22457047, 22537053, 22577062, 22637065 and 22687069. There is an increase in silicification towards the top of the Sago Pudding Sandstone which finally grades into a maximum of 3 metres of Cherty Rock. The Cherty Rock is characterised by vein quartz, vughs filled by quartz, but mainly appears to be sandstones replaced by chert. The chert is sometimes rhythmically banded and rarely shows a honeycomb structure of chert and limestone.

The Cherty Rock is also exposed along the foreshore to the north of Lossiemouth, between Lossiemouth Harbour and Maggie's Crag. To the east, the contact with the Sago Pudding Sandstone is normally gradational but to the west, in the vicinity of Maggie's Crag, the contact can often be identified. Where the limestone is unaltered, it is characteristically friable and includes randomly distributed quartz grains; occasionally, a laminated horizon occurs. At 22657098, veins are infilled with quartz and galena. The high degree of replacement of the caliche by chert appears to be associated with faulting at this locality, where the Old Red Sandstone is in juxtaposition with Triassic rocks.

At Spynie Hill, the Cherty Rock is only exposed in the main working quarry (22256565) and in the plantations above the quarry. The eastern face of the quarry is represented by the Lossiemouth Sandstone which shows an increase in silicification towards the upper parts of the quarry. The top metre of the quarry displays highly silicified sandstones with cavities infilled by soft ferruginous and manganiferous material. The top of the quarry appears to coincide with the contact of the Lossiemouth Sandstone with the Cherty Rock, as immediately above the quarry, 0.5 metres of grey and brown chert is exposed (22356560). The chert contains vughs infilled by quartz and calcite which, in thin section, can be seen to replace both sandstones and limestones.

At the Palace of Spynie (23106590), exposures at the base of the bank of the former Loch Spynie give the following section:

2 metres Dark chert with chalcedonic banding and cavities lined by calcite and quartz. Also disseminated galena (equivalent to the indurated caliche).

2 metres Pink and white limestone with scattered quartz grains grading down into a calcareous sandstone (equivalent to the friable caliche).

The Cherty Rock is also present in the upper horizon of the St. Peters Well Borehole, Duffus (17206874). A maximum of 1.5 metres is present and consists of sandy limestones which have been replaced by chert. This succession is similar to that at Inverugie where the sequence is well exposed. At Inverugie, several overgrown quarries in the grounds of Inverugie House and a quarry to the north of the house show the Cherty Rock overlying highly silicified sandstones (Sago Pudding Sandstone). However, the most complete succession occurs in a quarry to the north west of the house (1485685) where the Cherty Rock is relatively well exposed and the replacement does not obscure the original caliche. The following succession can be recognised:

0.5 metres Highly siliceous caprock characterised by rhythmically laminated chert and chalcedony (?Indurated caliche).

1.0 metre Highly indurated caliche with only a few quartz grains, pseudo-oolitic structures, laminated bands and generally a compact appearance. Often replaced by rhythmically banded chert and opal and chalcedony infill. Disseminated galena in places.

2 metres Green and white friable limestones showing relatively little replacement by chert. Characterised by floating quartz grains in the carbonate matrix which increase in amount towards the bottom of the section. Some vertical fractures infilled by quartz grades into

1.5 metres Siliceous sandstones with occasional calcareous nodules. Isolated veins of galena and quartz.

In the quarries to the east (1505687½), the succession is similar but the upper laminated horizon is absent. The Cherty Rock is also exposed at Gallows Hill (147684) and in a quarry to the east of the main Clarkly Hill quarries (1302684½). Here the silicified sandstones at the base of the caliche horizon are exposed but there is no evidence of the overlying limestones.

THE ORIGINAL CALICHE HORIZON OF THE CHERTY ROCK

Close examination of the Cherty Rock, where the original caliche can still be recognised, reveals that three main zones can be identified:

1. Upper = Indurated Caliche
2. Middle = Friable Caliche
3. Lower = Zone of Diagenetic Quartz

Fig. 12.1 shows a comparison of the Cherty Rock with modern day caliche profiles from the High Plains, Texas, described by Aristarain (1970) and Reeves (1970). The similarity to modern day caliche can clearly be seen.

1. Indurated caliche

The indurated caliche represents the upper horizon of the caliche profile and reaches a maximum thickness of 2 metres. It is characterised by a grey, hard flinty limestone which is often outlined by laminations and cavity infilling by both quartz and calcite. The form of the infilling is typically botryoidal.

The caliche horizon represents a favourable replacement structure both for chert, which replaces the limestone, and for quartz, which infills the vertical fractures. Galena is also found in these fractures, but the greater percentage is disseminated throughout the limestone. It is clear that the indurated caliche represents a most favourable channel for mineralisation.

Under the microscope, the most recognisable feature of the indurated caliche is the almost complete absence of detrital quartz (Plate 12.1A), the matrix being almost solely micritic calcite. Where quartz grains are present, they are generally quite large and unicrystalline suggesting that the less stable

1 CHERTY ROCK - Lossiemouth

2 CHERTY ROCK - Inverugie

3 CALICHE - High Plains.
[no present infiltration]

4 CALICHE - High Plains
[infiltration still taking place]

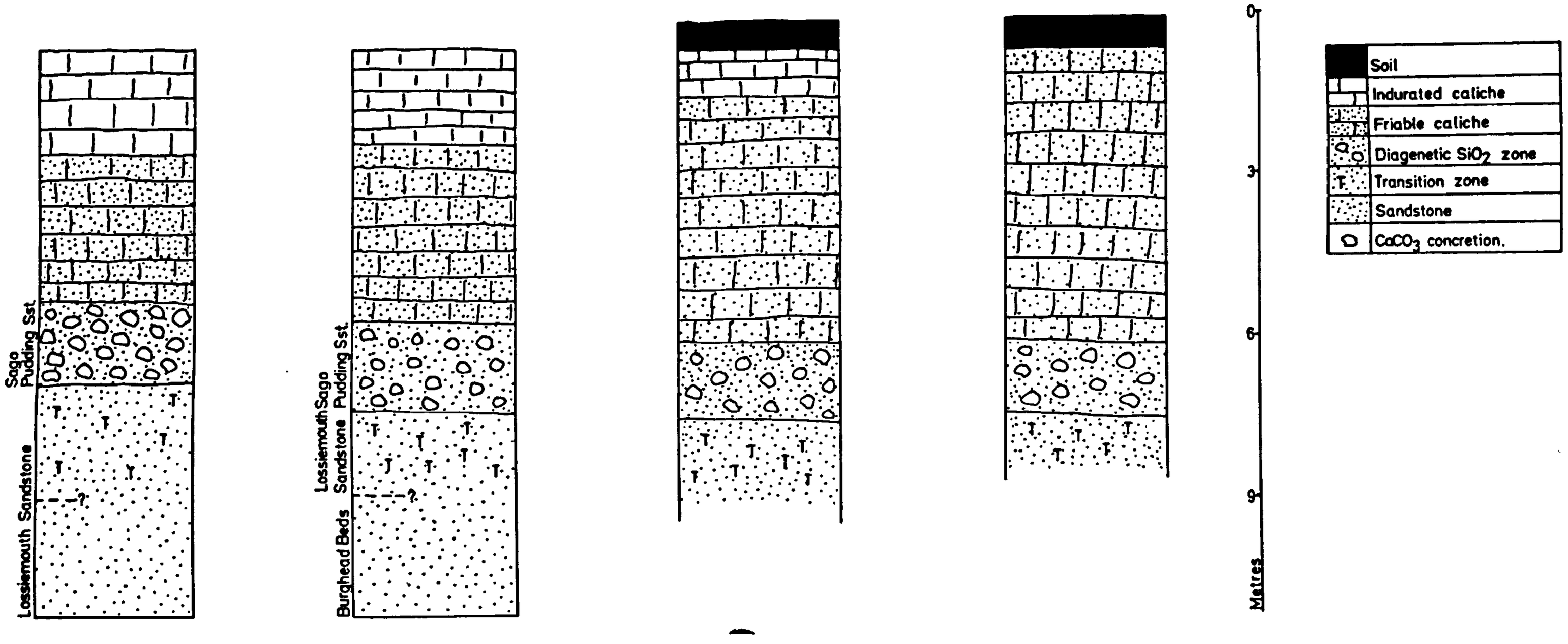

Fig. 12.1. Comparison of the Cherty Rock with modern day caliche horizons

EXPLANATION OF PLATE 12.1

INDURATED CALICHE OF THE CHERTY ROCK

A. Friable caliche illustrating the loose packing of the individual calcite grains. Some grains have a rhombic outline but this is rare except around the periphery of cavities. Stereoscan.

B. Solution features on the periphery of a detrital quartz grain embedded in a matrix of friable caliche. Stereoscan.

C. Impression of rhombic calcite/?dolomite due to solution of detrital quartz in the friable caliche. Stereoscan.

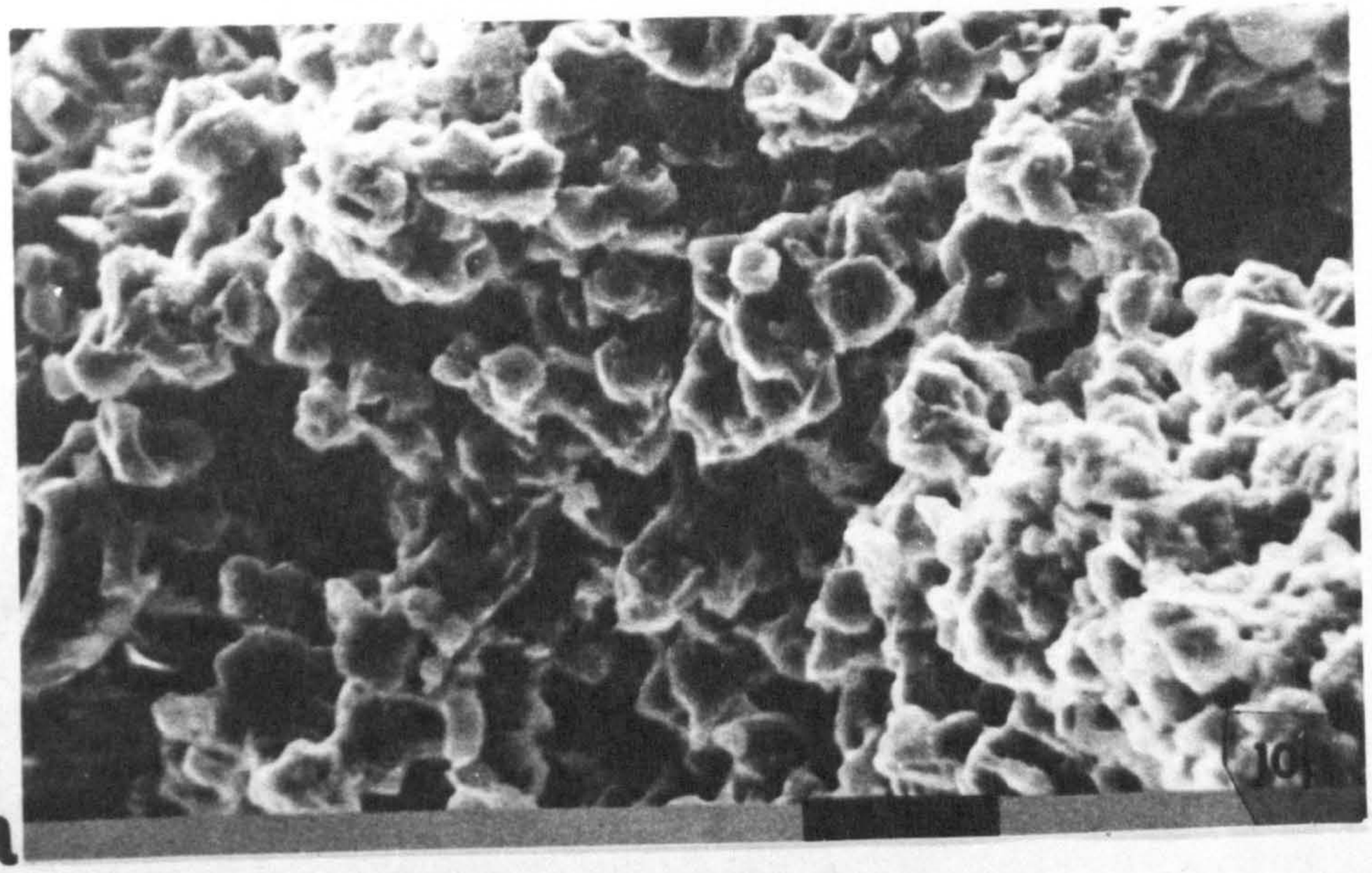

a

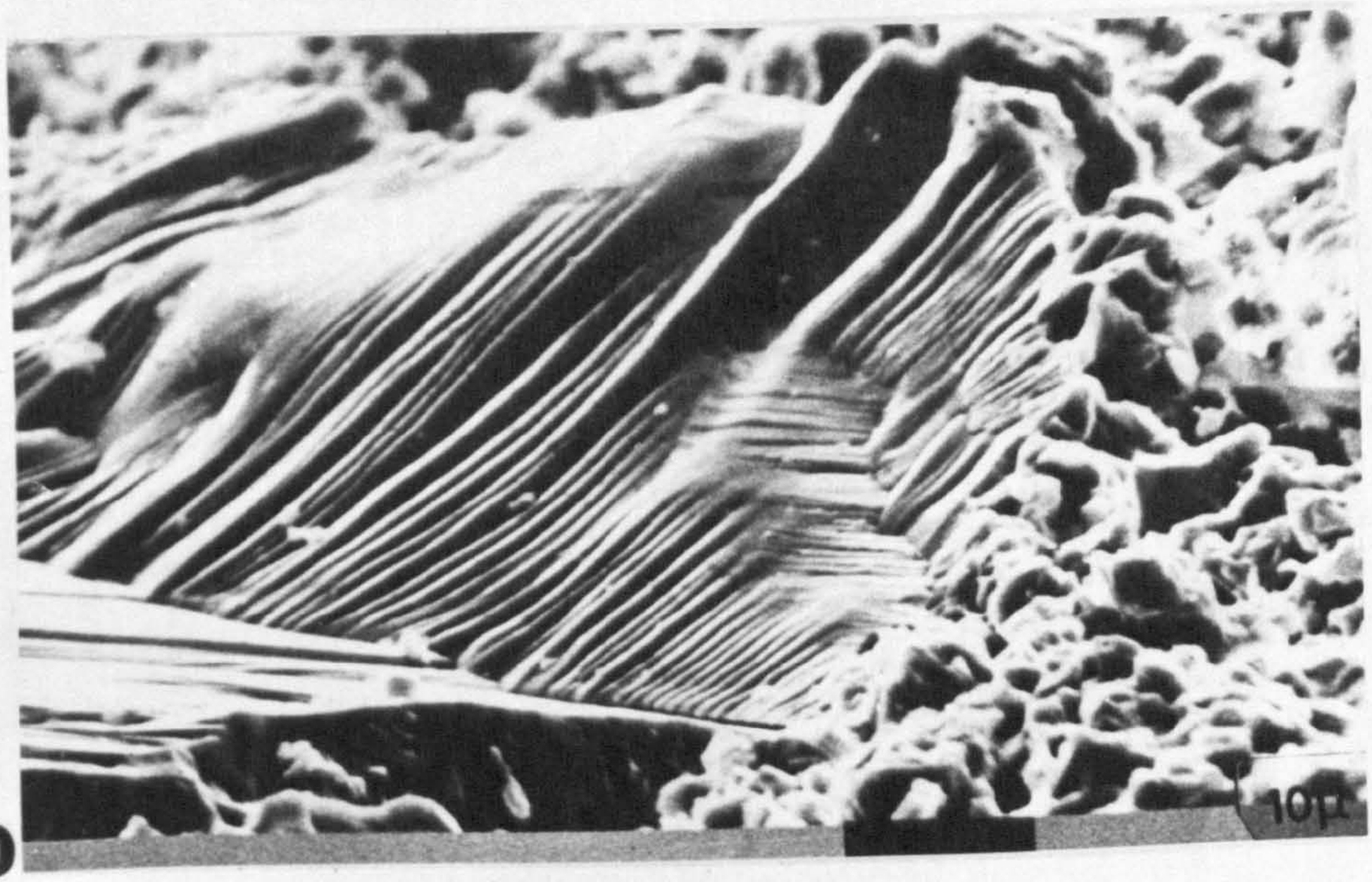

b

c

PLATE 12·1

EXPLANATION OF PLATE 12.2

INDURATED CALICHE OF THE CHERTY ROCK

A. Recrystallisation of the indurated caliche along a post depositional fracture. Scanning electron microscope.

B. Pseudo oolitic structure of the indurated caliche replaced by chert. Polarising microscope, crossed nicols.

C. Pseudo oolitic structure of the indurated caliche illustrating the middle of a botryoidal cavity fill. Some of the upstanding protruberances have been sectioned to display the characteristic pseudo oolitic structure. Polarising microscope, plane polarised light.

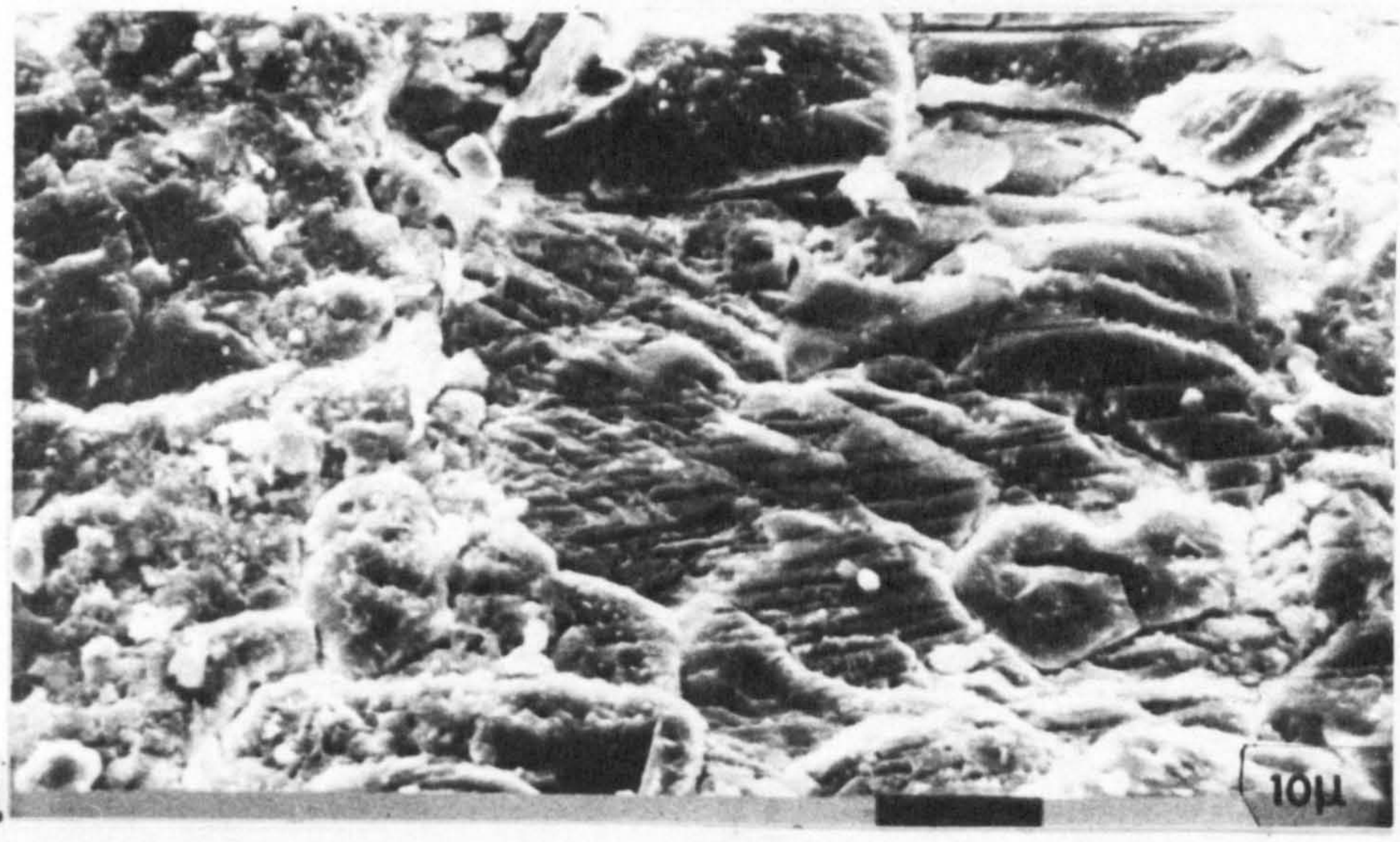

a

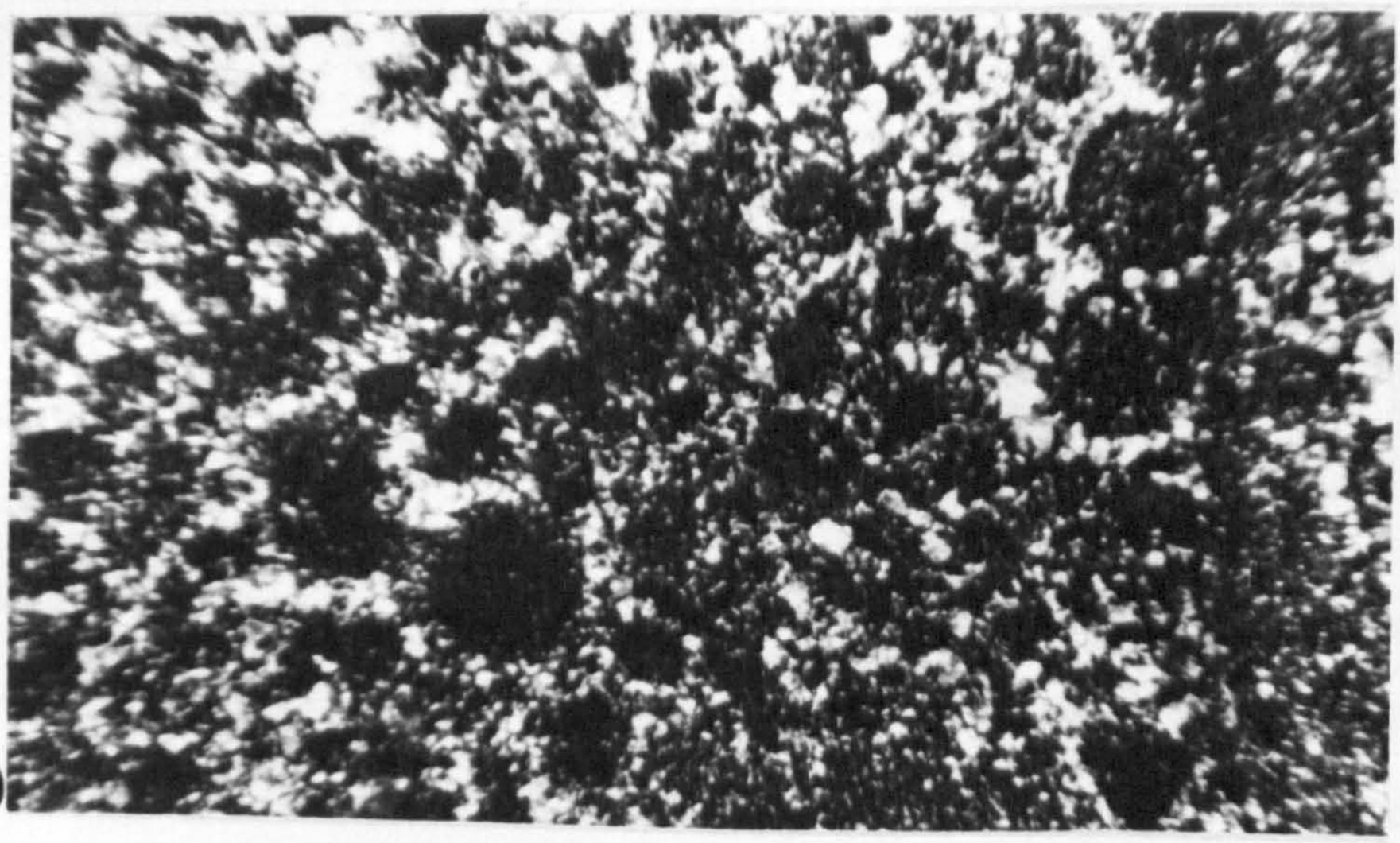

b

0 1mm.

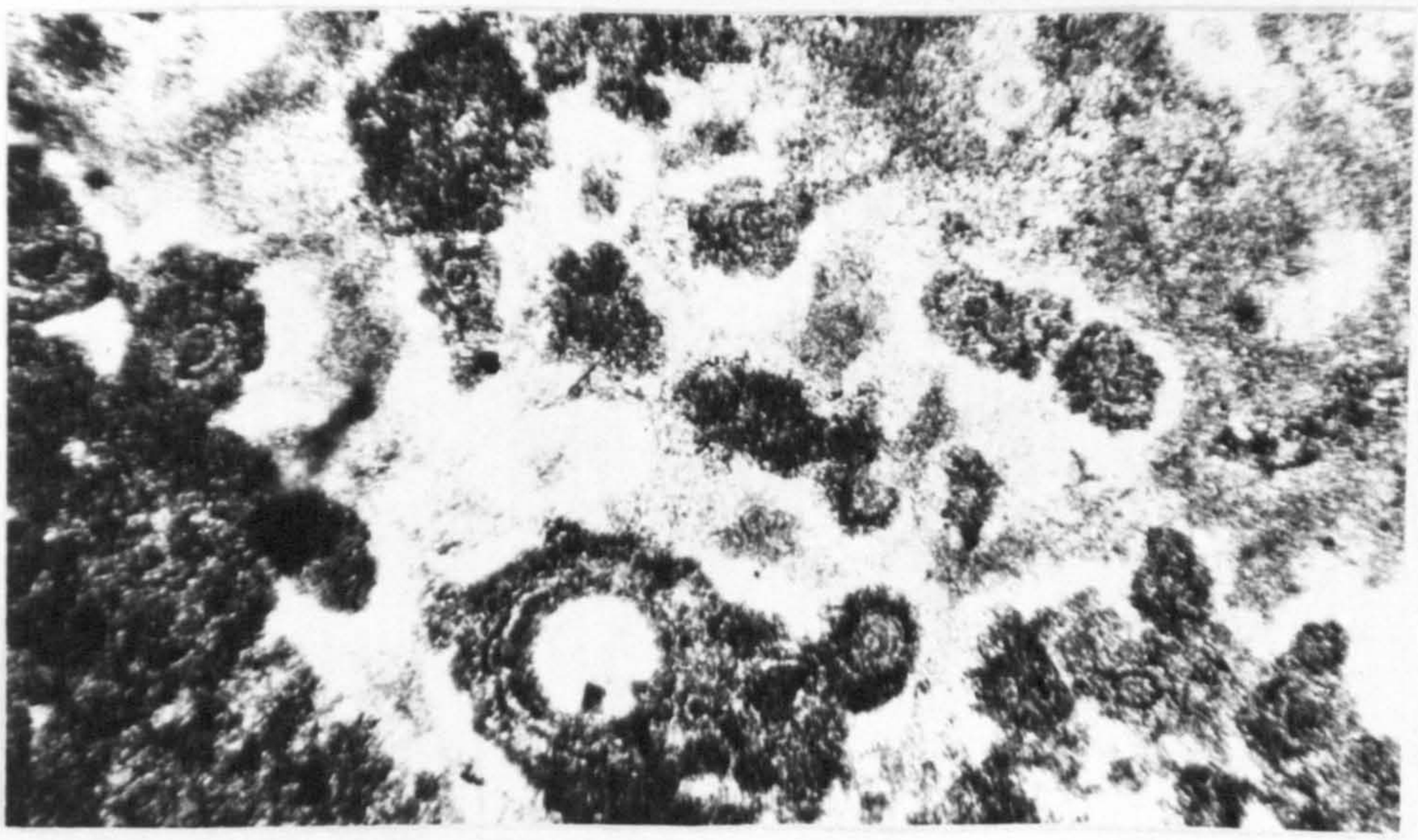

c

1mm.
0

PLATE 12·2

EXPLANATION OF PLATE 12.3

CHERTY ROCK CALICHE

A. Caliche forming around a detrital quartz nucleus. The indurated caliche matrix has been replaced by chert. Crossed nicols.

B. Friable caliche illustrating replacement of detrital quartz and recrystallisation to sparite grade calcite in the matrix. Crossed nicols.

C. Diagenetic quartz zone of the caliche illustrating quartz overgrowths around the detrital quartz. The contact between the original quartz and the overgrowth is represented by a thin film of iron oxide. Crossed nicols.

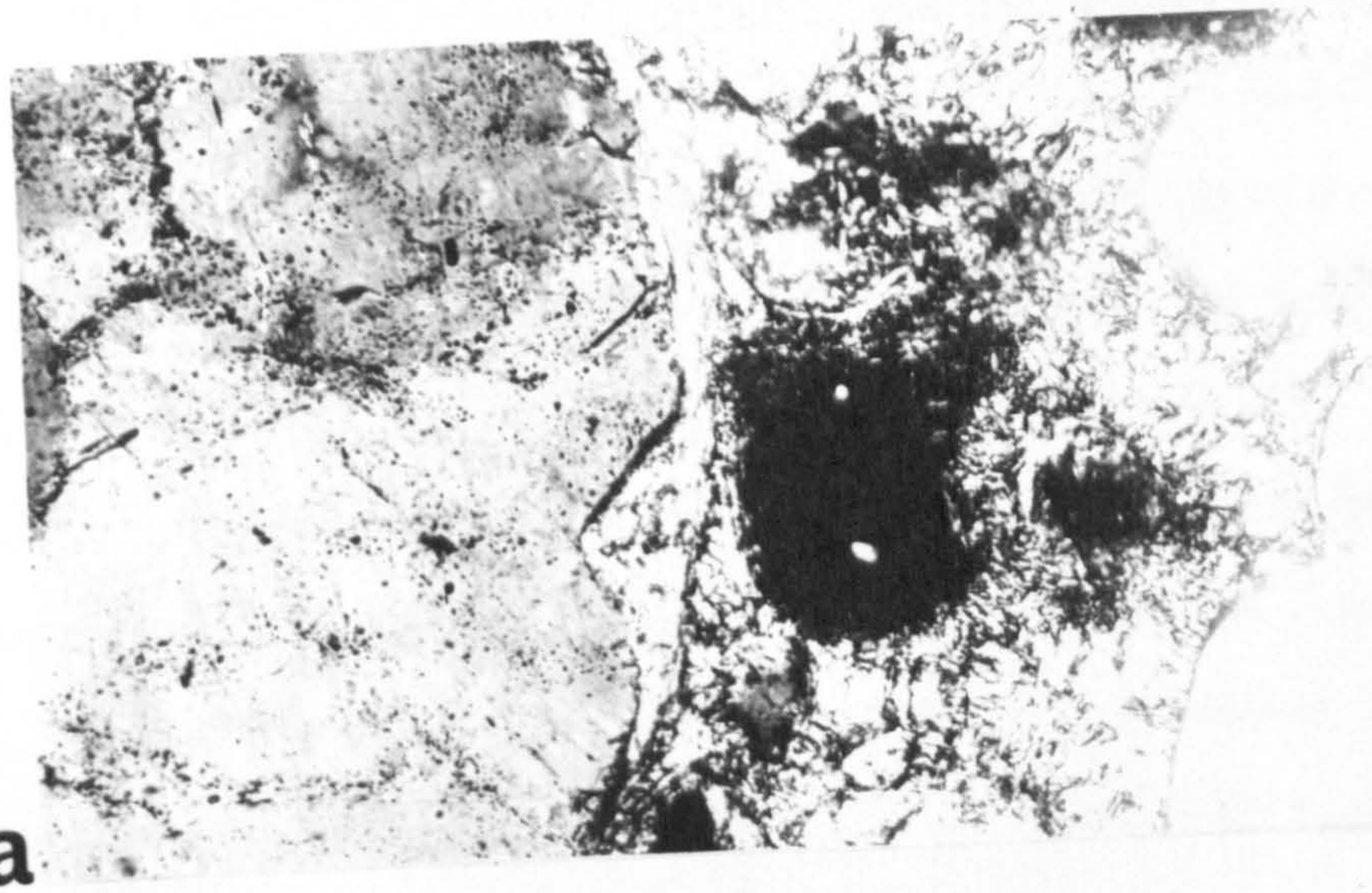

a

0·5mm.

0

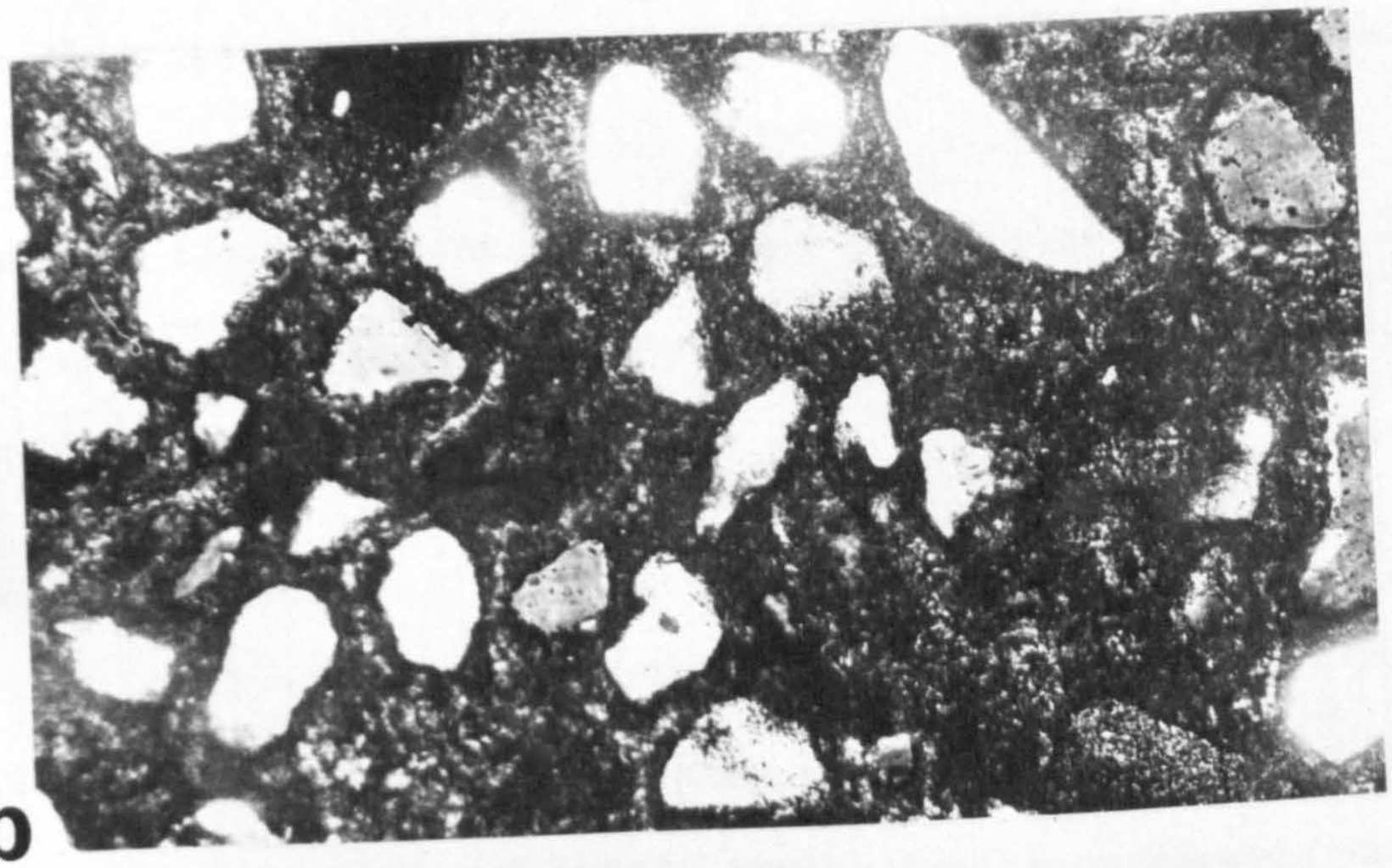

b

1mm.

0

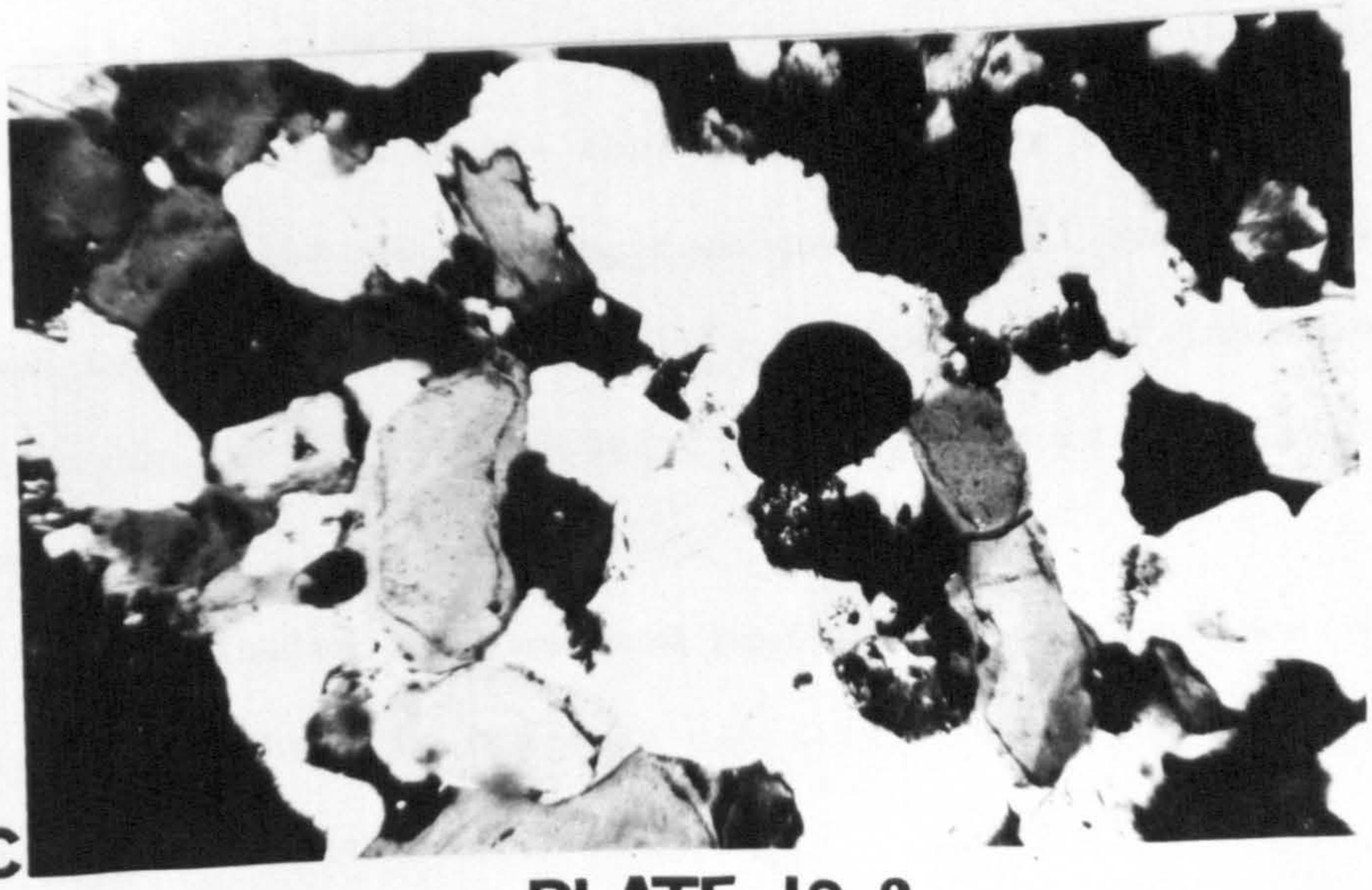

c

1mm.

0

PLATE 12·3

grains have been removed in solution. This is supported by work on the scanning electron microscope which has shown that the detrital quartz exhibit various types of solution features on their periphery (Plate 12.1A and 12.1B). Small fractures within the groundmass cause the micrite grade calcite to recrystallise to sparry calcite (Plate 12.2A). On the periphery of some of the detrital grains, a "skin" of caliche sometimes forms, this possibly representing the initial stages of concretion formation (Plate 12.3A).

Another characteristic feature of the horizon is the presence of horizontally laminated, microcrystalline calcite; this appears to represent precipitation of calcite along horizontal fractures. The calcite is often darker than the surrounding calcite, a feature which may be due to a concentration of iron or organic compounds. Pseudo-oolitic structures often occur between the laminated horizons but are more frequently found in cavities. The structures are thought to represent sections through botryoidal cavity infill (Plates 12.2B and 12.2C).

2. Friable caliche

Friable caliche is typically a white, light green or pink limestone in hand specimen, with quartz grains embedded into the friable matrix (Plate 12.3B). The percentage of quartz grains increases towards the base of the horizon until the limestone could be more aptly designated a calcareous sandstone. This horizon does not show so much silica replacement as the previous horizon, most of the chert being confined to small areas, giving the rock a honeycomb texture. This may be due to replacement of indurated caliche nodules in the more friable matrix. Vein quartz is also present in vertical fractures.

Laminated horizons and pseudo-oolitic structures are absent in the friable caliche. In the thin sections, the micritic calcite matrix is less dense and the detrital grains are floating in the groundmass, i.e. rarely are there any grain contacts. The contact between the matrix and the detrital

grains is marked by the occurrence of rhombic sparry calcite around the periphery of the grain. The quartz grains frequently have an etched and frosted appearance suggesting that they have been replaced by the matrix.

The clastic grains are similar to those in the underlying sandstones (Sago Pudding Sandstone, Lossiemouth Sandstones and Burghead Beds) although heavy minerals are rare; when present, they are normally zircon with occasional apatite or tourmaline. Microcline is the only common clastic grain other than quartz.

At the present day much of the microcrystalline calcite has recrystallised owing to later fracturing of the caliche.

3. Zone of diagenetic quartz

The lowest horizon is characterised by sandstones with quartz overgrowths. The sandstones are often red due to an iron oxide pellicle between the detrital quartz grain and the secondary overgrowth. Although the sandstones in fact represent the uppermost parts of the Burghead Beds, Sago Pudding Sandstone and the Lossiemouth Sandstones, the zone was silicified during formation of the caliche and is therefore included as one of the caliche zones.

Measurement of vertical successions at Spynie, Inverugie and Lossiemouth indicates that the percentage of quartz overgrowths decreases away from the Cherty Rock. At Spynie, sandstone immediately below the friable caliche are characterised by quartz overgrowths occupying 35 per cent of the total rock volume (Fig. 12.2). This amount steadily decreases away from the Cherty Rock, till at a depth of 15 metres below, the overgrowths occupy only 5 per cent of the total rock volume. At Inverugie, the percentage of overgrowths decreases to 5 per cent within 4 metres of the friable caliche. Although no vertical successions can be measured at Lossiemouth, the upper part of the Lossiemouth Sandstone and the Sago Pudding Sandstone are highly silicified whereas towards the base of the Lossiemouth Sandstone, the sandstones become increasingly cemented by calcite.

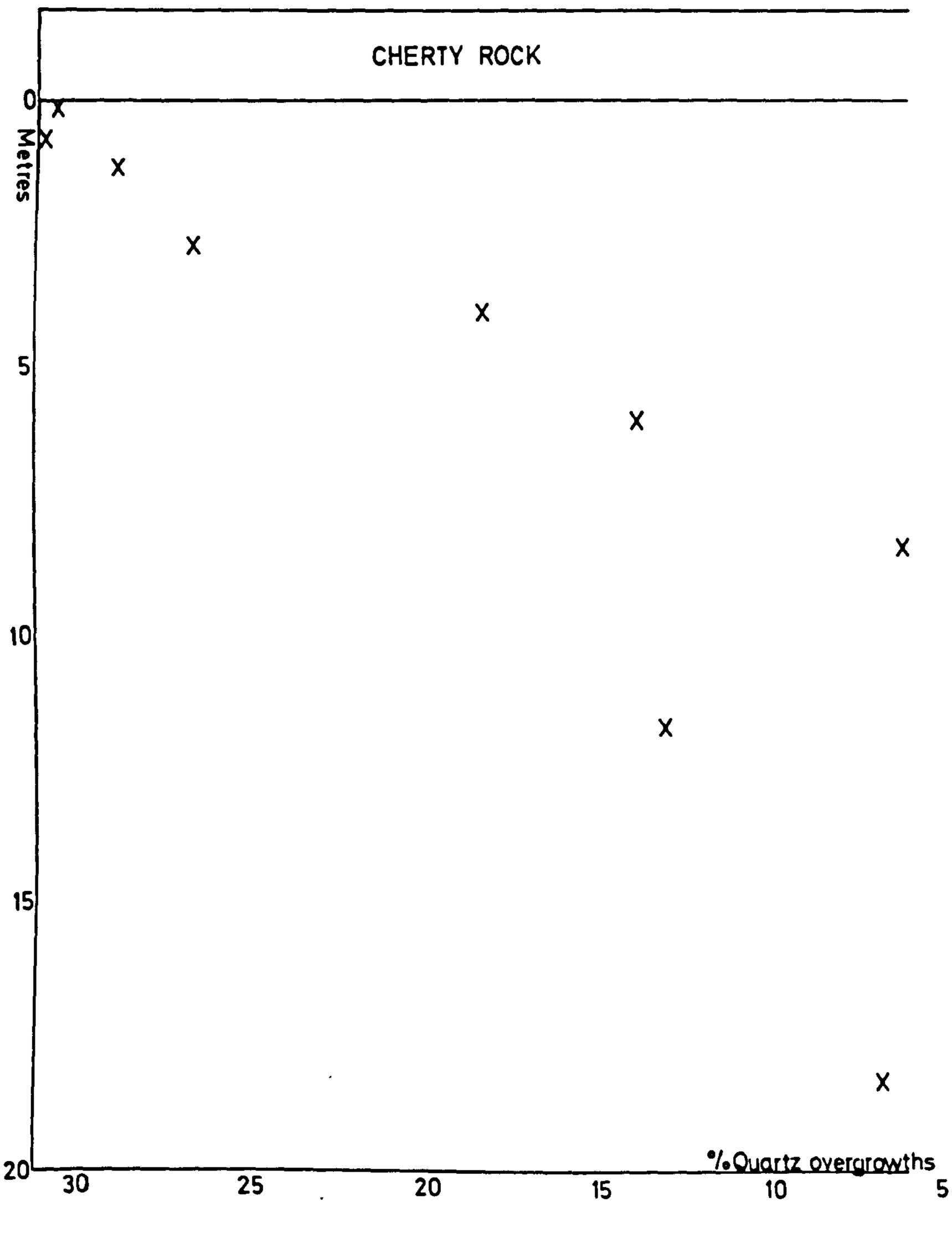

Fig. 12.2. Decrease in quartz overgrowths away from the Chert Rock with depth, Spynie Quarry.

The early diagenetic nature of the overgrowths is seen by the presence of calcium carbonate along the boundary of the detrital quartz and the secondary overgrowth. Zonal alternations of micritic calcite and quartz within multiple quartz overgrowths indicates that percolating solutions carrying calcium carbonate were present during the period of quartz overgrowth formation. They probably represent temperature inversions or changes in pH during deposition of the silica.

Where concretions of micritic calcite are present, there are little or no overgrowths around the detrital grains compared to the normal highly silicified sandstones (Plate 12.3C).

FORMATION OF MODERN DAY CALICHE

Brown (1956, p.14) concluded that caliche horizons were the "result of long continued soil processes operating in an aeolian aggrading profile". Calcium carbonate and silica gel are leached downwards to form a Cca horizon (caliche) of extremely pure calcium carbonate and silica. Reeves (1970) describes the ideal environment for the formation of caliche as, sufficient water to provide more than a superficial accumulation of carbonate, but not an excess, as this will cause leaching of the soluble material. Arkley (in Reeves, 1970) suggests that caliche generally forms in areas with a rainfall of 25 inches or more in a hot climate but may form in areas with less than 25 inches provided the rain is concentrated in a cool period. Carbonates are dissolved from the overlying soils by carbonic acid, produced by the mixing of rainfall with carbon dioxide from the atmosphere and the soil. The alkaline nature of the solutions allows supersaturation of silica in the form of H_4SiO_4 at the expense of carbonates, thus explaining the absence of chert and opal in the upper parts of the caliche.

The parent caliche appears to be similar to the friable caliche zone where the clastic grains "float" in a groundmass of calcium carbonate powder, Reeves (1970) suggests that all other types of caliche horizons can

be derived from this parent caliche by plugging of the profile, repeated exposure of the upper horizons and solution of the various clastic materials. He suggest that the transition from young to old caliche involves alteration of a small percentage of the quartz grains and considerable weathering of the alumino-silicates. Silica held in solution is deposited at the base of the profile as amorphous silica or as overgrowths around detrital quartz. An old caliche can thus be recognised by the presence of a diagenetic quartz zone.

The uppermost horizon of the caliche, the indurated caliche horizon, is the youngest part of the profile and is characterised by a hard flinty limestone with laminated and pseudo-oolitic structures. Reeves (1970) demonstrates that the induration in this horizon is due to repeated long exposure coupled with multiple plugging, solution and redeposition. This exposure causes repeated desiccation, which accounts for the many horizontal and vertical fractures in this horizon. Small fractures can be recognised by recrystallisation of the micrite to sparry calcite but the larger horizontal fractures are infilled by percolating solutions and produce the laminated bands and botryoidal cavity infill. The vertical fractures tend to be largest and thus frequently remain open or become infilled by soil. Detrital quartz is almost absent from this horizon owing to the removal by the highly alkaline nature of the percolating solutions.

Friable caliche horizons show no induration between the carbonate powder and the residual parent material purely because they have not been exposed to repeated desiccation and multiple plugging. The downward increase in detrital quartz probably indicates that there is a decrease in pH towards the base of the profile. Reeves also showed that when further infiltration of water occurs, solution and redeposition of the existing calcareous powder produces small nodules of indurated caliche producing a honeycomb texture of indurated and friable caliche. In the case of the Cherty Rock, the indurated caliche is normally replaced by chert producing a honeycomb of friable caliche and chert.

Precipitation of silica in the diagenetic quartz zone occurs where there is a lowering of the pH. In the case of the Cherty Rock, this appears to have occurred where the percolating solutions met stagnant water held in the voids of the underlying sandstones. Once established, the zone of diagenetic quartz would plug the horizon producing an automatic decrease in pH. This explains the decrease in quartz overgrowths with depth.

It can therefore be concluded that the various features present in the Cherty Rock indicate that it was originally a caliche horizon.

ORIGIN OF THE CALCIUM CARBONATE IN CALICHE SOILS

The origin of calcium carbonate in caliche soils is generally accepted to be from loess (Reeves, 1970; Aristarain, 1970; Brown, 1956). Caliche horizons are formed on the downwind side of the world's major deserts, this fact supporting the aeolian derivation. Studies of the carbonate content of the aeolian dust around New Mexico (Ruhe, 1967 in Reeves, 1970) indicate that between 16-31 tons of carbonate per acre have fallen during the past 10,000 years and that 30 per cent of this amount may have been trapped. The evaporitic carbonates of Permo-Triassic age of the Elgin Basin could provide a possible source of calcite in the Cherty Rock caliche. Walker (1967) notes that calcium carbonate can also be formed by intra-stratal solution of iron silicates and feldspars although the insignificant amount of these minerals in the parent material would suggest that th~~ey~~ is ~~were~~ was only a minor process.

SOLUTION AND PRECIPITATION OF THE SiO_2 IN THE CALICHE

Precipitation and solution of silica is determined by changes in temperature, pressure, partial pressure of carbon dioxide, but mainly by the pH (Krauskopf, 1959). Krauskopf also demonstrated that there was a marked increase in solution of silica above a pH of 9. As the solution and depositional properties of silica and calcite are reciprocal, Reeves (1970) suggested that the formation of massive caliche was formed simply due to the fluctuation of

temperature. However, Arkley (in Reeves, 1970) showed that soil is a very complex organic and mineral material, and that the kinetics of pure silica solutions simply did not apply. He suggested that the pH would remain fairly constant around 8.2 due to the depletion of carbon dioxide by calcium bicarbonate buffering. Parry and Reeves (1968) have noted that in the High Plains of New Mexico, the caliche soils are rich in illite and montmorillonite and thus a high pH could be created by cation exchange and subsequent release of silica in the clay size fractions. It is also interesting to note that Darragh et al (1966) obtained 80 p.p.m. silica in relatively stagnant environments in the Australian opal fields due to silica liberated from ferromagnesian minerals, kaolinised feldspars and solution of detrital quartz. It would therefore seem that a high pH is not necessary and that high concentrations of silica can form under other conditions.

It is however suggested that the source of the silica in the Cherty Rock caliche is due to liberation of silica from clays, feldspars, ferromagnesian minerals and solution of quartz grains. In the upper parts of the caliche, a pH of 9 or more is probably necessary to produce solution of silica and deposition of calcite. In the lower parts of the profile, the pH is probably closer to 8 as suggested by Arkley (in Reeves, 1970). This is indicated by the zonal nature of the micrite and quartz in the multiple quartz overgrowths. This would suggest that the pH was critical. Minor fluctuation in temperature and the amount of water in the caliche would cause the critical pH value of 8 to produce alternate solution and deposition of silica and calcite.

CHAPTER 13

DIAGENESIS AND MINERALISATION IN THE ELGIN NEW RED SANDSTONE

Diagenesis and mineralisation in the Elgin New Red Sandstones are intimately related with the result that many of the fabrics are highly complex and exceedingly difficult to interpret. The various fabrics transgress lithological boundaries and for this reason, these topics are dealt with together in a single chapter.

The most interesting feature of these sandstones are the various cementing agents, their origin and relationship to each other. Dunham (1952) has reviewed the petrography and distribution of the fluorite cemented Hopeman Sandstone, while Peacock (1968) recognised barytes, fluorite, silica, calcite, pyrite and haematite cements and gave a brief petrographical description of many of the sandstones. However, neither of these authors has discussed the depositional conditions of the various cements, with the result that no firm conclusions regarding the age and origin of the various phenomena have been made. It is the author's intention to discuss the many replacement features and the distribution of the various mineral cements in order to achieve some insight into the chronology of diagenesis and mineralisation events.

The result of the author's studies has been the recognition of many different fabrics (Fig. 13.1) which can be divided into the following four main stages of diagenesis and later mineralisation:

1. Diagenesis prior to the development of the caliche (Cherty Rock).
2. Diagenesis during the early stages of caliche development.
3. Diagenesis during the late stages of caliche development.
4. Post caliche diagenesis and silica-calcite-galena-haematite mineralisation.

The evidence for the various stages is discussed in the relevant sections.

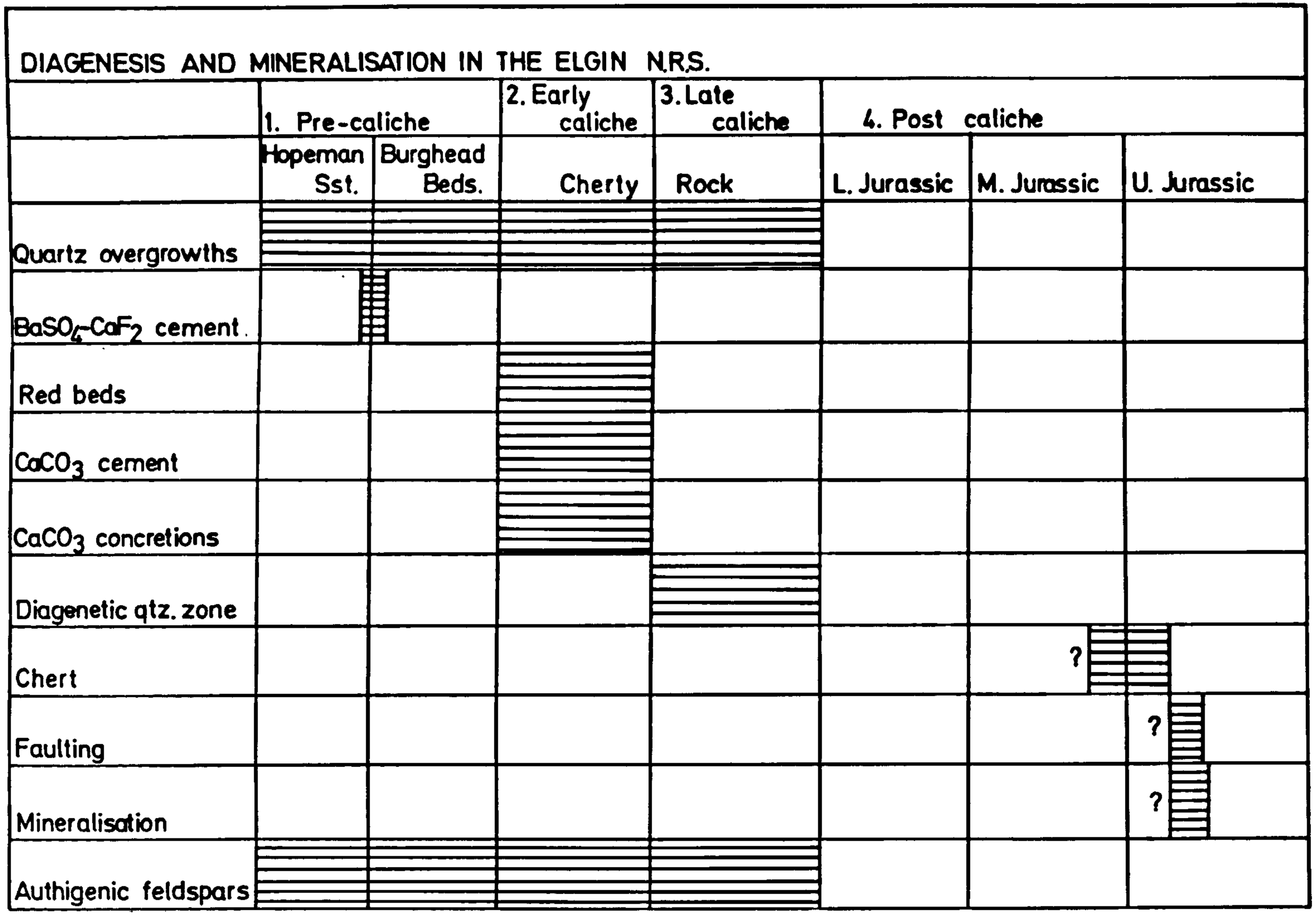

Fig. 13.1. Diagenesis and mineralisation in the Elgin New Red Sandstone.

1. DIAGENESIS PRIOR TO CALICHE DEVELOPMENT

Diagenesis prior to caliche development is defined as the period of time between the beginning of Hopeman Sandstone deposition and the end of the Sago Pudding Sandstone. In practice, the stage can be recognised by the various minerals which are being replaced by the calcite cement and caliche which were developed during the early stages of caliche development.

Fig. 13.1 shows that three main events can be recognised in this stage:

(a) Introduction of fluorite and barytes into the Hopeman Sandstone.

(b) Secondary quartz overgrowths.

(c) Authigenic feldspars.

The evidence for this stage is related to a calcite cemented sandstone (Concretionary Sandstone of Peacock, 1968) which will be shown to have been formed during the early stages of caliche development in the Hopeman Sandstone. Peacock (1968) noted that the distribution of fluorite was independent of the calcite cemented Hopeman Sandstones which occurred on the foreshore north of Greenbrae Quarry (13876955). He also noted that fracture zones infilled by fluorite cut both the fluorite and calcite cemented sandstones and therefore suggested that there were two different stages of fluorite deposition (it will be shown in the next section that the barytes and fluorite are intimately related and clearly deposited at the same time, so all references to stages of fluorite of deposition also relate to barytes), pre-calcite deposition and post-calcite deposition. A later section shows that remobilisation of the fluorite occurred during the post caliche mineralisation so the second stage in this case is therefore synonymous with the late stage mineralisation. It can therefore be concluded that fluorite and barytes cemented sandstones were developed prior to the caliche.

Similarly, the calcite cemented sandstones at this locality are also seen to replace secondary quartz overgrowths (plate 13.1C) and authigenic feldspars in the Hopeman Sandstones. These events are therefore also pre-caliche in origin.

(a) Distribution and origin of the fluorite and barytes cement

Peacock (1968) identified two main areas of fluorite and barytes in the Elgin area. The first occurred as cements in the Hopeman Sandstone, with other minor occurrences in the Lossiemouth and Sago Pudding Sandstones. However, in the case of the latter two horizons, there is no evidence of replacement of the secondary quartz overgrowths, the fluorite and barytes normally being exposed along joint surfaces and in pore spaces between the overgrowths (Plates, 13.4C and 13.6A). As the quartz overgrowths in the Sago Pudding Sandstone and the Lossiemouth Sandstones were formed during the late stages of caliche development (see later section), it is reasonable to assume that the fluorite in the sandstones is due to remobilisation during the late mineralisation stage (Plates 13.4C and 13.6A). Pre-caliche fluorite and barytes is therefore only present as a cementing material in the Hopeman Sandstone(Plates 13.4A and 13.4B).

The total absence of fluorite and barytes cements in the Lossiemouth Sandstones and the Burghead Beds and its presence in the H4 phase of the Hopeman Sandstone suggests that they were introduced during the period between the end of the Hopeman Sandstone and the beginning of the Burghead Beds. However, it has already been shown in Chapter 3 that there was probably no break in sedimentation between the two horizons. It is therefore probable that the mineralising fluids were introduced during the early stages of the Burghead Beds deposition when the wet fluviatile deposits would prove an unfavourable horizon for the introduction of fluorite and barytes compared to the aeolian sandstones.

In hand specimens, the fluorite is patchily developed giving the rock a spotted appearance upon weathering; a honeycomb texture is developed due to the weathering out of the non cemented part of the sandstone. The barytes either occurs as poikilitic cements, infillings along contemporaneous fractures or rarely as a homogeneous cement (Plate 13.4A).

The distribution of the fluorite and barytes in the Hopeman Sandstone has long been a problem (Elgin memoir, Fig. 14, p.55) but the subdivision of the Hopeman Sandstone and the recognition of primary and remobilised phases of fluorite and barytes has shed some light on the problem. The fluorite cemented sandstones are well developed at Greenbrae Quarry, Masonshaugh Quarry and along the foreshore between these quarries. Here, they cement dune sandstones of the H4, H3 and the top of the H2 phase of the Hopeman Sandstone. From the foreshore north of Greenbrae Quarry to the harbour at Hopeman, reefs and nodules of both barytes and fluorite are found as discrete units occupying the top of the H2 phases. The mineralisation appears to be controlled to a certain extent by later features suggesting that in part, the fluorite and barytes has been remobilised. From the harbour to the foreshore north of Clashach Quarry, the fluorite and barytes appears to have been channelled along the top of the H2 phase and the basal unit of the H3 phase. Barytes also occurs as nodules and veins in the contorted dunes of the H1 phase and the base of the H2 phase between Sir Roberts Stables and Covesea Lighthouse.

Three main zones of fluorite and barytes cementing the Hopeman Sandstone can therefore be recognised: (a) Fluorite zone, (b) Barytes and fluorite zone, and (c) Barytes zone. In the west, the sandstones are dominantly cemented by fluorite whereas to the east, they are mainly cemented by barytes. Fluorite also appears to be confined to the H3 and upper H2 phases whereas barytes is concentrated in the H1 and H2 phases. However, this may in part be due to the limited present day outcrop and the rapid thinning to the east.

The origin of the fluorite and barytes is a complex problem as there is little evidence of any method of introduction. Three main theories are put forward to explain their presence although the actual method may have been a combination of two or more suggestions.

<u>Theory 1 : Hydrothermal origin (Fig. 13.2)</u>

Fig. 13.3 (Gallagher, 1970) illustrates mineralisation in the Northern Highlands and particularly the frequent occurrence of both fluorite

THEORY 1

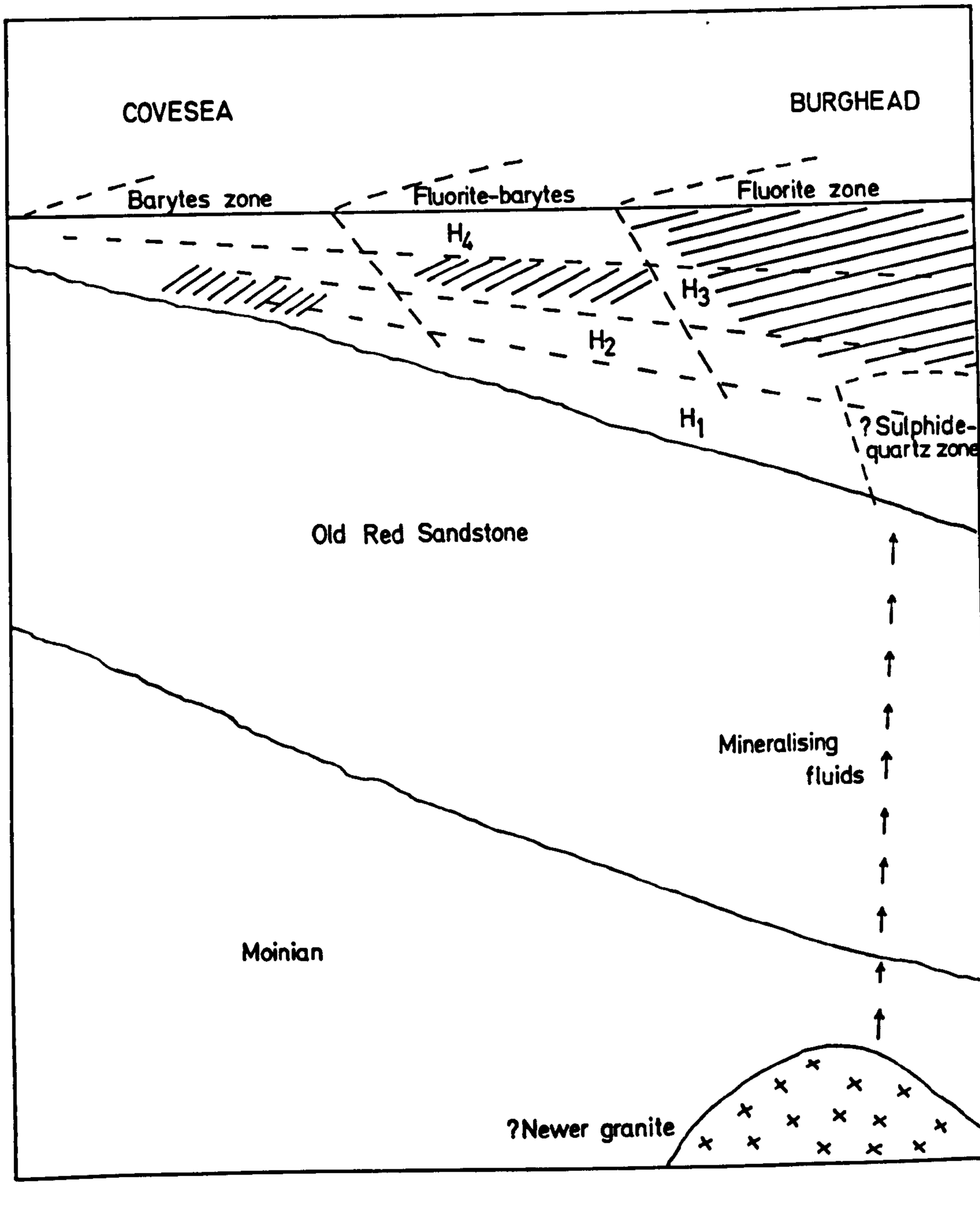

Fig. 13.2. Hydrothermal introduction of the fluorite and barytes into the Hopeman Sandstone.

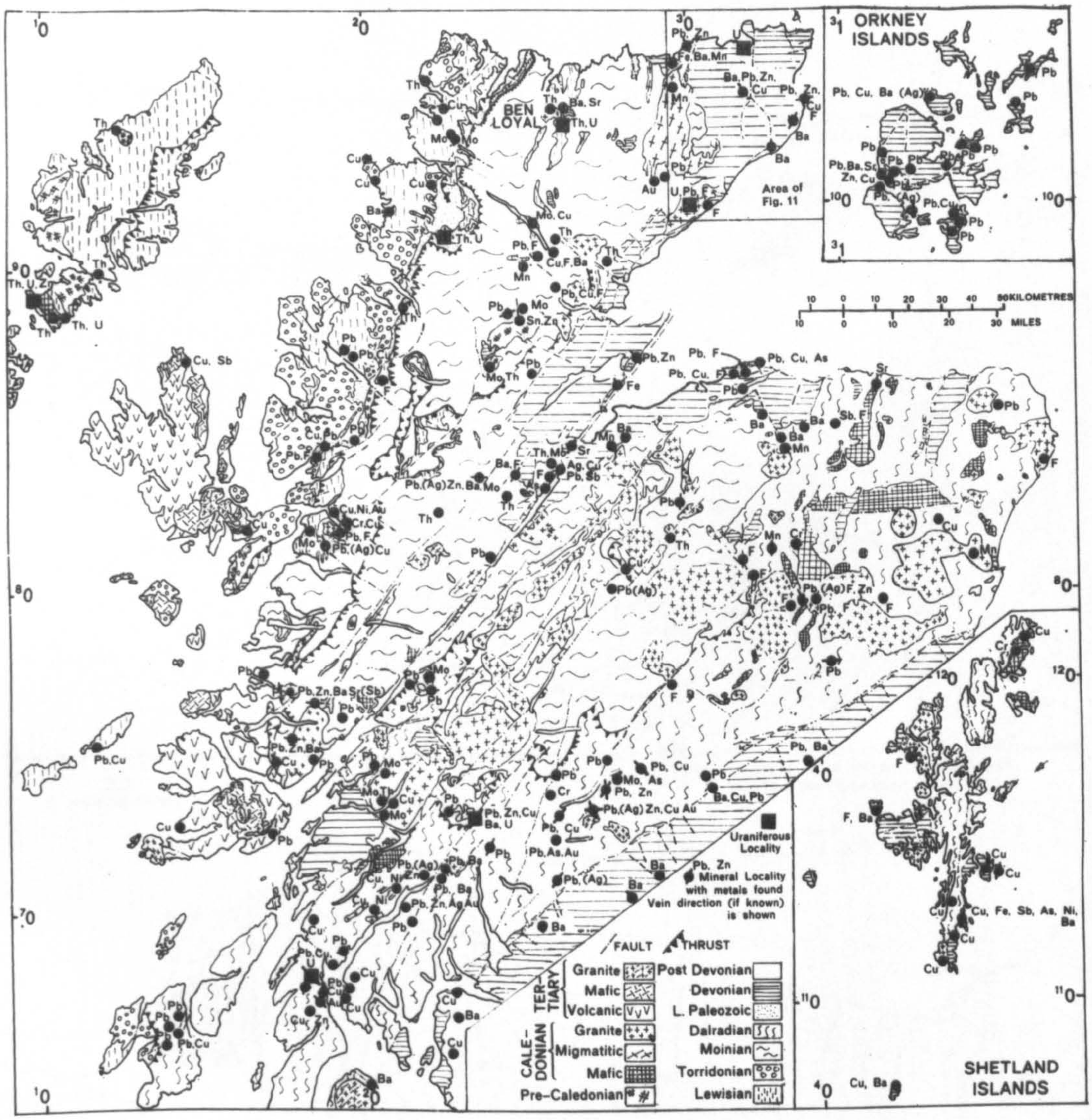

Fig. 13.3. Mineralisation in the Northern Highlands of Scotland (from Gallagher,1970).

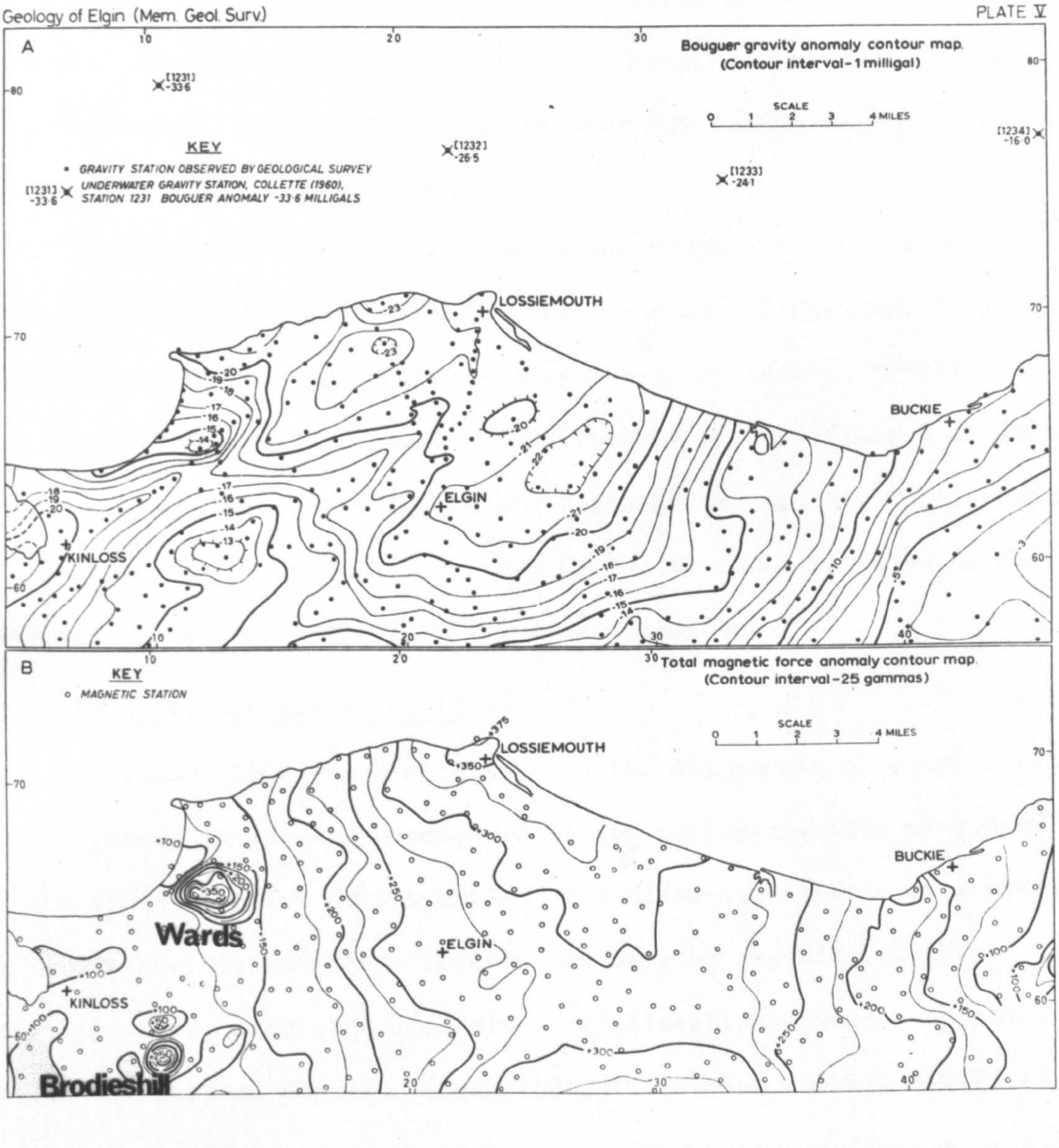

Fig. 13.4. Geophysical investigations in the Elgin district (from Fenning, 1968).

and barytes in the Moray Firth. Gallagher (1970) demonstrates that mineralisation in the Northern Highlands of Scotland is mainly limited to zones of transcurrent faulting and associated with granitic intrusions. Even in the case of the transcurrent faulting, the source is often the Newer Granites, as the minerals have been remobilised and introduced into the fault systems. Thus, the frequent occurrence of barytes and fluorite associated with the Newer Granites (Silurian or Devonian) as at Carn Chuinneag, Grudie and Helmsdale, (Gallagher, 1970; 1971) suggests they may have also been the original source of the Elgin fluorite and barytes.

Although there are no Newer Granites exposed in the Elgin district, two marked gravity and magnetic anomalies to the south of Burghead (Fig. 13.4) have been interpreted as deep seated igneous masses by Fenning (1968). Fig. 13.2 illustrates a hypothetical reconstruction of a possible hydrothermal source for the fluorite and barytes in the Elgin district. The later phase of mineralisation in the Jurassic may then be due to remobilisation of the higher temperature zones of the Triassic mineralisation.

Theory 2 : Evaporitic origin (Fig. 13.5)

Davidson (1964) suggested that in the diagenesis of evaporites, barium was released to local groundwaters on the anhydritisation of gypsum and again on the gypsificiation of anhydrite. The close association of evaporites with the occurrence of lead-zinc-fluorite and barytes deposits of the Mississippi type also suggested some close relationship between evaporites and fluorite and barytes deposits (Bush, 1971). However, Dunham (1966) thought that the amounts would be far too small and estimated that evaporites would only yield 2 p.p.m. of barium and 56 p.p.m. of fluorine upon total recrystallisation.

Bush (1971) suggests that the movement of groundwater is the result of evaporation caused by high daytime temperatures and that this evaporation concentrates the brines and subsequently lowers the water table. Brines enriched in base metals then migrate through the underlying rocks and become

THEORY 2

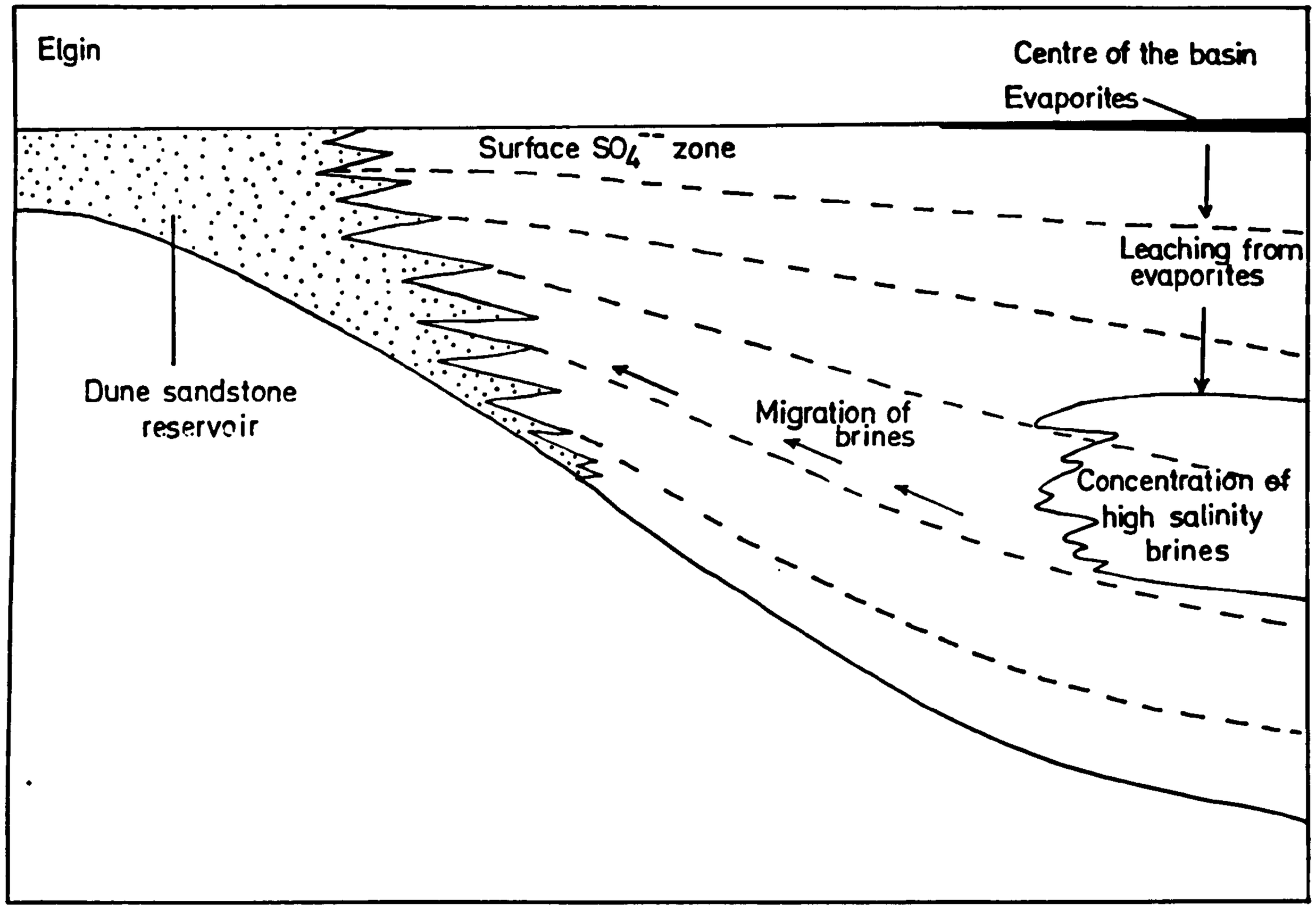

Fig. 13.5. Evaporites as the source of the fluorite and barytes cements in the Hopeman Sandstones.

trapped where further concentration and increase in salinity occurs. Associated sulphides could then be derived from the reaction between organic matter and anhydrite.

In the Elgin Basin, evaporites are present during the Zechstein and would provide a possible source for the fluorite and barytes. Burial and subsequent heating together with migration up dip to a higher level is possible, but the relatively low concentration of evaporites and lack of time would not make this a suitable theory in the case of the Elgin district.

Theory 3 : Deep formational water origin (Fig. 13.6)

Recent investigations of fluid inclusions in ore minerals suggests that the mineralising fluids are often more akin to brines of deep formational origin than to hydrothermal mineralising fluids. The theory that deep formational waters have been important as sources of mineralisation has been further strengthened by the discovery of recent brines capable of mineralisation in the Red Sea, Salton Sea and the Caspian Sea (Dunham, 1970).

The origin of these formation waters is extremely complex and multiple hypotheses regarding their source are unavoidable. The source may need the intervention of igneous activity, evaporites may or may not be a requisite, or the formation waters may originate in the ocean as meteoric waters. The various problems are adequately summed up in a recent review by Dunham, (1970). Suffice to say, concentration of buried brines have yielded concentrations of barium of 1550 p.p.m. and 1750 p.p.m. (White, Hem and Waring, 1957) indicating that these brines are capable of mineralisation.

In the case of fluorite and barytes, Dunham (1970) suggested that their precipitation yielded no problems, especially barytes, which would form on meeting the SO_4^- rich surface waters. The discovery of formation waters in the English Midlands (Llewellyn and Stubbins, 1968) and the North of England (Sawkins, 1966) similar to the composition of local mineralisation (Fluorite-barytes-galena-zincblende-chalcopyrites) favours the view that these deposits were formed by deep formation waters.

THEORY 3

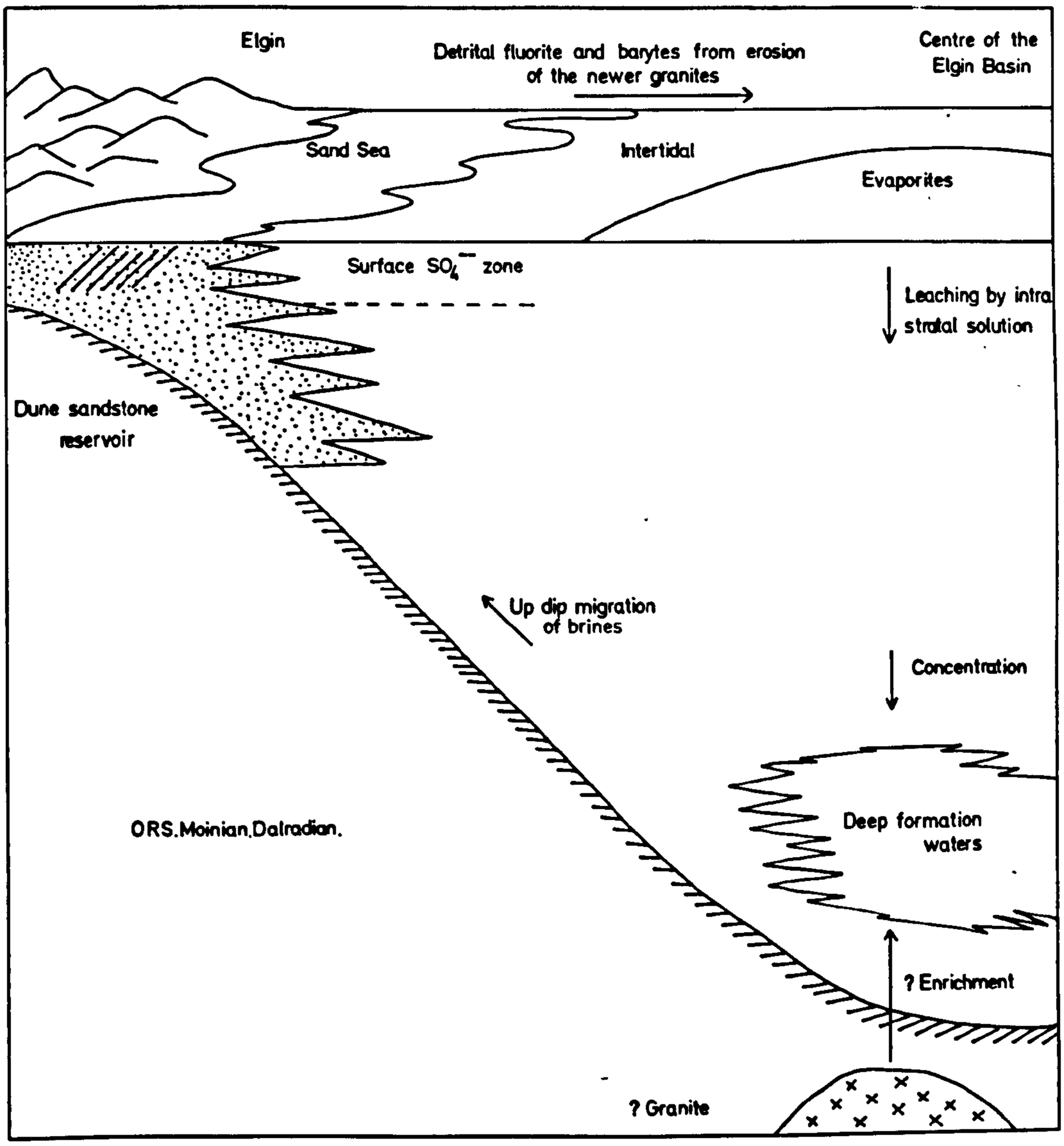

Fig. 13.6. Deep formation waters as the source of the fluorite and barytes cements in the Hopeman Sandstones.

In the case of the Elgin district, these deep formation waters may have migrated up dip from the centre of the basin or have been introduced along fault channelways; in either case, the dune sandstones would have provided an excellent reservoir. The source of the fluorite and barytes may however have been from either of the following sources:

(a) From the Newer Granites enriching the deep formation waters at depth.

(b) Erosion of pre-existing Newer Granites.

(c) Evaporites.

(d) A combination of two or more sources.

Whether the introduction of the fluorite and barytes was by the deep formation waters or the hydrothermal method, the most obvious original source is the Newer Granites.

(b) <u>Secondary quartz overgrowths</u>

Plate 13.1C illustrates a quartz overgrowth being replaced by the calcite cement which was formed during the early stages of caliche development, clearly indicating that quartz overgrowths were formed prior to the caliche. Quartz overgrowths also formed during the early late stages of caliche development and it is therefore difficult to distinguish between the various stages of quartz overgrowths. However in the late stages of caliche development, formation of quartz overgrowths appears to have been mainly confined to areas close to the caliche. Fig. 12.2 shows that the proportion of overgrowths decreased rapidly away from the Cherty Rock and it is therefore suggested that the Hopeman Sandstones was unaffected at this time. Similarly in the early stages of caliche development, the precipitation of calcite indicates unfavourable conditions for the precipitation of silica and it is more probable that solution of silica occurred at this period. It is suggested that most of the quartz overgrowths in the Hopeman Sandstone (with the exception of silica introduced along faults during later mineralisation) were developed during the pre-caliche period,

EXPLANATION OF PLATE 13.1

SECONDARY QUARTZ OVERGROWTHS

A. Pyramidical face of a secondary quartz overgrowth developed on a detrital unstrained quartz grain in the calcite cemented Hopeman Sandstone. Crossed nicols.

B. Prism faces of secondary quartz overgrowths developed on strained detrital quartz in the Hopeman Sandstone. Crossed nicols.

C. Bipyramidical faces developed as secondary overgrowths around a detrital quartz which is being replaced by calcite cement in the Hopeman Sandstone. Crossed nicols.

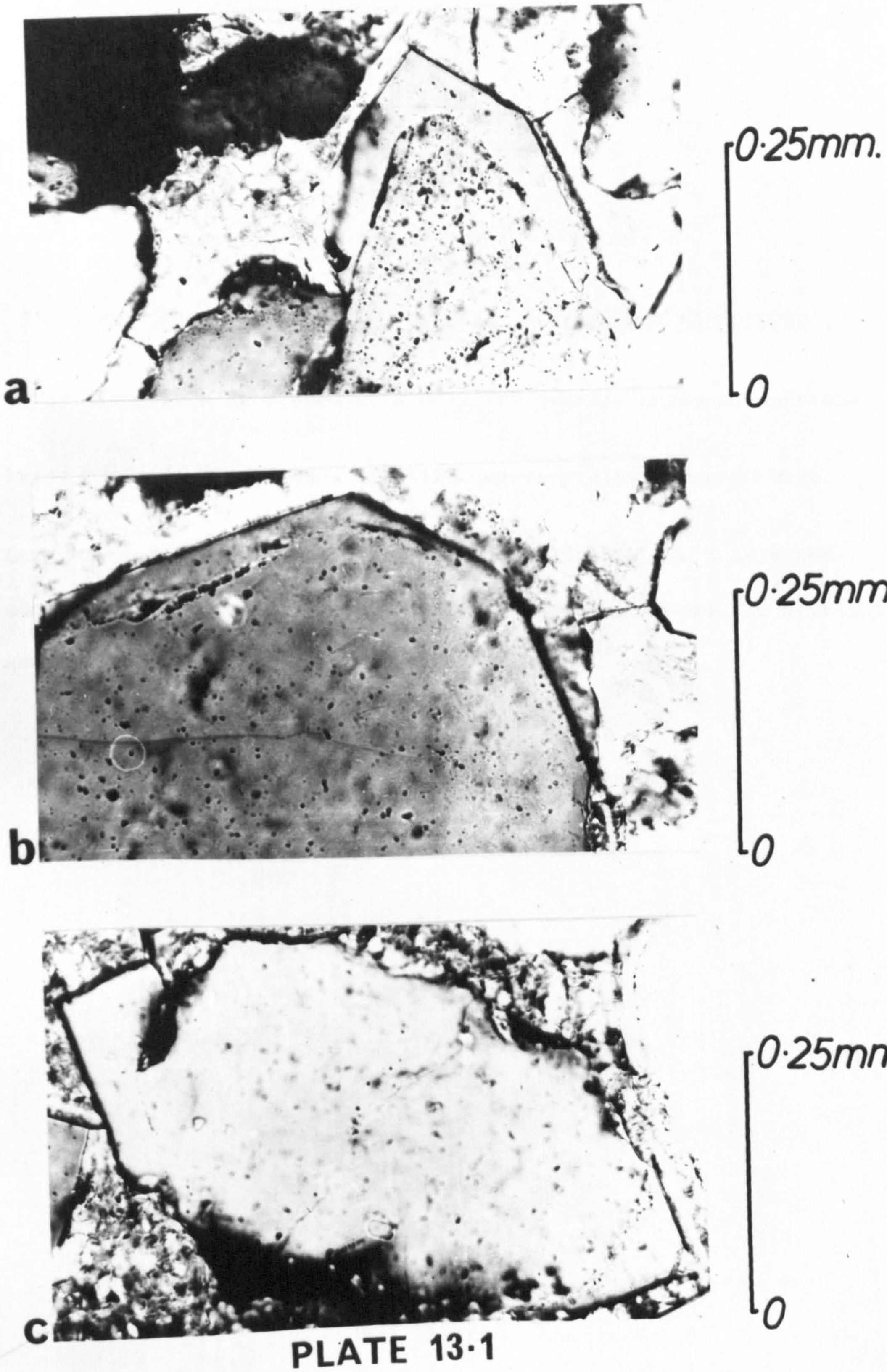

PLATE 13·1

EXPLANATION OF PLATE 13.2

SECONDARY QUARTZ OVERGROWTHS : SCANNING ELECTRON MICROSCOPE

A. Pyramidical face developed on a detrital quartz, Hopeman Sandstone.

B. Prism faces developed on a detrital quartz grain, Burghead Beds.

C. Several small quartz crystals growing parallel to the c axis and coalescing to form a secondary quartz overgrowth around the detrital quartz grain, Hopeman Sandstone.



PLATE 13·2

whereas in the Burghead Beds, Lossiemouth Sandstones and Sago Pudding Sandstones, most of the overgrowths are of the late caliche stage. The percentage of quartz overgrowths in the Hopeman Sandstone varies between 0-15 per cent but the distribution is completely random and no increase with depth is seen. However, coarse grained dune deposits and playa deposits do tend to have a higher percentage of overgrowths.

All stages in the formation of quartz overgrowths are seen in the Hopeman Sandstones although overgrowths are more pronounced on unimodal unstrained quartz as opposed to the strained and polycrystalline quartz. Both rhombohedral (Plates 13.1A and 13.1C) and prism faces (Plate 13.1B) are well developed although the rhombohedral faces are more common and preferentially developed. The various stages of development of the overgrowths as seen in Plate 13.2 follows that described by Waugh (1970, p.309), who stated that "Initial growth commences with the appearance of numerous oriented projections with rhombohedral and prismatic form on grain surfaces. Merging and overlap of the projections results in the formation of large crystal faces whose form is dependent on the initial location of the projections with respect to the internal crystallographic axes."

(c) Authigenic feldspars

There is also evidence of calcite cemented Hopeman Sandstone replacing authigenic feldspars although they were probably also developed during the formation of the caliche as well as prior to it. Plate 13.3 illustrates the typical habit of the overgrowths indicating that the overgrowths are optically continuous with the detrital grain. They show their best development on orthoclase feldspar although these tend to be the least common and most altered feldspar. Microcline also shows overgrowths but they are not so well developed.

In all cases, the overgrowths possess the adularia habit and, as in the case of quartz overgrowths, are better developed on the rhombohedral faces. Scanning electron micrographs illustrate their formation, (Plate 13.3C). Numerous oriented projections of minute (1-10 microns) adularia crystals

gradually coalesce to form larger crystals until the overgrowth produces a perfect overgrowth of adularia habit. The origin of the overgrowths is probably due to percolating solutions rich in potassium, sodium, aluminium and silica derived from the breakdown of pre-existing feldspars, clays, ferromagnesian minerals.

2. DIAGENESIS DURING THE EARLY STAGES OF CALICHE DEVELOPMENT

Diagenesis during the early stages of caliche development is defined as the period of time after deposition of the Sago Pudding Sandstone and prior to the development of the diagenetic quartz zone of the caliche profile. Three main fabrics were developed during this period:

(a) Friable and indurated zones of the caliche.

(b) Formation of iron oxide pellicles around the detrital grains in the diagenetic quartz zone.

(c) Formation of calcite cements in the Burghead Beds, Sago Pudding Sandstone, Hopeman Sandstone and Lossiemouth Sandstone.

The various fabrics can be placed in this stage as the formation of the diagenetic quartz zone in the late stages of caliche development effectively changes the diagenesis by plugging the horizon with the resulting barrier to percolating solutions. Thus, the diagenetic quartz zone preserves the iron pellicles by formation of overgrowths and stops effective downward percolation of calcium carbonate rich solutions. Although some redeposition of the underlying calcite cements may have occurred in the late stages, the source of the calcium carbonate had been effectively cut off.

(a) Friable and indurated caliche zones

The conditions prevalent during the early stages of caliche development have been discussed in Chapter 12 so only the essential points are included in this section. From their study of modern day caliche, Reeves (1970) and Aristarain (1970) demonstrate that the preliminary stages of caliche development are confined to the development of the friable caliche and also the indurated caliche, provided the profile is exposed.

EXPLANATION OF PLATE 13.3

AUTHIGENIC FELDSPARS

A. Secondary overgrowth in optical continuity with the detrital orthoclase feldspar, Hopeman Sandstone. Crossed nicols.

B. Authigenic feldspar with no evidence of a detrital nucleus.

C. Small feldspar crystals of adularia habit growing parallel to each other and making up part of a secondary overgrowth around a detrital orthoclase feldspar. Scanning electron microscope.

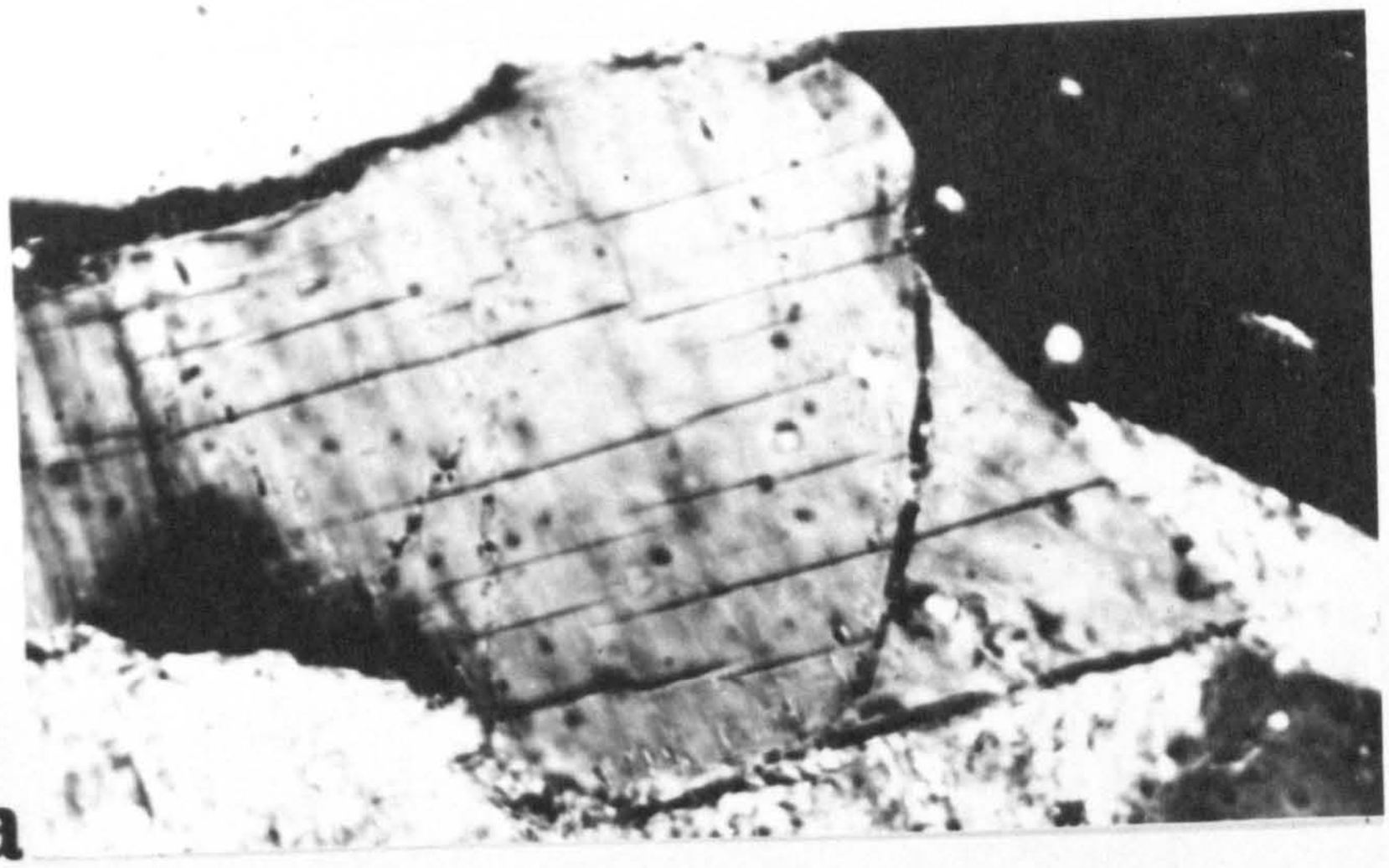

a

0·25mm.

0

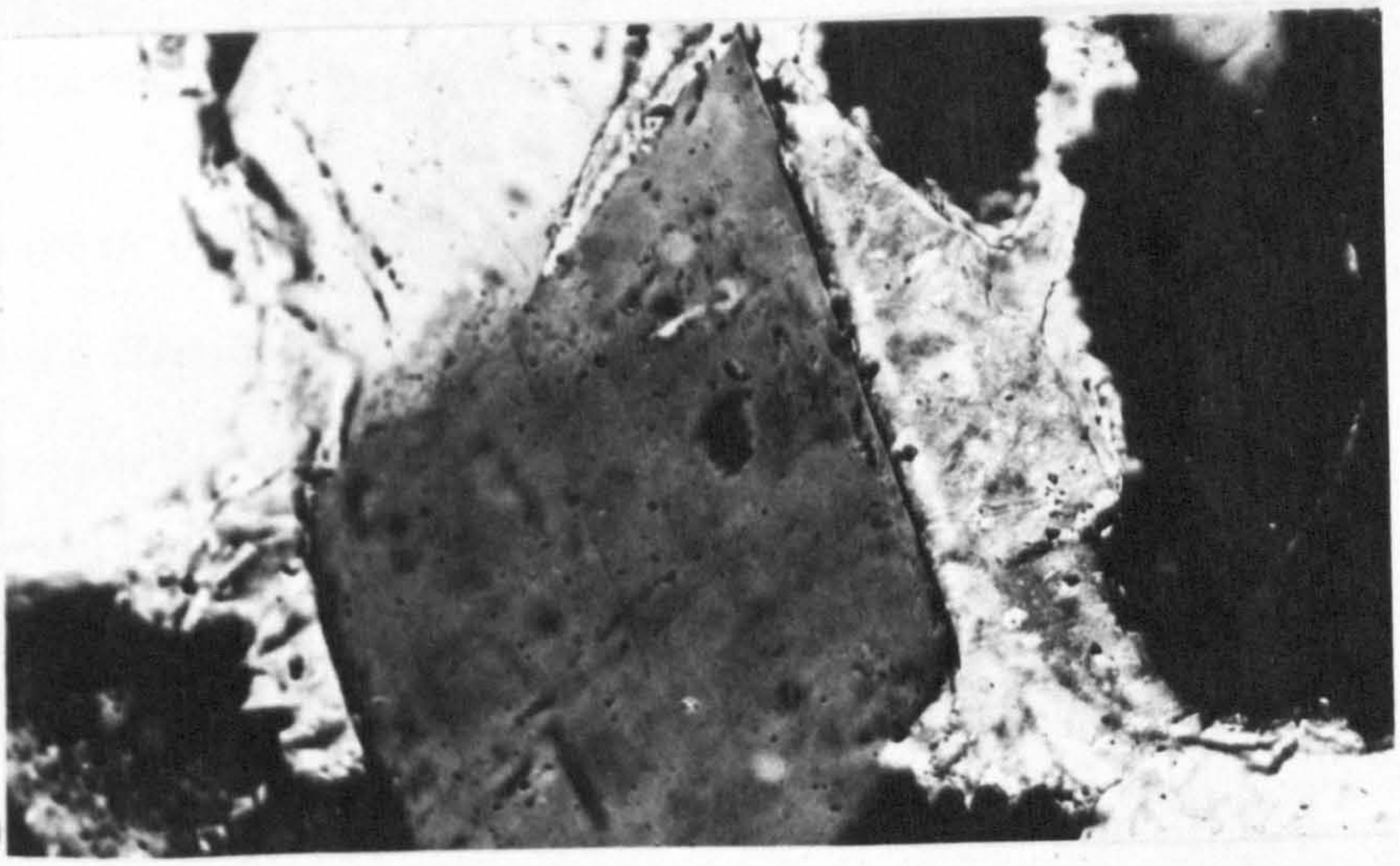

b

0·5mm.

0

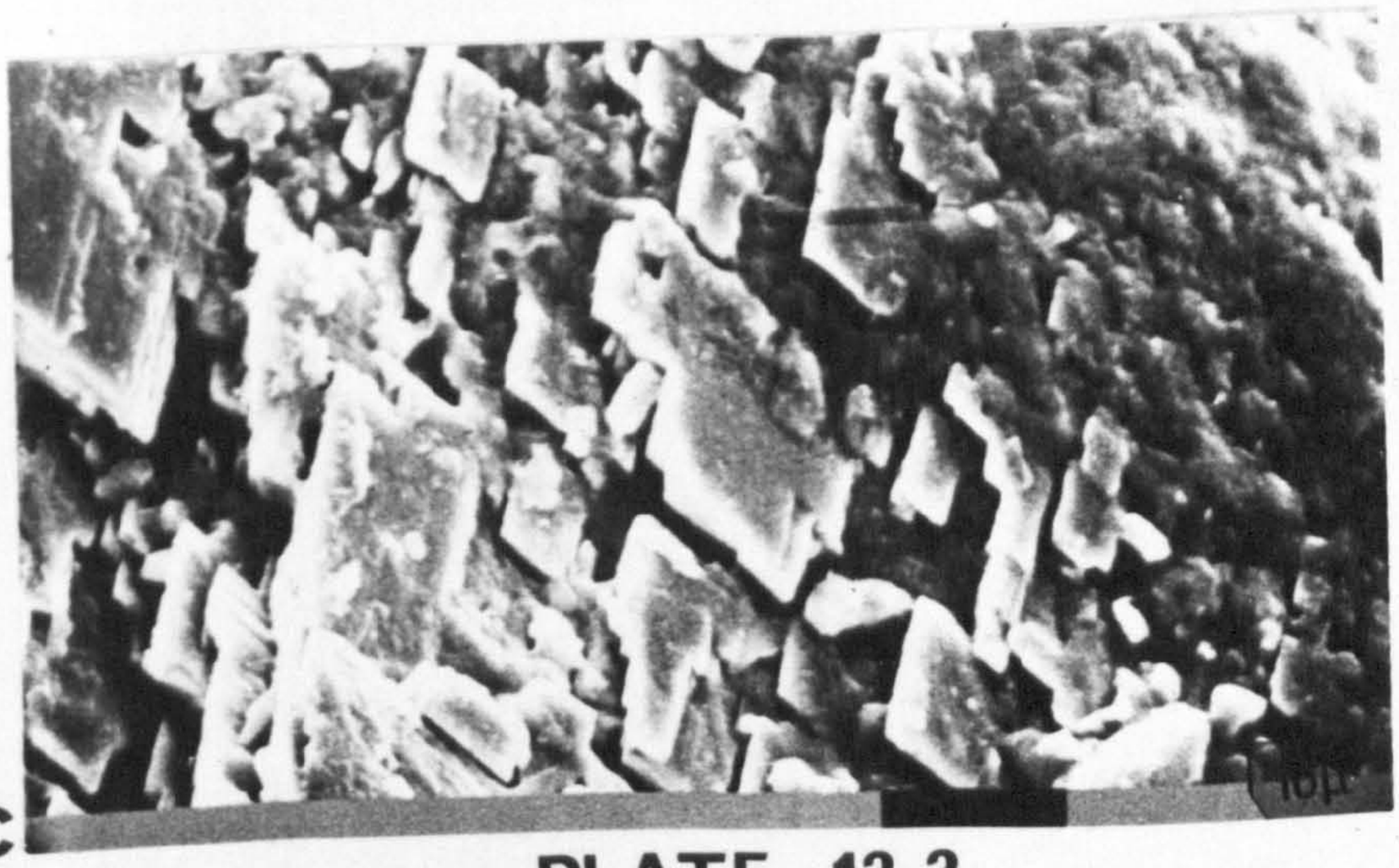

c

10μ

PLATE 13·3

EXPLANATION OF PLATE 13.4

FLUORITE AND BARYTES

A. Barytes cement replacing pre-caliche secondary quartz overgrowths in the Hopeman Sandstone. Crossed nicols.

B. Fluorite cement replacing pre-caliche secondary quartz overgrowths in the Hopeman Sandstone. Away from the fluorite cement, the overgrowths are complete. Plane polarised light.

C. Post-caliche fluorite in pore spaces between late caliche secondary quartz overgrowths in the Lossiemouth Sandstone. Plane polarised light.

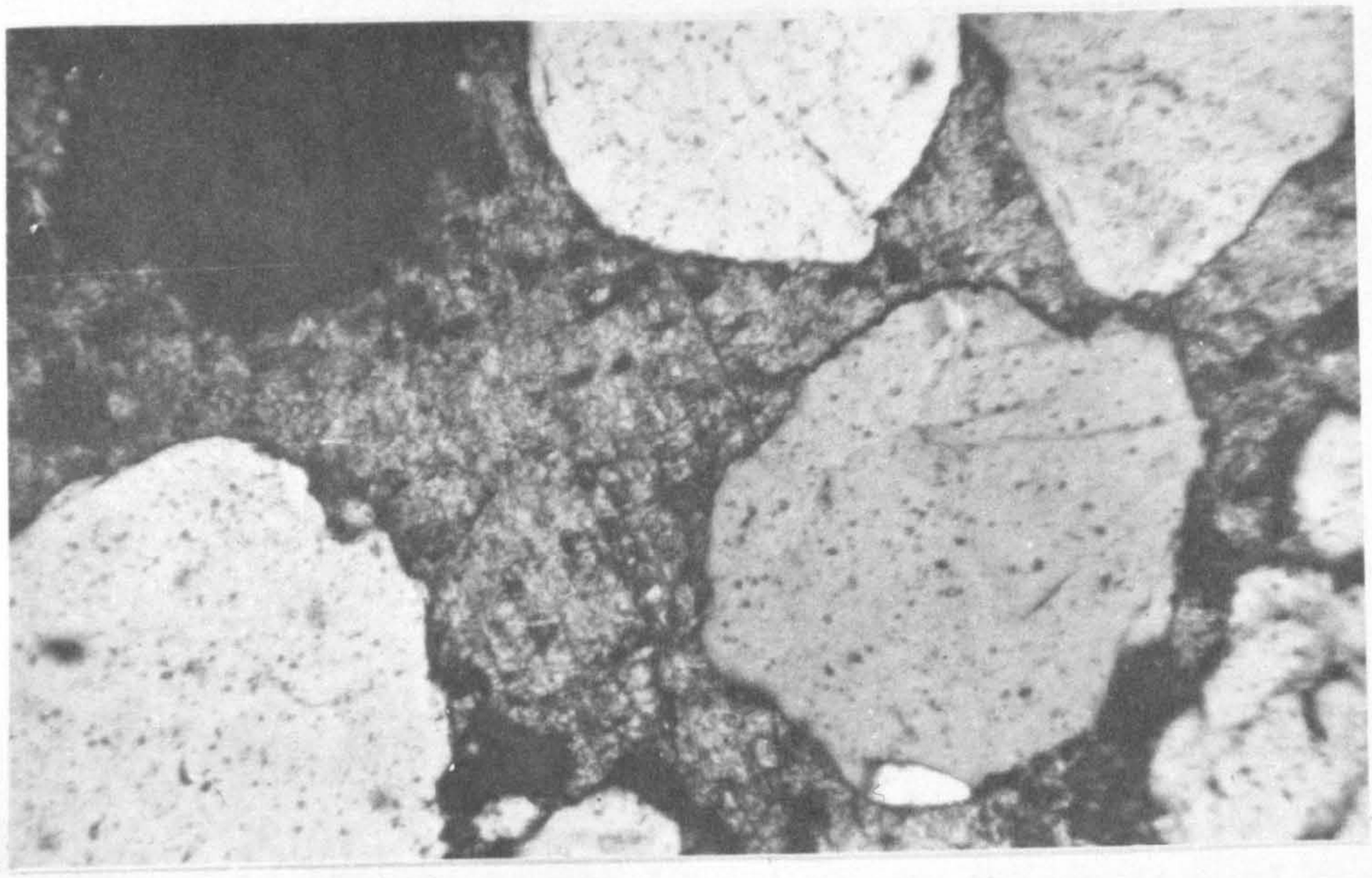

a

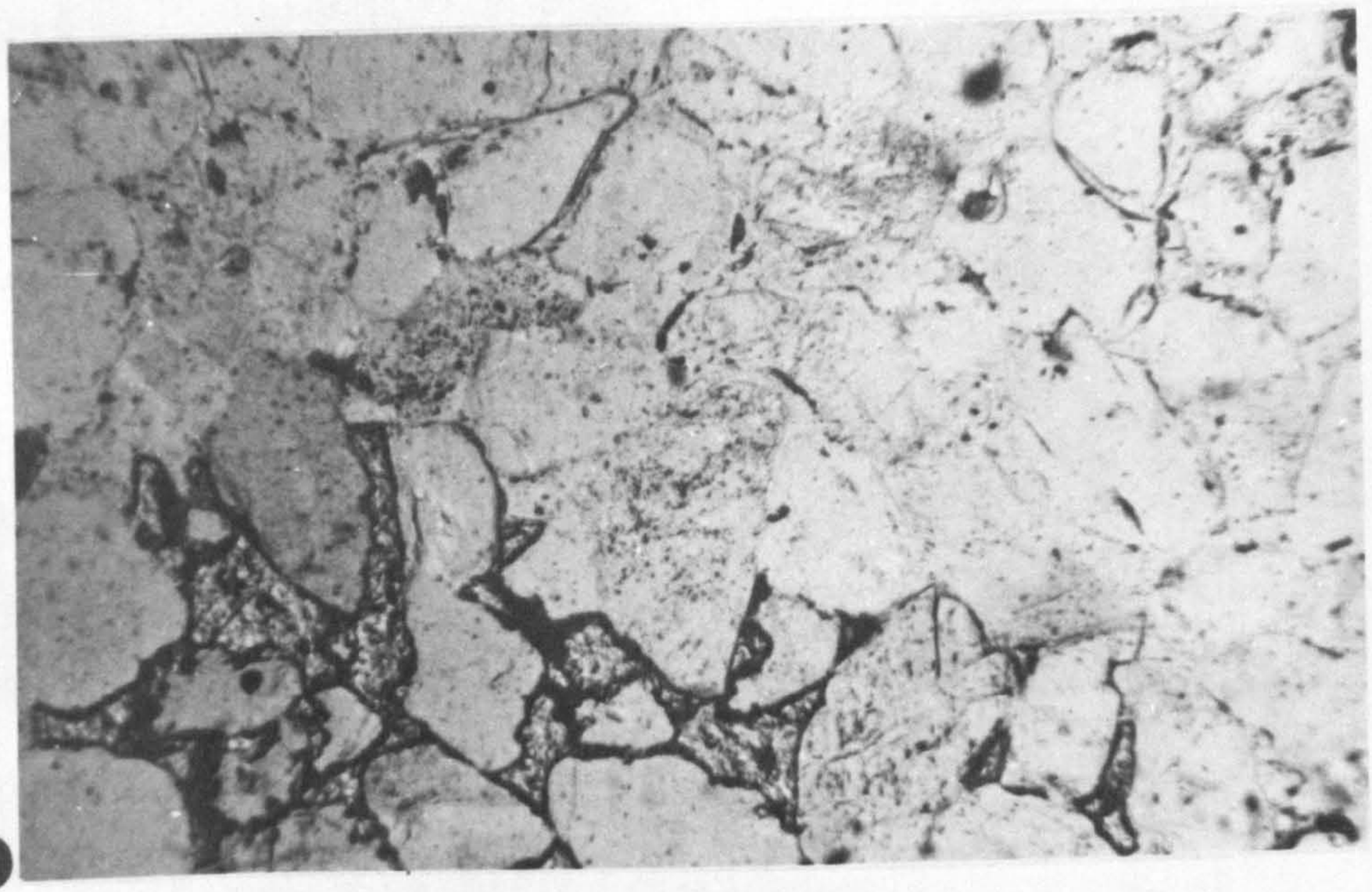

b

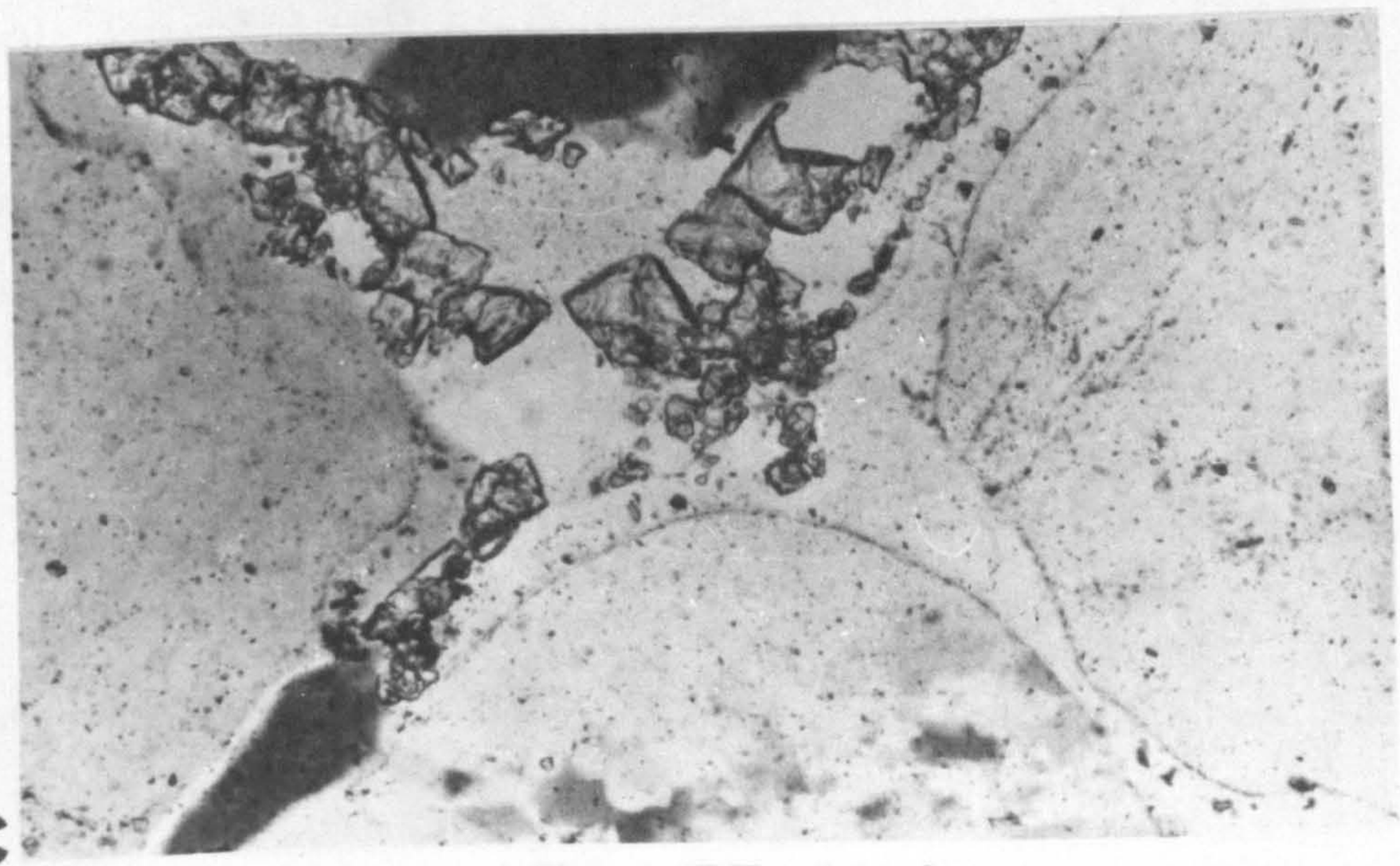

c

1mm.

0

PLATE 13·4

EXPLANATION OF PLATE 13.5

REPLACEMENT OF THE INDURATED CALICHE BY SILICA

A. Dolomite (clear) and calcite (grey) rhombs in a matrix of chert which has replaced the microcrystalline calcite groundmass. Plane polarised light.

B. Calcite rhombs in a chert matrix and chalcedony vugh infill. Scanning electron microscope.

C. Chert replacing the microcrystalline groundmass of the indurated caliche. The dark bands probably represent organic impurities from the original caliche. Pseudomorph after calcite is infilled by drusy quartz cavity infill. Crossed nicols.

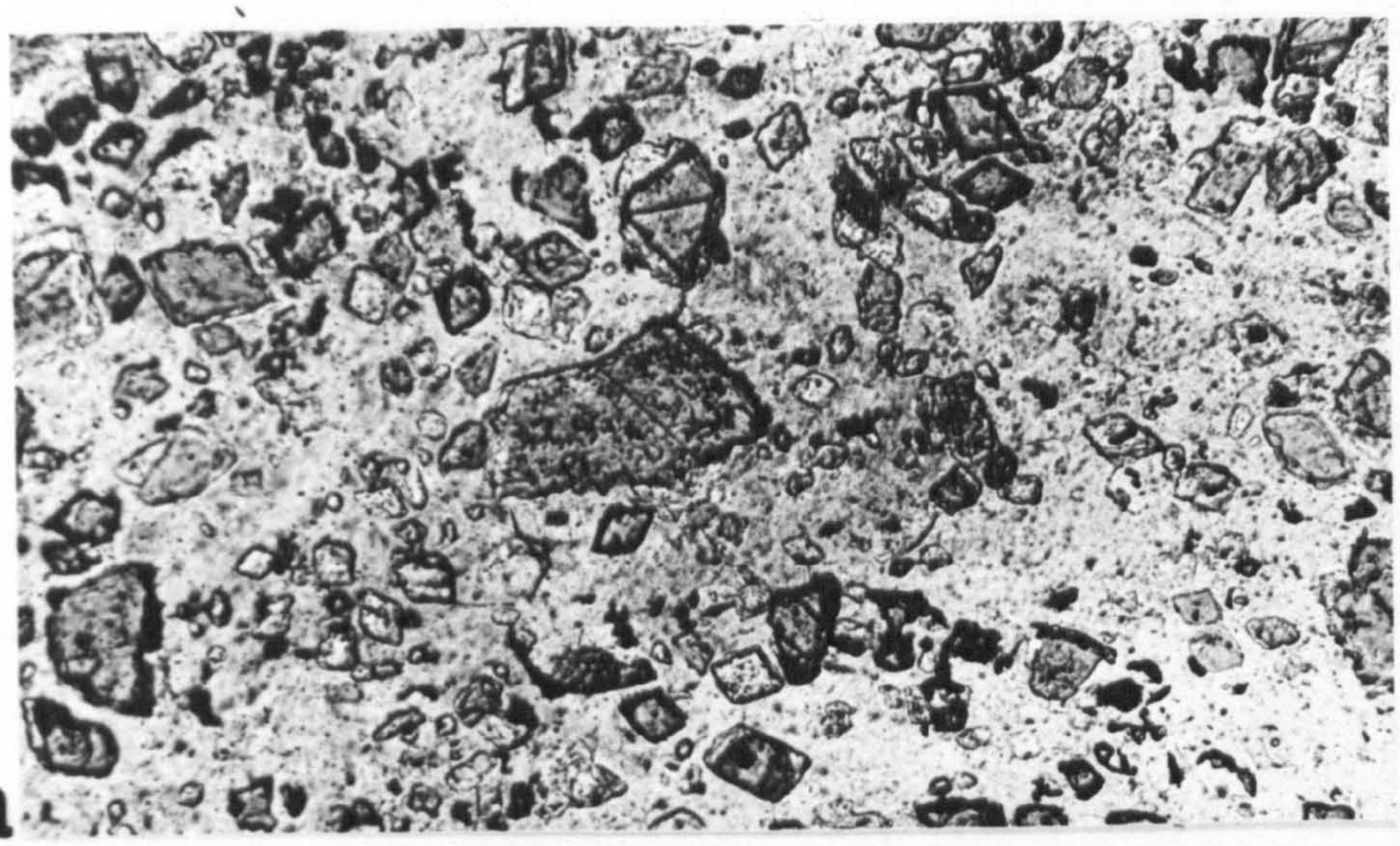

a

1mm.

0

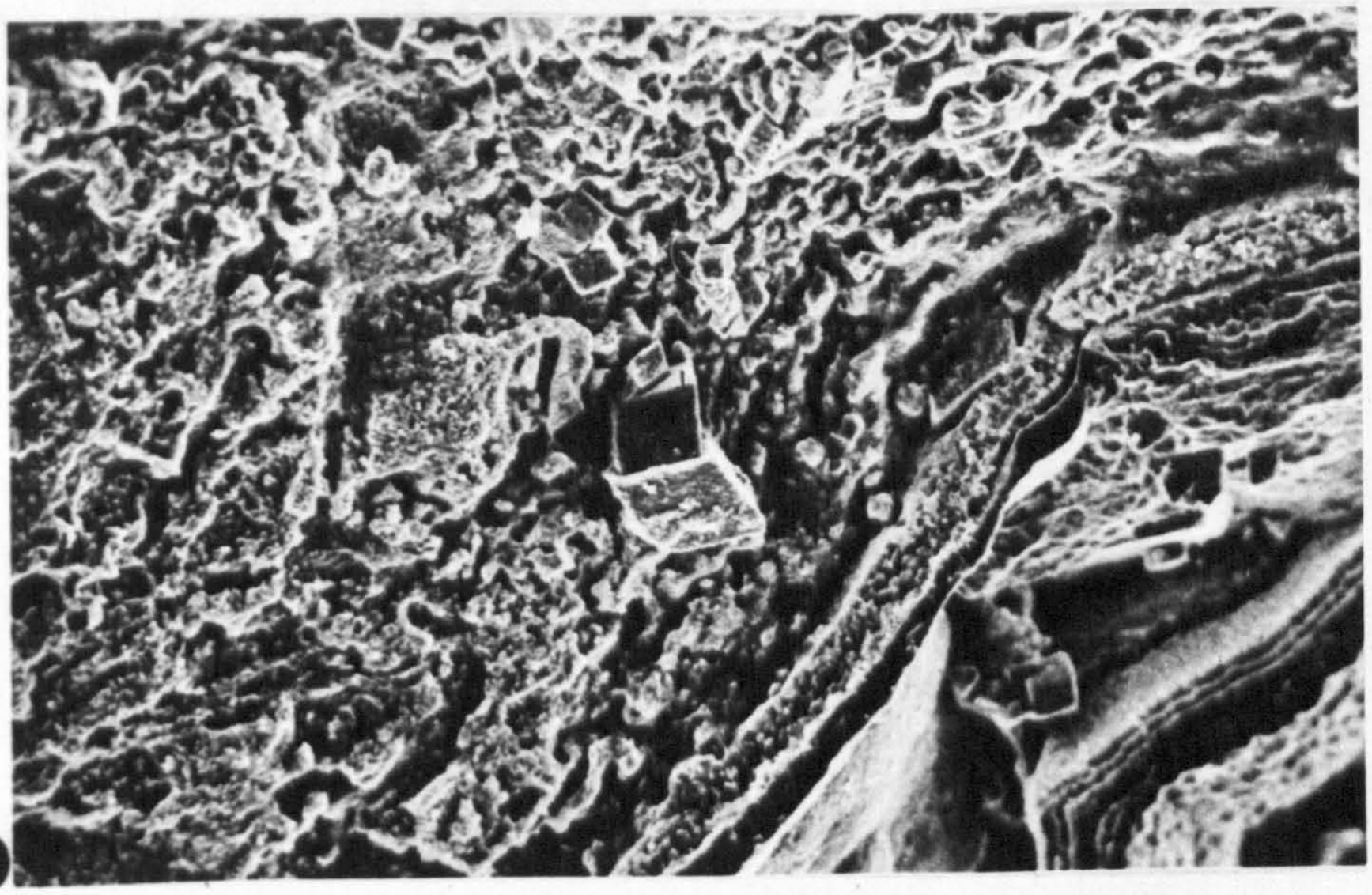

b

40μ

0

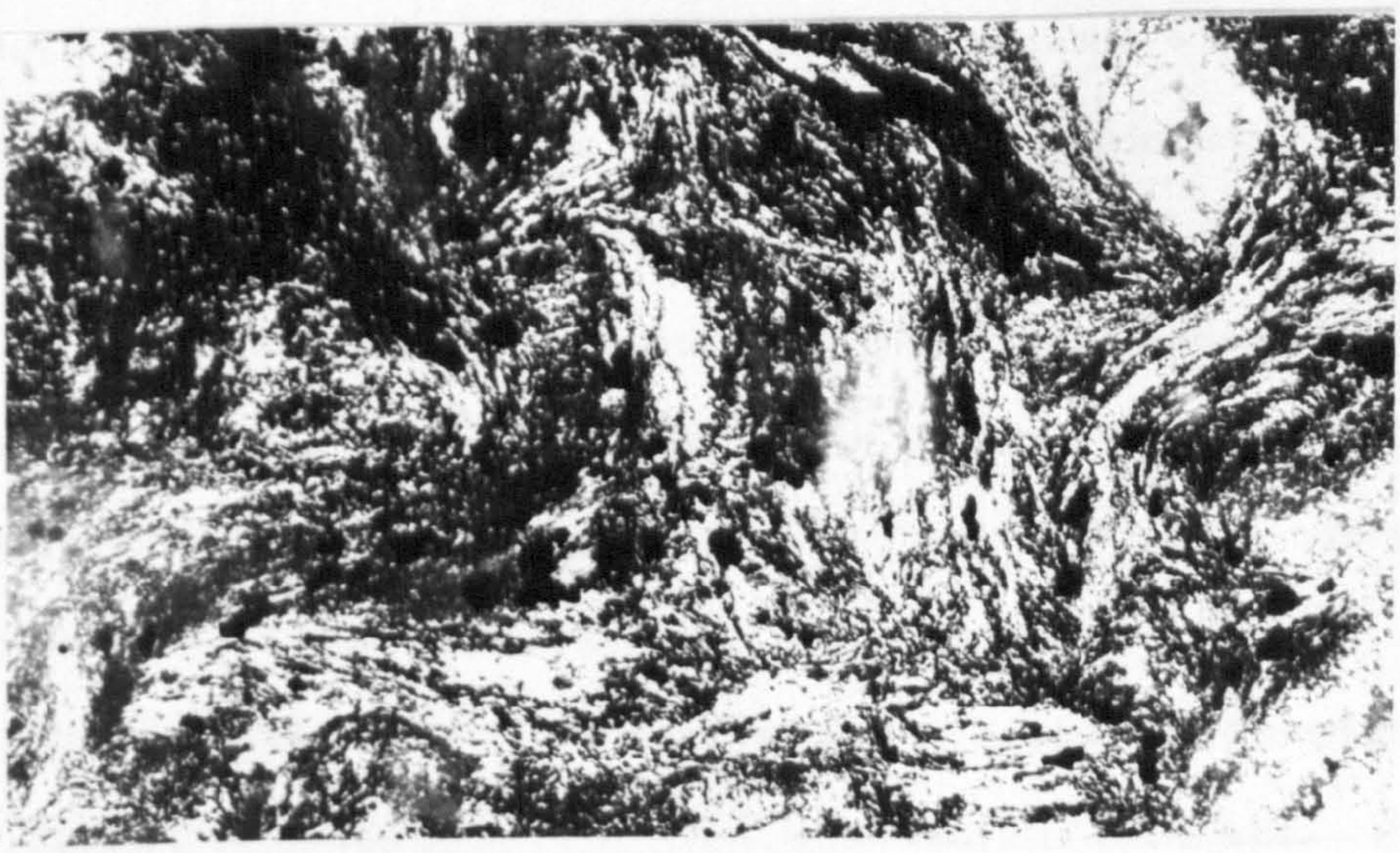

c

1mm.

0

PLATE 13·5

The dominant process in the formation of the caliche is the result of long continued soil processes operating in an aeolian aggrading environment. The extremely pure calcium carbonate horizon which results indicates a removal of detrital grains by alkaline solutions. Solution of detrital quartz decreases with depth. Experimental work (Krauskopf, 1959) suggests that silica is not removed in solution until a pH of 9 or more is reached and as the solution of silica and the precipitation of calcium carbonate occur under the same conditions, a pH of more than 9 would seem to be a pre-condition for the formation of a caliche profile. Arkley (in Reeves, 1970) however, showed that the kinetics of pure silica solution did not apply to soils and suggested that the pH remained fairly constant around 8·2. As solution of silica and precipitation of calcium carbonate decrease in the underlying sandstones it is suggested that there was a lowering in pH due to the decreasing movement of pore fluids.

(b) <u>Formation of iron pellicles around detrital grains</u>

The diagenetic quartz zone is essentially red in colour owing to a thin film of microcrystalline iron oxide between the detrital grain and the secondary quartz overgrowth. As the secondary overgrowths were formed during the late stages of caliche development, the iron oxide film is therefore early caliche in origin. The red bed horizon reaches a maximum of 4 metres in thickness and corresponds to the Sago Pudding Sandstone and, occasionally, the upper parts of the Lossiemouth Sandstone.

Micas are relatively common in both the Lossiemouth Sandstone and the Sago Pudding Sandstone. Muscovite is the commonest mica and is relatively unaltered compared to the rarer biotite which is only preserved as a relic nucleus surrounded by iron oxides and clay minerals. Walker (1967) regards the formation of red beds in an arid to semi arid environment as due to the <u>in situ</u> alteration of detrital iron bearing minerals. The occurrence of altered biotite clearly supports the view that this was a process in the formation of these red beds.

It is suggested that special conditions prevailed during the formation of the caliche and that the main reason for the absence of red beds in underlying horizons was the absence of clays and ferro-magnesian minerals due to the dominantly aeolian environment. However, upon formation of the caliche, a ready supply of clays and ferro-magnesian minerals, together with a high pH, produced ideal conditions for the formation of red beds. These red beds probably formed by both alteration of ferro-magnesian minerals (Walker, 1967) and from pre-existing oxides in the overlying caliche (Friend, 1966; Van Houten, 1968; Wilson, 1971). Solution of the detrital minerals from the overlying indurated and friable caliche were subsequently reprecipitated in the diagenetic quartz zone as ferric oxides which formed as thin films around the detrital grains. A rapid decrease in pH away from the caliche profile meant that conditions were unfavourable in the underlying sandstones leading to the relatively thin red bed horizon which is the only red horizon present in the Elgin New Red Sandstones.

During the late stages of the caliche, plugging of the horizon led to a decrease in pH at this horizon together with deposition of secondary overgrowths which closed the period of red bed formation.

(c) <u>Formation of calcite cements in the underlying sandstones</u>

Calcite cement is present in all the sandstones underlying the caliche but the distribution is extremely patchy and rarely provides more than 5 per cent of the total rock volume. The higher percentages are found in the coarser grained Burghead Beds and the concretionary Hopeman Sandstone but usually there is less than 1 per cent in any given sample and frequently the calcite cement is totally absent. However, calcite cements are most frequent in the horizons closest to the Cherty Rock suggesting that the source was from the overlying caliche. Formation of the diagenetic quartz zone effectively cut off the source of the calcium carbonate and suggests that the cements were formed during the early stages of caliche development although later redistribution may have occurred.

EXPLANATION OF PLATE 13.6

A. Post caliche fluorite and late caliche secondary quartz overgrowths in the Lossiemouth Sandstone. Scanning electron microscope.

B. Haematite introduced during post caliche mineralisation replacing late caliche secondary quartz overgrowths in the Lossiemouth Sandstone. Crossed nicols.

C. Fluorite cemented Hopeman Sandstone illustrating the etching of pre caliche secondary quartz overgrowths.



a

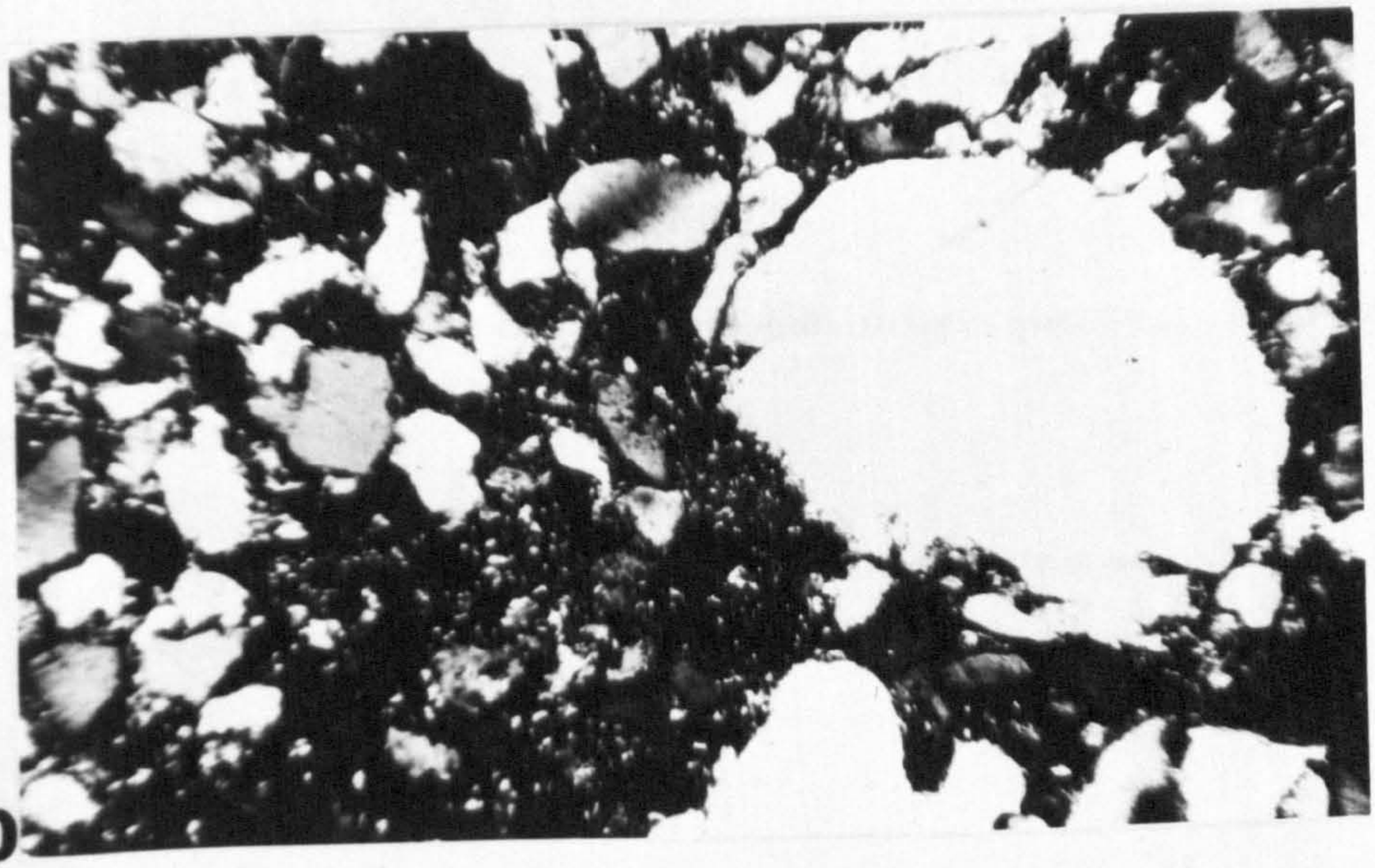

b



c

PLATE 13·6

EXPLANATION OF PLATE 13.7

SILICA MINERALISATION

A. Pseudomorphs after calcite infilled by drusy quartz embedded in a chert matrix. Crossed nicols.

B. Cavity infill by banded chalcedony and drusy quartz. Scanning electron microscope.

C. Quartz cavity infill. Scanning electron microscope.

At the top of the H2 horizon of the Hopeman Sandstone, the foreshore to the north of Greenbrae Quarry exposes a calcareous concretionary sandstone which has a calcite cement occupying as much as 15-20 per cent of the total rock volume. The form of the cement is typically poikilitic.

3. DIAGENESIS DURING THE LATE STAGES OF CALICHE DEVELOPMENT

This stage is defined as the period between deposition of the early caliche profile and prior to the deposition of the overlying Liassic sediments.

The essential diagenetic fabric which developed during this stage was the formation of the diagenetic quartz zone of the caliche profile. Secondary quartz overgrowths formed in the underlying sandstones but the effect diminished with depth until in the Hopeman Sandstone, there is only rare evidence of any quartz overgrowths forming during this period. Reeves (1970) demonstrates that during the late stages of modern day caliche profiles, a zone of diagenetic quartz develops at the base of the profile, provided infiltrating waters are not impaired by a reduced permeability. The diagenetic quartz zone is the natural progression of a caliche profile provided sufficient time is available, thus, explaining the presence of these siliceous zones in only the old caliche profiles.

The effect of the diagenetic quartz zone in the Cherty Rock caliche was to preserve the red bed horizon and to effectively plug the horizon with the result that no calcium carbonate infiltrated into the underlying sandstones. Instead, secondary quartz overgrowths were developed in the underlying sandstones although there was a rapid decrease in their formation with depth (Fig. 12.2). The source of the silica appears to have been solution of the detrital quartz grains from the overlying friable and indurated caliche with subsequent precipitation of the silica on reaching a lower pH in the diagenetic quartz zone and the underlying sandstones.

It may be argued that the quartz overgrowths were not formed by this process but by burial and pressure solution. Fig. 13.7 illustrates that

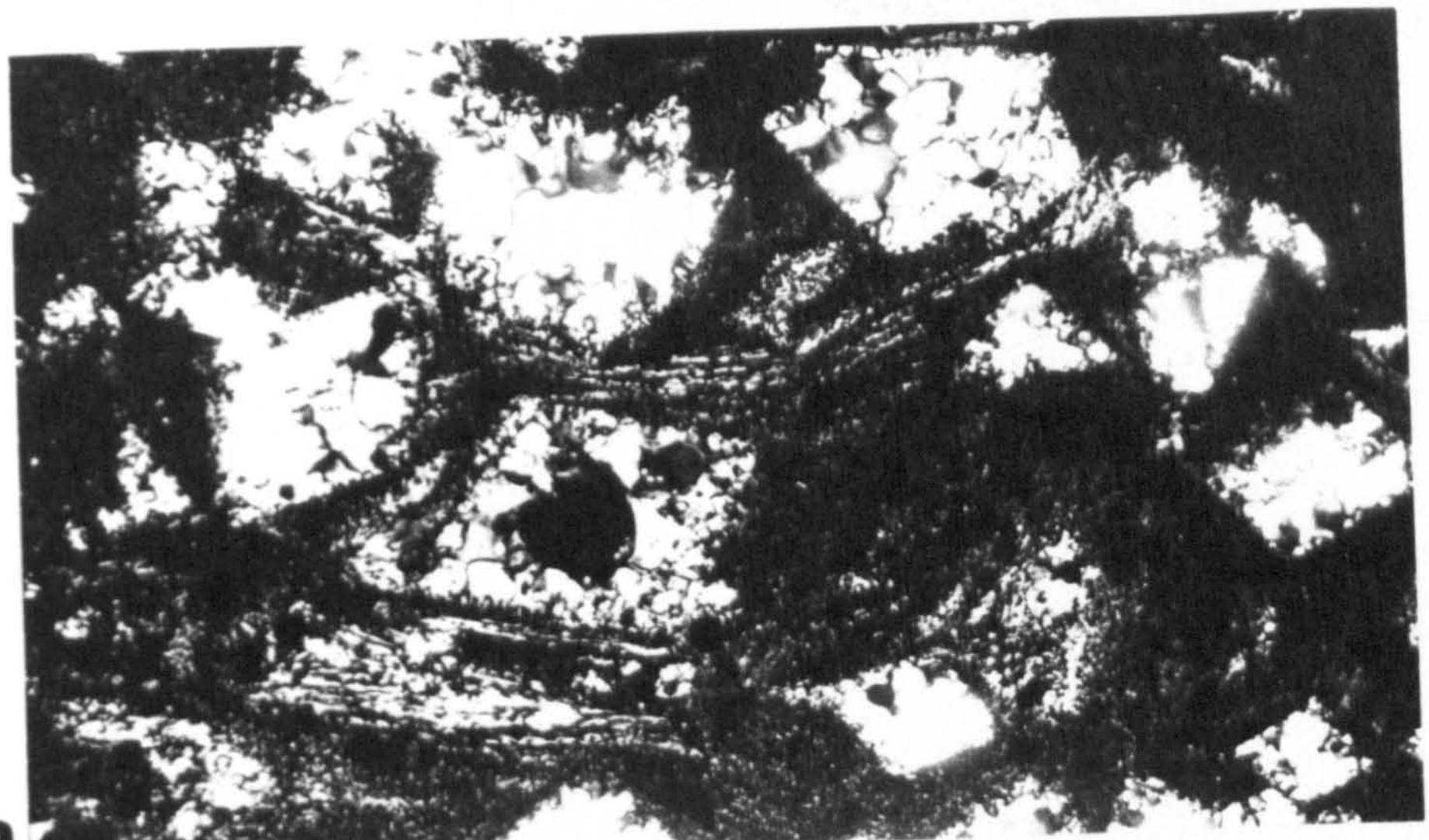

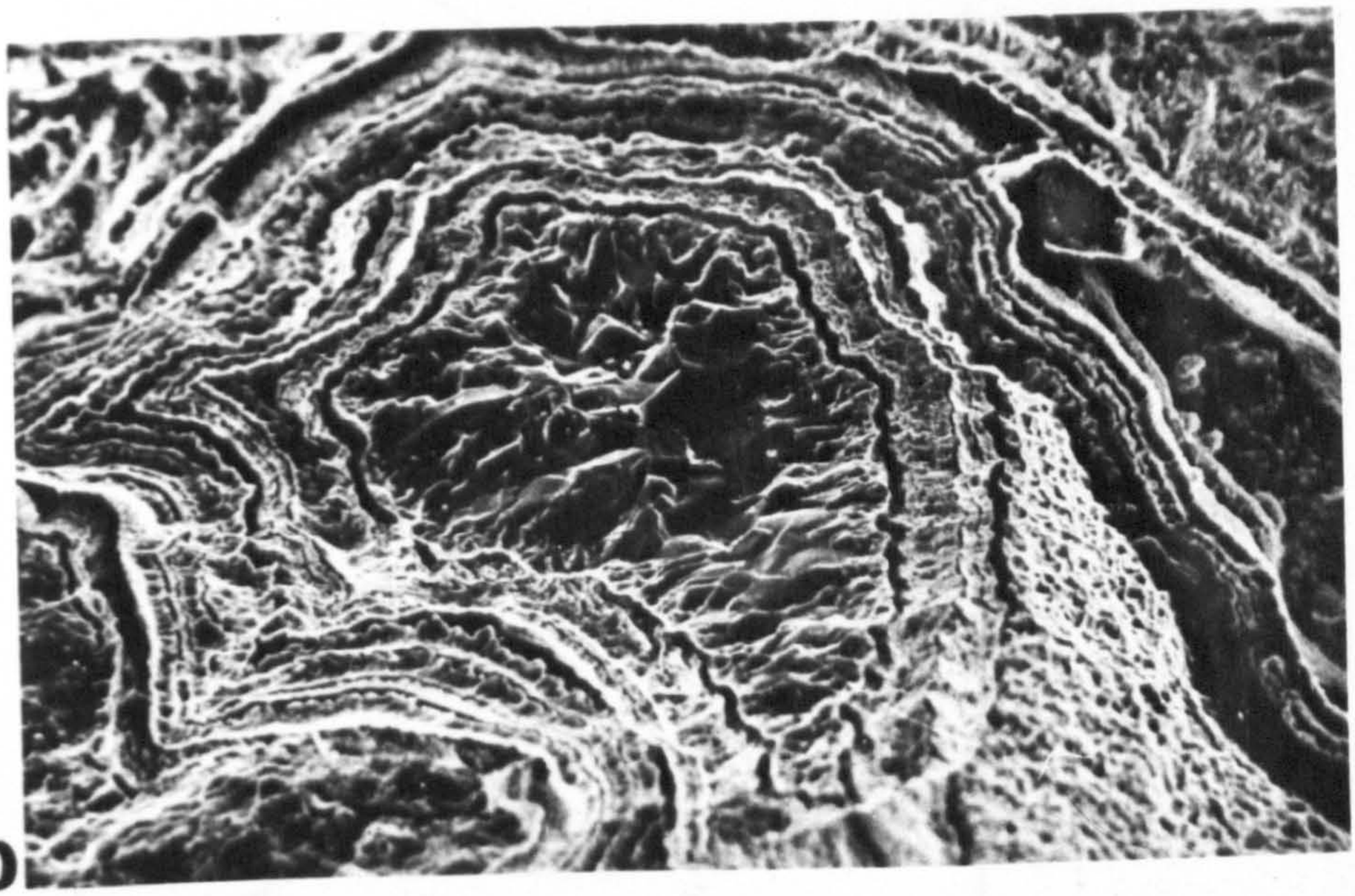



PLATE 13·7

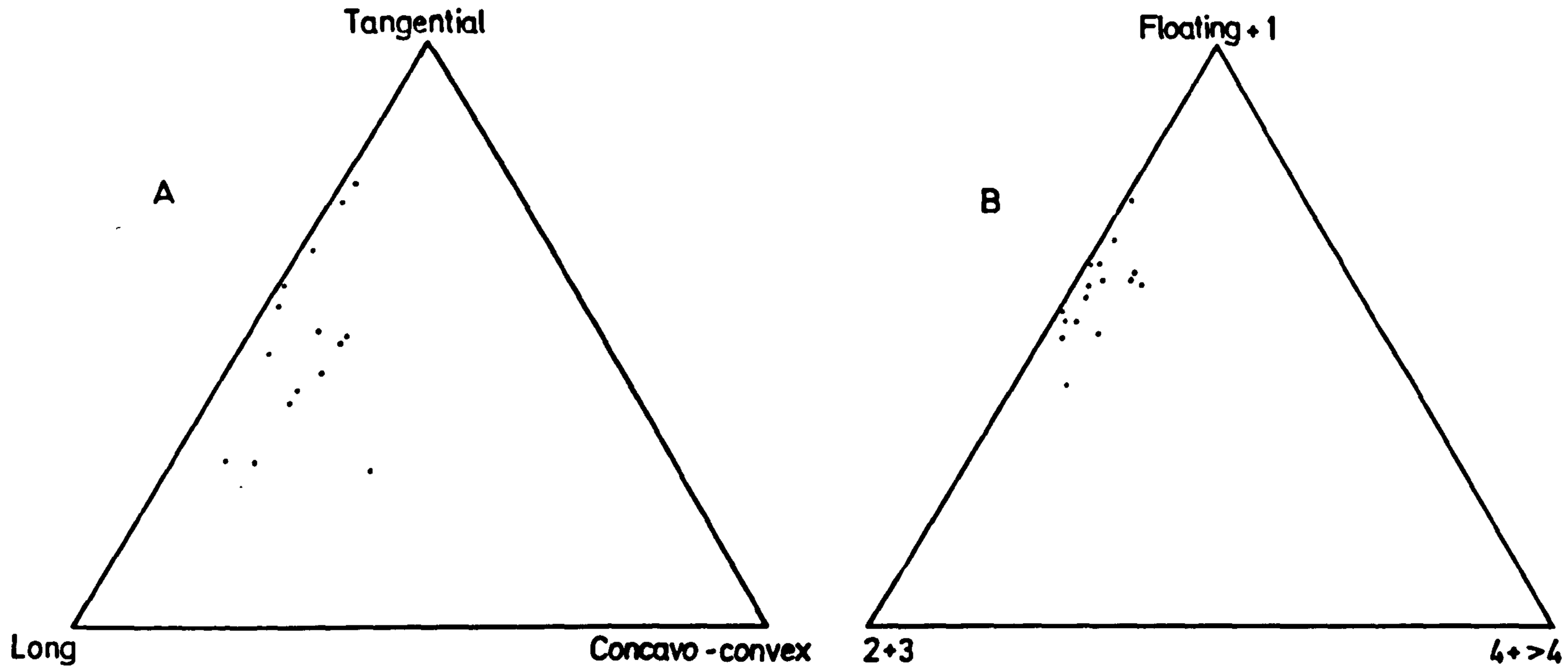

Fig. 13.7. Characteristics of the grain contacts in the diagenetic quartz zone.

the Sago Pudding Sandstones rarely show more than one or two contacts per grain and that the contacts are generally tangential. These features do not suggest pressure solution.

4. POST CALICHE DIAGENESIS AND MINERALISATION

A galena-haematite-fluorspar-barytes-calcite-quartz mineralisation is widely distributed although it is mainly associated with the Cherty Rock and faults and joints affecting pre-Jurassic rocks. A lower limit to the age of the mineralisation in the Elgin district is based on the presence of joint surfaces coated with fluorspar and galena in the Lower Jurassic rocks penetrated by the Geological Survey boreholes at Lossiemouth (Elgin memoir, p.126). Moorbath (1962, p.335) gives a date of 140±60 million years for the galena from veins at Stotfield giving a late Jurassic age to the mineralisation. It is also interesting to note that there is evidence for two periods of silicification which pre-date and post-date contemporaneous faulting. As there is evidence of dateable Lower Kimmeridgian faulting at Helmsdale (Gallagher, 1971; Hallam, 1970) and borehole evidence in the North Sea also suggests Upper Jurassic faulting, there is no reason to dispute the late Jurassic age suggested by Moorbath (1962).

Mineralisation pre-dating the faulting may only be recognized in the Cherty Rock where chertification of the caliche profile has occurred. Mineralisation post-dating the faulting is more varied and galena, haematite, fluorite, barytes, calcite and silica are the main components although it will be shown later that the fluorite, barytes and calcite probably represents remobilisation of pre-existing Triassic mineralisation.

(a) Pre-faulting mineralisation

The first stage of mineralisation is limited to silicification of the Cherty Rock and occasionally the underlying Sago Pudding Sandstones. The degree of alteration of the caliche profile decreases towards the base so that the indurated caliche is often totally replaced whereas the Sago Pudding only shows rare instances of replacement.

EXPLANATION OF PLATE 13.8

POST CALICHE MINERALISATION

A. Galena and microcrystalline chert replacing indurated caliche.
Crossed nicols.

B. Microcrystalline chert. Scanning electron microscope.

C. Drusy calcite vein infilling along a post caliche fracture.
Scanning electron microscope.

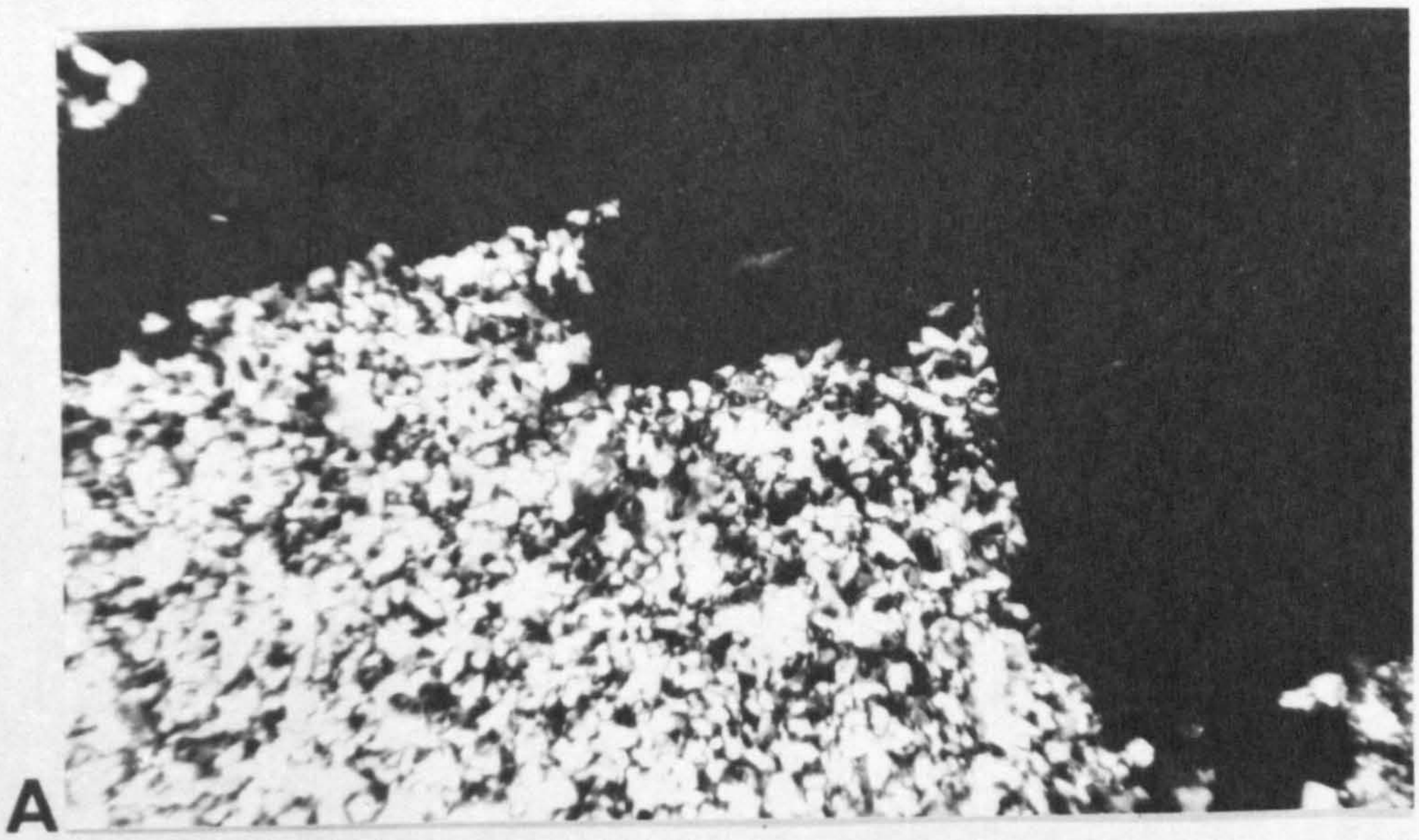

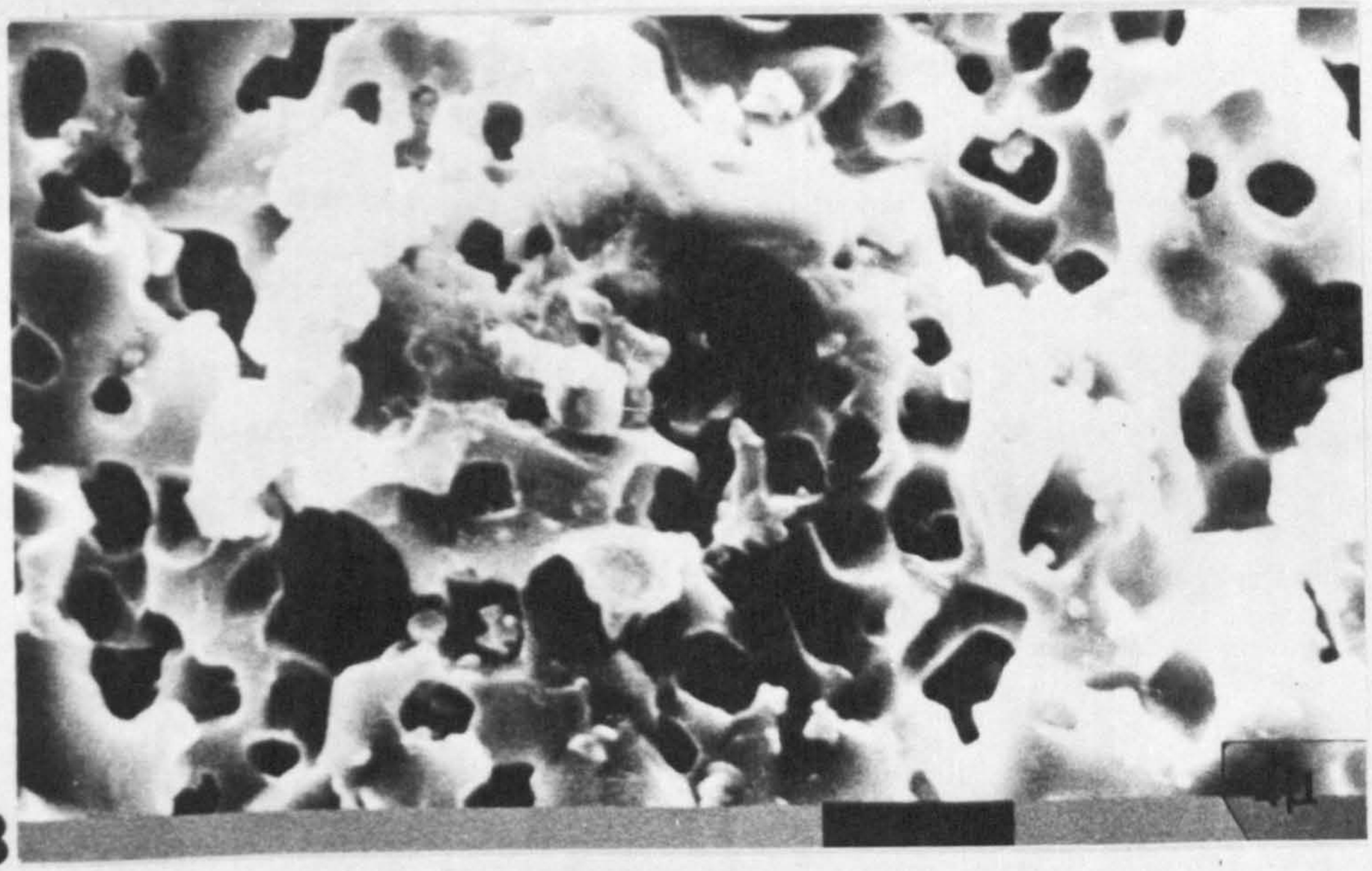

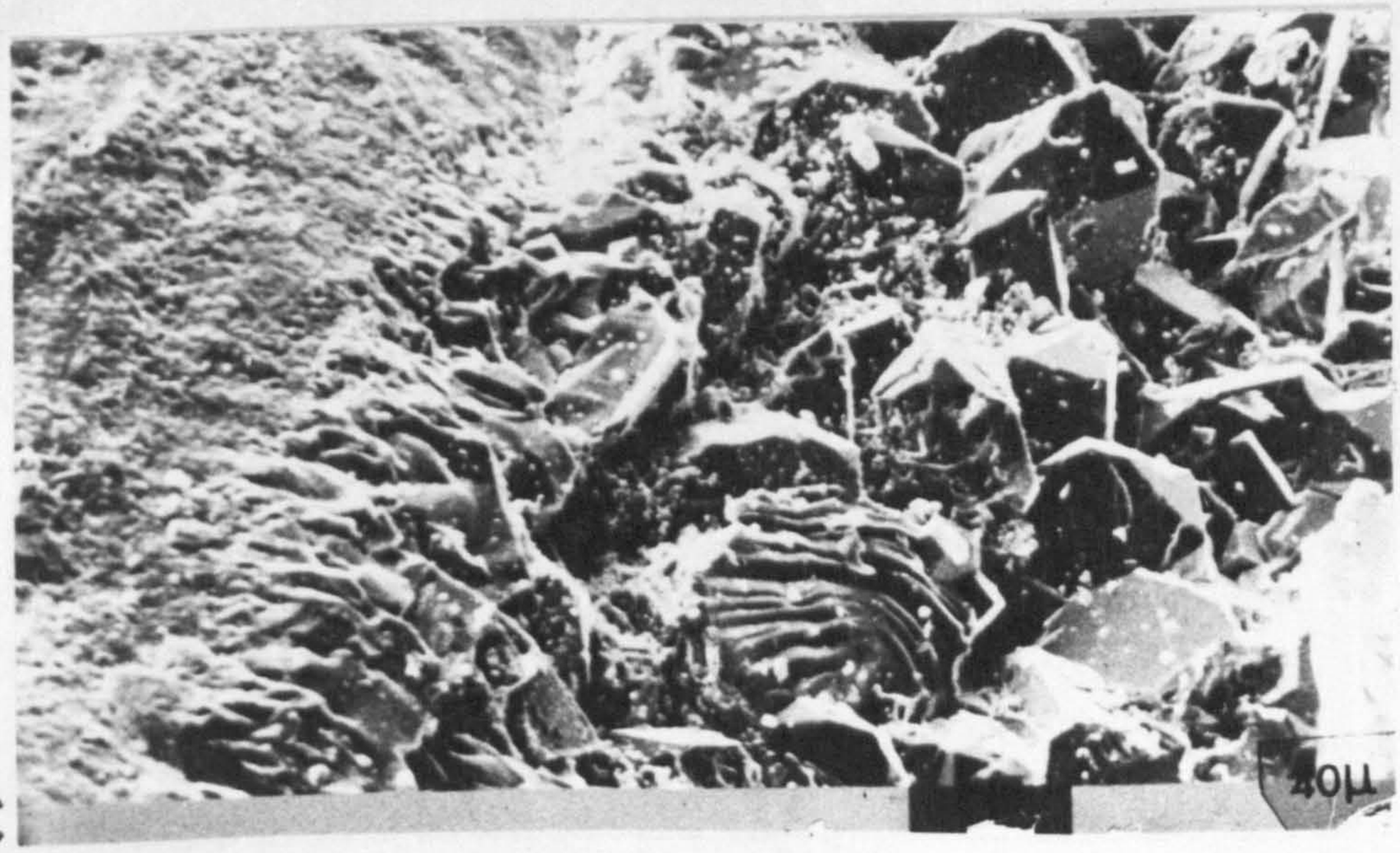

PLATE 13·8

EXPLANATION OF PLATE 13.9

SILICA MINERALISATION

A. and B. Zoned quartz illustrating several stages of development in cavity infilling.

C. Banded chalcedony in plane polarised light on the edge of a vein infilling.

PLATE 13·9

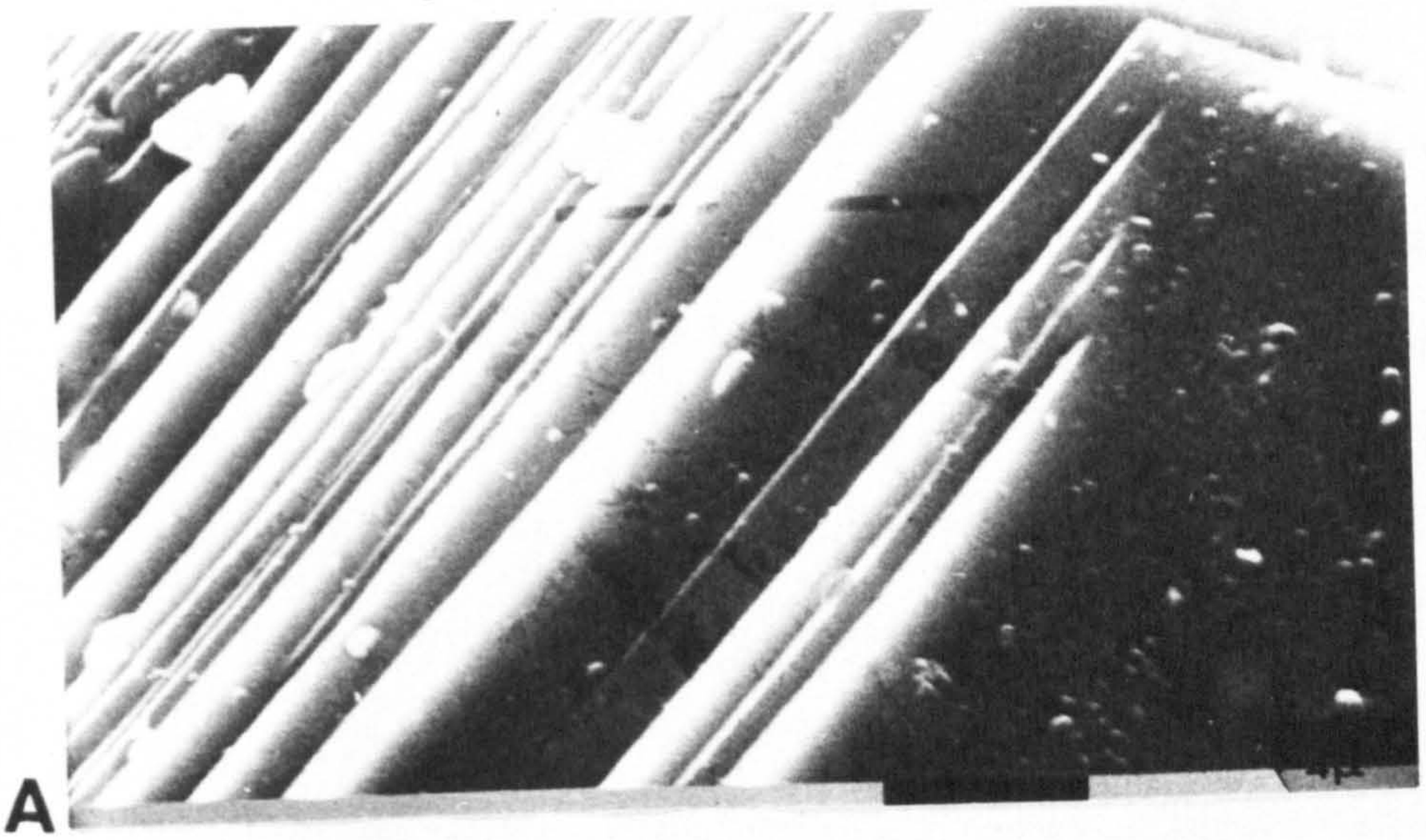



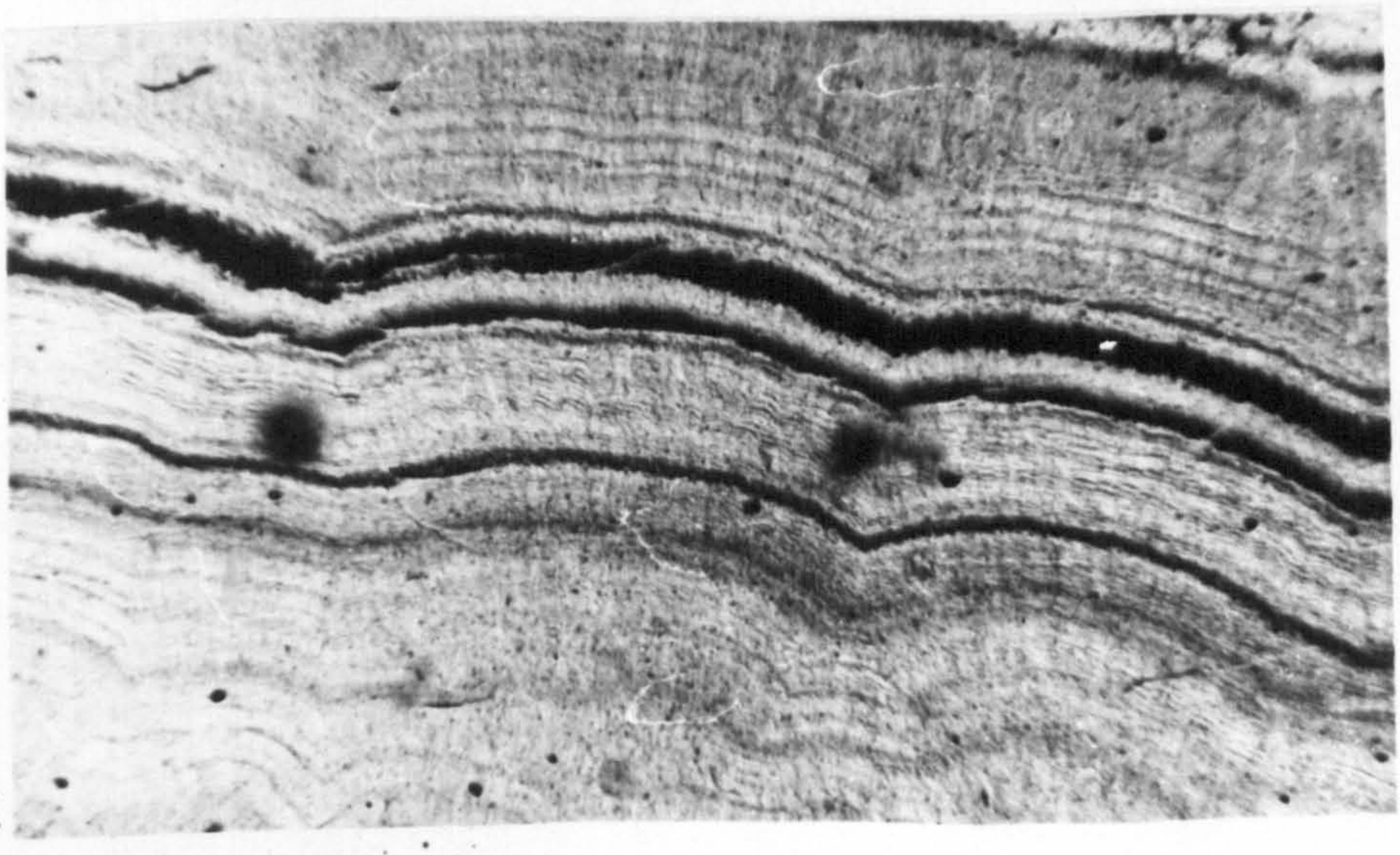

Alteration of the indurated caliche frequently involves complete replacement of the calcite so that no traces are left (Plates 13.8A and 13.8B). However traces of organic matter or residues of the calcite are often preserved (Plate 13.5). Commonly there is a transitional stage between the replacement of the micritic calcite by chert which can be recognised by the presence of calcite and dolomite rhombs on the boundary of the replacement (Plates 13.5A and 13.5B). The matrix is first replaced by chert, then the calcite rhombs are pseudomorphed and if the alteration is complete, finally the dolomite rhombs are replaced. However, various stages of the replacement are frequently preserved. The rhombs are frequently zoned showing several stages of growth and may even show alternations of dolomite and calcite. The rhombs probably represent re-crystallisation of replaced caliche which formed from the residual calcite. The chert also replaces the cavities and often preserves the laminations and pseudo oolitic textures of the indurated caliche. The laminations may be replaced by chert or opal but in most cases by chalcedony. The length slow chalcedony precludes an original caliche origin of the chalcedony (Folk, 1971).

Chertification of the friable caliche also occurs but is mainly confined to replacement of the microcrystalline calcite. However, the lack of original structure in this horizon means that the replacement chert is also structureless. Solution of the detrital grains occurs both in this horizon and in the diagenetic quartz zone. The grains are often highly etched by the chert matrix and in some cases may replace the secondary quartz overgrowths formed in the late stages of caliche development.

(b) <u>Post faulting mineralisation</u>

At Lossiemouth, Inverugie and Spynie, the chertified caliche is frequently cut by veins filled with vein quartz, calcite, galena, haematite, fluorite, barytes. Fault breccias with fragments of chertified caliche with calcite and dolomite rhombs clearly showing that the faulting post dates the early chertification. The faults are infilled by drusy quartz, chalcedony and

opal indicating a second phase of silicification. Recrystallisation of the microcrystalline calcite also occurs (Plate 13.8C).

The following forms of silica mineralisation have been recognised:

(a) Drusy cavity infill (Plates, 13.7C, 13.7B, 13.7A, 13.5B)

(b) Zoned quartz in cavities (Plates, 13.9A and 13.9B)

(c) Microcrystalline chert (Plate, 13.8B)

(d) Opal cavity infill

(e) Chalcedonic cavity infill (Plates, 13.9C, 13.7B, 13.5B)

(f) Quartz overgrowths in the Hopeman Sandstones, usually zoned.

With the exception of the latter, all these structures are confined to the Cherty Rock.

Galena occurs along vein infillings but is mainly disseminated in the chert matrix (Plate, 13.8A). Haematite also occurs as vein infillings and may occur as a cement in the vicinity of faults as at Findrassie (Plate 13.6B). Fluorite, barytes and calcite are limited in occurrence but are seen along fractures and sometimes in pore spaces (Plates, 13.6A and 13.4C) in the Sago Pudding and Lossiemouth Sandstones. They clearly post date overgrowths and are easily differentiated from the pre-overgrowth cements (Plates, 13.6C, 13.4A, 13.4B) of the Hopeman Sandstone. Fluorite veins cross cutting the calcite and fluorite cementing Hopeman Sandstones at Roddoch Wells are also of this stage. Their limited occurrence and association with pre-existing fluorite, barytes and calcite would suggest that they are due to remobilisation of the pre existing Triassic mineralisation.

Origin and distribution of the mineralisation

Peacock (1968) suggested that the preferential mineralisation of the Cherty Rock was due to the overlying Jurassic shales providing a damming effect and thus concentrating the mineralisation in the Cherty Rock. Although this was probably a major factor, a similar effect was produced in the Mississippian Ore fields where limestones were replaced in preference to

sandstones (Beal and Onasick, 1970). They suggested that this was due to trapping potential of carbonates.

The source of the mineralisation produces a similar problem to the origin of the fluorite and barytes and may be due either to a direct source or a remobilisation of a pre-existing mineralisation. In either case, the silica, galena, haematite, barytes, calcite and fluorite constituents are similar to mineralisation associated with Newer Granites to the south and west of the area (Gallagher, 1971).

CHAPTER 14

TRIASSIC ROCKS OF GOLSPIE, SUTHERLAND

In the south west of the Moray Firth, a series of Mesozoic sediments occupy a narrow coastal strip between Helmsdale to the north and Golspie to the south. This coastal tract varies in width from a few hundred metres to three kilometres (Fig. 14.1), and is bounded on the landward side by a fault which originated as a submarine scarp during Kimmeridgian times (Read 1925). The Mesozoic sediments young towards the north and are faulted against Moine Schists, Old Red Sandstones and the Helmsdale Granite.

The most recent account of the Triassic rocks of the Golspie area is that by Read (1925). Even at this early date he stated (p.35)"that the boundaries shown on the map are based to a large extent on old records of pits or quarries now covered up and no longer available for examination". This is even more the case at the present day and, as a result, many of the interpretations are speculative.

The lowest strata are only visible at extremely low tides as reefs, east of a small disused pier, 1 kilometre south south west of Dunrobin Castle. They are represented by a series of massive calcareous sandstones dipping at 5 degrees north, strike N35E. The base of the sandstones is not seen but at least 10 metres are exposed. These sandstones grade up into sandy limestones and marls, these comprising the cherty limestone of Judd (1873) and Read (1925). It is suggested that the sandy limestones are a diagenetic modification product of the underlying calcareous sandstone and that together with the marls, they represent a fossil caliche horizon.

The marls contain varying proportions of quartz grains, the percentage of which decreases from the base to the top. The marls are also preferentially replaced by chert, vein quartz and silica veins but, compared to the Elgin Cherty Rock, the degree of replacemnt is relatively small.

Although the contact of the marls and the overlying sandstones (Dunrobin Castle Sandstones) is not seen, a series of sandstones and conglomerates dipping at the same angle and strike are exposed just south of the old pier at Dunrobin. A fault separates them from similar sandstones occurring to the north of the pier where they are seen as low water reefs.

Three hundred metres north of the pier, a small reef of white sandstones is overlain by clays of Liassic age. It is not known if the sandstones are also of Liassic age as they are unfossiliferous. Read (1925) suggests that they are the same as the sandstones overlying the caliche and that they are Rhaetic in age. This interpretation is also accepted here although the white sandstones have not been environmentally analysed owing to the limited exposure.

Evidence of the marls and cherty limestone are again seen in Golspie Burn, 250 metres above the railway bridge (Fig. 14.1). Here 1-2 metres of marly limestones with scattered quartz grains are exposed in the river bank. The exposure is traversed by jointsfilled with opal and chalcedony and cavities filled with both calcite and vein quartz. The limestone varies from white to pink in colour. Fifty metres north of the bridge, another exposure of sandy marl outcrops in the river bank.

The following section therefore represents the Triassic succession of Golspie:

Read 1925		Williams 1972	
100 metres	Sandstones and pebbly sandstones	Dunrobin Castle Sandstones	
3 metres	Cherty limestone	Golspie Cherty Rock	= Indurated caliche
15 metres	Marls		= Friable caliche
	Calcareous Sandstone		= Calcareous Sst.

GOLSPIE CHERTY ROCK

The sequence from calcareous sandstones through sandy limestones to marls can be closely compared to the Elgin Cherty Rock, as noted by Judd (1873).

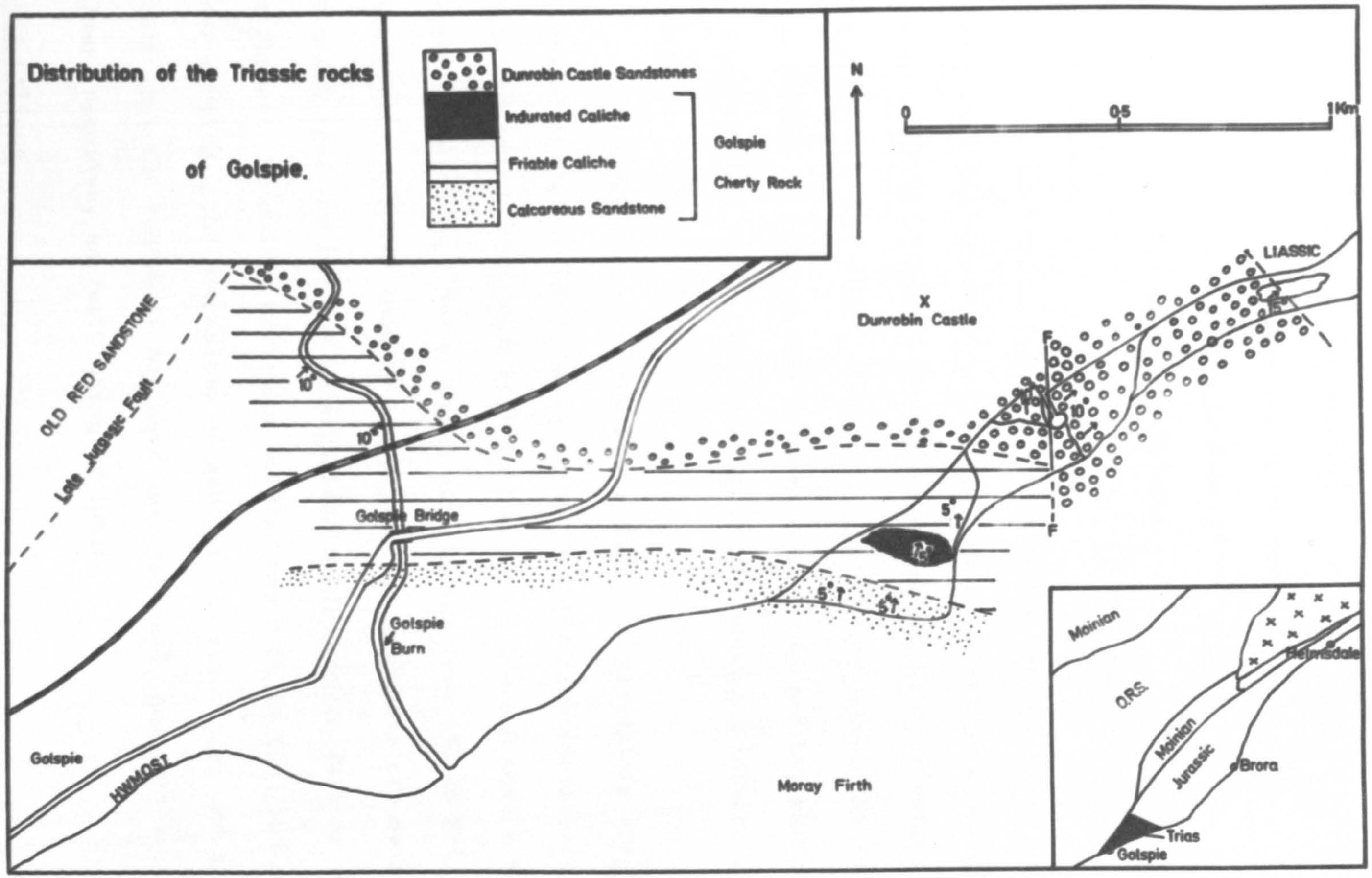

Fig. 14.1. Distribution of the Triassic rocks of Golspie.

However there are minor differences, and a closer comparison can be made to the immature caliche horizons described Aristarain (1970) from the High Plains, New Mexico (Fig. 14.2).

Detailed field mapping indicates that the Golspie Cherty Rock can be subdivided into three main horizons:

1. Calcareous Sandstone
2. Friable Caliche
3. Indurated Caliche

Calcareous sandstone

The base of the calcareous sandstones is not seen, and at the top they grade into the overlying friable caliche. As one proceeds up the calcareous sandstones towards the friable caliche, the percentage of calcite increases and the percentage of detrital grains decreases. At the base, the detrital grains show one to two contacts with other grains, whereas in the friable caliche the grains are floating in the microcrystalline calcite groundmass.

The sandstones, which are probably of floodplain origin, display an essentially massive appearance, no sedimentary structures being apparent. The detrital grains vary from high to low sphericity and have a dominantly subangular appearance. Median grain size varies from 1·7 to 2·6 phi which is generally finer grained than in the equivalent sediments of the Dunrobin Castle Sandstones; this can however be explained by deposition further away from the river channel. Standard deviation varies from 0.66 to 1.05 indicating moderate to poor sorting. The bimodality of some of the sandstones and absence of mica suggests that the sediments may have been reworked, possibly by wind. Skewness is always negative, kurtosis being variable.

Friable Caliche

The calcareous sandstones grade up into the friable caliche which may be recognised by the increase in calcium carbonate content and the decrease

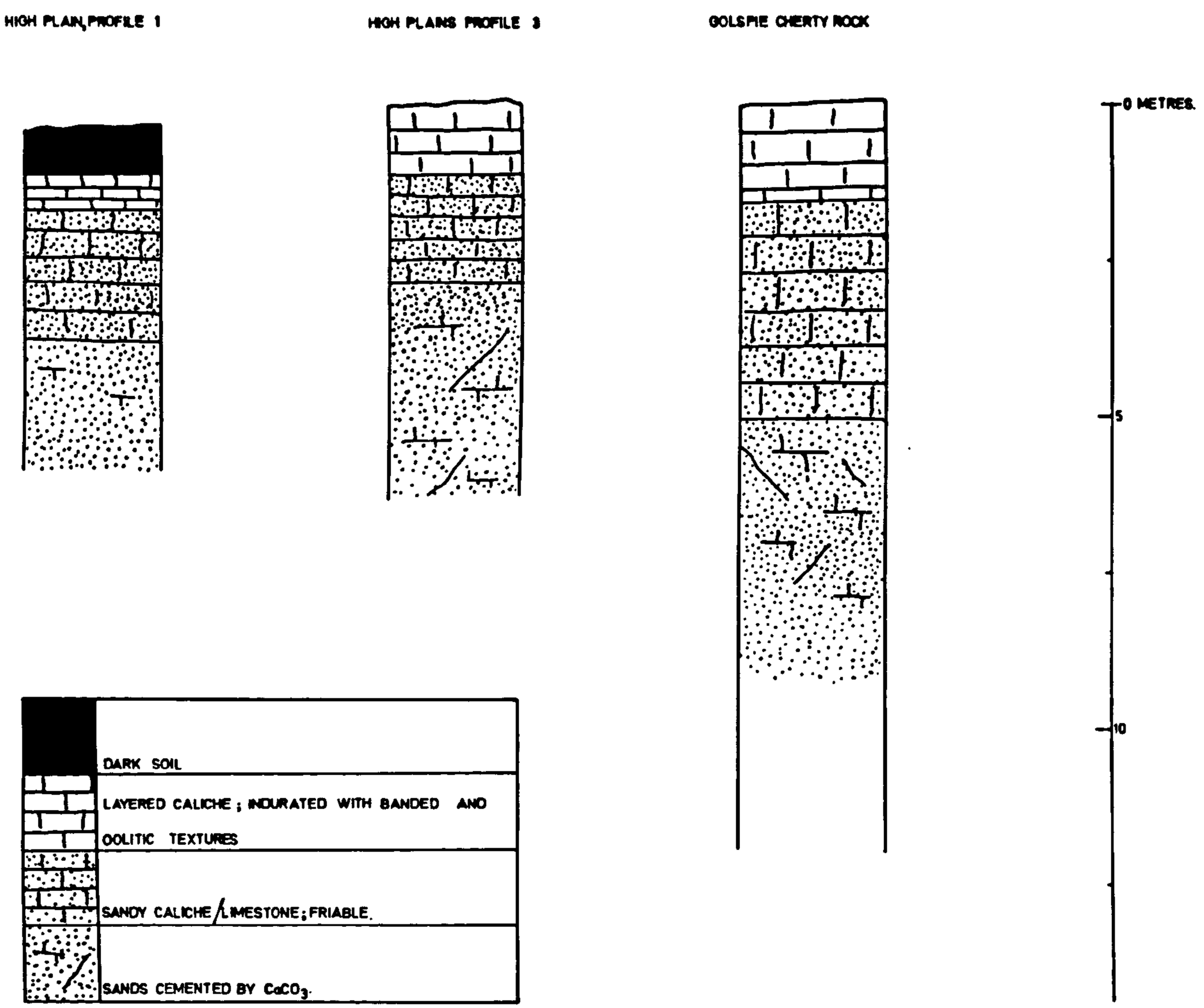

Fig. 14.2. Comparison of the Golspie Cherty Rock with modern day caliche profiles.

in detrital quartz grains. The quartz grains "float" in a microcrystalline calcite matrix.

This horizon shows similar characteristics to the friable caliche of the Elgin Cherty Rock although it is less compacted and little or no replacement by silica has taken place. However, siliceous veins and patchy areas of chert replacement are sometimes present.

The matrix is typically a white to green crumbly caliche with no evidence of laminated or pseudo oolitic structures. In places, the microcrystalline calcite has recrystallised along fractures. Sparry calcite is also present along the contact between the detrital grains and the surrounding matrix. In some areas, pockets of quartz grains suggest the presence of an original cavity where the detrital grains have been concentrated; these quartz grains are characterised by a rim of microcrystalline calcite impregnated by traces of organic material. The poorly developed matrix in these areas suggest that the quartz grains acted as nuclei along which precipitation took place.

The clastic grains are of a similar type to those seen in the underlying sandstones; some grains are etched along the contact with the matrix due to replacement by calcite.

Indurated Caliche

A further decrease in the percentage of quartz grains is again seen in the indurated caliche although pockets of quartz grains may be concentrated in some areas. The indurated caliche is typically grey and white in hand specimen and shows a higher degree of replacement by silica than the underlying horizons. The horizon is also much harder than the crumbly friable caliche and has a typically flinty appearance.

In thin section, the microcrystalline groundmass appears to be very dense except where recrystallisation along fractures has taken place. The most characteristic features are however the laminations and pseudo oolitic structures. The laminations appear to represent precipitation of calcite along horizontal fracture zones, the fractures having been formed by desiccation and shrinkage.

The pseudo oolitic structures represent sections through botryoidal cavity infillings.

Most areas are completely free of quartz grains and are characterised by the dense microcrystalline matrix. The reciprocal relationship between the proportion of calcite and quartz grains would suggest that the quartz has been removed in solution.

Chert frequently replaces the microcrystalline groundmass; vein quartz, chalcedony and opalline silica are also found infilling fractures. However, replacement is not as great as in the equivalent horizons at Elgin.

Formation of the caliche

The main points regarding the formation and origin of modern day caliche profiles have already been discussed in Chapter 11, and all the evidence suggests that the Golspie Cherty Rock was formed in a similar manner to the Elgin Cherty Rock. However, the absence of a diagenetic quartz zone at Golspie does suggest some difference in the conditions of formation.

Reeves (1970) showed that several stages of caliche formation could be recognised in modern day caliche profiles, the stages depending on the age of the profile. He showed that the friable caliche was the youngest stage of the profile and that all the later stages were due to modification of this unit. The indurated caliche which is present at both Golspie and Elgin is formed due to plugging of the profile by the diagenetic quartz zone or repeated exposure. As the diagenetic quartz zone is absent at Golspie, the indurated caliche probably formed due to exposure. Reeves (1970) also showed that the zone of diagenetic quartz is only formed in the old stages of the caliche profile so the Golspie Cherty Rock is therefore a relatively immature caliche.

Silica replacement of the Golspie Cherty Rock

The presence of replacement silica is mainly confined to the Golspie Cherty Rock, although silicification has been noted at one horizon in the Dunrobin Castle Sandstones along a fault zone close to Dunrobin Pier. This

appears to indicate a preferential replacement of carbonate as was also seen at Elgin. Three main types of silica can be identified:

1. Direct replacement of the caliche matrix by chert.
2. Chalcedonic and opalline silica along fractures and cavities.
3. Quartz cavity infill.

Direct alteration of the caliche is mainly confined to replacement of the indurated caliche horizon. The microcrystalline chert completely replaces the calcite and usually preserves the original laminations and pseudo-oolitic structures. In some cases, dolomite may be present at the contact of the caliche and the replacing chert, or in more advanced stages, entirely enclosed within the chert. A further stage of replacement may be seen where the dolomite rhombs are replaced by drusy quartz.

Chalcedony and opalline silica are common along fractures, particularly in the indurated caliche. They are also present in the friable caliche and the calcareous sandstones but their importance tends to diminish away from the indurated caliche. Larger fractures are infilled by drusy quartz and sometimes calcite, the later being interpreted as remobilised calcite.

The age of the mineralisation is clearly later than the Dunrobin Castle Sandstones which is silicified in places. The fault, which brings Mesozoic strata against the older rocks, has been dated as Kimmeridgian in age (Read, 1925; Gallagher, 1970; Hallam, 1970). Gallagher (1971), discussing mineralisation in the Helmsdale area has shown that there is no trace of mineralisation in the Kimmeridgian sediments. He therefore dates the Helmsdale mineralisation as pre-Kimmeridgian in age. It is therefore probable that the silicification took place during the Lower or Middle Jurassic.

DUNROBIN CASTLE SANDSTONES

The Dunrobin Castle Sandstones comprise a series of grits, sandstones and conglomerates overlying the Golspie Cherty Rock. The deposits consist of isolated channels of coarser material set in the commoner, massive bedded

sandstones. Two main facies can be recognised:

1. Channel conglomerates
2. Well sorted massive sandstones

Channel conglomerates

The conglomerates and pebbly, calcareous cemented sandstones occur as broad shallow channel fill deposits, 3 metres wide and 0·5 metre in depth. They are isolated in occurrence and cut down into the massive bedded sandstones. The poor exposure means that the lateral extent of the channels is difficult to define, but individual channels up to 10 metres in length have been recognised. Palaeocurrent directions are similarly difficult to obtain but three directions trending N70-80E and one trending N20E have been recorded. The channel deposits display trough cross stratification where the structures can be identified.

The individual grains range from angular to subrounded and are poorly sorted. Standard deviation is generally between 1·4-1·5 reflecting the poor coefficient of sorting. Mean grain size is generally 0-0·5 phi but the sediments are often bimodal or trimodal, the modes being variable. Skewness is generally negative (Table 14.1).

Well sorted massive sandstones

No sedimentary structures have been recognised in these sandstones, the general appearance being that of massive calcareous cemented sandstones. They are similar in appearance to the calcareous sandstones below the friable caliche and probably represent a similar facies.

Mean grain size varies from 0·4 to 2·6 phi and is always finer grained than the channel sandstones. However, they display a higher sorting coefficient, standard deviation varying from 0·47 to 1·05. This indicates moderate sorting on the classification of Folk and Ward (1957). Skewness is again normally negative and kurtosis between 0·50-0·59. The grains are of a high sphericity and angular to subrounded in outline.

Number	5th	16th	25th	50th	75th	84th	96th	ST.D.	Sk.	Kg.
Massive sandstones										
G10	0	0.90	1.60	2.15	2.55	2.80	3.45	0.92	-0.20	0.58
G11	0.20	0.55	0.75	1.70	2.30	2.50	3.00	1.05	-0.07	0.50
G12	0.95	1.90	2.20	2.60	3.10	3.25	3.75	0.66	-0.11	0.54
G13	0.80	1.70	2.05	2.50	3.00	3.20	3.60	0.79	-0.15	0.53
G2	0.25	0.60	0.70	1.05	1.40	1.70	2.20	0.47	+0.02	0.53
G5	-0.70	-0.30	-0.10	0.40	0.80	1.05	1.50	0.68	-0.01	0.50
G7	0.30	1.00	1.40	1.80	2.10	2.40	2.80	0.70	-0.04	0.51
Channel conglomerates and grits										
G1	-2.30	-1.80	-1.00	0.30	0.85	1.40	2.65	1.55	-0.04	0.52
G3	-1.70	-0.60	-0.30	0.60	1.20	1.60	2.25	1.40	-0.13	0.52
G6	-3.00	-2.00	-0.30	0.50	0.90	1.10	1.60	1.46	-0.06	0.61

TABLE 14.1. Grain size analyses of the Dunrobin Castle Sandstones

Parameters for McBride's Classification (1963)

Number	Quartz	Rock Fragments	Feldspar
G1	71.9	24.6	2.8
G2	93.6	4.8	1.6
G3	69.5	29.5	1.0
G4	79.0	20.0	1.0
G5	71.8	27.3	0.9
G6	68.4	29.9	1.7

Parameters for Pettijohn's Classification (1954)

Number	Quartz	R.F. and Feldspar	Matrix
G1	71.9	28.1	0
G2	93.6	6.4	0
G3	69.5	30.5	0
G4	79.0	21.0	0
G5	71.8	28.2	0
G6	68.4	31.6	0

Parameters for Williams' Classification (1972)

Number	Unimodal Quartz	Clay and Mica	Others
G1	46.0	0	54.0
G2	66.0	0	34.0
G3	43.0	0	47.0
G4	50.0	0	50.0
G5	41.6	0	58.4
G6	51.6	0	48.4

TABLE 14.2.

Classification of the Dunrobin Castle Sandstones

The dual classification proposed in Chapter 5 is again used to classify the Dunrobin Castle Sandstones together with the classification of McBride (1963). Figs. 14.3A and 14.3B show the results of Tables 14.1 and 14.2 plotted with reference to the classification of McBride (1963) and Pettijohn (1954). In both classifications, the sandstones plot as litharenites.

Fig. 14.3C illustrates the results plotted on the auxiliary classification and demonstrates that the sandstones plot in a similar position to the flood deposits of the Elgin district. However, the absence of clays and micas may probably indicate that the sandstones were originally aeolian prior to their incorporation into the fluviatile system.

The maturity indices of Pettijohn (1954) indicate (a. 50:1, b. 3:1) a low maturity and a dominantly supracrustal source area. The provenance ratio is 8:1 in favour of rock fragments, again indicating a predominantly supracrustal source. Fluidity gives an anomalous reading as the absence of both clay and mica indicate a high fluidity although the sediments are clearly waterlain and of a low fluidity depositing media. This is probably due to aeolian influences prior to their deposition.

Detrital components of the Dunrobin Castle Sandstone

Strained and unstrained quartz

Unicrystalline quartz constitutes 43-60 per cent of the total rock volume. The most common type is where black dust particles are aligned along fractures in the quartz grain; this type of quartz is always strained and probably represents the alignment of impurities during metamorphism. Randomly distributed black dust particles do however occur, but these are less common. Inclusions may also be present, normally in the form of round bubbles, together with needle like fluid inclusions. The presence of rare quartz with iron oxide staining along fractures suggests possible derivation from the Old Red Sandstones although these may be dicyclic.

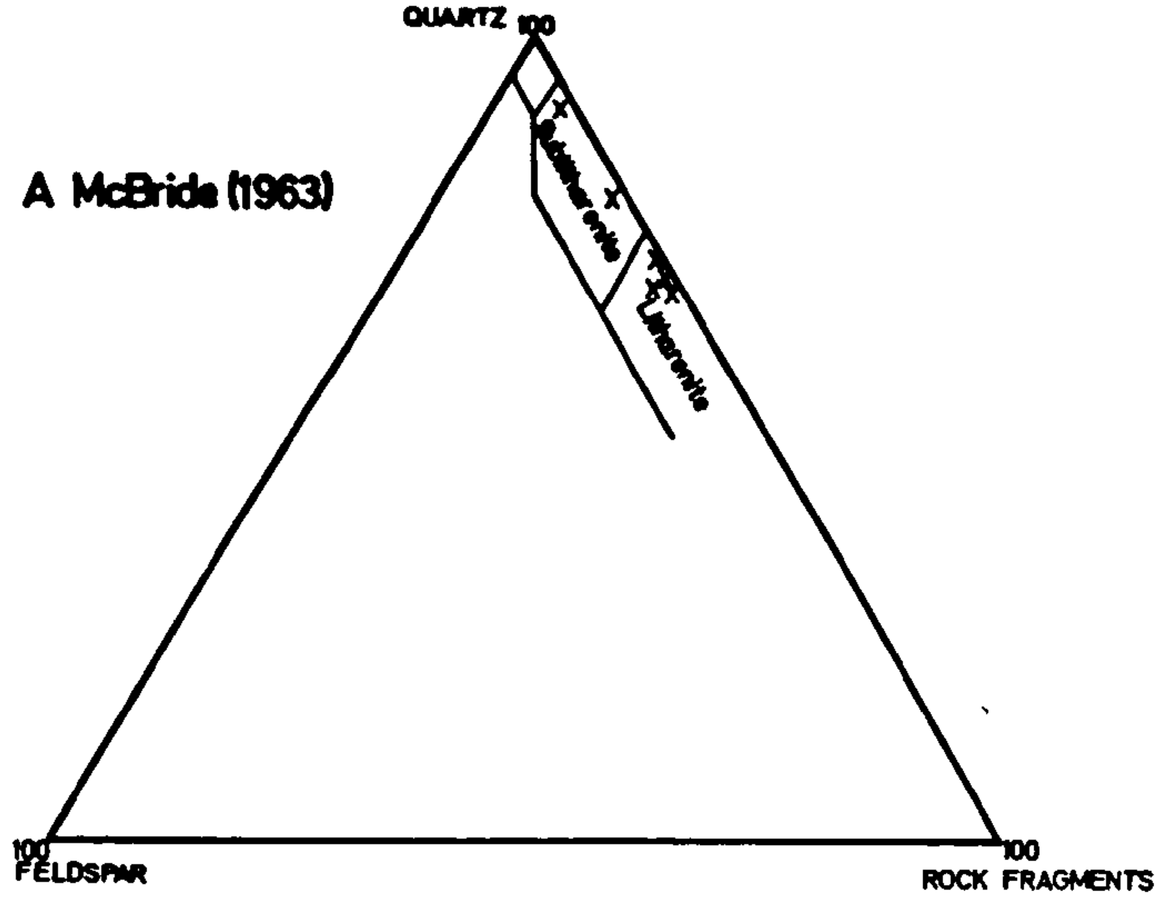

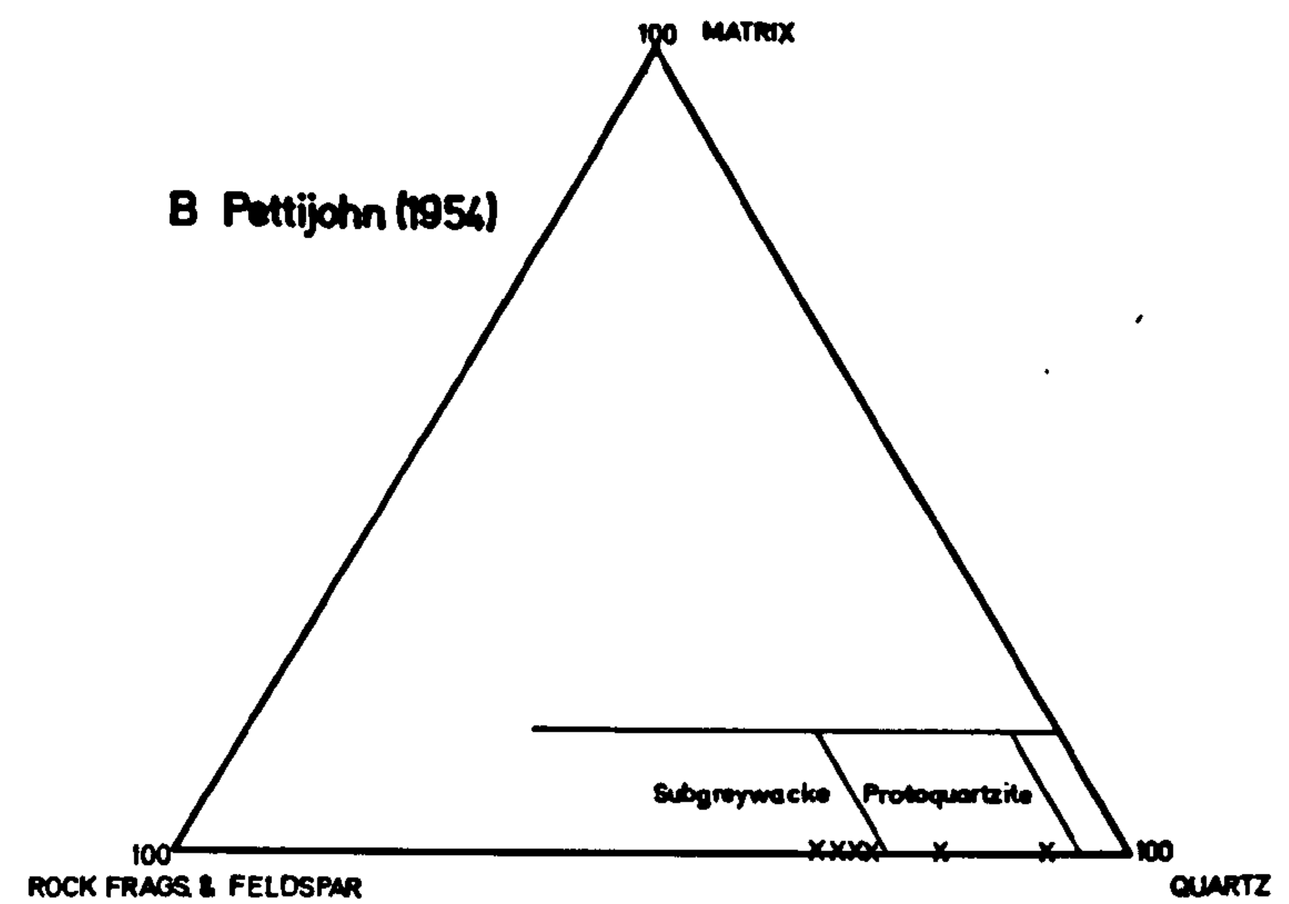

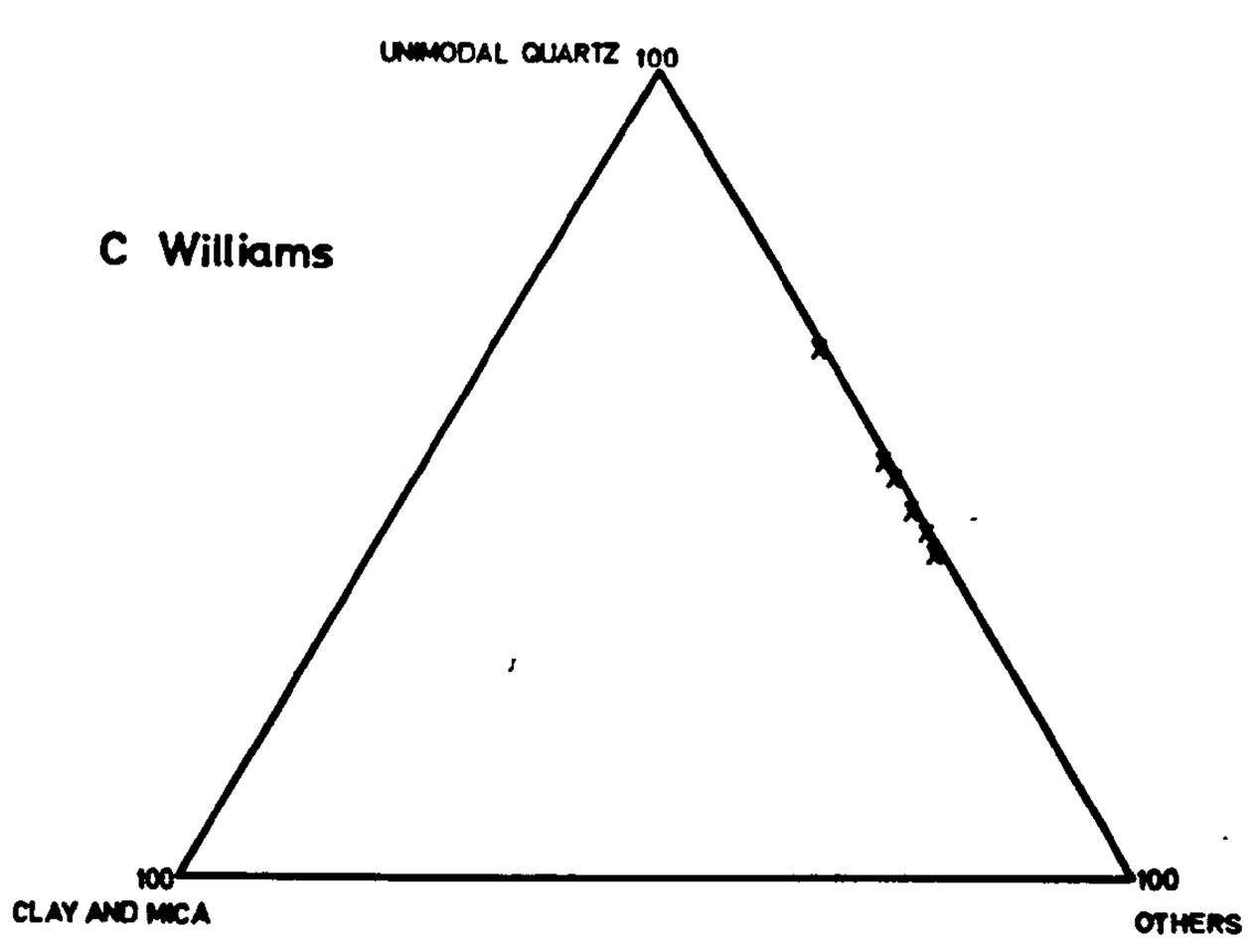

Fig. 14.3. Classification of the Dunrobin Castle Sandstones.

Polycrystalline quartz

Polycrystalline quartz constitutes 15-30 per cent of the total detrital grains, the highest percentage being found in the coarser grained grits and conglomerates. Two main types of polycrystalline can be identified, these being termed schistose and globular polycrystalline quartz.

The schistose polycrystalline quartz grains display highly strained quartz units elongated parallel to a lineation. The grains are highly sutured at the contacts and this, together with their strained appearance, suggest that they were derived from high grade metamorphic areas. This type of quartz represents 3-8 per cent of the total rock volume.

The globular polycrystalline quartz is more common and constitutes approximately 20 per cent of the total rock volume. No elongation of the quartz units is seen suggesting that the globular polycrystalline quartz are derived from a lower grade metamorphic rock.

It is suggested that both these types of quartz were originally derived from the metamorphic Moinian quartzites and granulites although their immediate source may have been from the Old Red Sandstone.

Rock Fragments

Rock fragments contribute 10-35 per cent of the total detrital grains and are characterised solely by caliche and chertified cornstones. The caliche can be recognised as being mainly derived from the indurated zone and represents 4-24 per cent of the total rock volume. The high percentage would suggest that it has been derived locally from the underlying Golspie Cherty Rock. The fragments rarely contain quartz and illustrate the characteristic dense microcrystalline calcite of the induratedcaliche. Some examples do show pseudo oolitic and laminated structures. Friable caliche is rare suggesting that either they were not exposed or that it was less likely to be preserved; the former is thought to be most probable.

Chertified cornstones are less common, the chert tending to be coarser grained and illustrating similar replacement features to those from

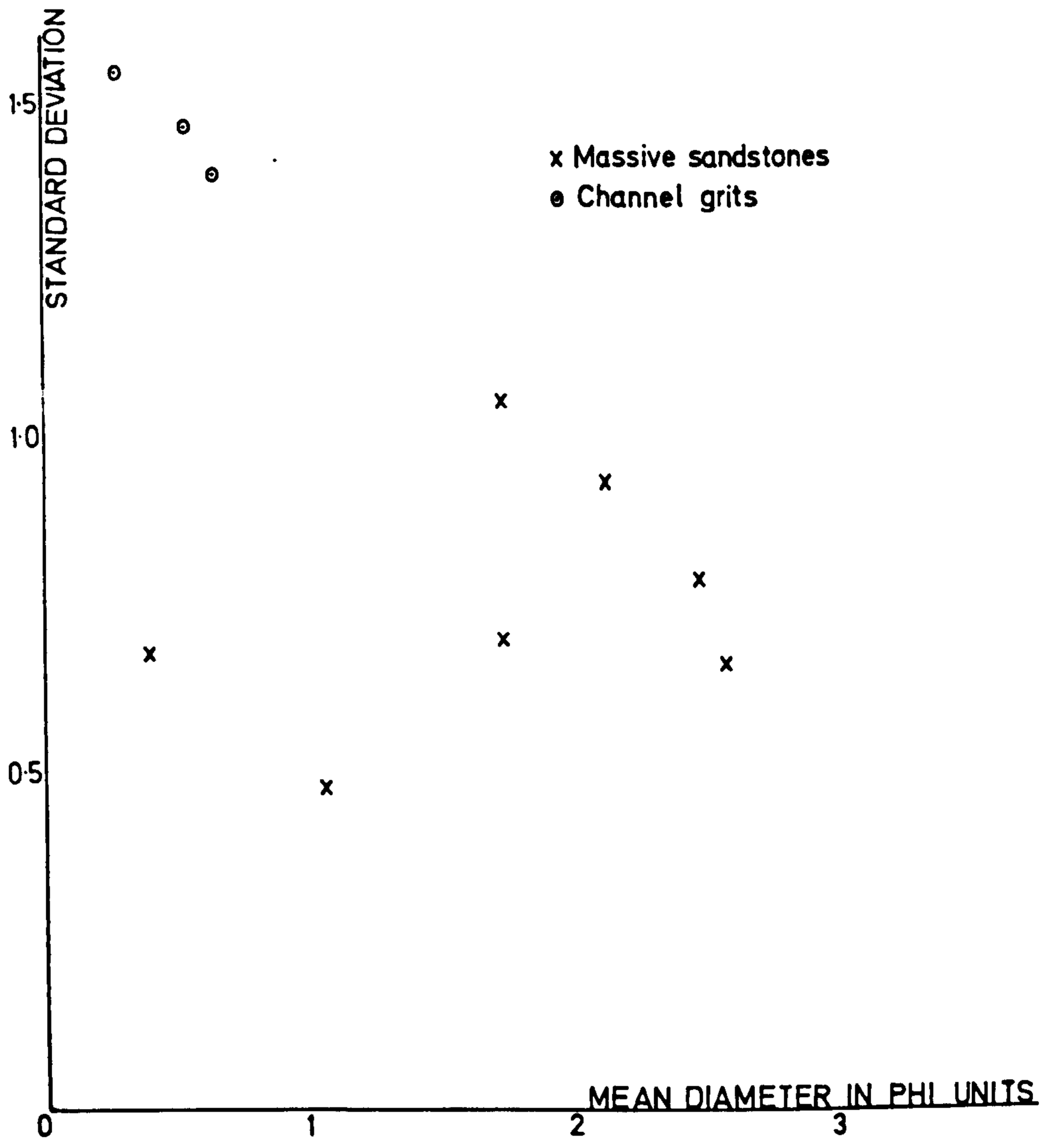

Fig. 14.4. Standard deviation plotted against mean diameter for the Dunrobin Castle Sandstones.

the Old Red Sandstone of the Elgin area. This view is substantiated by the iron staining in the cornstones which is not present in the Triassic caliches.

Feldspar

The maximum percentage of feldspar found in any sample was 3 per cent but the average percentage was generally nearer to 1 per cent. Orthoclase is the commonest feldspar and normally is found in a highly weathered state; they are often sericitised and stained by iron oxides. Microcline is also rarely present but no evidence of plagioclase feldspar has been found.

Heavy minerals, clays and mica

The Dunrobin Castle Sandstones display a total absence of clays and micas and also a relative paucity of heavy minerals. Where present, the heavy minerals are generally zircon although rare grains of apatite and tourmaline have been identified.

DEPOSITIONAL FRAMEWORK OF THE GOLSPIE TRIASSIC

The dominant source of the Golspie Triassic was clearly the Old Red Sandstone, local caliche and metaquartzites of Moinian age. The lack of granitic fragments suggests that they were either not exposed at this time or, more probably, that the sediments were essentially local in origin.

The three main sediment types are recognised: caliche, channel conglomerates and massive sandstones. It is suggested that they represent the deposits of the distal end of an alluvial fan. The massive sandstones can be compared to sheetflood-like deposits, the lack of sedimentary structures being partially original and partially due to later obliteration by percolating caliche solutions. The channel conglomerates were formed during periods of large scale flooding carrying coarser material further away from the source area. During long periods of sub-aenal exposure the alluvial fan would be stabilised by the development of a caliche soil horizon. This association of facies is common to many modern day alluvial fans in Baja California (Walker, 1967). The absence of clays and micas can then be explained by removal of the finer material from the top of the alluvial fans by aeolian agencies.

CHAPTER 15

MORAY FIRTH BOREHOLE DATA

The search for oil and gas in the North Sea began in 1964 and has expanded ever since. The results from the boreholes have enabled the Permo-Triassic succession to be correlated over a wide area with a resultant greater understanding of the associated sedimentological problems. Much of the information remains on closed file but the author is indebted to Hamilton Brothers Oil Company and Total Oil Marine for their close co-operation and for the results which are discussed in the following sections.

Preliminary geophysical investigations in the Moray Firth (Collette, 1968) indicated the possible existence of a basin occupying the position of the present day Moray Firth during Permo-Triassic times. The presence of a large negative anomaly was first interpreted as a granite batholith by Collette, (1968) but the general opinion now, is that the anomaly represents a large sedimentary basin (e.g. Sunderland, 1972); it was first called the Elgin Basin by Audley-Charles (1970). Palaeocurrent data from the Triassic of Golspie and Elgin also indicate drainage into a basin occupying the approximate position of the present day Moray Firth.

The following results are a summary of Hamilton Brothers Oil Company Well 12/26-1:

	DEPTH
Lower Bajocian sediments	
Unconformity	
Sandstones alternating with silts, thick anhydrites and limestones. The sands are fine to very fine grained and angular in outline. Dolomites are sometimes present. 31m.	1304m.
Red to maroon sandstones alternating with minor silts. Sandstone predominates by approximately 5:1. Silts reach a maximum of 5 metres in thickness and frequently have associated gypsum. 182m.	1335m.

	DEPTH
Red kaolinitic silts with minor sandstones up to 5m in thickness. Silts are highly micaceous. 76m.	1517m.
Alternating limestones and anhydrite, with anhydrite predominating. Sandstones intercalate with the evaporites and represent 50 per cent of the horizon. 24m.	1593m.
Red to maroon silts with minor micaceous sandstones. 51m.	1617m.
Thick sequence of anhydrite and limestones (?dolomites) alternating with minor sandstone horizons. 76m.	1668m.
Thick sandstones with infrequent gypsum horizons. 28m.	1744m
End of drilling.	1772m.

The results from 12/26-1 can be further supplemented by the following information released by the Total Oil Marine Company (personal communication). The information is based on drilling results from wells 12/26-1, 12/21-1, 12/22-1 and 12/23-1.

1. The Elgin Basin was open to the east, probably from the very beginning of the Permian.
2. An important marine incursion occurred during some part of the Zechstein but terrigenous sedimentation persisted.
3. After the marine incursion a thick series of silts accumulated.
4. In their lower part these bear some evidence of marine influence but appear to have been continental deposits for the main part.
5. A marine incursion (after a period of erosion) closed sedimentation in the Permo-Trias.

Brunstrom (1969) notes that in the southern part of the North Sea Basin, the deposition of evaporites marks the incoming of a marine incursion. Fig. 3.3 illustrates a summary of the sedimentation in borehole 12/26-1 and indicates a distinct cyclicity in the pattern of Permo-Triassic stratigraphy

in the Elgin Basin. This cycle is designated the Ideal Cycle and is discussed in the following section.

IDEAL CYCLE

Fig. 3.3 indicates that the deposition of evaporites is generally followed by marine silts, intertidal silts and finally continental sandstones. There are therefore four main units to the cycle:

(a) Evaporites

(b) Marine silts

(c) Continental or Intertidal silts

(d) Continental sandstones

(a) Evaporite unit

The Elgin Basin was open to the east where it was periodically joined to the main Norwegian Basin during periods of marine incursion. At other times, the basin acted as a discrete unit and continental sedimentation prevailed. The interdigitation of the evaporites with intertidal silts would suggest that they are of a shallow water origin. The boreholes only indicate the presence of dolomites, limestones and anhydrite but the limited nature of the boreholes does not rule out potash/magnesium salts being deposited elsewhere in the basin. Brunstrom (1969) suggests that the presence of anhydrite indicates that the limit of the marine incursion was within a few miles of their site of deposition. From the position of the boreholes this would suggest that the evaporites were confined to the centre of the basin.

(b) and (c) Silt unit

Brunstrom (1969) documents the presence of silts interbedded with evaporites in the Southern North Sea Basin and notes that these are intertidal in origin. In the Elgin Basin, the silts are marine at the base and grade up into intertidal silts with no marine fauna. The environment envisaged for the evaporites and silts of the Elgin Basin is similar to that seen in Baja California at the present day (Thompson, 1968).

(d) Sandstone unit

The sandstones are composed of fine to very fine grained angular quartz of continental origin. The presence of thin laminae of interbedded gypsum would support the theory that they represent the upper horizons of the intertidal flat. Continental evaporites are at present forming in similar environments of the upper intertidal flat of the Persian Gulf (Shearman, 1966) and Baja California (Thompson, 1968) and there is also evidence of analagous deposits in the Southern North Sea during the Permo-Trias (Brunstrom, 1969; Kent and Walmsley, 1970). The high carbonaceous content of some of the sandstones indicates the possible proximity of deltaic deposits (Texaco Oil Company, personal communication). This assumption is substantiated by the presence of coarse grained point bar deposits at Elgin which, in modern rivers, often progress into deltaic deposits.

CHAPTER 16

PALAEGEOGRAPHY, FRAMEWORK AND HISTORY OF THE NEW RED SANDSTONE ELGIN BASIN

Evidence for a basin occupying the position of the present day Moray Firth is first seen during the Lower Old Red Sandstone when a series of lacustrine sediments were laid down in a fault bounded basin (Geikie, 1878; Compagnie Francais des Petroles, 1969). Deposition continued into the Upper Old Red Sandstone but no evidence of Carboniferous sedimentation is seen at the present day.

Onshore evidence at Elgin indicates that deposition began again during the Upper Permian or early Triassic. However, the borehole results from the Moray Firth indicate that deposition in the centre of the basin began much earlier in the Permian. Sedimentation has continued from Permian times until the present day (Total Oil Marine and Hamilton Brothers Oil Company, personal communication). It is suggested that the basin was fault controlled and that the beginning of sedimentation during the Permian is intimately associated with secondary movement along Caledonian faults during the initial stages of the opening of the North Atlantic (Hallam, 1970).

The presence of a deep sedimentary basin occupying the present day position of the Moray Firth is now generally accepted (Kent, 1967; Audley-Charles, 1970; Warrington, 1970; Wills, 1970; Sunderland, 1972). However, reconstruction of the Permo-Triassic Elgin Basin must take into account the major structural events which have occurred since the Triassic. The controlling structural feature of the basin is the Great Glen Fault, a sinistral wrench fault with a displacement of 65 miles. The main movement took place between the Lower and Middle Old Red Sandstone although recent work by Holgate (1969) indicates that a dextral movement of 26 miles occurred in the Tertiary. There is also evidence for movement along faults parallel to the Great Glen Fault during the Jurassic (Helmsdale Fault) and thus movement along the Great Glen Fault probably

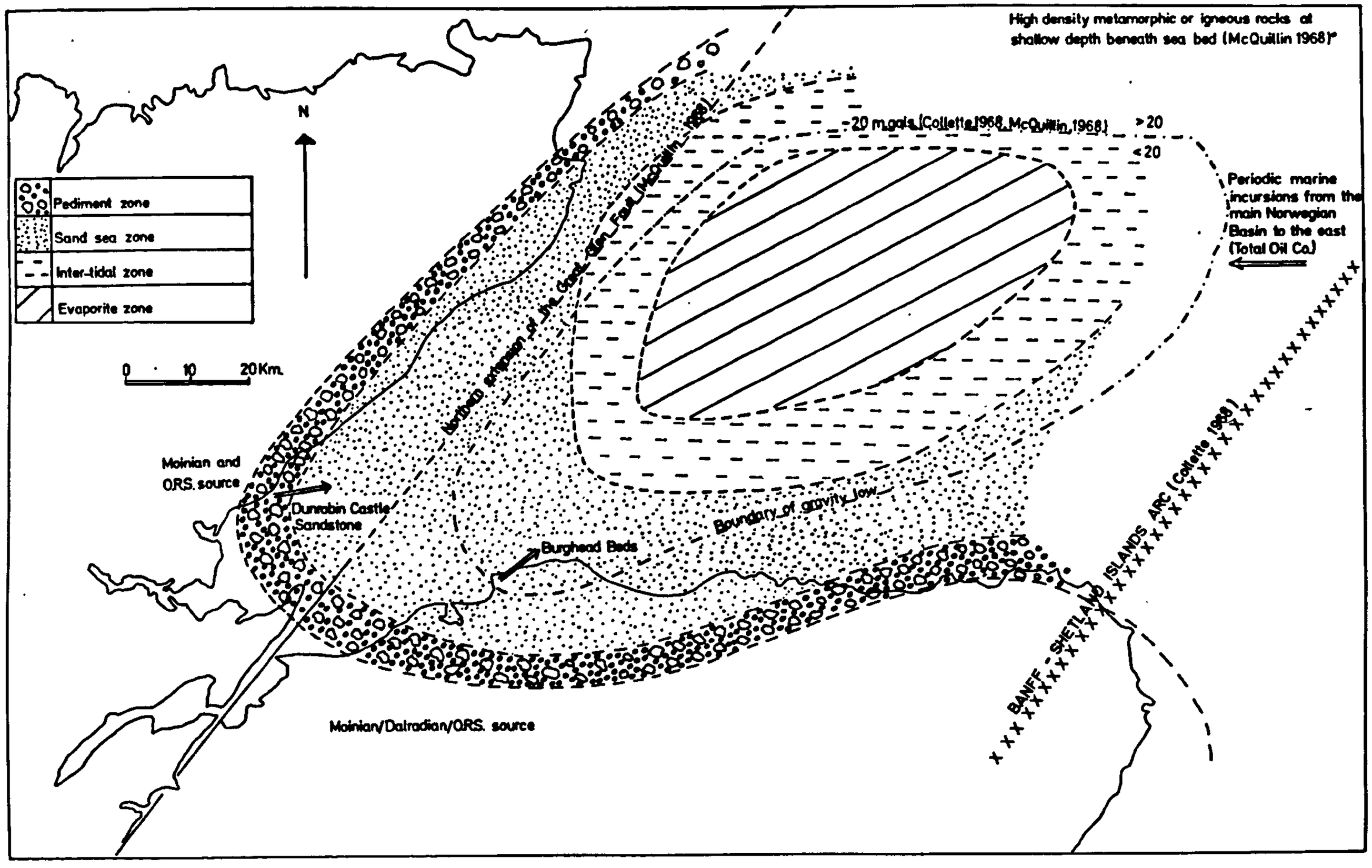

Fig. 16.1. Palaeogeography of the New Red Sandstone Elgin Basin

continued from the Old Red Sandstone through to the Tertiary. However, as there are no precise measurements of this movement, all reconstructions of the Permo-Triassic Elgin Basin only include a dextral movement of 26 miles along the Great Glen Fault relative to the present day position (Fig. 16.1).

Definition of the northern limit of the basin shown in Fig. 16.1 is based on the work of McQuillin (1968) who suggests that a negative anomaly to the north of Wick represents the northern limit of the basin in the Moray Firth. He interprets the anomaly as being due to a series of high density igneous or metamorphic rocks at a shallow depth beneath the sea bed. The western limits of the basin are based on the lateral extent of the Triassic alluvial fan deposits at Golspie which would indicate that the source was within a few miles to the west. As the basin is fault controlled, the edge of the basin is put parallel to the main north east to south west Helmsdale Fault which appears to have controlled sedimentation during both the Old Red Sandstone and the Jurassic.

In the Elgin area, on the southern margin of the basin, deposition did not begin until the Upper Permian or early Triassic. Sedimentation commenced with a series of sheetflood deposits indicating the proximity of the source at this time (Fig. 16.2). As the faulting in this region generally has an east-west trend, the southern limit of the basin is drawn as an east-west line to the south of Elgin.

The Elgin Basin was periodically joined to the main Norwegian Basin to the east which was dominantly marine, whereas the Elgin Basin was dominantly continental in character. The periodic nature of the marine incursions may indicate that some sort of barrier existed between the two basins. It is therefore tentatively suggested that the eastern limit of the basin is defined by the Banff-Shetland Islands Arc (Collette, 1968).

Four main zones of sedimentation can be recognised in the Permo-Triassic Elgin Basin and although minor variations may exist, the model fits in well with similar environments in the south of the Permo-Triassic North Sea Basin (Figs. 16.1 and 16.2).

PEDIMENT ZONE

The pediment zone represents an area probably within 3-4 kilometres of the mountain source where the principal sediments are sheetflood and alluvial fan deposits. The source of the sediment in the pediment was the weathered talus which formed in response to the chemical and mechanical break up of the source material, and which was then deposited during periods of flash flooding. Petrological evidence clearly indicates that the material was derived from a dominantly Moinian and Old Red Sandstone source area.

The alluvial deposits formed as alluvial fans around valley mouths and in confined channels. These pass laterally into more extensive sheetflood deposits (Fig. 16.2). Caliche soil horizons are also sometimes present in this zone especially associated with the alluvial fans. Reptiles, found in association with the sheetflood deposits, probably lived in shallow pools on the edge of the sand sea and the pediment zone. There is little diversity in the remains which would suggest that the reptiles were highly specialised for this particular environment.

SAND SEA ZONE

The pediment zone graded laterally into extensive aeolian deposits of the sand sea zone; the aeolian deposits extended over a large area and may have occupied up to 50 per cent of the total area of the basin.

Near to the source area, seif dunes often formed where the mountain source diverted the dominant north east winds to produce a complex helicoidal flow necessary to form seif dunes. However, away from the source, the greater percentage of the sand sea was occupied by barchan dunes formed by the dominant north east trade winds.

This dominant north east palaeowind direction is in agreement with the results obtained from other Permo-Triassic dune sands British Isles by several workers (Shotton, 1937; Shotton, 1956; Runcorn, 1962; Opdyke, 1961; Laming, 1966; Thompson, 1969; Piper, 1970; Waugh, 1970). The palaeowind direction

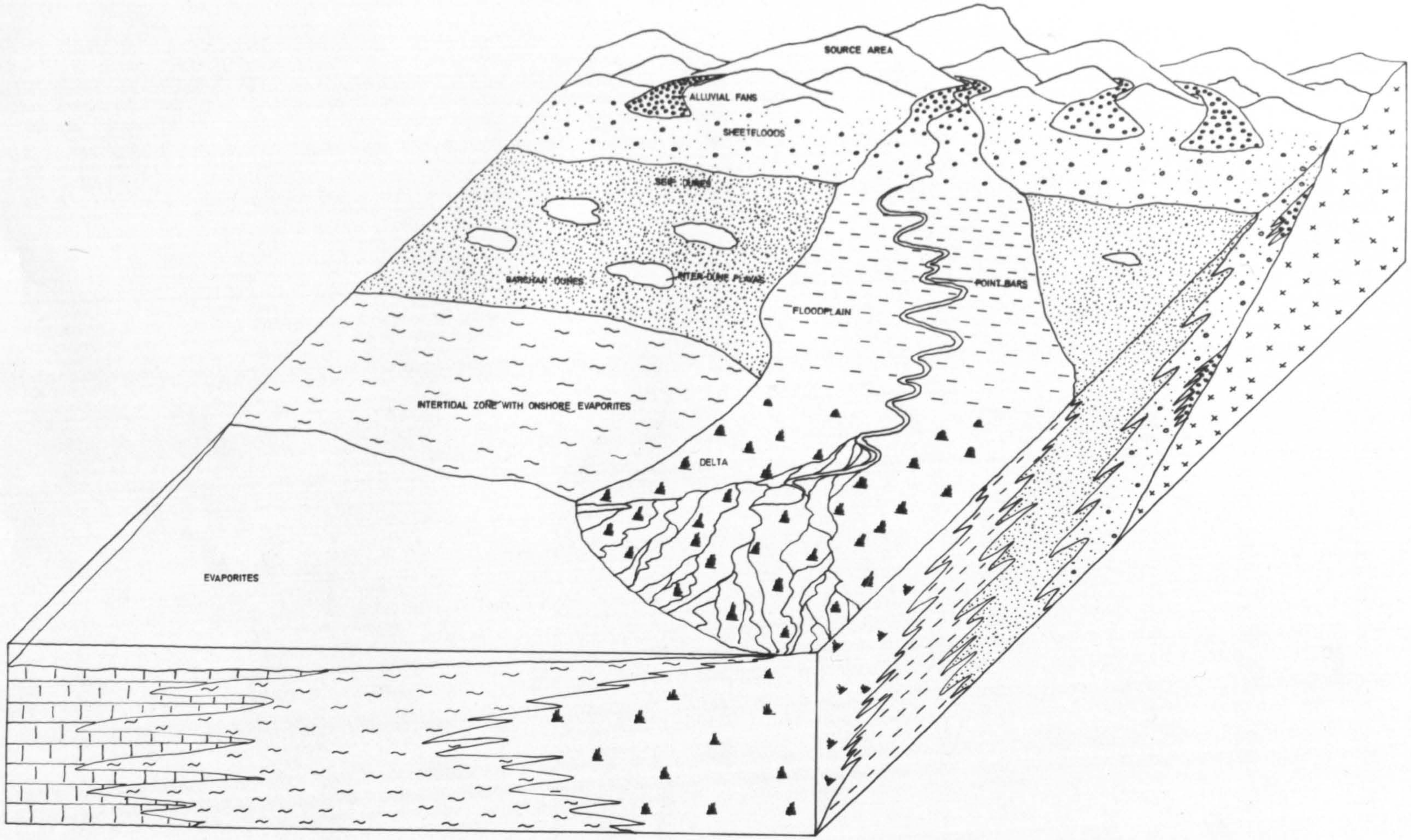

Fig. 16.2. Reconstruction of the southern part of the Elgin Basin during Triassic times.

of the Lossiemouth Sandstone (Fig. 16.3) is the first Upper Triassic record from the British Isles. The south westerly palaeowind direction, and the absence of any easterly winds, indicates that the North of Scotland was not under the influence of the Trade Wind Belt at this time, and it is probable that Elgin was either:

1. Under the influence of the Westerly Wind Belt during the Upper Triassic or,
2. It was in a position equivalent to the present day Horse Latitudes, in which case the south west winds are purely local in origin.

The sheetfloods of the pediment zone had their lateral extension in the form of playa lake deposits which were formed where the progress of the floods were halted by the damming effect of the large barchan dunes. The downstream equivalents of the alluvial fans were coarse grained point bar deposits. This type of fluvial system is characterised by low sinuosity, gradients of 2-3 feet per mile, bank stabilisation by vegetation and short duration peak flow. During the peak discharge the river formed large point bars but quickly reverted to a shallow braided river system and finally to complete desiccation. The rivers also had associated floodplain deposits which reached distances of up to 3-5 kilometres from the main channel. However, these floodplain deposits were frequently reworked by the wind and replaced by dunes.

Reptilian remains which have been found in this zone (Walker, 1961) have been shown to be adapted to two different modes of life. The first probably lived on floodplains whereas the second type, which was adapted to a life on a sandy terrain, probably lived on the aeolian dunes on the edge of the floodplain or close to the interdunal areas.

INTERTIDAL ZONE

Basinwards, a series of alternating fine grained sandstones and silts are interpreted as intertidal deposits. Where the fine grained sandstones predominate, interbedded gypsum also occurs suggesting that this lithology may represent the upper intertidal flat. The high carbonaceous content of some of

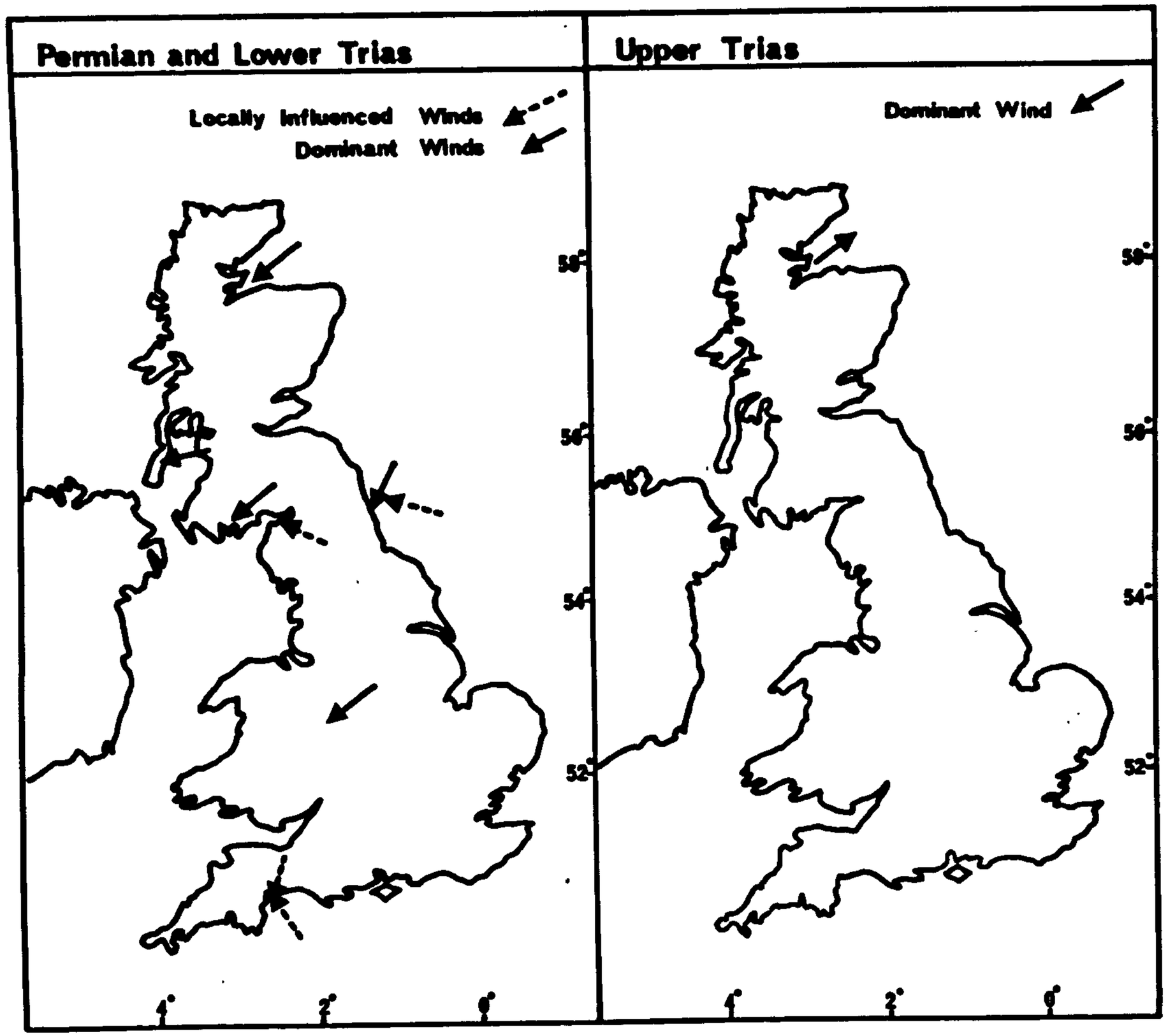

Fig. 16.3. Palaeowind directions in the British Isles during New Red Sandstone times.

the sediments may indicate the presence of deltas, these being the downstream extension of the point bar deposits as seen in many modern day rivers. The environment is thought to have been similar to the present day intertidal areas of Baja California (Thompson, 1968).

EVAPORITE ZONE

Towards the basin centre, the Moray Firth boreholes show the presence of limestones, dolomites and anhydrite which were formed subsequent to marine incursions from the main Norwegian Basin to the east. However, even while the evaporites were forming, terrestrial sedimentation persisted. The evaporites are thus thought to have formed in extremely shallow water until they were ultimately replaced by the intertidal sediments.

REFERENCES

ALLEN, J. R. L., 1965 — Origin and characteristics of recent alluvial sediments. Sedimentology, 5,89-191

ALLEN, J. R. L., 1970 — Physical processes of sedimentation. Unwin, London. 248 pp.

ARISTARAIN, L. F., 1970 — Chemical analyses of caliche profiles from the High Plains, New Mexico. J.Geol., 78,201-212

AUDLEY-CHARLES, M. G., 1970 — Stratigraphic correlation of the Triassic rocks of the British Isles. Q.J1.geol. Soc. London, 129,19-48

BAGNOLD, R. A., 1941 — The physics of blown sand and desert dunes. Methuen. London. 265 pp.

BAGNOLD, R. A., 1953 — The surface movement of blown sand in relation to meteorology. In Desert Research. UNESCO. Jerusalem. pp. 89-96

BAGNOLD, R. A., 1954 — Some flume experiments on large grains but little denser than the transporting fluid, and their implications. Inst. Civ. Eng. Proc. Paper, 6041, 174-205

BEAL, M. A., and ONASICK, E. P., 1970 — Stratigraphic habitat of Mississippi Valley type orebodies. Trans. Instn. Min. Metall., 79,B145-154

BERNARD, H. A. and MAJOR, C. F., 1963 — Recent meander belt deposits of the Brazos River; an alluvial sand model. Bull. Am. Assoc. Petrol. Geol., 47:350 (abstract)

BLATT, H. and CHRISTIE, J.M., 1963 — Undulatory extinction in quartz of igneous and metamorphic rocks and its significance in provenance studies in sedimentary rocks. J. sedim. Petrol., 33,559-579

BOERSMA, J. R., VAN de MEENE, E. A., and TJALSMA, R. C., 1968 — Intricated cross stratification due to the interaction of a mega ripple with its leeside system of backflow ripples. Sedimentology, 11,147-162

BROWN, C. N., 1956 — The origin of caliche on the north eastern Llano Estacado, Texas. J. Geol., 64,1-15

BRUNSTROM, R. G. W., and WALMSLEY, P. J., 1969 — Permian evaporites in the North Sea Basin. Bull. Am. Assoc. Petrol. Geol., 53,870-883

BUSH, P. R., 1970 — Chloride rich brines from sabhka sediments and their possible role in ore formation. Trans. Instn. Min. Metall., 79,B137-144

COLLETTE, B. J., 1960 — The gravity field of the North Sea. Gravity Exped. Sea., 5,47-96

COLLETTE, B. J., 1968 — On the subsidence of the North Sea area. In Donovan, 1968, Geology of the Shelf Seas. Oliver and Boyd. Edinburgh. 160 pp.

COMPAGNIE FRANCAIS des PETROLES, 1969 — Contribution a l'etude sedimentologique des terrains Devoniens du Nord-Est de L'Ecosse. Notes et Memoires, 9, 83 pp.

COOPER, J. R., 1943 — Flow structures in the Berea Sandstone and Bedford Shale of central Ohio. J. Geol., 51,190-203

CRAIG, G. Y. — The geology of Scotland. Oliver and Boyd. Edinburgh

DARRAGH, P. J., GASKIN, A. J., TERRELL, B. C., and SANDERS, J. V., 1966 — Origin of precious opal. Nature, 209,13-16

DAVIDSON, C. F., 1964 — Some genetic relationships between ore deposits and evaporites. Trans. Instn. Min. Metall., 75,B216-225

DONOVAN, D. T., 1968 — Geology of the Shelf Seas. Oliver and Boyd. Edinburgh. 160 pp.

DUNHAM, K. C., 1952 — Fluorspar. 5th edit. Mem. Geol. Surv. U.K. Min. resources, 4. 30 pp.

DUNHAM, K. C., 1966 — Role of juvenile solutions, connate waters and evaporitic brines in the genesis of lead, zinc, fluorine-barium deposits. Trans. Instn. Min. Metall., 75,B226-229

DUNHAM, K. C., 1970 — Mineralisation by deep formation waters; a review. Trans. Instn. Min. Metall., 79,B127-136

EDEN, R. A., SMALL, A. V. E., and McQUILLIN, R., 1970 — Preliminary report on the marine geological and geophysical work off the east coast of Scotland, 1966-1968. Inst. geol. Sci. Rep. No. 70/1

FAIRBRIDGE, R. W., 1947 — Possible causes of intraformational disturbances in the Carboniferous varve rocks of Australia. Roy. Soc. N.S.W. J., 70,114-120

FENNING, P. J., 1968 — in Geology of the Elgin district. Mem. Geol. Surv. U.K.

FOLK, R. L. 1954 — The distinction between grain size and mineral composition in sedimentary rock nomenclature. J. Geol., 62,344-359

FOLK, R. L., 1968 — Bimodal supermature sandstones; product of the desert floor. Int. Geol. Congr. Prague, 8,9-32

FOLK, R. L., 1970 — Longitudonal dunes of the northwest edge of the Simpson Desert, Northern Territory, Australia. 1. Geomorphology and grain size relationships. Sedimentology, 16,5-54

FOLK, R. L., 1971 — Length slow chalcedony; a valuable criterion for the recognition of evaporitic strata. Int. Sedim. Congr. 1971. Heidelberg, (abstracts)

FOLK, R. L., and WARD, W. C., 1957 — Brazos River Bar; a study in the significance of grain size parameters. J. sedim. Petrol. 27,3-26

FRAZIER, D. E. and OSANICK, A., 1961 — Point-bar deposits, Old River Locksite, Louisiana. Trans. Gulf Cst. Ass. Geol. Socs. 11,121-137

FRIEND, P. F., 1966 — Clay fractions and colours of some Devonian red beds in the Catskill Mountains, U.S.A. Q. J1. geol. Soc. London, 122,273-292

GALLAGHER, M. J., 1970 — Galena-fluorite mineralisation near Lairg, Sutherland. Trans. Instn. Min. Metall. 79,B182-184

GALLAGHER, M. J., 1971 — New evidence of uranium and other mineralisation in Scotland. Trans. Instn. Min. Metall. 80,B150-173

GEIKIE, A., 1878 — On the Old Red Sandstone of Western Europe. Trans. Roy. Soc. Edin. 34,345-452

GILBERT, C. M., 1955 — in Williams, H., Turner, F. J., and Gilbert, C. M. Petrography. W. H. Freeman. San Francisco. 406 pp.

GLENNIE, K. W., 1970 — Desert sedimentary environments. Developments in Sedimentology, 14. Elsevier. Amsterdam

GREENSMITH, J. T., 1963 — Clastic quartz, provenance and sedimentation. Nature, 197,345-347

GUY, H. P., SIMONS, P. B., and RICHARD, E. V., 1966 — Summary of alluvial channel data from flume experiments, 1956-1961. Prof. Pap. U.S. Geol. Surv. 462-I. 96 pp.

HALLAM, A., 1970 — Mesozoic geology and the opening of the North Atlantic. J. Geol. 79,129-157

HOLGATE, N., 1969 — Palaeozoic and Tertiary transcurrent movements on the Great Glen Fault. Scott. J. Geol. 5,97-139

INMAN, D. L., 1952 — Measures for describing the size distribution of sediments. J. sedim. Petrol. 22,125-145

INMAN, D. I., EWING, G. C., and CORLISS, J. B., 1966 — Coastal sand dunes of Guerro Negro, Baja California, Mexico. Bull. Geol. Soc. Am. 77,787-802

JONES, J. P., 1962 — Deformed cross stratification in the Cretaceous Bima Sandstone, Nigeria. J. sedim. Petrol. 32,231-239

JUDD, J. W., 1873 — The secondary rocks of Scotland. Q. Jl. Geol. Soc. London. 29,97-197

JUDD, J. W., 1886 — Presidential address to section C (Geology) Rep. Brit. Assoc., Aberdeen. 1885. 994-1013

KENT, P. E., 1967 — Outline geology of the southern North Sea Basin. Proc. Torks. geol. Soc. 36,1-22

KENT, P. E., and WALMSLEY, P. J., 1970 — North Sea progress. Bull. Am. Assoc. Petrol. Geol. 54,168-181

KRAUSKOPF, K. B., 1956 — Dissolution and precipitation of silica at low temperatures. Geochim. cosmochim. Acta. 10,1-26

KRUMBEIN, W. C., 1941 — Measurement and geological significance of shape and roundness of sedimentary particles. J. sedim. Petrol. 11,64-73

KUENEN, PH. H., 1949 — Slumping in the Carboniferous rocks of Pembrokeshire. Q. Jl. Geol. Soc. London. 104,365-385

KUENEN, PH. H., 1960 — Experimental abrasion, 4; Eolian action. J. Geol. 68,427-449

LAMING, D. J. C., 1958 — Fossil winds. J. Alberta. Soc. Petrol. Geol. 6,179-183

LAMING, D. J. C., 1966 — Imbrication, paleocurrents and other sedimentary features in the Lower New Red Sandstone, Devonshire, England. J. sedim. Petrol. 36,940-959

LAND, L. S., 1964 — Eolian cross bedding in the beach dune environment, Sapelo Island, Georgia. J. sedim. Petrol. 34,389-394

LLEWELLYN, P. G., and STUBBINS, R., 1968 — Lower Carboniferous evaporites and mineralisation in the eastern and central Midlands of Britain. Trans. Instn. Min. Metal.. 77,B170-173

MACKIE, W., 1897 — The sands and sandstones of Eastern Moray. Trans. geol. Soc. Edin. 7,148-172

MACKIE, W., 1901 — The occurrence of barium sulphate and calcium fluoride as cementing substances in the Elgin Trias. Rep. Brit. Assoc., Glasgow, 1901. 649-650

MACKIE, W., 1901 — The pebble band of the Elgin Trias and its wind worn pebbles. Rep. Brit. Assoc., Glasgow, 1901. 650-651

MACKIE, W., 1925 — The principles that regulate the distribution of particles of heavy minerals in sedimentary rocks, as illustrated by the sandstones of the North East of Scotland. Trans. Edin. geol. Soc. 11,138-164

McBRIDE, E. F., 1960 — A classification of common sandstones. J. sedim. Petrol. 33,664-669

McGOWEN, J. H. and GARNER, L. E., 1969 — Physiographic features and stratification types of coarse grained point bars; modern and ancient examples. Sedimentology 14,77-111

McKEE, E. D., 1966 — Structures of dunes at White Sands National Monument, New Mexico. Sedimentology 7,1-69

McKEE, E. D., CROSBY, E. J., and BERRYHILL, H. L., 1967 — Flood deposits, Bijou Creek, June 1965. J. sedim. Petrol. 37,829-851

McKEE, E. D., REYNOLDS, M. A., and BAKER, C. H., 1962 — Experiments on intraformational recumbent folds in cross-bedded sand. U.S. Geol. Surv. Profess. Papers 450D,155-160

McKEE, E. D., and TIBBITTS, G. C., 1964 — Primary structures of a seif dune and associated deposits in Libya. J. sedim. Petrol. 34,5-17

McKEE, E. D., and WEIR, G. W., 1953 — Terminology for stratification and cross stratification in sedimentary rocks. Bull. Geol. Soc. Am. 64,381-390

McQUILLIN, R., 1968 — Geophysical surveys in the Orkney Islands. Inst. geol. Sci. Geophysical Paper No. 4. 18 pp.

MOORBATH, S., 1962 — Lead isotope abundance studies on mineral occurrences in the British Isles and their geological significance. Phil. Trans. Roy. Soc. A. 254,295-360

MURCHISON, R. I., 1859 — On the sandstones of Morayshire containing reptilian remains; and on their relations to the Old Red Sandstone of that country. Q. Jl. Geol. Soc. London, 15,419-439

NEWTON, E. T., 1893 — On some new reptiles from the Elgin Sandstones. Phil. Trans. Roy. Soc. Series B 184,431-503

NORRIS, R. M., 1969 — Dune reddening and time. J. sedim. Petrol. 39,7-11

OPDYKE, N., 1961 — The palaeoclimatological significance of desert sandstones. In Nairn (editor), Descriptive palaeoclimatology. Interscience Publishers, New York

PARRY, W. T., and REEVES, C. C., 1968 — Clay mineralogy of pluvial lake sediments, southern High Plains, Texas. J. sedim. Petrol. 38,516-579

PEACOCK, J. D., BERRIDGE, N. G., HARRIS, A. L. and MAY, F., 1966 — Contorted beds in the Permo-Triassic aeolian sandstones of Morayshire. Bull. Geol. Surv. Gt. Brit. No. 24. 157-162

PEACOCK, J. D., 1968 — Geology of the Elgin district. Mem. Geol. Surv. U.K.

PETTIJOHN, F. J. 1954 — Classification of sandstones. J. Geol. 62,360-365

PHILLIPS, J. G., 1886 — The Elgin sandstones. Rep. Brit. Assoc., Aberdeen, 1885. 1023-24

PIPER, D. J. W., 1970 — Eolian sandstones in the basal New Red Sandstone of Arran. Scott. J. Geol. 6,295-308

POWERS, M. C., 1953 — A new roundness scale for sedimentary particles. J. sedim. Petrol. 23,117-119

READ, H.H., 1925 — Geology of the country around Golspie, Sutherlandshire. Mem. Geol. Surv. U.K.

REEVES, C. C., 1970 — Origin, classification and geological history of caliche on the southern High Plains, Texas and eastern New Mexico. J. Geol. 78,352-362

RIGBY, J. K., 1958 — Mass movement in Permian rocks of Trans-Pecos, Texas. J. sedim. Petrol. 28,298-315

RILEY, N. A., 1941 — Projection sphericity. J. sedim. Petrol. 11,94-97

RUNCORN, S. K., 1962 — Climatic changes through geological time in the light of the palaeomagnetic evidence for polar wandering and continental drift. Q. J1. Roy. met. Soc. 87,282-313

SAWKINS, F. J., 1966 — Preliminary fluid inclusion studies of the mineralisation associated with the Hercynian granites of south west England. Trans. Instn. Min. Metall. 75,B109-112

SELLEY, R. C., SHEARMAN, D. J., SUTTON, J., and WATSON, J., 1963 — Some underwater disturbances in the Torridonian of Skye and Raasay. Geol. Mag., 100,224-243

SHEARMAN, D. J., 1966 — Origin of marine evaporites by diagenesis. Trans. Instn. Min. Metall. 75,B208-215

SHOTTON, F. W., 1937 — The Lower Bunter Sandstone of north Worcestershire and east Shropshire. Geol Mag. 174,534-553

SHOTTON, F. W., 1956 — Some aspects of the New Red Sandstone desert in Britain. Lpool. Manchr. geol. J. 1,450-465

SLATER, G., 1927 — The structure of the disturbed deposits of the Mens Klint, Denmark. Trans. Roy. Soc. Edin. 55,289-302

SOLOMON, M., RAFTER, T. A. and DUNHAM, K. C., 1971 — Sulphur and oxygen isotype studies in the Northern Pennines in relation to ore genesis. Trans. Instn. Min. Metall. 80,B259-275

SORBY, H. C., 1880 — On the structure and origin of non calcareous stratified rocks. Proc. geol. Soc. 36,46-92

SORBY, H. C., 1908 — On the application of quantitative methods to the study of structures and history of rocks. Q. J1. geol. Soc. London. 64,171-232

STEWART, H. B., 1956 — Contorted sediments in modern coastal lagoon explained by laboratory experiments. Bull. Am. Assoc. Petrol. Geol. 40,153-179

SUNDERLAND, J., 1972 — Deep sedimentary basin in the Moray Firth. Nature 236,24-25

THOMPSON, D. B., 1969 — Dome shaped aeolian dunes in the Frodsham member of the so-called "Keuper" Sandstone formation (Scythian-? Anisian; Triassic) at Frodsham, Cheshire, England. Sedim. Geol. 3,263-289

THOMPSON, R. W., 1968 — Tidal flat sedimentation in the Colorado River delta, north western Gulf of California. Geol. Soc. Am. Mem. 107

TRASK, P. D., 1932 — Origin and environment of source sediments of petroleum. Gulf Publishing Co. Houston, Texas. 323 pp.

VAN HOUTEN, F. B., 1968 — Iron oxides in red beds. Bull. Geol. Soc. Amer. 79,399-416

WADELL, H., 1934 — Some new sedimentation formulas. J. Appl. Phys. 5,281-291

WALKER, A. D., 1961 — Triassic reptiles from the Elgin area; Stagonolepsis, Dasygnathus and their allies. Phil. Trans. Roy. Soc. Series B, 244,102-204

WALKER, T. R., 1967 — Formation of red beds in modern and ancient deserts. Bull. Geol. Soc. Amer. 79,399-416

WARRINGTON G. W., 1970 — The stratigraphy and palaeontology of the Keuper series of the central midlands of England. Quart. J1. Geol. Soc. London, 126,183-223

WATSON, D. M. S., 1909 — The Trias of Moray. Geol. Mag. 6,102-107

WATSON, D. M. S., and HICKLING, G., 1914 — On the Triassic and Permian rocks of Moray. Geol. Mag. 1,399-402

WATSON, D. M. S., WESTOLL, T. S., WHITE, E. I. and TOOMBS, H. A., 1948 — Guide to excursion C.16., vertebrate palaeontology. 18th Int. Geol. Cong. London.

WAUGH, B., 1967 — Environmental and diagenetic studies of the Permo-Triassic clastic and carbonate Sediments of the Vale of Eden. Ph.D. thesis. (unpublished). Univ. of Newcastle.

WAUGH, B., 1970 — Formation of quartz overgrowths in the Penrith Sandstone (Lower Permian) of north west England as revealed by scanning electron microscopy. Sedimentology, 14,309-320

WESTOLL, T. S., 1951 — The vertebrate bearing strata of Scotland. 18th Int. Geol. Cong. London, 9,5-21

WHITE, D. E., HEM, J. D., and WARING, G. A., — Chemical composition of subsurface waters. U.S. Geol. Surv. Prof. Papers, 440F. 67 pp.

WILLIAMS, P. F., and RUST, B. R., 1969 — The sedimentology of a braided river. J. sedim. Petrol. 39,649-679

WILLS, L. J., 1970 — The Triassic succession in the central Midlands in its regional setting. Quart. J1. Geol. Soc. London. 126,225-286

WILSON, M. J., 1971 — Clay mineralogy of the Old Red Sandstone (Devonian) of Scotland. J. sedim. Petrol. 41,995-1007